

**Endogenous retroviruses and the
association with TDP-43 and
inflammation in the cause and
progression of Motor Neuron
Disease**

By

Megan Fowler
BBehSci, BMedSci (Hons)

*Thesis
Submitted to Flinders University
for the degree of*

Doctor of Philosophy

College of Medicine and Public Health
August 2024

ABSTRACT

Motor Neuron Disease (MND), also known as amyotrophic lateral sclerosis (ALS) is a progressive neurological disorder characterised by the death of upper and lower motor neurons. The aetiology of MND remains unknown and treatment options are limited. A hallmark of MND pathology is altered localisation of the transactive response (TAR) DNA binding protein 43 kDa (TDP-43), which is normally found within the nucleus of neuronal and glial cells and is involved in RNA regulation. In MND, TDP-43 aggregates within the cytoplasm and facilitates motor neuron degeneration.

The exact mechanism of how TDP-43 mislocalisation results in neurodegeneration is still unclear. One proposed mechanism involves endogenous retroviruses (ERVs). ERVs are genomic remnants of ancient viral infection events, with most being inactive and not retaining the capacity to encode a fully infectious virus. However, some ERVs retain the ability to be activated and transcribed, and ERV transcripts have been found to be elevated within the brain tissue of MND patients. Therefore, ERVs, specifically human endogenous retrovirus type K (HERV-K), have been proposed to be involved in the cause and propagation of neurodegeneration.

Due to the association between ERVs and their potential role in neurodegeneration, antiretroviral therapy to target ERVs was proposed as a treatment. A phase II clinical trial of an antiretroviral therapy, Triumeq, showed promising results for reducing HERV-K levels in a small cohort of MND patients. While this a promising result for identification of a novel therapy for MND, further research into this treatment is needed.

The aim of the current study was to test the efficacy of Triumeq in a TDP-43 mouse model of MND to further elucidate the mechanisms of action of Triumeq in MND. The study first assessed the tolerability of Triumeq in a small cohort of TDP-43 transgenic mice where it was deemed tolerable before testing in a larger cohort. The mice studies identified a significant improvement in motor performance in TDP-43 mice treated with Triumeq. However, this significant difference was only seen at Day 17 of the study and no further differences were observed by the time the mice reached the ethical end point. This difference in motor

performance also coincided with a significantly lower level of urinary p75^{ECD} in the treated mice. At this same point of disease, there was also a significantly lower number of motor neurons in the lumbar region of untreated mice compared to treated mice. Other disease progression measures including weight loss were not significantly different between Triumeq-treated mice and untreated mice at any point of the study. Real Time Quantitative Polymerase Chain Reaction (RT-qPCR) was employed to measure the mRNA expression of inflammatory markers within the brain of the treated and untreated mice. While there were no significant differences in expression between treatment groups, there was a correlation between TDP-43 expression and an inflammatory cytokine C-X-C motif chemokine ligand 10 (CXCL10), a chemokine known to be increased in MND patients with influence on neurodegenerative mechanisms.

Based on the results from Chapter 3, an increased dose of Triumeq was tested in the mice to determine any further therapeutic benefit. While only a small cohort was used for this study, no significant differences between mice treated with an increased dose of Triumeq and untreated mice were observed for any measure of disease progression. These findings, alongside the findings from Chapter 3, suggest that Triumeq could be reducing neurodegenerative mechanisms at the current dose used in the human clinical trials.

In addition to the mice studies, this study also aimed to further elucidate the mechanism of Triumeq on TDP-43 and HERV-K relationship *in vitro*. To do this, the expression of HERV-K and TDP-43 in multiple cell lines, including a primary cell, was analysed. Using one of the analysed cell lines, exogenous viral infection was shown to increase the levels of HERV-K expression, independent of TDP-43 expression but associated with increased inflammatory cytokine expression.

This study provides valuable insight into the use of Triumeq as a treatment for MND and further elucidate the involvement of HERV-K in MND pathology, specifically involving TDP-43 and inflammatory pathways. Further elucidating the functional relationship between HERV-K, neuroinflammation and TDP-43 will allow for a greater understanding of potential therapeutics to target the intersection of these mechanisms and hopefully slow or halt MND disease progression.

DECLARATION

I certify that this thesis does not incorporate without acknowledgment any material previously submitted for a degree or diploma in any university; and the research within will not be submitted for any other future degree or diploma without the permission of Flinders University. To the best of my knowledge and belief it does not contain any material previously published or written by another person except where due reference is made in the text.

Signed Megan Dubowsky

Date 18/04/2024

ACKNOWLEDGEMENTS

Firstly, I would like to thank Associate Professor Mary-Louise Rogers, for the support and supervision over the last 7 years. Thank you for trusting in me from the beginning days during my research placement, through to finally finishing my PhD.

Thank you to my co-supervisor, Professor Jill Carr. I am very grateful for the input and support you have provided over my PhD project. To the other members of the Carr lab, thank you for your help and support throughout this project. Thank you also to my adjunct supervisor, Dr. Frances Theunissen. Your support both in my scientific endeavours and my personal life is something I will always appreciate.

I'd also like to thank Professor Anthony Akkari who has been an incredible support during the last couple of years of my PhD. Thank you for pushing me over the finish line. To the rest of the members at the Perron Institute, thank you also for your help and support over the last 2 years.

A big thank you to the members of the lab during my PhD. Steph, Dani and Billy, I would not have made it through without your support. Thank you for the constant laughs, for listening to my rants, allowing me to yell, the welcome distractions, the long conversations, putting up with my questionable music choices and the constant rustling coming from my snack drawer. Mephassalini also deserves an honourable mention here.

This degree would not have been possible without the support of my family and friends. To Joshua, for being a wealth of knowledge about all things science. To my son Leo, for his understanding and resilience while both his parents finish a PhD. It has been a long and difficult process but your smile at the end of each day got me through. To Rosie, Gary, Amy, Rachel, David and Callum, your support was unwavering. Thanks for putting up with presentation practices and letting me vent about my PhD. A particular thank you to my adorable nephews, Dawson and Maxwell.

I would also like to thank Andrew, for his support while finishing this PhD. I would not have made it through without your coffees, amazing dinners, forest walks, constant encouragement and emotional support through my mental breakdowns while writing this up.

I acknowledge the contribution of an Australian Government Research Training Program Scholarship throughout my candidature.

I dedicate this thesis in memory of Ian and Gail Fowler (1930/1942-2022). I will never forget your tremendous love and support.

FUNDING

2019-2023

Australian Research Training Program Scholarship

2019 – 2023

Motor Neuron Disease Research Association Top-up Scholarship

PUBLICATIONS AND PRESENTATIONS

PUBLICATIONS

Chapter 1:

Dubowsky, M., Theunissen, F., Carr, J.M., and Rogers, M.L., 2023. The Molecular Link Between TDP-43, Endogenous Retroviruses and Inflammatory Neurodegeneration in Amyotrophic Lateral Sclerosis: A Potential Target for Triumeq, an Antiretroviral Therapy. *Molecular Neurobiology*, 60(11), pp.6330-6345.

Other:

Dubowsky, M., Shephard, S.R. and Rogers, M.L., 2021. Neurotrophic Therapy for ALS/MND. *Handbook of Neurotoxicity*, pp.1-37.

Shephard, S.R., Karnaros, V., Benyamin, B., Schultz, D.W., **Dubowsky, M.**, Wu, J., Chataway, T., Malaspina, A., Benatar, M. and Rogers, M.L., 2022. Urinary neopterin: A novel biomarker of disease progression in amyotrophic lateral sclerosis. *European Journal of Neurology*, 29(4), pp.990-999.

PRESENTATIONS

Dubowsky, M.K., *Endogenous retroviruses as a cause of Motor Neuron Disease (2019)*, Oral Presentation, Flinders University College of Medicine and Public Health Emerging Leaders Showcase, Adelaide, South Australia

Dubowsky, M., Carr, J., Theunissen, F., Walker, A.K., Gold, J., Rogers, M.L. Amyotrophic Lateral Sclerosis and Frontotemporal Degeneration. Abstracts from the 31st International Symposium on ALS/MND 2020 (Virtual), Theme 7: Pre-clinical strategies, p1-30, DOI: 10.1080/21678421.2020.1828775

Dubowsky, M.K., Carr, J., Gold, J., Walker, A., Rogers, M-L., *Effects of antiretroviral therapy on motor behaviour, TDP-43 proteinopathy and immune response in a motor neuron disease mouse model (2021)*, Poster/Oral Presentation (Virtual), Macquarie Neurodegeneration Meeting

Dubowsky, M.K., *Endogenous retroviruses as a cause of Motor Neuron Disease (2022)*, Oral Presentation, Flinders University College of Medicine and Public Health Emerging Leaders Showcase, Adelaide, South Australia

Dubowsky, M.K., Carr, J., Gold, J., Walker, A., Rogers, M-L., *Effects of antiretroviral therapy on motor behaviour, TDP-43 proteinopathy and immune response in a motor neuron disease mouse model (2022)*, Poster/Oral Presentation, Australian and New Zealand Research Symposium, Brisbane, Australia

Dubowsky, M.K., Carr, J., Gold, J., Walker, A., Rogers, M-L., *Effects of antiretroviral therapy on motor behaviour, TDP-43 proteinopathy and immune response in a motor neuron disease mouse model (2023)*, Poster/Oral Presentation, Australian and New Zealand Research Symposium, Wollongong, Australia

Dubowsky, M., Carr, J., Theunissen, F., Walker, A.K., Gold, J., Rogers, ML. Amyotrophic Lateral Sclerosis and Frontotemporal Degeneration. Abstracts from the 34th International Symposium on ALS/MND 2023, Basel, Switzerland, Theme 7: Pre-clinical strategies, p191, DOI:10.1080/21678421.2023.2260198

LIST OF FIGURES

Figure 1.1 Structure of TDP-43.....	31
Figure 1.2 Proposed mechanisms of motor neuron degeneration in MND.....	47
Figure 1.3 Schematic of a Dox-suppressible system for hTDP-43 expression resulting in cytoplasmic mislocalisation of TDP-43.....	64
Figure 1.4 Classification of Human Endogenous Retroviruses.....	68
Figure 1.5 Endogenisation of retroviruses from exogenous retroviral infection.....	69
Figure 1.6 Structure of the HERV-K (HML-2) full-length provirus.....	72
Figure 1.7 Proposed pathway leading to motor neuron disease involving neuroinflammation and HERV-K.....	77
Figure 1.8 Proposed interaction of HERV-K, TDP-43 and inflammatory mediators in the process of neurodegeneration in MND.....	82
Figure 2.1 Experimental timeline of the validation and pilot studies for Triumeq treatment in hTDP-43 Δ NLS mice.....	93
Figure 2.2 Experimental timeline of the Triumeq treatment in hTDP-43 Δ NLS mice.....	94
Figure 3.1 hTDP-43 expression and mislocalisation in the cortex of the hTDP-43 Δ NLS mouse model.....	110
Figure 3.2 Urinary p75 ^{ECD} levels in hTDP-43 Δ NLS mice on Dox and 2, 4 and 6 weeks off Dox.....	112
Figure 3.3 Removal of Dox initiates MND-like symptoms in hTDP-43 Δ NLS mice.....	114
Figure 3.4 Percentage weight change and neurological score after Triumeq treatment in hTDP-43 Δ NLS mice.....	116
Figure 3.5 Latency to fall on the wirehang test between treated and untreated hTDP-43 Δ NLS mice.....	117
Figure 3.6 Percentage weight change and neurological score in a large cohort of hTDP-43 Δ NLS mice.....	119
Figure 3.7 Latency to fall on the wirehang test for a large cohort of hTDP-43 Δ NLS mice.....	121
Figure 3.8 Gait analysis including stride length and stride width in treated and untreated hTDP-43 Δ NLS mice.....	122

Figure 3.9 Urinary p75^{ECD} levels in treated and untreated hTDP-43ΔNLS mice on day 1 and day 15 post-treatment onset	124
Figure 3.10 Histological presentation of motor neurons within the lumbar spinal cord from treated and untreated hTDP-43ΔNLS mice	126
Figure 3.11 Motor neuron count from lumbar spinal cord of treated and untreated hTDP-43ΔNLS mice	127
Figure 3.12 mRNA analysis of brain tissue from treated and untreated hTDP-43ΔNLS mice	130
Figure 3.13 Relationship between TDP-43 expression and TNF-α and CXCL10 expression from brain tissue of treated and untreated hTDP-43ΔNLS mice	132
Figure 4.1 Percentage weight change and neurological score in a cohort of hTDP-43ΔNLS mice after increased dose of Triumeq treatment	143
Figure 4.2 Percentage weight change of treated single dose and double dose hTDP-43ΔNLS mice compared to untreated mice	144
Figure 4.3 Latency to fall from the wirehang test for the double dose study	146
Figure 4.4 Gait analysis including stride length and stride width in double dose treated and untreated hTDP-43ΔNLS mice	148
Figure 4.5 Urinary p75^{ECD} levels in double dose treated and untreated hTDP-43ΔNLS mice across study course	150
Figure 4.6 Urinary p75^{ECD} levels in double dose treated and untreated hTDP-43ΔNLS compared to single dose treated and untreated mice	151
Figure 5.1 Change of TDP-43 expression to untreated SH-SY5Y after treatment with various concentrations of a PMO against TARDBP	164
Figure 5.2 Expression of HERV-K and inflammatory markers at different concentrations of a PMO against TARDBP	165
Figure 5.3 Correlation of TDP-43 expression to Pan HERV-K and HERV-K env expression in a TDP-43-knockdown SH-SY5Y cell line	166
Figure 5.4 Correlation of TDP-43 expression to ICAM-1 and TNF-α expression in a TDP-43-knockdown SH-SY5Y cell line	167
Figure 5.5 TDP-43 and HERV-K expression from olfactory neuroepithelial derived stem cells from MND patients and controls	169

Figure 5.6	HERV-K expression in multiple cell lines.....	171
Figure 5.7	Expression of TDP-43 and HERV-K in a HeLa cell line with Dengue Virus Infection and LPS stimulation.....	174
Figure 5.8	Expression of pan HERV-K and HERV-K env in ARPE-19 with Zika virus or dengue virus infection and LPS and Poly-IC stimulation.....	176
Figure 6.1	Proposed therapeutic targets and interaction of HERV-K, TDP-43 and inflammatory mediators in MND.....	191
Figure A.1	Formation of a provirus from exogenous retroviral infection to release from a host cell.....	195
Figure A.2	Motor neurons within the lumbar spinal cord of a hTDP-43ΔNLS mouse.....	196
Figure A.3	Example gait analysis from a healthy litter-matched control mouse.....	197
Figure A.4	HERV-K pol, HERV-K gag, HERV-K env primer validation in ARPE-19.....	198
Figure A.5	Inflammatory expression in DENV and ZIKV-infected ARPE-19.....	199
Figure A.6	TDP-43 primer binding locations shown on TDP-43 sequence.....	200

LIST OF TABLES

Table 1.1 Types of Motor Neuron Disease and the motor neurons involved, presentation of disease and life expectancy of each type	24
Table 1.2 Summary of treatments and therapies for MND and their mechanism of action and benefit.....	60
Table 2.1 Primer sequences used for amplification of mRNA.....	89
Table 2.2 Antibodies used in ELISA and Immunofluorescence	90
Table 2.3 Buffers used in this project.....	91
Table 2.4 Neurological score explanation for TDP-43 mice (Adapted from Leitner et al., 2009)	96
Table 2.5 Cell lines used for RNA analysis provided for this project.....	105
Table 3.1 Overview of significant effects from Triumeq treatment on the pathways from brain through to muscle	139
Table 5.1 Transcription factors upstream of full length HERV-K and the number of binding sites across 20 HERV-K loci	159
Table 5.2 Transcription factors predicted to regulate HERV-K expression showing the number of binding sites on each locus with red representing no binding sites and green representing 1 or more binding sites	161

ABBREVIATIONS

ALS – Amyotrophic Lateral Sclerosis
ALSFRS-R – ALS Functional Rating Scale Revised
AMPA - α -amino-3-hydroxy-5-methyl-4-isoxazolepropionic acid
ART – Antiretroviral Therapy
ARVs – Antiretrovirals
C9orf72 – Chromosome 9 Open Reading frame 72
cGAS - cyclic GMP-AMP Synthase
CSF – Cerebrospinal Fluid
CXCL10 - C-X-C motif chemokine ligand 10
DCTN1 - Dynactin Subunit 1
Dox – Doxycycline
DPR – Dipeptide Repeat Proteins
DENV – Dengue Virus
EAAT2 - Excitatory Amino Acid Transporter 2
ELISA – Enzyme-linked Immunosorbent Assay
ER – Endoplasmic Reticulum
ERV – Endogenous Retrovirus
fALS – Familial ALS
FTD – Frontotemporal Dementia
FUS – Fused in Sarcoma
GluR2 - Ionotropic Glutamate Receptor 2
HEK – Human Embryonic Kidney
HERV – Human Endogenous Retrovirus
HERV-K – Human Endogenous Retrovirus Type K
HIV – Human Immunodeficiency Virus
hMPCs – Human Mesenchymal Progenitor Cells
hTDP-43 – Human TDP-43
ICAM-1 - Intracellular Adhesion Molecule 1
IFN – Interferon
IGF-2 – Insulin-like Growth Factor Receptor 2
IHC – Immunohistochemistry
IIs – Integrase Inhibitors
IL – Interleukin
iPSC – Induced Pluripotent Stem Cells
IRF – Interferon Regulatory Factor
KoRV – Koala Retrovirus
LMN – Lower Motor Neurons
LTR – Long Terminal Repeat
LPS - Lipopolysaccharide

MMTV – Mouse Mammary Tumour Virus
MND – Motor Neuron Disease
MS – Multiple Sclerosis
NEK1 - NIMA-related Kinases
NF- κ B - Nuclear Factor Kappa-light-chain-enhancer of Activated B Cells
NF-L – Neurofilament Light Chain
NIV – Non-invasive Ventilation
NMDA - N-methyl-D-aspartate Receptor
NMJ – Neuromuscular Junction
NNRTIs – Non-nucleoside Reverse Transcriptase Inhibitors
NRTIs - Nucleoside Reverse Transcriptase Inhibitors
ONS – Olfactory Neuroepithelial-derived Stem Cells
OPTN – Optineurin
p75^{ECD} - The Extracellular Domain of the p75 Neurotrophin Receptor
PBP - Progressive Bulbar Palsy
PBS – Phosphate Buffered Saline
PCR – Polymerase Chain Reaction
PIs – Protease Inhibitors
PLS – Primary Lateral Sclerosis
PMA – Primary Muscular Atrophy
PMO - Phosphorodiamidate Morpholino Oligomers
pNF-H – Phosphorylated Neurofilament Heavy Chain
ROS – Reactive Oxygen Species
RT – Reverse Transcriptase
RT-qPCR – Real Time Quantitative Polymerase Chain Reaction
sALS – Sporadic ALS
SOD1 – Cu/Zn Superoxide Dismutase
STAT – Signal Transducer and Activator Of Transcription
STING – Stimulator of Interferon Genes
TBK1 – TANK Binding Kinase 1
TDP-43 – TAR DNA Binding Protein 43
TLR – Toll-like Receptor
TNF- α – Tumour Necrosis Factor Alpha
TRAF - TNF Receptor-associated Factor
TRIF - TIR-domain-containing adapter-inducing Interferon- β
UI - Uninfected
UMN – Upper Motor Neurons
UPR – Unfolded Protein Response
UPS – Ubiquitin Proteasome System
ZIKV – Zika Virus

TABLE OF CONTENTS

1	INTRODUCTION.....	20
1.1	Motor Neuron Disease	20
1.1.1	A Neurodegenerative Disease	20
1.1.2	Epidemiology of Motor Neuron Disease.....	21
1.1.3	Heterogeneity of Motor Neuron Disease	21
1.1.4	Pathology of Motor Neuron Disease	25
1.1.5	Molecular Genetics of Motor Neuron Disease	25
1.1.5.1	Superoxide Dismutase 1.....	26
1.1.5.2	Chromosome 9 Open Reading Frame 72	27
1.1.5.3	TAR DNA Binding Protein 43	28
1.1.5.4	Fused in Sarcoma	32
1.1.5.5	TANK-binding Kinase 1	32
1.1.6	Risk Factors of Motor Neuron Disease	32
1.1.6.1	Older Age and Gender as a Risk Factor of MND.....	32
1.1.6.2	Environmental Risks of MND.....	33
1.1.6.3	Lifestyle Risk Factors	36
1.1.7	Underlying Pathogenesis of Neurodegeneration	38
1.1.7.1	Susceptibility of Motor Neurons to Degeneration	38
1.1.7.2	Excitotoxicity as a Cause of Neurodegeneration in MND	39
1.1.7.3	Impaired Proteostasis	40
1.1.7.4	Axonal Transport.....	41
1.1.7.5	TDP-43 Pathology and its Role in Neurodegeneration.....	42
1.1.7.6	Mitochondrial Dysfunction.....	45
1.1.7.7	The Role of Neuroinflammation in Neurodegeneration	48
1.2	Disease Characteristics: From Diagnosis to Treatment.....	52
1.2.1	Diagnosis.....	52
1.2.2	Progression of MND.....	53
1.2.3	Prognostic Factors Associated with MND.....	53
1.2.4	Biomarkers of MND	54
1.2.4.1	p75 Extracellular Domain as a Prognostic, Progression and Pharmacodynamic Biomarker of MND	54
1.2.4.2	TDP-43 as a Biomarker of Disease Progression.....	56
1.2.5	Current Treatments and Therapy	57
1.2.5.1	Pharmaceutical Treatment for MND.....	57
1.2.5.2	Ventilation as Supportive Therapy for MND	58
1.2.5.3	Need for Further Treatment Development.....	59
1.3	Models of MND	61
1.3.1	In Vitro Models	61
1.3.1.1	Induced Pluripotent Stem Cells.....	61
1.3.2	In Vivo Models	61
1.3.2.1	SOD1 Mice Models	61
1.3.2.2	TDP-43 Mice Models	62
1.4	Endogenous Retroviruses as a Proposed Cause of MND	65
1.4.1	Retroviruses	65
1.4.2	Endogenous Retroviruses: Structure and Function	66
1.4.3	HERV Benefit and Role in Disease.....	70
1.4.4	Human Endogenous Retrovirus Type-K is Associated with MND	73
1.4.4.1	Interaction Between HERV-K, TDP-43 and Inflammation may Cause Neurodegeneration in MND	74
1.4.5	Anti-retroviral Therapy	78
1.4.6	Treatment of HERV-K-associated MND Through Antiretroviral Therapy	79
1.4.7	Mouse Endogenous Retroviruses and their association with TDP-43	84

1.5	Concluding Remarks.....	84
1.6	Hypothesis and Aims.....	86
2	MATERIALS AND METHODS.....	88
2.1	Materials.....	88
2.1.1	Primers.....	88
2.1.2	Antibodies.....	88
2.1.3	Buffers.....	88
2.2	Methods.....	92
2.2.1	Animal Welfare.....	92
2.2.2	Triumeq Treatment Administration of TDP-43 mice.....	92
2.2.3	Mouse Behavioural testing.....	95
2.2.3.1	Weight Measurement.....	95
2.2.3.2	Neurological Scores.....	95
2.2.3.3	Grip Duration using the Wirehang Test.....	97
2.2.3.4	Gait Analysis.....	97
2.2.3.5	Mice Urine Collection.....	97
2.2.4	Spinal Cord and Brain Extraction for Immunohistochemistry.....	98
2.2.5	Brain Extraction for RNA Analysis.....	98
2.2.6	Enzyme-linked Immunosorbent Assay.....	98
2.2.7	Urinary Creatinine Analysis.....	99
2.2.8	Urinary p75 ^{ECD} calculations.....	99
2.2.9	RNA Analysis.....	100
2.2.9.1	RNA Extraction.....	100
2.2.9.2	DNase I Treatment.....	100
2.2.9.3	Reverse Transcription.....	101
2.2.9.4	Real-time Quantitative Polymerase Chain Reaction (RT-qPCR).....	101
2.2.10	Tissue Imaging.....	102
2.2.10.1	Brain Immunofluorescence.....	102
2.2.10.2	Cresyl Violet Staining.....	102
2.2.10.3	Motor Neuron Counts.....	103
2.2.11	Cell Culture.....	103
2.2.11.1	Cell Maintenance.....	103
2.2.11.2	Viral and Inflammatory Stimulation of HeLa Cells.....	103
2.2.11.3	Cell Lines Provided.....	104
2.2.12	Data Analysis.....	106
3	EFFECTS OF TRIUMEQ TREATMENT ON AN MND MOUSE MODEL.....	108
3.1	Introduction.....	108
3.2	Results.....	109
3.2.1	Validation of hTDP-43 Expression and Mislocalisation in hTDP43ΔNLS mice.....	109
3.2.2	Validation of Urinary p75 ^{ECD} Levels in hTDP43ΔNLS mice after Removal from Dox.....	109
3.2.3	Pilot Study for the Validation of MND Progression in hTDP43ΔNLS Mice off Doxycycline.....	113
3.2.4	Pilot Study to Assess the Tolerability and Palatability of Triumeq in hTDP43ΔNLS Mice.....	115
3.2.4.1	Triumeq Does not Influence Disease Progression.....	115
3.2.4.2	Triumeq Influences Motor Performance at 15 Days Post-treatment Onset.....	115
3.2.5	Effects of Triumeq Treatment in hTDP43ΔNLS Mice.....	118
3.2.5.1	Triumeq Treatment Does Not Influence Disease Progression According to Weight Loss and Neurological Score.....	118
3.2.5.2	Triumeq Treatment Influences Motor Performance.....	120
3.2.5.3	Triumeq Treatment Influences Gait.....	120
3.2.5.4	Triumeq Influences p75 ^{ECD} Levels.....	123
3.2.5.5	Triumeq Influences Motor Neuron Count in the Spinal Cord.....	125
3.2.5.6	Triumeq Does Not Influence Expression of TDP-43, MMTV, TNF-α or CXCL10.....	128

3.2.5.7	TDP-43 Expression Correlates with Inflammatory Marker Expression	129
3.3	Discussion.....	133
3.3.1	Summary.....	133
3.3.2	Dox Removal in hTDP-43ΔNLS Mice Induces Disease.....	133
3.3.3	Pilot Study for Triumeq Use in hTDP-43ΔNLS Mice	134
3.3.4	Effects of Triumeq Treatment on Disease Progression and Pathology	135
3.3.5	Conclusions.....	138
4	EFFECTS OF AN INCREASED DOSE OF TRIUMEQ TREATMENT ON AN MND MOUSE MODEL.....	141
4.1	Introduction	141
4.2	Results.....	142
4.2.1	Increased Triumeq Dose Does Not Influence Disease Progression	142
4.2.2	Increased Triumeq Dose Does Not Affect Weight Loss	142
4.2.3	Increased Triumeq Dose Does Not Influence Motor Performance According to Wirehang	145
4.2.4	Increased Triumeq Dose Does Not Influence Gait.....	147
4.2.5	Increased Triumeq Dose Does Not Influence Urinary p75 ^{ECD}	149
4.3	Discussion.....	152
4.3.1	Summary.....	152
4.3.2	Increasing the Dose of Triumeq in a small cohort of hTDP-43ΔNLS mice	152
4.3.3	Conclusions.....	154
5	INVESTIGATING THE RELATIONSHIP BETWEEN HERV-K, TDP-43 AND INFLAMMATION IN VITRO	157
5.1	Introduction	157
5.2	Results.....	158
5.2.1	<i>In silico</i> Analysis of Transcription Factors Predicted to Regulate HERV-K Gene Expression.....	158
5.2.2	Antisense Oligonucleotide against TARDBP reduces TDP-43 expression	162
5.2.3	TDP-43 Expression is Not Correlated with HERV-K Expression <i>In Vitro</i>	162
5.2.4	TDP-43 Expression is Correlated with Immune Markers <i>In Vitro</i>	163
5.2.5	HERV-K and TDP-43 Expression is Not Increased in a Primary Cell Line of MND.....	168
5.2.6	Expression of HERV-K in Multiple Cell Lines	170
5.2.7	Dengue Virus Infection or LPS stimulation does not increase HERV-K or TDP-43 expression in a HeLa cell line	173
5.2.8	Expression of HERV-K pan and HERV-K env is Increased Following Zika Virus Infection <i>In Vitro</i>	175
5.3	Discussion.....	177
5.3.1	Summary.....	177
5.3.2	<i>In Silico</i> Analysis of Transcription Factors Regulating HERV-K Expression.....	177
5.3.3	Analysis of HERV-K and TDP-43 Expression in Multiple Cell Lines.....	178
5.3.4	Conclusions.....	182
6	DISCUSSION	184
6.1	Overview	184
6.1.1	Triumeq Treatment in a TDP-43 mouse model of MND	184
6.1.2	<i>In Vitro</i> Analysis of HERV-K and TDP-43.....	188
6.2	The future of Triumeq treatment for MND.....	190
6.3	Future directions.....	192
6.4	Conclusions	193
7	APPENDIX.....	195

REFERENCES 201

CHAPTER 1. INTRODUCTION

An excerpt from the following chapter was published in *Molecular Neurobiology*:

Dubowsky, M., Theunissen, F., Carr, J.M. and Rogers, M.L., 2023. The Molecular Link Between TDP-43, Endogenous Retroviruses and Inflammatory Neurodegeneration in Amyotrophic Lateral Sclerosis: a Potential Target for Triumeq, an Antiretroviral Therapy. *Molecular Neurobiology*, pp.1-16

1 INTRODUCTION

1.1 Motor Neuron Disease

1.1.1 A Neurodegenerative Disease

Motor Neuron Disease (MND), also known as amyotrophic lateral sclerosis (ALS), is a progressive neurological disorder with amyotrophic lateral sclerosis (ALS) the most common form of MND. MND was first identified by French Physician, Jean-Martin Charcot in 1869 (Charcot, 1869) and is characterised by death of upper motor neurons (UMN) and lower motor neurons (LMN) (Chiò and Traynor, 2015, Foster and Salajegheh, 2018). UMNs emanate from the primary motor cortex with axons terminating in the brain stem and spinal cord. LMNs emanate from the brainstem and spinal cord to control movements of the face, eyes and tongue. LMNs emanating from the spinal cord synapse with skeletal muscles to form the neuromuscular junctions (Mora and Chiò, 2015). Death of motor neurons controlling muscle movements results in muscular atrophy, the eventual inability to activate muscles of the body and control vital functions such as respiration (Foster and Salajegheh, 2018, Kiernan, 2018). However, particular muscles remain intact throughout disease progression such as the muscles controlling the bladder, bowel and eye movements (Shaw *et al.*, 2014).

Two opposing hypotheses are proposed for the place of origin of neurodegeneration within the neurons, the dying-forward hypothesis and the dying-back hypothesis. The dying-forward hypothesis suggests that neurodegeneration occurs first in corticomotoneurons resulting in downstream anterior horn neurodegeneration from excitotoxicity. The dying-back hypothesis suggests that neurodegeneration begins in the neuromuscular junction from neurotrophin deficiency and results in retrograde neurodegeneration (Williamson and Cleveland, 1999, Eisen *et al.*, 1992, van den Bos *et al.*, 2019). The cause of MND remains elusive and with no cure and approximately a year between symptom onset and diagnosis, life expectancy of MND sufferers lies between 2-5 years from diagnosis (Hardiman *et al.*, 2011, Foster and Salajegheh, 2018). To put an end to this discouraging statistic, Motor Neuron Disease research continues with its search for a cause, disease-halting treatments and a cure.

1.1.2 Epidemiology of Motor Neuron Disease

The global prevalence of MND is 4.5 per 100,000 people (Logroscino *et al.*, 2018). In Australia, approximately 2000 people have MND with two people diagnosed and two people losing their life to the disease, each day (Deloitte Access Economics (Report), 2015). In Australia, the prevalence rate of MND is approximately 8.7 per 100,000. There is great variability in prevalence rate among different countries with the global prevalence rate ranging from 1 per 100,000 to 11 per 100,000 (Chiò *et al.*, 2013). The countries with the lowest prevalence rate were in Sub-Saharan Africa with prevalence rates of lower than 1 per 100,000 people. The highest rates were parts of North America with rates of approximately 20 per 100,000 people (Logroscino *et al.*, 2018). MND is socially, economically and personally burdensome with the cost of the disease at \$1.1 million AUD per individual, reported by Deloitte Access Economics (2015). The annual economic cost of the disease is primarily due to costs associated with loss of productivity at \$35,510 per individual with MND and health care costs at \$77,776 per individual.

1.1.3 Heterogeneity of Motor Neuron Disease

Motor neuron disease does not present homogeneously among patients (Al-Chalabi *et al.*, 2016, Ticozzi and Silani, 2018). Heterogeneity is observed in the type of MND, the site of onset, presence of concomitant cognitive impairments and the lifespan of affected individuals. MND presents either sporadically or with a genetic origin (Byrne *et al.*, 2010 as reviewed by Mathis *et al.*, 2019). Sporadic MND (also known as sALS) affects 90% of MND cases (Mathis *et al.*, 2019) with the remaining 10% of cases having a familial cause (fALS). fALS usually presents at an earlier age with the average age of onset of 45 while sALS has a later average age of onset of 55 (Mehta *et al.*, 2019, Cady *et al.*, 2015). Multiple genetic causes are implicated in fALS, discussed in section 1.1.5, furthering the heterogeneity in the cause of the disease (Nguyen *et al.*, 2018, Ticozzi and Silani, 2018). This heterogeneity results in difficulties determining potential causes and hence ways to prevent MND.

The site of onset is another aspect of MND that varies among patients. Symptoms are first reported either in limbs, classified as limb onset, or in speech and swallowing, classified as bulbar onset (Brown and Al-Chalabi, 2017). Limb onset is more common than bulbar onset

with 70% of MND patients exhibiting limb onset compared to 30% exhibiting bulbar onset (Shellikeri *et al.*, 2017). Both types ultimately result in death due to failure of the motor neurons involved in respiration within 2-5 years from diagnosis (Kiernan, 2018).

Another aspect of heterogeneity of MND is the presence of behavioural or cognitive symptoms. Ringholz *et al.*, (2005) reported that 50% of patients exhibit mild cognitive impairments including slight changes in executive functioning and language. It was also reported that 15% on MND patients have concurrent Frontotemporal Dementia (FTD) as determined by neuropsychological examination. MND-FTD is a severe cognitive impairment involving difficulties with learning, executive function, behaviour and personality changes and learning (Raaphorst *et al.*, 2012). Various rates of concurrent MND-FTD have been reported ranging between 5-30% of MND patients (Benjaminsen *et al.*, 2018, Vinceti *et al.*, 2019). This inconsistency in the reported prevalence may be due to poor sensitivity of the FTD diagnostic criteria. Regardless of the prevalence rate, these statistics illustrate the heterogeneity of MND.

MND is diagnosed when symptoms of both upper and lower motor neuron dysfunction are present. In the early stages of MND, it can often be difficult to distinguish MND from other motor diseases including primary lateral sclerosis (PLS) and progressive muscular atrophy (PMA), again adding to the heterogeneity. PLS is characterised by degeneration of upper motor neurons while PMA is characterised by degeneration of lower motor neurons (Brown and Al-Chalabi, 2017). These are outlined in **Table 1.1** and are often misdiagnosed as MND, influencing treatments and prognosis. MND is a rapidly progressive disease with poor prognosis whereas PLS and PMA develop slowly, with average life expectancies of 10-20 years (Statland *et al.*, 2015, Liewluck and Saperstein, 2015, Turner *et al.*, 2020).

Another aspect of heterogeneity seen in MND is the life expectancy with varying rates of survival among MND patients. Although the survival rate for a large proportion of MND patients is 2-5 years, there is a small proportion of patients that live beyond 5 years. There are varying reported percentage rates of long-term survival of MND patients. An Italian longitudinal study reported 10% of MND patients with long term survival, as considered by

survival of 8 years or more (Zoccolella *et al.*, 2008). However, other population studies in Denmark and Taiwan have identified prolonged survival in 20% (Jennum *et al.*, 2013) and 25% (Lee *et al.*, 2013) of MND cases respectively (Pupillo *et al.*, 2014). The reasons behind these population specific long-term survival rates are unknown but younger age at onset and delay in diagnosis, suggesting slower disease progression, are predictors of long-term survival across populations (Calvo *et al.*, 2017). Misdiagnosis of other slower progressing forms of MND, such as PMA and PLS, may influence studies on survival rates (Pupillo *et al.*, 2014, Pupillo *et al.*, 2017). The heterogeneity of MND outlined above indicates the difficulty in identifying the cause of MND and hence, delays treatment development.

Table 1.1 Types of Motor Neuron Disease and the motor neurons involved, presentation of disease and life expectancy of each type

Disease Name	Motor neuron involvement	Presentation of disease/onset	Life expectancy
Amyotrophic Lateral Sclerosis (ALS)	Upper and lower motor neurons	Limb or bulbar onset with limb weakness	2-5 years from diagnosis
Progressive Muscular Atrophy (PMA)	Lower motor neurons	Limb onset with generalised muscle weakness	5-10 years
Primary Lateral sclerosis (PLS)	Upper motor neurons	Limb onset with stiffness and weakness of muscles	20 years
Progressive Bulbar Palsy (PBP)	Upper and lower motor neurons	Bulbar presentation with difficulties with speech and swallowing	2-5 years from diagnosis

1.1.4 Pathology of Motor Neuron Disease

At autopsy, macroscopic pathology is rare to see and not deemed a characteristic of MND pathology. Gross atrophy of the brain is more common in PLS and in MND with concomitant FTD. The main pathological sign of MND is the loss of motor neurons within the anterior and lateral columns of the spinal cord and the primary motor cortex of the brain and is seen microscopically. This has been well characterised in mouse models expressing MND-associated genes. In humans, immunofluorescent staining of cervical and lumbar spinal cord sections shows the progressive loss of motor neurons across the disease course compared to healthy controls (Dai *et al.*, 2017).

A pathological characteristic of MND is the presence of bunina bodies in the lower motor neurons of the anterior horn of the spinal cord, first described in 1962 (Bunina, 1962). Bunina bodies are eosinophilic cytoplasmic inclusions present in sporadic and familial forms of the disease (Saber *et al.*, 2015). Immunohistochemical analysis of bunina bodies showed the inclusions are positive for cystatin C (Okamoto *et al.*, 1993) and transferrin (Mizuno *et al.*, 2006) and negative for ubiquitin (Leigh *et al.*, 1991, Saber *et al.*, 2015).

Ubiquitin-positive inclusions are a hallmark of MND pathology also found within the anterior horn neurons. Neumann *et al.*, (2006) identified TAR DNA binding protein 43 (TDP-43; discussed further in 1.1.5.3) as the main component of the ubiquitinated inclusions. TDP-43 pathology is now considered a hallmark of MND with the presence of ubiquitinated TDP-43 aggregates with cytoplasmic mislocalisation, found in 50% of FTD cases and 97% of MND cases (Birsa *et al.*, 2019). This contrasts with bunia bodies, not found in all MND cases. However, TDP-43 inclusions are not present in a small proportion of MND patients with MND-associated superoxide dismutase (SOD1) mutations. TDP-43 involvement in MND will be further discussed in sections 1.1.7.5 and 1.4.4.1.

1.1.5 Molecular Genetics of Motor Neuron Disease

An inherited genetic cause of MND explains only 10% of cases, while the remaining 90% are regarded as sporadic (Hardiman *et al.*, 2017b). Interestingly, twin studies have revealed there is 60% heritability of fALS (Al-Chalabi *et al.*, 2010).

Within the 10% of familial cases, 65-70% are accounted for by 4 genes including GGGGCC (G₄C₂) hexanucleotide repeats in chromosome 9 open reading frame 72 (*C9orf72*; 40%) (DeJesus-Hernandez *et al.*, 2011, Renton *et al.*, 2011), missense mutations in the SOD1 Cu/Zn superoxide dismutase 1 (*SOD1*; 15-20%) (Rosen *et al.*, 1993, Wijesekera and Nigel Leigh, 2009), point mutations in TAR DNA binding protein 43 (*TDP-43*; 4%) (Neumann *et al.*, 2006) and point mutations in the Fused in Sarcoma gene (*FUS*; 4%) (Vance *et al.*, 2009, Kwiatkowski *et al.*, 2009). The prevalence of these mutations will be discussed below. More recently identified MND-associated gene mutations including TANK-binding Kinase 1 (*TBK1*) and NIMA-related Kinase 1 (*NEK1*) and unidentified genes are thought to explain the genetic cause behind the remaining 40% of familial cases (Nguyen *et al.*, 2018). Familial genes are also implicated in sALS (Ryan *et al.*, 2019).

1.1.5.1 Superoxide Dismutase 1

Missense mutations in *SOD1* account for 15-20% of the fALS cases (Wijesekera and Nigel Leigh, 2009). The association between *SOD1* mutations and inheritance of MND was found in 1993 and was the first genetic link found for MND (Rosen *et al.*, 1993). Since then, over 150 mutations within the *SOD1* gene have been associated with MND (Wijesekera and Nigel Leigh, 2009). The *SOD1* enzyme, encoded by the *SOD1* gene is located on chromosome 21 (Tafari *et al.*, 2015). The *SOD1* protein has copper and zinc binding sites that binds these ions to enable the conversion of free superoxide radicals to reactive oxygen species and hydrogen peroxide which is then broken down further by another cellular catalase enzyme (Ighodaro and Akinloye, 2017). This breakdown of free radicals protects cells from their damaging effects. Hence, *SOD1* can be considered protective against events such as oxidative stress and build-up of free radicals, as described below.

There are many potential causes of neuronal apoptosis in MND related to the *SOD1* mutation. The original hypothesis for *SOD1*-related neurodegeneration was the loss of effective *SOD1* enzyme function, resulting in a build-up of damage-causing free radicals (Rosen *et al.*, 1993; Deng *et al.*, 1993; as reviewed by Saccon *et al.*, 2013). However, Reaume *et al.* (1996) suggested that loss-of-enzyme function was not the cause of neurodegeneration since neurodegeneration was not observed in *SOD1* knock-out mice. Instead, a gain-of-toxic

function of the mutated SOD1 enzyme was postulated (as reviewed by Saccon *et al.*, 2011). First reported in 1994, a transgenic mouse model with a single amino acid change from alanine to glycine at position 93 (SOD1:p.Gly93Ala), has been shown to accurately reflect human disease progression and has identified SOD1-related neurodegenerative mechanisms (Gurney *et al.*, 1994 as reviewed by Joyce *et al.*, 2011). Using this model, evidence for SOD1 gain-of-function was demonstrated, including motor neuron degeneration from SOD1 overexpression (Gurney *et al.*, 1994; as reviewed by Turner and Talbot, 2008). SOD1-related toxicity is thought to influence multiple cellular pathways involving endoplasmic reticulum (ER), proteasome and mitochondrial stress, altered axonal transport and RNA-processing defects (Dion *et al.*, 2009).

1.1.5.2 Chromosome 9 Open Reading Frame 72

In over 40% of fALS patients, there is an increased number of hexanucleotide repeats in the short arm of chromosome 9 open reading frame 72 (*C9orf72*). The association between MND and the increased number of hexanucleotide repeats was discovered in 2011 by two independent research labs (DeJesus-Hernandez *et al.*, 2011, Renton *et al.*, 2011). *C9orf72* explains 40% of fALS, making it the most common familial cause of MND (Renton *et al.*, 2014). *C9orf72* typically contains 20-30 GGGGCC (G₄C₂) hexanucleotide repeats, MND patients have a pathogenic *C9orf72* variant containing hundreds of G₄C₂ hexanucleotide repeats (DeJesus-Hernandez *et al.*, 2011). This hexanucleotide repeat is believed to cause neurodegeneration through one or more pathways (Gitler and Tsuiji, 2016). One hypothesis is that the hexanucleotide repeat results in loss-of-function of *C9orf72*, decreasing available functioning protein and resulting in disease due to haploinsufficiency (Ciura *et al.*, 2013, Gitler and Tsuiji, 2016). Furthermore, hypermethylation of the *C9orf72* promoter at the hexanucleotide repeat expansion has been proposed to suppress gene expression and also cause loss-of-function (He and Todd, 2011). Multiple studies have provided evidence for this loss-of-function hypothesis by showing reduced *C9orf72* transcript levels in MND models (DeJesus-Hernandez *et al.*, 2011, Renton *et al.*, 2011, Gijssels *et al.*, 2012). This process has been observed in other repeat expansion disorders such as Fragile X syndrome, which is caused by an expansion of a repeat region of the *FMR1* gene (Bozdagi *et al.*, 2012).

Another suggested pathway of *C9orf72*-related neurodegeneration is gain-of-function due to the formation of toxic RNA foci from the expanded G₄C₂ repeat (DeJesus-Hernandez *et al.*, 2011, Gitler and Tsuiji, 2016). These RNA foci sequester RNA-binding proteins and effect RNA processing. RNA foci are also formed from the antisense GGCCCC (G₂C₄), sequestering further RNA binding proteins. However, research using a *Drosophila* model with 160 G₄C₂ repeat expansions demonstrated that the accumulation of G₄C₂ sense RNA foci did not affect RNA processing or cause neurodegeneration (Tran *et al.*, 2015). This finding suggests that the accumulation of toxic RNA foci is insufficient to cause neurodegeneration in this model. Lastly, abnormal transcription leading to repeat-associated non-AUG-initiated (RAN) translation into aggregation-prone dipeptide repeat proteins (DPRs) could also be responsible for the neurodegeneration in *C9orf72*-caused MND (Gitler and Tsuiji, 2016). RAN translation of sense G₄C₂ and antisense G₂C₄ transcripts generates 6 DPRs, glycine-alanine (GA), glycine-proline (GP), glycine-arginine (GA), proline-alanine (PA) and proline-arginine (PR) (Mori *et al.*, 2013). Several studies have identified DPR-related neurodegeneration in *C9orf72*-related MND (Shi *et al.*, 2018). By contrast, human post-mortem studies have found no correlation between the DPR protein levels and degree of neurodegeneration (Mackenzie *et al.*, 2015). As there is evidence for each mechanism, neurodegeneration resulting from the *C9orf72* hexanucleotide repeat expansion could be a result of one or a combination of these pathways.

1.1.5.3 TAR DNA Binding Protein 43

While a majority of fALS cases can be explained through mutations in the *SOD1* and *C9orf72* genes, a small portion (5%) are attributed to mutations in the gene that encodes TAR DNA-binding protein 43kDa (TDP-43; *TARDBP*) (Zufiria *et al.*, 2016).

As shown in **Figure 1.1**, TDP-43 contains a nuclear localisation sequence, nuclear export signal, two highly conserved RNA recognition motifs and a glycine-rich domain (Cohen *et al.*, 2011). The nuclear localisation sequence and nuclear export signal enable the transport of TDP-43 between the nucleus and the cytoplasm through importin- α (Pinarbasi *et al.*, 2018). The functions of TDP-43 are thought to occur predominately within the nucleus where TDP-43 binds to precursor mRNA and regulates transcription. The RNA recognition motifs enable

the identification and binding of the protein to RNA and the glycine rich domain of TDP-43 is important for protein-protein interactions (Buratti and Baralle, 2001, Buratti *et al.*, 2005, Heyburn and Moussa, 2017).

The functions of TDP-43 occur predominately within the nucleus where TDP-43 binds to DNA and RNA and is involved in transcriptional regulation, RNA splicing and stability, and transport of mRNA (Lee *et al.*, 2011, Reddi, 2017). TDP-43 also has cytoplasmic functions including translation, mRNA transport and stress granule formation (Alami *et al.*, 2014, Gao *et al.*, 2018, Colombrita *et al.*, 2009). TDP-43 was first described as a transcription factor that regulates the transcription of the human immunodeficiency virus (HIV) trans-activation response (TAR) element to repress HIV-1 transcription (Ou *et al.*, 1995). Since then, TDP-43 has been identified as a transcriptional repressor involved in the repression of a spermatid-specific acrosome vesicle gene (*ACRV*) with the promotor region containing TDP-43 binding sites (Acharya *et al.*, 2006).

Lalmansingh *et al.* (2011) experimentally identified a role of TDP-43 in transcriptional repression of *ACRV*, localising the repressor activity to the RRM1 region of TDP-43. Mutations in TDP-43 causing dysfunctional RRM1 mitigated the repressor activity of TDP-43. In addition, TDP-43 was also found to be involved in the alternative splicing of human cystic fibrosis transmembrane conductance regulator (*CFTR*) exon 9 (Buratti *et al.*, 2001) and human survival of motor neuron 2 (*SMN2*), a gene associated with sporadic MND (Bose *et al.*, 2008). Furthermore, TDP-43 also regulates the alternative splicing of ciliary neurotrophic factor receptor (*CNTFR*), a protein that is implicated in neurodegeneration (Hashimoto *et al.*, 2009, Tollervey *et al.*, 2011, Polymenidou *et al.*, 2011).

Although it has been implicated in disease, particularly MND, TDP-43 is indispensable for healthy development. Wu *et al.* (2010) demonstrated the importance of the protein through TDP-43 knock-out mice, which caused embryonic lethality. The link between TDP-43 and fALS was identified in 2006 through the presence of ubiquitinated TDP-43 inclusions in MND patients (Neumann *et al.*, 2006). Since then, approximately 35 MND-causing mutations related to TDP-43 have been discovered (Gendron *et al.*, 2013, Sreedharan *et al.*, 2008). These mutations are all dominant missense mutations located within the glycine-rich domain of the

protein (Cohen *et al.*, 2011). These single nucleotide mutations interrupt important function of the protein glycine-rich domain of the protein and it has been proposed to involve impairment of TDP-43 phosphorylation from altered phosphorylation sites (Pesiridis *et al.*, 2009). This has been hypothesised to result in accumulation of protein aggregates, potentially causing neurodegeneration, further discussed below in section 1.1.7.5 (Guo *et al.*, 2011, Scotter *et al.*, 2015). Furthermore, TDP-43 regulates its own expression through binding to 3'UTR sequences in its own mRNA, promoting degradation to decrease TDP-43 levels (Ayala *et al.*, 2011). This self-regulating negative feedback loop may be affected by non-functional TDP-43 aggregates that are unable to bind the mRNA, increasing TDP-43 levels and perpetuating neurodegenerative processes. While only 5% of fALS cases can be attributed to mutations of TDP-43, 97% of MND cases have TDP-43 pathology characterised by cytoplasmic aggregation and nuclear clearance and the protein (Neumann *et al.*, 2006, Heyburn and Moussa, 2017).

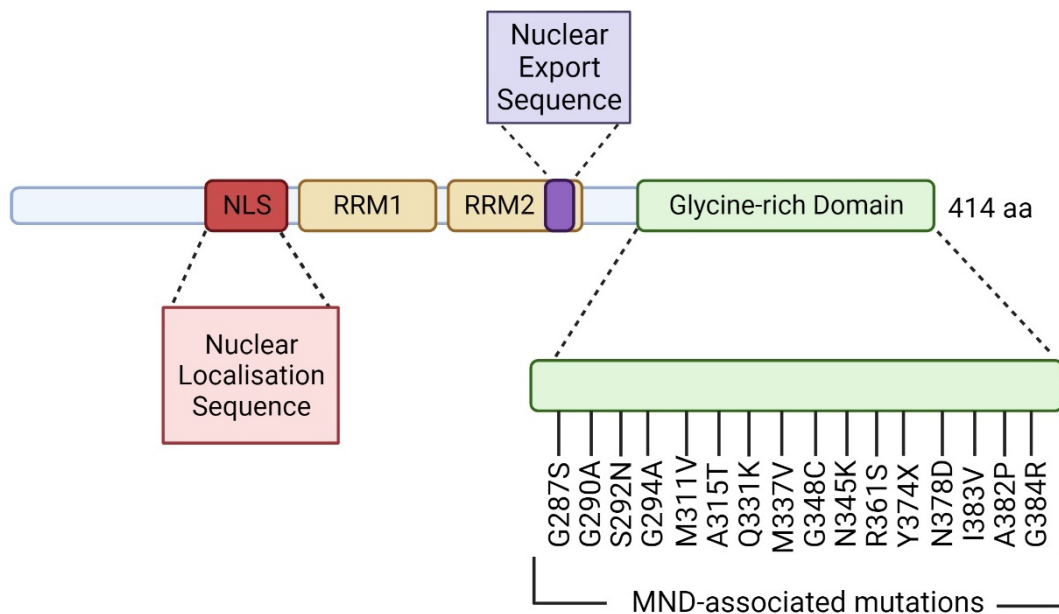


Figure 1.1 Structure of TDP-43

The TDP-43 protein contains a nuclear localisation sequence (red), 2 RNA recognition motifs (RRM; yellow), with a nuclear export sequence (purple) and a glycine-rich domain (green). The MND-associated mutations are localised within the glycine-rich domain (Cohen et al., 2011). Figure made in BioRender.

1.1.5.4 *Fused in Sarcoma*

A further 5% of the known familial causes of MND can be explained by mutations within the Fused in Sarcoma (*FUS*) gene (Vance *et al.*, 2009, Kwiatkowski *et al.*, 2009). Along with TDP-43, *FUS* encodes a nucleic acid binding protein, involved in transcription regulation and RNA processing including alternative splicing (Sun *et al.*, 2011). Over 50 MND-associated missense mutations have been defined, with a majority located in the nuclear localisation sequence (Kwiatkowski *et al.*, 2009, Deng *et al.*, 2014). Similarly, to TDP-43, *FUS* pathology is characterised by loss of nuclear *FUS* and formation of cytoplasmic *FUS* aggregates which results in both loss-of-function toxicity and gain-of-function toxicity, leading to neurodegeneration (Ratti and Buratti, 2016, Ishigaki and Sobue, 2018).

1.1.5.5 *TANK-binding Kinase 1*

Loss-of-function or missense mutations in TANK-binding Kinase 1 (*TBK1*) have also been observed in MND, explaining a small portion of fALS (Nguyen *et al.*, 2018, Cirulli *et al.*, 2015). *TBK1* mutations reduces the expression of functional protein and is proposed to result in MND development through haploinsufficiency (Freischmidt *et al.*, 2017). *TBK1* regulates immune response, inducing production of interferon- α (IFN- α) and IFN- β . *TBK1* mutations in MND have shown to reduce function of the neuronal autophagy system, causing neurodegeneration due to protein aggregation (Oakes *et al.*, 2017). The involvement of *TBK1* in neuroinflammation-mediated neurodegeneration is discussed further in section 1.1.7.7.

1.1.6 Risk Factors of Motor Neuron Disease

Aside from known causative genes, other factors including environmental and lifestyle factors, increase the risk of developing MND.

1.1.6.1 *Older Age and Gender as a Risk Factor of MND*

MND can affect adults at any age, although the average age of onset is 55 (Deloitte Access Economics Report, 2015). Age as a risk factor for MND appears most prevalently between the

ages of 65-74. The total prevalence rate of MND in Australia increases from 12.3 per 100,000 people at ages 45-54 to 28.4 per 100,000 people at ages 65-74. However, there is a drop in the prevalence for the age groups of 75-84 and 85+ to 23.1 per 100,000 people and 11.3 per 100,000 people respectively (Deloitte Access Economics (Report), 2015). This pattern of age-related prevalence has been consistently reported across populations (Marin *et al.*, 2018, Benjaminsen *et al.*, 2018, Mehta *et al.*, 2018). Age is hence described as a biphasic risk factor for the development of MND.

The male gender is another risk factor for the development of MND. The prevalence rate for males is consistently higher than for females across all age groups with the average all-age proportion of male/female cases at 1.5:1 (Deloitte Access Economics (Report), 2015). The reason for the greater prevalence rate among males is still unclear. It has been hypothesised, however, that the greater proportion of male MND patients may be due to differences in hormone influences, environmental risks and lifestyle risks, further discussed below (McCombe and Henderson, 2010, Chiò *et al.*, 2011).

1.1.6.2 Environmental Risks of MND

Environmental factors have been linked to the development of MND. With 90% of MND occurring sporadically, it is hypothesised that the following environmental risks are involved in the development of MND. Exposure to environmental risks as a cause of MND could provide a partial explanation for MND epidemiology.

1.1.6.2.1 β -N-methylamino-L-alanine BMAA

Cyanobacteria have been proposed as a cause of neurodegenerative disease, including MND. The cyanobacteria neurotoxin, β -N-methylamino-L-alanine (BMAA), is found in bodies of water with algal blooms, including sources of drinking water, and cycad plants. BMAA has been implicated as a cause of MND, especially among third-world countries (Cox *et al.*, 2018). The implication of BMAA as a cause of MND originated from a high incidence within a small community in Guam (Baugh, 2017, Cox *et al.*, 2018, Holtcamp, 2012). Kurland *et al.*, (1994) hypothesised BMAA in commonly consumed foods in Guam, namely foods made from cycad

seeds or consumption of animals that feed on cycads, resulted in neurological illness . It has been hypothesised that biomagnification could link BMAA to MND through consumption of seafood in the Western world also (Lance *et al.*, 2018, Brand *et al.*, 2010). Similarly, Li *et al.* (2019) identified bioaccumulation of BMAA from BMAA-rich soil into crops in China. The increased exposure of BMAA through foods has then been thought to cause MND through accumulation of BMAA causing toxic aggregates with nerve cells through its misincorporation into proteins, replacing amino acid L-serine and resulting in apoptosis (Dunlop *et al.*, 2013 as reviewed by Cox *et al.*, 2018). Administration of L-serine to target BMAA has been assessed in a Phase I clinical trial which showed a reduction in disease progression according to the ALSFRS-R compared to placebo control patients (Levine *et al.*, 2017). Research is required to further decipher the link between MND and BMAA and determine the benefit of targeting BMAA as a treatment for MND.

1.1.6.2.2 Metals

Exposure to metals is another environmental risk factor that has been proposed to cause neurodegeneration in MND (Ingre *et al.*, 2015). Although some metals have important biological function, excess exposure to metals has been linked to the development of neurodegenerative diseases, including MND (Cicero *et al.*, 2017, Roos, 2017). Examples of heavy metals implicated in MND are copper, zinc, lead, selenium and manganese but most have conflicting results about their specific role in disease development (Roos, 2017, Peters *et al.*, 2016). The link between MND and heavy metal exposure was first identified through patients with chronic lead poisoning presenting with symptoms that mimicked MND (Livesley and Sissons, 1968). Exposure to metals can occur through respiration, consumption of certain foods and through skin contact (Rehman *et al.*, 2018). High prevalence of MND have been identified in those with occupations with high heavy metal exposure, such as construction work and manufacturing (Andrew *et al.*, 2017). Metal exposure is proposed to increase the risk of MND through increased production of reactive oxygen species resulting in oxidative stress and consequential neuronal apoptosis (Bozzo *et al.*, 2017, Cicero *et al.*, 2017).

Comparisons of metal concentration within cerebrospinal fluid (CSF) of MND patients versus controls identified increased copper, zinc, manganese and lead levels for MND patients (Roos,

2013 as reviewed by Roos, 2017). Furthermore, increased copper levels have been identified within serum from MND patients compared to controls. However, in a larger study, this finding was not replicated (Peters *et al.*, 2021, Peters *et al.*, 2016). This study also found the inverse association for zinc levels in blood and risk of MND, potentially due to the involvement of zinc in SOD1 function (Hilton *et al.*, 2015). Manganese, a well-established neurotoxicant, is another metal associated with MND due to its excessive accumulation within neurons (Horning *et al.*, 2015, Sarkar *et al.*, 2019). Multiple studies have identified high levels of manganese within CSF of MND patients compared to controls (Roos *et al.*, 2012, Peters *et al.*, 2016).

As previously stated, lead exposure has been implicated as a risk factor of MND for over 50 years (Livesley and Sissons, 1968). Many studies since then have identified increased lead levels in blood and CSF of MND patients compared to controls (Wang *et al.*, 2014, Fang *et al.*, 2010, Roos, 2013, Peters *et al.*, 2016). Recent research has implicated lead as a potential risk factor of MND through its direct association with TDP-43 pathology, with excess lead leading to accumulation of TDP-43, *in vitro* (Ash *et al.*, 2018). However, a case-controlled study of MND patients did not find the same association between lead and MND development, with no significant differences in CSF lead levels between MND patients and age-matched healthy controls (Vinceti *et al.*, 2017a). Further research is required to determine the extent of metal exposure as a risk factor for MND and examine potential treatments based on deficiency or excess exposure to metals.

1.1.6.2.3 Pesticides

High pesticide exposure has been linked to certain occupations such as agriculture with the use of pesticides on plants (Vinceti *et al.*, 2017b, Dickerson *et al.*, 2019). The effect of pesticide exposure on MND risk has been consistently reported across time and populations with studies showing a significant increase in risk of development from high pesticide exposure (Su *et al.*, 2016, Bonvicini *et al.*, 2010, Kamel *et al.*, 2012, Mostafalou and Abdollahi, 2017, Gunnarsson *et al.*, 1992, Morahan and Pamphlett, 2006). High level of pesticide exposure is also correlated with shorter survival time (Goutman *et al.*, 2019). Pesticides are long lasting within the body and have neurotoxic effects (Jayaraj *et al.*, 2016). The mechanism of pesticide

causing MND is unknown, but pesticides are proposed to irreversibly affect the central nervous system through excitotoxic mechanisms from acetylcholinesterase inhibition (Chen, 2012). Oxidative stress is also implicated as a mechanism of neurodegeneration from pesticide exposure (Zepeda-Arce *et al.*, 2017, Mostafalou and Abdollahi, 2017). Thus, antioxidant therapy has been investigated as a therapy against oxidative stress and to restore acetylcholinesterase activity (Fakhri-Bafghi *et al.*, 2016). Pesticide and MND risk analysis studies rely on self-reported pesticide exposure and do not provide a description of specific pesticides used and their chemical properties (Malek *et al.*, 2012). Although a risk has been identified, further investigation is required to determine particular pesticides and length and time of exposure that may be associated with MND prior to clinical translation of these findings.

1.1.6.3 Lifestyle Risk Factors

1.1.6.3.1 Diet factors as a risk factor of MND

Nutrition is implicated as a risk factor for many diseases (Tarry-Adkins and Ozanne, 2017, Tollefsbol, 2018). In MND specifically, a high carbohydrate diet and low-fat diet have been associated with increased risk of disease development (Okamoto, 2019, Ingre *et al.*, 2015). Murine models have identified the benefits of a low-carbohydrate diet in not only reducing the risk of development of MND but improving the survival of remaining motor neurons in animals with MND (Zhao *et al.*, 2006 as reviewed by Paoli *et al.*, 2014). Although the mechanisms remain unclear, low carbohydrate diets are proposed to improve motor function in neurological disease through an increased production of ketone bodies (Veyrat-Durebex *et al.*, 2018). Ketone body production can reduce neurodegeneration through the removal of reactive oxygen species, and repairs mitochondrial dysfunction, a mechanism implicated in the neuropathogenesis of MND (Veyrat-Durebex *et al.*, 2018, Veech, 2014). The benefits of a ketogenic diet have been identified in *in vivo* models of other neurological disorders, such as epilepsy. Danial *et al.* (2013) and Martin *et al.* (2016) used a mouse model of epilepsy to investigate the effects of a ketogenic diet on seizures. They demonstrated a reduction in number of seizures in the mice on a ketogenic diet compared to those on a standard diet. This research suggests the ketogenic diet can influence neuronal excitability (Martin *et al.*, 2016,

Danial *et al.*, 2013). Therefore, treatment with ketone bodies or a strict ketogenic diet could be a novel avenue for treating neurodegenerative diseases, including MND (Sharma *et al.*, 2014, Vandoorne *et al.*, 2018). Further research including clinical trials investigating the safety and tolerability of the ketogenic diet in MND patients is required prior to clinical use.

Along with low-carbohydrate diets, higher intake of polyunsaturated fatty acids has been suggested to have a neuroprotective effect with low-fat diets also considered a nutritional risk factor of MND (Fitzgerald *et al.*, 2014). This is proposed to be due to anti-inflammatory and antioxidant properties of polyunsaturated fatty acids such as docosahexaenoic acid (Mori *et al.*, 2018, Fitzgerald *et al.*, 2014). This research is promising for the neuroprotective effect of low-carbohydrate, higher fat diet for MND. However, safety and tolerability clinical trials are required prior to their use in a clinical setting.

1.1.6.3.2 Smoking increases risk of MND development

. Most studies suggest smoking results in an increased risk of developing MND (de Jong *et al.*, 2012, Wang *et al.*, 2011, Bryan *et al.*, 2016, Zhan and Fang, 2019). Armon (2018) suggested smoking leads to MND development through cumulative DNA damage that results in neurodegeneration. A toxic ingredient within cigarette smoke, formaldehyde, passes through the blood-brain barrier (Shcherbakova *et al.*, 1986, as reviewed by Seals *et al.*, 2017) and is implicated as a risk factor for the development on MND (Roberts *et al.*, 2016, Seals *et al.*, 2017). It has been hypothesised to cause neurodegeneration through protein aggregation and oxidative damage (Spencer, 2018).

1.1.6.3.3 Physical Fitness as a risk factor of MND development

Physical fitness and sports are considered a risk factor of MND (Ingre *et al.*, 2015, Okamoto, 2019). A United States-based study on professional football players identified a 40-fold greater risk of developing MND among the professional football players compared to the general population (Abel *et al.*, 2007 as reviewed by Larcorte *et al.*, 2016). Similarly, an increased risk of MND development has been identified in population-based studies on professional soccer players (Belli *et al.*, 2005, Chiò *et al.*, 2009 as reviewed by Larcorte *et al.*,

2016). The reason for increased risk of MND among athletes is unclear but multiple hypotheses have been proposed. One hypothesis for the association between sports and MND is the increased exposure to mild traumatic brain injury (mTBI) (Gardner and Yaffe, 2015). High-contact sports, such as football, result in risk of mTBI and although inconclusive, mTBI has been shown to be linked with later MND development. This may be caused from stress granule formation (Anderson *et al.*, 2018) and neuroinflammation (Loane *et al.*, 2014).

1.1.7 Underlying Pathogenesis of Neurodegeneration

The exact process underlying neurodegeneration in MND remains elusive. However, the identification of genes involved in MND pathology has helped in the understanding of neurodegenerative mechanisms. This includes oxidative stress, protein aggregates, RNA/DNA processing and many other neurodegenerative processes (Taylor *et al.*, 2016). Possible neurodegenerative processes involved in MND, and susceptibility of motor neurons are discussed below and shown in **Figure 1.2**.

1.1.7.1 Susceptibility of Motor Neurons to Degeneration

Motor neurons are particularly vulnerable to damage due to their large size, low expression of glutamate receptor α -amino-3-hydroxy-5-methyl-4-isoxazole propionic acid (AMPA) receptor subunit 2 (GluR2) and lack of intracellular calcium controlling proteins (Ferraiuolo *et al.*, 2011). The size of the motor neurons increases their susceptibility to neuronal damage due to the higher energy requirements. Given the reduced ATP production that occurs from mitochondrial dysfunction in MND, the large motor neurons with high energy demands are highly susceptible compared to other neuron subtypes with lower energy needs (Le Masson *et al.*, 2014, Ragagnin *et al.*, 2019). Furthermore, the large axons of the motor neurons mean they rely on functioning axonal transport systems for maintaining healthy cell function (Ragagnin *et al.*, 2019, De Vos and Hafezparast, 2017). Both mitochondrial function and axonal transport systems are dysfunctional in MND, as discussed below, which provides further explanation for the susceptibility.

Low expression of GluR2 also influences their susceptibility to neurodegeneration due to increased influx of Ca^{2+} . With Ca^{2+} permeability determined by the GluR2 subunit, low

expression of GluR2 increased calcium permeability and increases AMPA-mediated excitotoxic events that results in neurodegeneration (Gregory *et al.*, 2020, Nijssen *et al.*, 2017). Similarly, motor neurons lack important calcium buffering proteins, parvalbumin and calbindin D28k, that bind to calcium ions and maintain healthy levels of intracellular Ca^{2+} . Without these proteins, there is increased intracellular Ca^{2+} , potentially resulting in damaging excitotoxic events (Fairless *et al.*, 2019). Excitotoxicity is further explained below in section 1.1.7.2. Insulin-like growth factor 2 (IGF-2) receptor expression is also proposed to play a role in the susceptibility of motor neurons. Motor neurons that are susceptible to damage in MND do not express IGF-2 receptors while other motor neuron subtypes that are not affected in MND, such as oculomotor neurons, express this receptor (Ferraiuolo *et al.*, 2011, Allodi *et al.*, 2016). Further research is required for comprehensive understanding of selective resistance and vulnerability of neuronal subgroups in MND.

1.1.7.2 Excitotoxicity as a Cause of Neurodegeneration in MND

Excitotoxic mechanisms have been proposed as a cause of neurodegeneration in MND (King *et al.*, 2016, Staats and VanDenBosch, 2014). Excitotoxicity is mediated by glutamate, the main excitatory neurotransmitter within the CNS (Spalloni *et al.*, 2019). An early study identified increased levels of glutamate within the blood of MND patients compared to healthy controls (Rothstein *et al.*, 1990) which lead to the proposed involvement of excitotoxicity in MND. Glutamate reuptake from the synaptic cleft is important for reducing the levels of glutamate to avoid glutamate-induced toxicity (Spalloni *et al.*, 2019). One potential cause of the glutamate accumulation within the synaptic cleft is due to damage to the EAAT2 glutamate transporter responsible for the removal of glutamate into nearby astrocytes (Rothstein *et al.*, 1993 as reviewed by Spalloni *et al.*, 2019). Excessive glutamate within the synaptic cleft leads to increased activation of glutamate receptors, α -amino-3-hydroxy-5-methyl-4-isoxazole propionic acid (AMPA) and N-methyl-D-aspartate (NMDA) on the post-synaptic neuron. Increased neuronal excitability results in a cascade of detrimental downstream effects, including increases in intracellular Ca^{2+} , leading to neuronal death (Kwak *et al.*, 2010).

Dysregulation of intracellular calcium has detrimental effects for neurons such as mitochondrial dysfunction from calcium accumulation and increase of harmful free radicals (Turner *et al.*, 2013a, Spalloni *et al.*, 2019). As previously mentioned, research has shown that motor neurons in MND have altered expression of glutamate receptors containing the GluR2 subunit that may influence their calcium permeability and result in excitotoxic events, leading to neurodegeneration (Blizzard *et al.*, 2015). MND-associated gene mutations have been shown to increase the vulnerability of motor neurons to excitotoxic events with mutant SOD1 influencing glutamate uptake (Hayashi *et al.*, 2016, Trotti *et al.*, 1999). Due to the involvement of excitotoxicity in neurodegeneration, Riluzole, a glutamate antagonist, is used as a therapy for MND to reduce glutamate-induced excitotoxicity and reduce the progression of neurodegeneration (Lacomblez *et al.*, 1996). This is further discussed in section 1.2.5.1.

1.1.7.3 Impaired Proteostasis

Protein homeostasis (proteostasis) is a vital aspect of maintaining healthy cell function. Molecular chaperones, including heat shock proteins, maintain proteostasis through detection and control of misfolded proteins by refolding or through removal (Hartl *et al.*, 2011, Balchin *et al.*, 2016).

MND-causing pathogenic variants including SOD1 and TDP-43 discussed above, impair proteostasis within motor neurons and is thought to be one of the main processes involved in neurodegeneration (Ruegsegger and Saxena, 2016, Hipp *et al.*, 2014). Misfolded protein accumulation can lead to impaired proteostasis through multiple pathways. The Ubiquitin Proteasome System (UPS) is involved in degradation of misfolded protein to avoid toxic accumulation. However, impairment of this system may result in neuronal death. Farrarwell *et al.* (2018) used a mutant SOD1 cell model to investigate any alteration of ubiquitin homeostasis within the cells expressing MND-associated genes. Overexpression of mutant SOD1 resulted in the sequestration of free ubiquitin to the mutant SOD1 aggregates. Furthermore, altered ubiquitin homeostasis within the SOD1 aggregates resulted in altered mitochondrial morphology and dysfunction. This promotes the potential of MND-associated genes that form protein aggregates, such as mutant SOD1 and TDP-43, to cause neurodegeneration through dysfunctional ubiquitin homeostasis.

The unfolded protein response (UPR) system may also be impaired in MND. The UPR is initiated through proteins from the ER, regulating degradation of misfolded proteins to maintain ER homeostasis (Hetz *et al.*, 2015). In normal cells, misfolded proteins will induce the UPR, resulting in refolding or removal of these proteins. If these misfolded proteins overwhelm the UPR, it results in ER-stress and induction of cell death. In MND, misfolded proteins such as mutant SOD1, alter ER homeostasis, requiring the UPR to remove or refold the proteins. Similarly, when ER homeostasis cannot be maintained, ER-stress occurs leading to neuronal cell death (Shore *et al.*, 2011; as reviewed by Ruegsegger and Saxena, 2016). Saturation of chaperone proteins such as heat shock proteins from misfolded protein accumulation further increases protein accumulation, eventually resulting in neuronal death (Carra *et al.*, 2012).

1.1.7.4 Axonal Transport

Transport of material, such as neurofilaments and membrane-bound organelles, between the cell body and axonal terminal along the axon is vital for neuronal function. Axonal transport disruption can result in neuronal apoptosis (Morfini *et al.*, 2009, Taylor *et al.*, 2016). Axonal transport defects may originate from mutations of motor proteins, accumulation of axonal filaments causing axonal strangulation or from mitochondrial dysfunction resulting in lower energy production in the neuron (Brady and Morfini, 2017). Regardless of aetiology, axonal transport defects contribute to motor neuron degeneration in MND.

Gene mutations in motor proteins influence axonal transport and have been demonstrated to effect neurodegeneration (Araki *et al.*, 2014, Ikenaka *et al.*, 2013). Point mutations in *DCTN1* encoding dynactin subunit 1 is one axonal transport-affecting mutation associated with MND, identified in both sALS and fALS (Araki *et al.*, 2014, Brown and Al-Chalabi, 2017). Dynactin is a biochemical regulator of the motor protein dynein, vital for retrograde transport of organelles to maintain neuronal health. Thus, dynactin mutations affect the function of dynein, inhibiting retrograde transport, and resulting in neurodegeneration observed in MND. Similarly, Ikenaka *et al.*, (2013) observed inhibited axonal transport and subsequent neurodegeneration from knockdown of dynein-dynactin in motor neurons in a *Caenorhabditis elegans* model.

Neurofilament light (NF-L) protein mutations result in impaired axonal transport due to accumulation of neurofilaments from overexpression of neurofilament heavy (NF-H) and neurofilament medium (NF-M) (Gaiani *et al.*, 2017). Research with a transgenic mouse model expressing human mutant *SOD1*, discussed in section 1.3.2, has demonstrated the effects of neurofilament accumulation on slow axonal transport, early in the disease process (Bilsland *et al.*, 2010). Prior to motor neuron degeneration, neurofilaments accumulate and impair axonal transport, which depletes the motor axons and synapses of important nutrients and materials necessary for cell survival, including oxygen and mitochondria (Millecamps and Julien, 2013).

1.1.7.5 TDP-43 Pathology and its Role in Neurodegeneration

Only 5% of familial MND can be explained by direct TDP-43 mutations (Neumann *et al.*, 2006). TDP-43 pathology, observed as cytoplasmic TDP-43 aggregation, is present in both familial and sporadic MND (Cairns *et al.*, 2007). With the exception of those with fALS caused by *SOD1* mutations, 95% of people with MND have cytoplasmic inclusions containing TDP-43. In healthy cells, TDP-43 is localised with the nucleus of the neuron (Mackenzie *et al.*, 2007). However, in neurons and some glial cells of people with MND, TDP-43 inclusions are present within the cytoplasm. Cytoplasmic TDP-43 inclusions have been implicated as a major player in the initiation and progression of neurodegeneration (Gao *et al.*, 2018, Afroz *et al.*, 2019). These aggregates undergo post-translational modifications including phosphorylation and ubiquitylation, which are not observed in healthy brain tissues. Currently, it is unclear whether phosphorylation of TDP-43 occurs early in the disease process or after the formation of the cytoplasmic aggregates. However, due to the presence of phosphorylated but not ubiquitinated TDP-43 inclusions, it is proposed that phosphorylation occurs prior to ubiquitination (Neumann *et al.*, 2006, Dong and Chen, 2018). Although the protein is ubiquitinated, failure of the UPS to degrade these proteins results in formation of ubiquitinated TDP-43 inclusions (Dong and Chen, 2018, Scotter *et al.*, 2014).

One hypothesis for neurodegeneration from TDP-43 is a loss of function of nuclear TDP-43. DNA damage and impaired DNA repair system has been proposed as a cause of neurodegeneration resulting in loss of nuclear TDP-43 (Mitra *et al.*, 2019). In neuronal SH-

SY5Y cells with an inducible TDP-43 depletion system, an increase in unrepaired DNA double-strand breaks correlated with the level of TDP-43 depletion in a dose-dependent manner and was independent of cytoplasmic aggregations (Mitra *et al.*, 2019). Similarly, changes in expression of genes related to DNA damage has been observed in pathology-affected neurons from neocortex brain tissue from MND patients and associated with loss of nuclear TDP-43 (Liu *et al.*, 2019). Loss of nuclear TDP-43 has been suggested to cause neurodegeneration by altering RNA processing as determined by altered patterns of gene splicing in shRNA-mediated TDP-43 knock-down in NSC34 cells (Highley *et al.*, 2014). Furthermore, functional TDP-43 within the nucleus is vital for splicing of stathmin-2 (STMN2), an important regulator of axonal health. Pathological TDP-43 results in cryptic splicing of STMN2, producing non-functional STMN2 RNA and increases axonal degeneration (Spence *et al.*, 2024, Klim *et al.*, 2019). A similar mechanism has also been shown for UNC13A, where loss of neuronal TDP-43 through CRISPR inhibition in human induced pluripotent stem cell (iPSC)-derived motor neurons caused inclusion of a cryptic exon in *UNC13A* and caused a reduction in synaptic transmission (Brown *et al.*, 2022, Ma *et al.*, 2022).

In addition to loss of function TDP-43-associated neurodegeneration, a gain of toxicity from the cytoplasmic TDP-43 inclusions may also induce neurodegeneration. Barmada *et al.* (2010) used rat primary cortical neurons transfected with constructs encoding human ALS-linked mutant TDP-43 or wild-type TDP-43, to identify the effects of TDP-43 nuclear clearance and cytoplasmic aggregation on neuronal death. Transfection of mutant TDP-43 increased the presence of cytoplasmic TDP-43 aggregates compared to the wild-type TDP-43 transfected cells and the level of cytoplasmic TDP-43 was an accurate predictor of cell death, indicating gain-of-function toxicity (Barmada *et al.*, 2010, Gao *et al.*, 2018).

Gain-of-function toxicity from cytoplasmic TDP-43 occurs through both the disruption of protein synthesis and transport (Bjork *et al.*, 2022) and mitochondrial dysfunction (Gao *et al.*, 2019). Aberrant TDP-43 accumulation within the cytoplasm results in the formation of stress granules and ribonucleoprotein complexes and reduces protein synthesis within the axon and synapse (Narayanan *et al.*, 2013, Colombrita *et al.*, 2009). These translation deficits influence synaptic function and reduce the integrity of the neuromuscular junction, resulting in muscular atrophy. In human induced pluripotent stem cell (iPSC)-derived motor neurons,

clearance of the axonal accumulation of TDP-43 restored the function of the neuromuscular junctions (Altman *et al.*, 2021).

A gain of function toxicity from cytoplasmic TDP-43 can also influence mitochondrial function. Using transgenic mice expressing wild-type human TDP-43 (hTDP-43) under a mouse prion promoter, Xu *et al.* (2010) identified aberrant mitochondrial aggregation and dysfunctional mitochondrial mechanics from TDP-43 overexpression in the cytoplasm. Similarly, TDP-43 was found to be aggregated within mitochondria isolated from spinal cord and cortex neurons in MND patients (Wang *et al.*, 2016). In HEK-293 cells overexpressing wild-type or mutant TDP-43, TDP-43 localised within the mitochondria and disrupted mitochondrial function determined through increased mitochondrial fragmentation and reduced ATP levels (Wang *et al.*, 2016). Blocking TDP-43 localisation via genetic ablation of the mitochondrial localisation sequence, reduced TDP-43 localisation to the mitochondria and reduced the neuronal loss and mitochondrial fragmentation compared mutant TDP-43.

The combined effects of both loss of nuclear TDP-43 and the gain of toxic cytoplasmic TDP-43 aggregates should not be ruled out as the cause of TDP-43-related neurodegeneration. Knockdown of endogenous TDP-43 by siRNA in murine spinal cord x neuroblastoma hybrid cell line (NSC-34) was used to measure cell viability in the absence of cytoplasmic TDP-43 aggregates. Neuronal toxicity was indicated by both a significant reduction in cell viability and an increase of caspase-3 activity was found, suggestive that loss-of-function toxicity can occur without the need for TDP-43 aggregation. However, a similar result was found when TDP-43 inclusion bodies were intracellularly delivered via a plasmid expressing human TDP-43 into the NSC-34 cell line to mimic cytoplasmic aggregation. The relative contributions of loss-of-function and gain-of-function toxicity were calculated and determined to equally contribute to neuronal toxicity (Casella *et al.*, 2016).

TDP-43 is also proposed to be involved neurodegeneration through inflammation. The TDP-43 promoter contains binding sites for Interferon regulatory factor 1 (IRF3), IRF3 and nuclear factor kappa-light-chain-enhancer of activated B cells (NF- κ B) (Douville *et al.*, 2011). Swarup *et al.* (2011) identified TDP-43 dependent increases in NF- κ B from immunoprecipitation experiments in MND spinal cord samples. They also demonstrated the toxicity of TDP-43

overexpression through transfection of mutant TDP-43 within a SH-SY5Y cell line activating the immune response. Further *in vivo* experiments using TDP-43 transgenic mice demonstrated a reduction in MND-related motor deficits from administration of an NF- κ B inhibitor (Swarup *et al.*, 2011). This promotes the role of neuroinflammation-mediated neurodegeneration from TDP-43. It has also been suggested TDP-43 proteinopathy is involved in neurodegeneration through endogenous retroviruses (ERVs), involving a feedback loop between ERV transcription, TDP-43 cytoplasmic accumulation, DNA damage and inflammation (Chang and Dubnau, 2019). This is further discussed further in section 1.1.7.7.

1.1.7.6 Mitochondrial Dysfunction

Mitochondrial dysfunction is typically seen in MND and has been proposed as a cause of neurodegeneration (Bozzo *et al.*, 2017). This dysfunction is primarily related to oxidative stress through unregulated production of reactive oxygen species (ROS) and loss of energy to the neuron (Bhat *et al.*, 2015). There is a proposed positive feedback loop between the production of ROS and mitochondrial dysfunction, with an increase in ROS causing further mitochondrial damage and mitochondrial damage resulting in an increase in ROS, eventually resulting in apoptosis (Ježek *et al.*, 2018). Protein aggregates are thought to be a driving factor in the initial cause of mitochondrial dysfunction (Carrì *et al.*, 2017). Intracellular adenosine triphosphate (ATP) levels have been found to be significantly reduced in lymphocytes from MND patients (Ghiasi *et al.*, 2012). Similarly, reduced neuronal ATP production has been shown in iPSC motor neurons from MND patients compared to controls (Hor *et al.*, 2021).

Alterations to mitochondrial function is seen in both familial and sporadic cases of MND (Carrì *et al.*, 2017). However, some altered function has been linked to specific familial mutations, such as *SOD1* (Tafari *et al.*, 2015, Pickles *et al.*, 2016). Mutant *SOD1* has been shown to impair mitochondrial activity through the binding of BCL2, an antiapoptotic protein and through *SOD1* protein aggregation leading to oxidative stress (Tan *et al.*, 2014). Similarly, TDP-43 aggregation also influences mitochondrial function by localising within mitochondria and reducing ATP production and inducing mitochondrial fragmentation, perturbing functional mitochondrial networks (Wang *et al.*, 2013, Wang *et al.*, 2016, Shah *et al.*, 2019). Mouse models of TDP-43 and *SOD1* both show impaired mitochondrial morphologies (Gurney *et al.*, 1994, Xu *et al.*, 2010). Morphologic changes such as mitochondrial swelling and

mislocalisation have also been observed in post-mortem spinal cord tissue from MND patients using electron microscopy (Sasaki and Iwata, 2007, Smith *et al.*, 2019).

With a high number of mitochondria at the neuromuscular junction (NMJ), mitochondrial dysfunction is thought to begin at the NMJ and provides support for the dying back hypothesis of neurodegeneration (Shi *et al.*, 2010, Chung *et al.*, 2017). Targeting mitochondrial function, such as increasing mitochondrial biogenesis through pharmaceutical modulation of biogenesis signalling pathways, could provide therapeutic benefits in MND by increasing the number of functioning neuronal mitochondria (Golpich *et al.*, 2017, Uittenbogaard and Chiaramello, 2014).

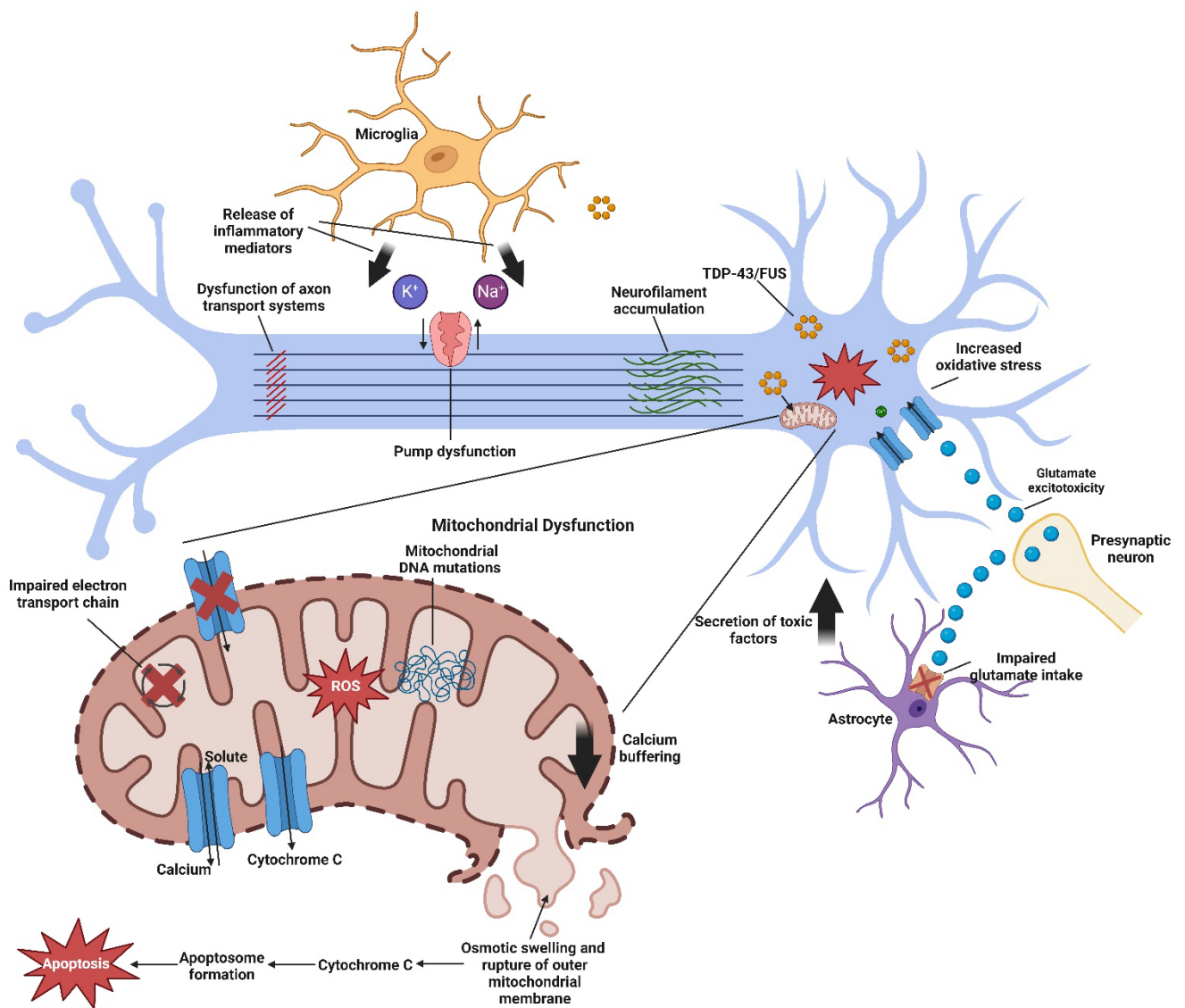


Figure 1.2 Proposed mechanisms of motor neuron degeneration in MND

Neurodegeneration in MND may be caused by one or multiple mechanisms including axonal transport deficits, non-neuronal cell involvement including microglia and astrocytes, excitotoxicity, protein aggregation from TDP-43, FUS and SOD1, mitochondrial dysfunction and oxidative stress. Figure adapted from Turner *et al.* (2013). Figure made in BioRender.

1.1.7.7 *The Role of Neuroinflammation in Neurodegeneration*

The impact of inflammation has been well established in MND with dysregulation of inflammatory cytokines in MND patients, involvement of astrocytes and microglia, and T lymphocyte infiltration into the CNS linked to MND disease progression (Appel *et al.*, 2021). Animal models of MND including *SOD1*, *C9orf72* and *TARDBP* also have dysregulated inflammatory processes, as seen in human ALS (Sheean *et al.*, 2018, Rudnick *et al.*, 2017, Beers and Appel, 2019). Transgenic mice with a loss of function *C9orf72* mutation had increased inflammatory cytokine expression within plasma and reduced survival rates compared to wild-type controls (Burberry *et al.*, 2016). Furthermore, a TDP-43^{Q331K} mouse model was used to investigate the inflammatory processes with the transgenic TDP-43 mice showing increased microglial activation that correlated with motor deficits and subsequent increased progression of neurodegeneration compared to WT mice (Lee *et al.*, 2018).

Modulation of the inflammatory processes evident in these animal models has provided evidence for slowing motor neuron degeneration and extending animal survival. For instance, cytotoxic CD8 T cells infiltrate the CNS selectively destroying motor neurons in mutant *SOD1*^{G93A} mice and increase the expression of interferon- γ (IFN- γ) (Coque *et al.*, 2019). Removal of this cell population via genetic ablation results in a slowing of this selective motor neuron degeneration. Whilst the role of the immune system has been explored in the more common forms of inherited ALS, less frequent mutations in *OPTN*, *SQSTM1*, *VCP* and *TBK1* are also associated with inflammation (Beers and Appel, 2019, Yu and Cleveland, 2018). In addition, patients with sporadic MND exhibit an activated immune phenotype including changes in cytokine concentrations including tumour necrosis factor – alpha (TNF- α), and interleukins (IL), IL-1 β , IL-4, IL-6 and IL-10 in serum (Jin *et al.*, 2020, Sun *et al.*, 2021, Huang *et al.*, 2020). Other inflammatory markers that can be detected within CSF, serum or urine of MND patients include monocyte chemoattractant protein 1 (MCP-1), C-reactive protein (CRP), neopterin and C-X-C motif chemokine ligand 10 (CXCL10) (Gille *et al.*, 2019, Huang *et al.*, 2020, Shepherd *et al.*, 2022, Tateishi *et al.*, 2010). MCP-1 has also been found to be present within activated microglia within the motor cortex of sporadic and familial MND patients with co-localisation of MCP-1+ activated microglia and degenerating Betz cells within the cortex (Jara *et al.*, 2017).

1.1.7.7.1 Dysregulation of the cGAS/STING pathway influences immune-mediated neurodegeneration in MND

The cyclic guanosine monophosphate-adenosine monophosphate (cGAMP) synthase (cGAS) and stimulator of interferon genes (STING) pathway (cGAS/STING) pathway has been implicated in neuroinflammation-mediated neurodegeneration (Yu *et al.*, 2020a, Fryer *et al.*, 2021). cGAS detects danger signals such as double stranded DNA (dsDNA) within the cytoplasm and triggers the formation of cyclic cGAMP. cGAMP binds to STING and subsequently activates TBK1 resulting in phosphorylation of interferon regulatory factor (IRF) 3, IRF7 and release of NF- κ B from the cytoplasm. These transcription factors move to the nucleus and subsequently induce transcription of mRNA for multiple inflammatory factors such as IL-6 and TNF- α , interferons (IFNs) including IFN- α and IFN- β and released from the cell (Shu *et al.*, 2014, Decout *et al.*, 2021, Ouyang *et al.*, 2023). Translation and release of IFN- α and IFN- β from these cells can act on neighbouring cells via the IFN- α/β receptor (IFNAR) to activate the Janus-associated kinase (JAK) and signal transducer and activator of transcription (STAT) pathway and induce transcription for interferon stimulated genes (ISGs) such as CXCL10 (Taylor *et al.*, 2018).

Under normal physiological conditions, the cGAS/STING pathway is neuroprotective and produces an immune response to clear unwanted pathogens and prevent cell death (Fryer *et al.*, 2021). However, aberrant activation of this pathway has been linked to neurodegeneration, where increased IFN production results in faster disease progression (Hofer and Campbell, 2013, Paul *et al.*, 2021). MND mouse models have been used to investigate the role of cGAS/STING in neurodegeneration. In *C9orf72*^{-/-} mice, there is an upregulation of Type 1 IFNs resulting in systemic CNS inflammation due to increased cGAS-STING pathway signalling (McCauley *et al.*, 2020). Through *STING*^{-/-} in a neurodegenerative disease model, Nazmi *et al.* (2019) proposed a STING-dependent toxic increase in IFNs, resulting in neurodegeneration through microglial phenotype modulation. Furthermore, a recent investigation has demonstrated that TDP-43 cytoplasmic mislocalisation results in mitochondrial DNA release that also activates the cGAS/STING pathway, resulting in the upregulation of NF- κ B and IFN pathways (Yu *et al.*, 2020a). In contrast, inhibition of STING using a validated STING inhibitor, H-151 (Haag *et al.*, 2018) in MND patient derived iPSCs and

a TDP-43 mouse model normalises IFN levels, resulting in reduced neuronal loss and improved motor performance in mice (Yu *et al.*, 2020a). Furthermore, manganese has been shown to directly bind to cGAS, increasing its sensitivity to dsDNA (Wang *et al.*, 2018, Sun *et al.*, 2023). As described in section 1.1.6.2.2, MND patients have significantly higher levels of manganese within CSF compared to healthy controls (Roos *et al.*, 2012, Peters *et al.*, 2016). Thus, the neuronal accumulation of manganese in MND patients and its ability to drive the cGAS/STING pathway may suggest a role of metals such as manganese influencing inflammatory pathways in MND.

To further outline the role of the immune response in neurodegeneration, TBK1 mutations causing disease through haploinsufficiency have also been linked to MND in a small number of familial MND cases (Cirulli *et al.*, 2015, Freischmidt *et al.*, 2015). TBK1 is involved in the cGAS/STING pathway and induces IFNs whilst also being involved in autophagy mechanisms (Ahmad *et al.*, 2016). The dysregulation of TBK1 could be contributing to neurodegeneration through disrupted autophagy resulting in aberrant protein aggregation or through increased neuroinflammation from activation of the inflammatory pathways involving TBK1 (Oakes *et al.*, 2017).

1.1.7.7.2 Non-neuronal cells and release of pro-inflammatory cytokines in MND

Neuroinflammation in MND includes the activation of microglia and the polarisation of microglia into two different phenotypes, either pro-inflammatory, M1, or anti-inflammatory, M2 (Beers and Appel, 2019). Activated microglia that produce a neuroprotective response with production of anti-inflammatory cytokines, such as IL-4 and IL-10, are referred to as M2 microglia (Cherry *et al.*, 2014, Puentes *et al.*, 2016). As indicated by mouse models of MND, further into MND disease progression, microglia become activated into the M1 phenotype with neurotoxic properties, releasing pro-inflammatory cytokines including IL-1 β , TNF- α , IL-6 and IL-18 (Geloso *et al.*, 2017, Clarke and Patani, 2020). In MND, levels of pro-inflammatory cytokines including TNF- α and IL-6 are increased in blood and CSF from MND patients compared to healthy controls as disease progresses (Tortarolo *et al.*, 2017, Ono *et al.*, 2001, Garbuzova-Davis *et al.*, 2018). TNF- α also mediates the activation of NF- κ B which has

apoptotic and neurotoxic properties, with increased activation of the NF- κ B signalling pathway in ALS, driving further inflammatory cytokine release (Appel *et al.*, 2021, Frakes *et al.*, 2014). TDP-43 and SOD1 aggregates within microglia are likely to induce a pro-inflammatory M1 phenotype due to increased NF- κ B signalling pathways and NLRP3 inflammasome (Zhao *et al.*, 2015, Hunter *et al.*, 2021). Furthermore, the formation of the NLRP3 inflammasome within microglia produces IL-18 and IL-1 β and induces microglia pyroptosis, exacerbating the pro-inflammatory M1 state (Wu *et al.*, 2022).

Astrocyte-mediated neurotoxicity has been proposed to be caused by protein aggregation such as mutant SOD1 and TDP-43 (Nagai *et al.*, 2007, Tong *et al.*, 2013). Furthermore, astrocytes may contribute to neurodegeneration through alteration of secreted factors (Vaz *et al.*, 2021). In healthy function, astrocytes provide the surrounding motor neurons with neurotrophic factors such as brain derived neurotrophic factor (BDNF) (Brigadski and Leßmann, 2020). In MND, astrocytes release toxic factors such as nitric oxide, transforming growth factor β 1 (TGF- β 1) and pro-inflammatory cytokines to the surrounding motor neurons and microglia (Endo *et al.*, 2016, Tripathi *et al.*, 2017). Overexpression of astrocyte-derived TGF- β 1 in SOD1^{G93A} mice was shown to reduce the neuroprotective state of microglia and resulted in faster disease progression (Endo *et al.*, 2015). Moreover, a rat astrocyte cell line treated with CSF from MND patients showed impaired regulation of nitric oxide and release of pro-inflammatory cytokines, IL-6 and TNF- α compared to control CSF and reduced release of neurotrophic factors (Mishra *et al.*, 2016). In the pro-inflammatory state, T-helper type 1 cells also release IFN- γ which can further activate IRF-1, NF- κ B and CXCL10 (Malaspina *et al.*, 2015, Ottum *et al.*, 2015).

In conclusion, while the exact mechanism of neuroinflammation-mediated neurodegeneration remains unknown, it is proposed to occur through a perpetual cycle of motor neuron death and sustained microglia and astrocyte activation with neurotoxic pro-inflammatory cytokine increases. Cell-to-cell spread of toxicity occurs between non-neuronal cells and surrounding motor neurons to propagate neurodegeneration (Lee and Kim, 2015, Polymenidou and Cleveland, 2011). An example of this cell-to-cell spread to propagate neurodegeneration involves astrocytic release of saturated lipoproteins, apolipoprotein E (APOE) and apolipoprotein J (APOJ). The release of APOE and APOJ, along with pro-

inflammatory cytokines, from neurotoxic reactive astrocytes causes neuronal death in surrounding motor neurons (Guttenplan *et al.*, 2021).

Use of anti-inflammatories has been used to target neuroinflammation-mediated neurodegeneration *in vitro* including Tocilizumab, an IL-6 receptor antagonist (Mizwicki *et al.*, 2012) and lenalidomide and thalidomide, a TNF- α antagonist (Kiaei *et al.*, 2006, Liu and Wang, 2017). However, a phase II clinical trial of thalidomide in MND patients did not show any differences in disease progression according to the ALS functional Rating Scale Revised (ALSFRS-R), compared to historical controls, and no significant changes in serum levels of TNF- α were determined (Stommel *et al.*, 2009). A phase II clinical trial of an immune regulator, NPO01, identified slower progression of MND in patients with higher C-reactive protein levels at baseline but failed to reach significance in the whole cohort (Miller *et al.*, 2015). Targeting other players involved in neuroinflammation such as the cGAS/STING pathway has been proposed as another potential therapeutic avenue for ALS, with STING inhibitors already in development (Van Damme and Robberecht, 2021).

1.2 Disease Characteristics: From Diagnosis to Treatment

1.2.1 Diagnosis

The average time between reported symptom onset and diagnosis is approximately one year. Diagnosis of MND uses the revised El Escorial World Federation of Neurology criteria (Agosta *et al.*, 2015, Rutter-Locher *et al.*, 2016). This diagnosis criteria relies on several assessments to identify MND-related symptoms, including electrophysiological measures, ruling out other potential causes (Paganoni *et al.*, 2014). The heterogeneity in presentation of MND negatively impacts the diagnostic delay (van Es *et al.*, 2017). Time from symptom onset to diagnosis is influenced by gender and site of onset with both fALS and bulbar onset associated with shorter time to diagnosis (Paganoni *et al.*, 2014). However, due to the large number of diagnostic tests required for MND to rule out potential mimic syndromes, misdiagnosis of MND is low (Williams, 2013).

Diagnostic biomarkers of MND have been investigated to reduce time between onset and diagnosis. However, while some biomarkers have diagnostic value, discussed below, there are no biomarkers that can be used as a standalone diagnostic tool. At present, the lack of effective treatment means research into diagnostic markers of MND is not a priority.

1.2.2 Progression of MND

Currently, progression of MND is reliant on the revised ALS Functional Rating Score (ALSFRS-R) (Kaufmann *et al.*, 2005). This is a questionnaire-based score between 0 (no function) and 48 (normal function), that records activity of daily living. It is powerful over time, but subjective. Disease progression can also be monitored by magnetic resonance imaging and assessment of motor function and respiratory function (Chipika *et al.*, 2019). ALSFRS-R is measured monthly from symptom onset and is used in clinical trials to measure progression. MND progresses at a rapid rate with many factors associated with faster or slower disease progression.

1.2.3 Prognostic Factors Associated with MND

There are factors that may influence the prognosis of MND such as demographic factors, clinical factors and cognitive factors (Creemers *et al.*, 2015). At present, being male and having bulbar onset of MND signifies a shorter disease duration to death, and thus, poor prognosis (Moura *et al.*, 2015, Turner *et al.*, 2013b). Wolf *et al.* (2015) identified an association between gender and disease course outcome, with males showing poorer prognosis than females. However, contrary to this, other population-based studies found no significant difference in disease outcome between genders indicating ineffectiveness of sex as an appropriate prognostic factor (Calvo *et al.*, 2017, Mandrioli *et al.*, 2018). The anatomical site of onset can also largely impact prognosis. Bulbar onset occurs in 15-20% of MND patients and results in poorer prognosis than those with spinal onset, with a life expectancy of less than 2 years post diagnosis (Turner *et al.*, 2013a, Moura *et al.*, 2015). This effect has been consistently reported (Dorst *et al.*, 2019, Calvo *et al.*, 2017, Stevic *et al.*, 2016). Cognitive function is also considered a prognostic factor for MND with poor cognitive function and comorbid frontotemporal syndrome associated with shorter survival, with a life expectancy of 2.5 years post diagnosis (Govaarts *et al.*, 2016, Hardiman *et al.*, 2017a, Ratti *et al.*, 2016).

Various environmental factors, some described previously, have been shown to influence prognosis as well as risk of development. While exposure to metals and pesticides have been shown to increase the risk of development, higher levels within serum and plasma of MND patients have also been shown to correlate with poor survival (Goutman *et al.*, 2019, Oggiano *et al.*, 2018). Similarly, lifestyle factors can also affect prognosis. Dietary factors such as vitamin intake have been proposed to influence the prognosis of MND, with levels of vitamin E and D positively correlated with life expectancy (Camu *et al.*, 2014). However, there are inconsistent results of vitamin E and D associated with MND progression (Blasco *et al.*, 2017, Libonati *et al.*, 2017, Paganoni *et al.*, 2017). Pre-diagnostic BMI has prognostic value, with both low BMI (below 24kg/m²) and a high BMI (above 35kg/m²) correlated with shorter life expectancy (Calvo *et al.*, 2017, Paganoni *et al.*, 2011).

1.2.4 Biomarkers of MND

Biomarkers are important for the classification of diseases, determination of disease course and for the determination of effective treatments via clinical trials (Biomarkers Definitions Working Group, 2001). Biomarkers can be further categorised into progression markers, prognostic markers, pharmacodynamic markers and diagnostic markers. Currently investigated biomarkers for MND include p75^{ECD}, TDP-43, uric acid, neurofilament heavy (NfH) and light (NfL) chain, neuroimaging and electrophysiological measures. Due to conflicting results and limited studies, further research is required prior to use of TDP-43, NfH and NfL, uric acid and electrophysiological markers as standalone biomarkers for MND (Vu and Bowser, 2017, Vucic and Rutkove, 2018, Benatar *et al.*, 2016). Both p75^{ECD} and TDP-43 will be discussed further due to their use in the current project.

1.2.4.1 p75 Extracellular Domain as a Prognostic, Progression and Pharmacodynamic Biomarker of MND

Neurotrophins are growth factor proteins that are involved in nervous system development and function. They bind to two types of receptors, tyrosine kinase receptors (Trk) and pan-neurotrophin receptor (p75) (Meeker and Williams, 2015). Trk consists of three receptors, TrkA, activated by nerve growth factor (NGF), TrkB, activated by brain-derived neurotrophic

factor (BDNF) and TrkC, activated by neurotrophins 3 and 4 (NT3 and NT4). In contrast, p75 neurotrophin receptor can bind all neurotrophins, NGF, BDNF and NT3/4/5 (Bothwell, 2016). The binding of these neurotrophins to Trk promotes cell survival and proliferation. However, binding of neurotrophins to p75 in motor neurons without co-expression of Trk receptors results in cell death. (Bothwell, 2016, Meeker and Williams, 2015). The p75 receptor, involved in promoting cell death, is expressed on motor neurons twice throughout life. Upregulation of p75 is first observed during embryonic development through synaptic pruning in motor neurons (Singh *et al.*, 2008, Je *et al.*, 2013). After embryonic development, p75 expression is down regulated and is only re-expressed after neuronal injury, including MND onset. Increased p75 expression after neuronal injury has been shown in many studies. Volosin *et al.* (2008) identified seizure-induced hippocampal expression of p75, and Rostami *et al.* (2014) identified increased p75 expression after traumatic brain injury in mice, via *in situ* hybridization. Importantly, p75 is re-expressed on spinal motor neurons (Copray *et al.*, 2003) and Schwann cells (Ahmad *et al.*, 2015) in MND. Apoptotic motor neurons from SOD1^{G93A} mice also express p75 (Smith *et al.*, 2015).

In embryonic development and after injury (including in MND), neurotrophins and pro-neurotrophins bind to the available p75 receptors. These bound ligands promote the recruitment of adaptor proteins to stimulate apoptotic pathways, such as the activation of c-Jun N-terminal kinase (JNK). Through tumour necrosis factor alpha converting enzyme (TACE), p75 undergoes proteolysis resulting in the cleavage of the intracellular domain (ICD) by γ -secretase and the release of the extracellular domain. The unbound ICD binds with NRIF, T6 and a DNA-binding protein, which promotes NRIF ubiquitination and allows NRIF translocation into the nucleus to initiate the apoptosis process. The extracellular domain (50kDa) is cleaved from the membrane (Pathak and Carter, 2017).

An early study showed that p75^{ECD} appeared in rat urine after a sciatic nerve injury (DiStefano and Johnson, 1988). Our group has since identified p75^{ECD} in the SOD1^{G93A} mice model and in humans living with MND (Shepherd *et al.*, 2014). Hence, p75^{ECD} is proposed to be transported from injured nerves and Schwann cells to the CSF and blood and eventually secreted in urine. This finding led to the identification of p75^{ECD} as a potential urinary

biomarker for MND that can provide additional value to the current clinical criterion (Gold *et al.*, 2019, Shepherd *et al.*, 2017).

With the ALSFRS-R being the only current way to determine disease progression, a biomarker with progression value is of vital importance for MND research. Shepherd *et al.* (2017) identified a positive correlation between p75^{ECD} levels within urine of MND patients, as measured by Enzyme-linked Immunosorbent Assay (ELISA), and ALSFRS-R score, indicating that levels of p75^{ECD} increase with decline in motor function. Notably, the levels of p75^{ECD} in urine increased at a measurable rate of 0.19 ng/mg per month over disease progression (Shepherd *et al.*, 2017). This was the first time a fluid-based biomarker has been described to increase at a measurable rate over disease progression in MND and was confirmed in a follow up study (Shepherd *et al.*, 2022).

Shepherd *et al.* (2017) also showed that baseline levels of urinary p75^{ECD} are a predictor of survival. Patients with MND that had higher levels of p75^{ECD} above the median level had decreased survival time than those with baseline p75^{ECD} levels below the median. This finding suggests that levels of p75^{ECD} within urine has prognostic value (Shepherd *et al.*, 2017). Since urinary p75^{ECD} is a progression marker, it may also be pharmacodynamic (Benatar *et al.*, 2016). Investigating the use of p75^{ECD} levels in a clinical trial may indicate treatment efficacy. Therapeutic interventions that are efficient in reducing or stabilising the levels of urinary p75^{ECD} (as described in Gold *et al.*, 2019) could suggest effective MND treatments.

1.2.4.2 TDP-43 as a Biomarker of Disease Progression

As outlined earlier in section 1.1.5.3, cytoplasmic TDP-43 aggregation occurs in MND. This accumulation of TDP-43 has been proposed to be a biomarker of disease progression and may also have prognostic value. The presence of TDP-43 has also been suggested to aid in the diagnosis of MND, as it is present in 97% of all MND cases (Majumder *et al.*, 2018). The aggregation of phosphorylated TDP-43 occurs in stages in MND, first occurring in motor cortex and spinal cord and in later stages occurring in other cortices including the frontal and temporal cortex (Brettschneider *et al.*, 2013). This finding suggests phosphorylated TDP-43 may have value as a progression biomarker of the disease. However, these stages and evident

increases in pTDP-43 with disease progression is not as evident within biofluids of MND patients as it is in post-mortem tissue (Feneberg *et al.*, 2018), making it difficult to use as a diagnostic or progression biomarker.

While some studies have identified an increase in the levels of TDP-43 from CSF from MND patients compared to healthy controls (Bourbouli *et al.*, 2017, Noto *et al.*, 2011), increases in the level of TDP-43 as the disease progresses were not found. This reduces the value of TDP-43 as biomarker of disease progression. Moreover, regular collection of CSF for monitoring disease progression is not ideal compared to collection of a less invasive biofluid such as urine. Regardless of the increase observed in MND patients compared to healthy controls, TDP-43 could not be used as a diagnostic biomarker for MND due to the presence of TDP-43 proteinopathy in other neurological disorders such as Alzheimer's disease (McAleese *et al.*, 2017, Chang *et al.*, 2016). While TDP-43 pathology is a hallmark of MND and observable in post-mortem tissue, it has not yet been established as a prognostic or progression biomarker for MND. However, further research with advances in TDP-43 detection and further understanding of the pathophysiology of TDP-43 may result in its use as a biomarker for the disease in the future.

1.2.5 Current Treatments and Therapy

1.2.5.1 *Pharmaceutical Treatment for MND*

There is no cure for MND and only four approved pharmaceutical treatments, Riluzole, Edaravone, Relyvrio and Qualsody, discussed below.

1.2.5.1.1 Riluzole

The first approved pharmaceutical treatment is Riluzole, a glutamate antagonist that reduces calcium-mediated toxic events leading to motor neuronal damage (Doble, 1996 as reviewed by Viswanad *et al.*, 2017). Original clinical trials of Riluzole indicated it increases survival by 2-3 months (Miller *et al.*, 1996, Bensimon *et al.*, 1994, Lacomblez *et al.*, 1996), with more recent data suggesting an increase of survival between 6-19 months (Thakore *et al.*, 2022).

1.2.5.1.2 Edaravone

The second pharmaceutical treatment, Edaravone, is an antioxidant which could reduce the progression of motor neurons through the removal of reactive oxygen species (Ikeda and Iwasaki, 2015, Watanabe *et al.*, 2018). However, Edaravone is only effective in a small subset of MND patients (5%) with fast disease progression and life expectancy is only increased by 2-3 months (Yoshino and Kimura, 2006, Abe *et al.*, 2017).

1.2.5.1.3 Relyvrio

Relyvrio, a combination of sodium phenylbutyrate and taurursodiol, targets cellular stress involving the mitochondria and ER and reduces apoptotic mechanisms reducing neuronal death (Paganoni *et al.*, 2020). A phase II clinical trial identified a slower progression according to the ALFSRS-R and increased survival by 6 months in the treated patients (Paganoni *et al.*, 2022). A phase III clinical trial is currently ongoing to determine further clinical benefit.

1.2.5.1.4 Qualsody

Qualsody, also known as Tofersen, is a recently approved pharmaceutical therapy for MND. It is an antisense oligonucleotide therapy targeting *SOD1* mRNA and reducing levels of mutant *SOD1* protein. While only effective in those with *SOD1*-associated MND, clinical trials have shown Qualsody is effective in reducing the levels of NfL, suggesting a slower progression of neurodegeneration (Miller *et al.*, 2022)

1.2.5.2 Ventilation as Supportive Therapy for MND

Non-invasive ventilation (NIV) is a common therapy option for MND patients. As respiratory failure is the main cause of death from MND, NIV aims to increase survival by providing mechanical breathing support. Berlowitz *et al* (2016) identified a significant increase in survival for those with NIV treatment compared to non-treated patients. This effect was observed regardless of age and gender. However, for NIV to provide patient benefit, adequate ventilation is required to reduce upper airway obstruction (Georges *et al.*, 2016, Schellhas *et*

al., 2018). NIV does not slow the progression of the disease but it has shown to increase quality of life (Vandoorne *et al.*, 2016).

1.2.5.3 Need for Further Treatment Development

While the treatments discussed above, and outlined in **Table 1.2**, provide short-term benefits, there is a lack of treatments that provide any long-term benefits such as a significant increase in survival. With a fast-progressing disease such as MND, a treatment that could reduce the progression of neurodegeneration should be investigated. Determining causative factors of neurodegeneration is vital for the discovery and effectiveness of further treatment options. Discussed further in section 1.4.6, anti-retroviral therapy is being investigated as a treatment for MND based on the association with human endogenous retroviruses (HERVs) (Gold *et al.*, 2019).

Table 1.2 Summary of treatments and therapies for MND and their mechanism of action and benefit

TREATMENT/THERAPY	MECHANISM OF ACTION	CLINICAL AVAILABILITY	PATIENT BENEFIT	REFERENCE
Riluzole	Glutamate antagonist to reduce excitotoxicity	Available for use as MND treatment	Increased survival by 2-3 months	(Doble, 1996a, Miller <i>et al.</i> , 1996, Bensimon <i>et al.</i> , 1994, Lacomblez <i>et al.</i> , 1996)
Edaravone	Removal of free radicals	Available for use as MND treatment	Increased survival by 2-3 months	(Watanabe <i>et al.</i> , 2018, Yoshino and Kimura, 2006, Ikeda and Iwasaki, 2015)
Relyvrio	Reduces cellular stress involving mitochondria and ER	Available for use as MND therapy	Increased survival by 6 months	(Paganoni <i>et al.</i> , 2022)
Qualsody	Reduces SOD1 mRNA	Available for use as MND therapy	Slowed functional decline	(Miller <i>et al.</i> , 2022)
Ventilation	Reduce respiratory symptoms	Available for use as MND therapy	Quality of life increase	(Vandoorne <i>et al.</i> , 2016)
Triumeq	Reduce expression of endogenous retroviruses	Not yet available – ongoing Phase III clinical trial	To be determined	(Gold <i>et al.</i> , 2019)

1.3 Models of MND

1.3.1 In Vitro Models

1.3.1.1 *Induced Pluripotent Stem Cells*

Induced pluripotent stem cells (iPSCs) derived from MND patients have been used to model MND *in vitro*. Dimos *et al.* (2008) identified the ability to generate motor neurons from skin fibroblasts of MND patients and healthy controls to compare pathogenesis. Pathological differences in differentiated motor neurons were identified between the two groups with a time-dependent neuronal loss observed from MND patient iPSCs. This finding allowed for examining patient specific differences in neuropathogenesis, an ideal way of studying MND given the heterogeneity. Comparison of motor neuron pathology can also be examined between sALS patients and fALS patients, allowing for determination of mutation-specific differences in pathogenesis (Sances *et al.*, 2016). iPSCs derived from patients with specific mutations, such as TDP-43 and SOD1, develop pathologies such as neurodegeneration, as seen in post-mortem brain and spinal cord tissue from MND patients (Egawa *et al.*, 2012). Furthermore, MND patient-derived iPSCs can provide insight into TDP-43 pathologies as they contain endogenous levels of TDP-43.

1.3.2 In Vivo Models

1.3.2.1 *SOD1 Mice Models*

The first transgenic mouse model of MND was a mutant SOD1 expressing mouse (SOD1^{G93A}) and is the most commonly used mouse model of MND (Gurney *et al.*, 1994). The SOD1^{G93A} model expresses 25 copies of mutant human SOD1, with a single change of glycine to alanine at position 93. The SOD1^{G93A} mice develop pathologies that are similar to human MND. Starting at 70-90 days of age, the mice develop signs of motor deficits. This includes gait abnormalities and reduction in muscle strength. By 20 days post symptom onset, the mice have 30% remaining muscle strength and severe gait abnormalities, with total hind limb paralysis by end-stage at 130 days of age. Microscopic pathologies are evident in the lumbar region of the spinal cord, preceding motor behavioural changes. This includes loss of motor neurons, reaching a total 50% motor neuron loss at end-stage. Further microscopic pathologies include axonal degeneration, mitochondrial dysfunction and SOD1 protein

aggregation (Gurney *et al.*, 1994). This model has been used extensively in research, providing evidence of MND pathogenesis mechanisms including excitotoxicity, protein aggregation and oxidative stress (De Giorgio *et al.*, 2019). After thorough investigation of the SOD1^{G93A} mice model, particular guidelines have been determined for their use in MND treatment research. This includes the minimum number of mice required to power experiments and quantitative genotyping to assess mutant SOD1 copy number (Scott *et al.*, 2008).

Other mutant SOD1 expressing transgenic mouse models have been developed, with single amino acid changes at various positions, including SOD1^{G85R} (Bruijn *et al.*, 1998), SOD1^{G37R} (Wong *et al.*, 1995) and SOD1^{D90A} (Jonsson *et al.*, 2006). These models vary in disease onset from early to late and in disease progression rate from slow to fast. The SOD1^{G93A} is the gold standard for MND research and the only one used in pharmaceutical trials for MND due to its similarity to human MND. However, similar to cases of human MND with SOD1 mutations, SOD1^{G93A} mice do not have TDP-43 pathology including cytoplasmic mislocalisation (Penndorf *et al.*, 2017) and is therefore, not an appropriate mouse model for research involving TDP-43.

1.3.2.2 TDP-43 Mice Models

With TDP-43 proteinopathy being a hallmark of MND, a TDP-43 mouse model is ideal for investigating the disease. Many transgenic TDP-43 mouse models have been developed since the discovery of MND-associated TDP-43 mutations in 2006 (De Giorgio *et al.*, 2019). Due to the importance of TDP-43 for embryonic and early development, issues arose in the development of a mouse model expressing mutant TDP-43 from mouse TDP-43 promoters expressed during development (Wegorzewska and Baloh, 2011). Instead, postnatally expressed TDP-43 promoters were used to induce mutant TDP-43 expression in the mice. One TDP-43 model commonly used in MND research consists of mouse promoter-controlled expression of mutant TDP-43, with a change of an alanine to threonine at position 315 (TDP-43^{A315T})(Wegorzewska *et al.*, 2009). These mice develop pathologies consistent with MND including significant gait abnormalities. Furthermore, these mice show spinal cord pathologies observed in human MND such as reduced innervation of neuromuscular junctions, motor neuron loss and ubiquitinated protein inclusions (Hatzipetros *et al.*, 2014, Wegorzewska *et al.*, 2009). However, TDP-43^{A315T} mice also develop gastrointestinal

abnormalities that interfere with MND disease progression unless controlled for with an easily digestible gel diet and presence of TDP-43 cytoplasmic inclusions are yet to be identified (Hatzipetros *et al.*, 2014). Due to these caveats, this TDP-43 mouse model has questionable use for MND research.

A more recent development in TDP-43 mouse models of MND is an inducible mutant TDP-43 overexpression mouse model (Walker *et al.*, 2015). This model is a Doxycycline (Dox)-suppressible neurofilament heavy chain (NEFH) promoter-driven system with defective nuclear localisation signal expressing human TDP-43 (hTDP-43 Δ NLS). When these mice are given Dox-lacking chow, the tetracycline transactivator (tTA) protein is active, activating the tTA promoter (*tetO*) and causes expression of hTDP-43 Δ NLS (**Figure 1.3**). These mice are bred on a C57BL/6J background.

Following hTDP-43 Δ NLS expression, the mice develop disease characteristics and symptoms that recapitulate human MND (Walker *et al.*, 2015). After 2 weeks off Dox, the hTDP-43 Δ NLS mice develop a behavioural phenotype that is consistent with MND. This includes claspings of the limbs, development of a tremor, gait abnormalities as measured by the rotarod test and loss of hind limb control as measured by the wirehang test. These motor deficits progress significantly until end stage disease at approximately 6 weeks off Dox. Pathological changes within the brain and spinal cord can also be observed in these mice such as loss of NMJ innervation and motor neuron loss. Importantly, TDP-43 pathology is evident within the brain and spinal cord with cytoplasmic TDP-43 inclusions and nuclear clearance, consistent with human MND.

With TDP-43 proteinopathy being a driving factor in neurodegeneration in almost all other MND patients, a mouse model that mimics the TDP-43 pathology within the spinal cord and brain is ideal for investigating causative factors and treatments. With the proposed association between TDP-43 and endogenous retroviruses, and TDP-43 pathology being a hallmark of MND, the hTDP-43 Δ NLS mouse model provides a logical model choice for investigating endogenous retroviruses in MND.

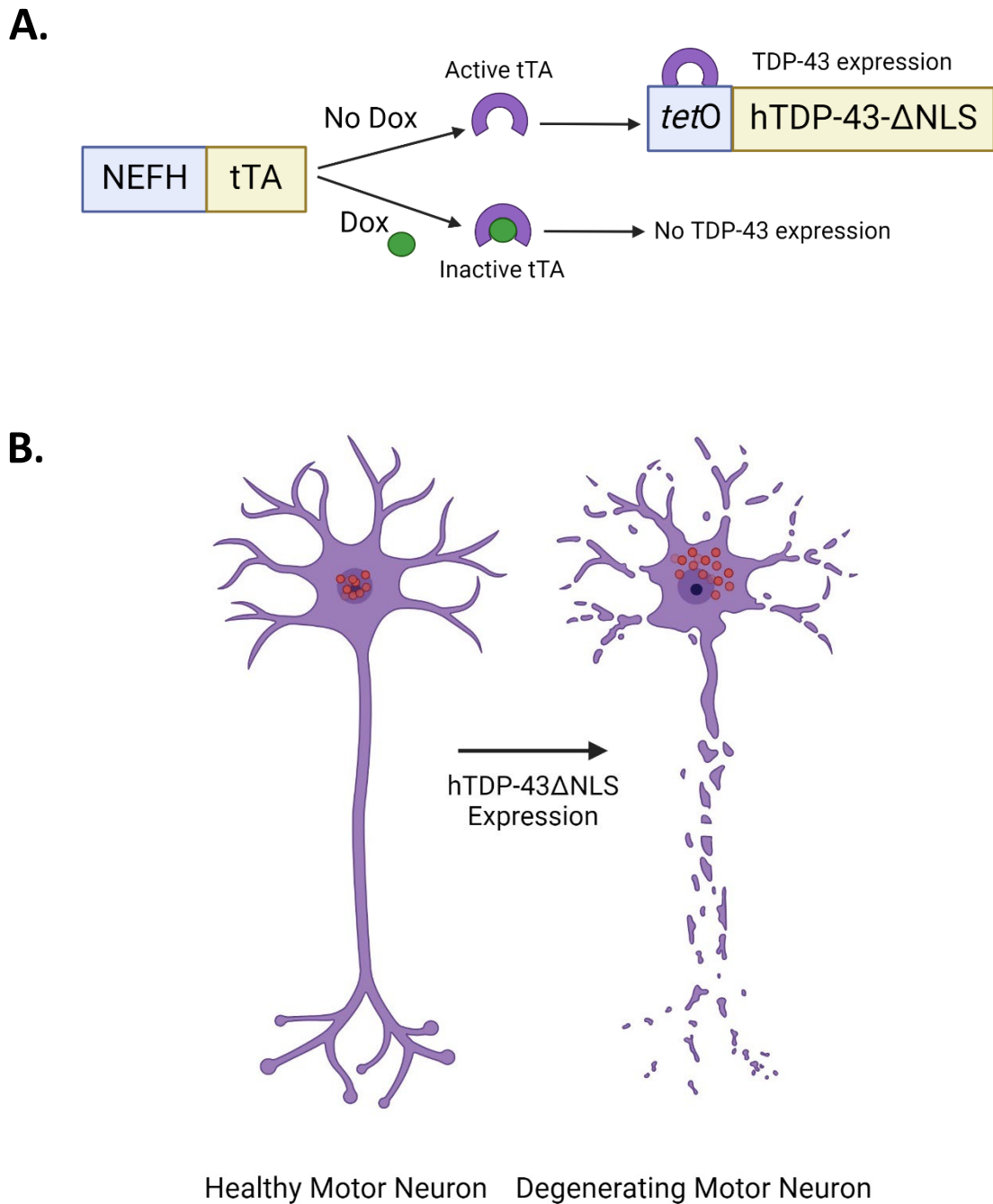


Figure 1.3 Schematic of a Dox-suppressible system for hTDP-43 expression resulting in cytoplasmic mislocalisation of TDP-43

The hTDP-43 Δ NLS mouse model uses a Dox-suppressible TDP-43 expression system **A**. Schematic of the Dox-regulated expression of hTDP-43 Δ NLS **B**. The hTDP-43 Δ NLS expression results in mislocalisation of hTDP-43 (depicted as red circles) from the nucleus to the cytoplasm. Adapted from Walker *et al.* (2015). Figure made in BioRender.

1.4 Endogenous Retroviruses as a Proposed Cause of MND

1.4.1 Retroviruses

Retroviruses are enveloped, positive-sense single stranded RNA viruses (Saxena, 2016). Retroviruses use an RNA-dependent DNA polymerase (RdDpol), termed reverse transcriptase (RT), that enables transcription of their viral RNA to viral DNA during replication. This is a unique property of some viruses and not a normal function found in eukaryotic cells. Instead, in eukaryotic cells, transcription of cellular genes converts DNA to RNA by DNA dependent RNA polymerase (DdRpol); (Coffin, 2018). Retroviruses that are transmitted between individuals are considered as exogenous retroviruses. Two pathogenic exogenous retroviruses that infect humans are HIV and human T cell leukemia virus type 1 (HTLV-1) (Isache *et al.*, 2016). The retrovirus particle consists of an RNA genome packaged with replication machinery, including integrase and RT inside the capsid core and surrounded by the envelope containing viral glycoproteins and lipid derived from cell membranes. When an exogenous retrovirus infects a cell, the genomic RNA is reverse transcribed into double stranded DNA in the cytoplasm, that then moves to the nucleus and integrates into the chromosome of the host cell forming a provirus. The process of exogenous retroviral infection into the host cell and release from the cell can be seen in Appendix **Figure A.1**

The proviral DNA genome consists of *gag*, *pol* and *env* coding regions, flanked by long terminal repeats (LTRs). *Gag* (Group specific antigen) encodes structural proteins including the capsid, matrix and nucleocapsid, *pol* encodes the enzymatic functions of the virus, viral protease, RT and integrase and the *env* encodes the surface and transmembrane glycoproteins, gp120 and gp140 (Coffin, 2018). Complex retroviruses also contain accessory genes such as *tat* within the HIV genome, encoding a transcriptional activator. Each LTR consists of a unique 3' region (U3) a repeat (R) and unique 5' region (U5). The U3 region of the LTRs serve as the viral promoter regions controlling gene expression. The R region contains the trans-activation response element (TAR), which interacts with viral *tat* protein during transcription and recruits cellular factors to enhance viral gene transcription (Coffin, 2018).

1.4.2 Endogenous Retroviruses: Structure and Function

ERVs are a type of transposable element which is a type of mobile genetic element that can move to other locations in the genome. Transposable elements are classified as DNA transposons or RNA transposons. Based on the presence of LTRs, retrotransposons are further classified into non-LTRs including short interspersed nuclear elements (SINE) and long interspersed nuclear elements (LINE) or ERVs with LTRs. LTR retrotransposons can be transcribed from the host cell genome into ERV RNA, then, in the same cell, reverse transcribed back into double stranded DNA and re-integrated into another site of the host genome (Gifford *et al.*, 2018, Bourque *et al.*, 2018). This would have the potential to be damaging to the host cell genome and hence many species, including humans, have cellular processes to restrict this from happening (Zhang *et al.*, 2022). ERVs are then classified into three different classes based on their homology to exogenous retroviruses genera. Class I encompasses Gammaretroviruses, class II encompasses Betaretroviruses and Class III, Spumaviruses (Gifford *et al.*, 2018) The relationship between classification of transposable elements and ERVs is seen in **Figure 1.4**. One type of ERV, HERV-K (HML-2), and its association with MND is discussed further below.

While exogenous retroviruses are capable of horizontal transmission from person to person and produce infectious virions, ERVs, in contrast, are traditionally not thought to produce infectious virions and are not horizontally transmitted. Instead, ERVs have integrated into the host genome and are vertically transmitted through the germ lines (Diehl *et al.*, 2016, Gifford *et al.*, 2018). The process of germ-line integration of ERVs occurred millions of years ago with the subsequent process of endogenisation. After endogenisation within the genome, the virus no longer produces an infectious particle and lacks the capacity to infect as an exogenous retrovirus (Küry *et al.*, 2018). Eventually, ERVs will be fixed within the genome and inherited within every member of the species (**Figure 1.5**). The koala retrovirus is believed to be an example of a current exogenous retrovirus in the process of endogenisation in the koala population (Nishat *et al.*, 2020). In humans, ERVs compose 8-10% of the human genome, usually thought to be transcriptionally silent and lack the ability to transpose (Lander *et al.*, 2001, Gifford *et al.*, 2018). In contrast, 10% of the mouse genome is comprised of endogenous

retroviruses and, unlike human ERVs, most murine ERVs remaining transcriptionally active and mobile within the mouse genome (Stocking and Kozak, 2008a, Li *et al.*, 2012a).

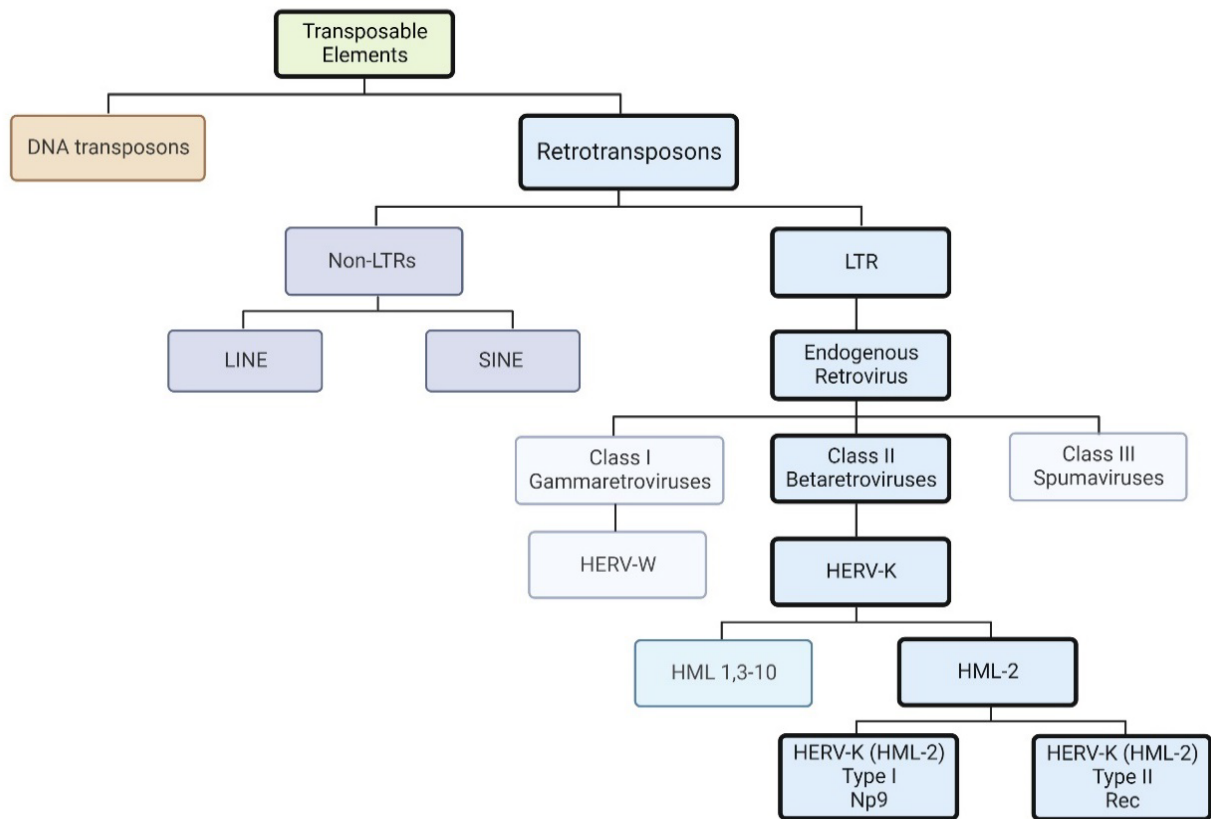


Figure 1.4 Classification of Human Endogenous Retroviruses

Betaretrovirus, that are long terminal repeat (LTR) containing retrotransposons present within the human genome. HERV-K are distinct from other endogenous elements such as DNA transposons, the non-LTR retrotransposons such as long interspersed nuclear elements (LINE) and short interspersed nuclear elements (SINE). HERV-K are related to other LTR-containing endogenous retroviruses such as HERV-W (a Class I Gammaretrovirus) and the Class III Spumaviruses. The HERV-K family is further subdivided into 10 human mammary tumor like (HML) elements, where HERV-K (HML-2) is further grouped into Type I (np9) and Type II (rec) based on the envelope sequence. Figure made in BioRender.

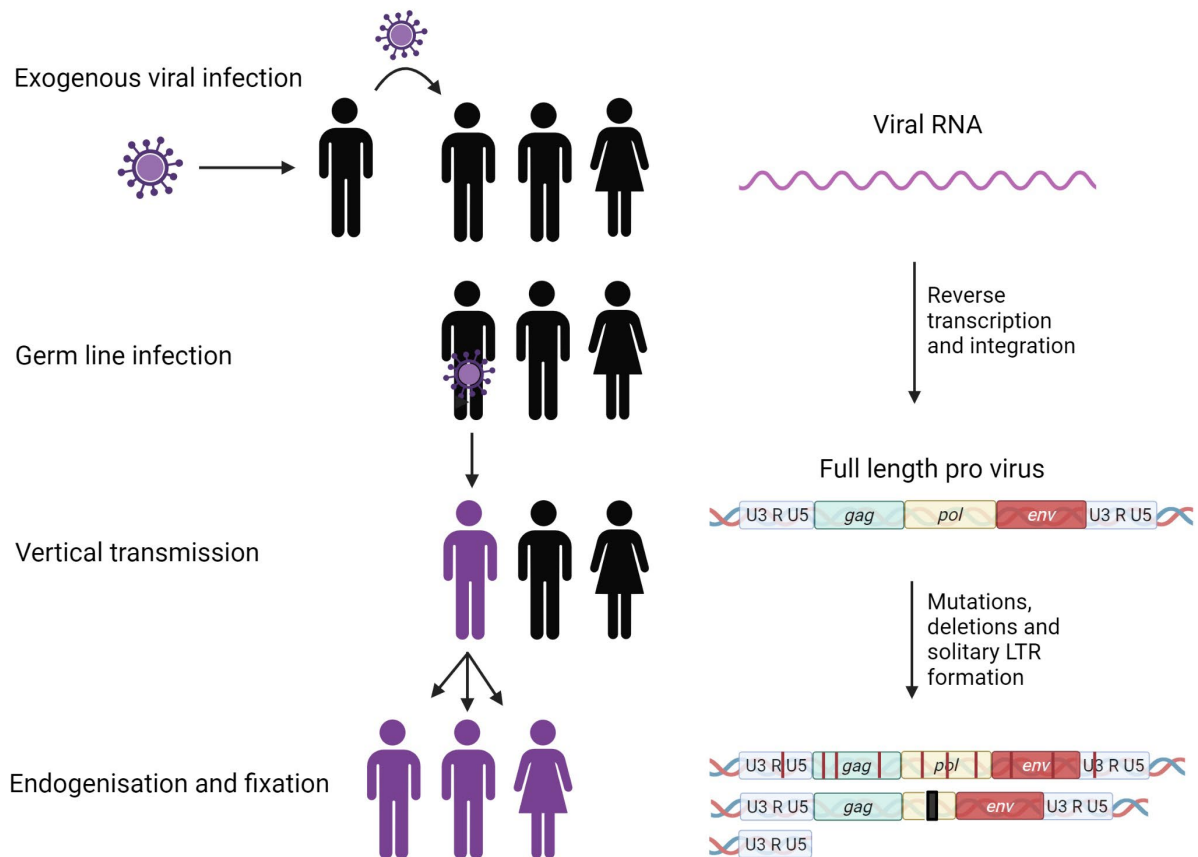


Figure 1.5 Endogenisation of retroviruses from exogenous retroviral infection

Originally, exogenous retrovirus infected humans and were horizontally transmitted and integrated into germ line cells. This resulted in vertical transmission and eventual endogenization and fixation into the genome. Full length retroviruses genomes integrated into the host genome but over time, point mutations and deletions have resulted in truncated endogenous retroviral elements (Grandi and Tramontano, 2017). Figure made in BioRender.

1.4.3 HERV Benefit and Role in Disease

Most human endogenous retroviruses (HERVs) are not transcribed and contain deletions and mutations resulting in a lack of functional protein production and lack the components required for a functional virus (Lenz, 2016). Recently, however, transcriptional activation of ERV elements in humans has been proposed as a causative factor or progressive factor for a multitude of diseases, including MND (Li *et al.*, 2015, Suntsova *et al.*, 2015, Nexø *et al.*, 2016, Douville and Nath, 2014). One type of HERV, HERV-W, does have a physiological benefit to the host with an important placental protein, Syncitin-1, encoded by the HERV-W envelope gene (Mi *et al.*, 2000). Syncitin-1 aids in trophoblast fusion and is a necessary step in the healthy formation of the placenta (Chuong, 2018). Abnormal expression of syncitin-1 has been associated with pregnancy-related disorders, such as pre-eclampsia and other placenta-related pathologies (Qiao *et al.*, 2017). While this type of HERV-W plays an important role in placental development, HERV-W expression has also been associated with multiple sclerosis (MS) pathology (Dolei, 2018). Several studies have identified increased levels of HERV-W env protein within brain tissue and human peripheral blood mononuclear cells (PBMCs) from MS patients compared to healthy controls (Kremer *et al.*, 2018, Ruprecht and Mayer, 2019, Rasmussen *et al.*, 1995, Perron *et al.*, 2012). The reactivation of HERV-W and the association with MS has been proposed to be caused by an exogenous viral infection from Epstein-Barr Virus (Dolei, 2018, Pérez-Pérez *et al.*, 2022, Soldan and Lieberman, 2023). Thus, while some HERVs have physiological importance, dysfunctional expression of these HERVs can have detrimental effects on the host. Other HERVs have been correlated with a variety of diseases; HERV-K, HERV-E and HERV-W are associated with cancers such as ovarian cancer and breast cancer (Grandi and Tramontano, 2018, Christensen, 2010, Rycaj *et al.*, 2015, Wang-Johanning *et al.*, 2003), HERV-W and HERV-K are associated with autoimmune diseases such as rheumatoid arthritis and systemic lupus erythematosus (Mameli *et al.*, 2017, Grandi and Tramontano, 2018) and HERV-W with schizophrenia (Leboyer *et al.*, 2013, Slokar and Hasler, 2016).

The evolutionarily youngest ERV to enter the human genome is HERV type K (HERV-K), which is predicted to have endogenised into the human genome approximately 700,000 years ago (Zimmer, 2019). While HERV-K is the most recent insertion into the human genome, it is no

longer considered to be mobile within the human genome (Magiorkinis *et al.*, 2015). HERV-K is a class II ERV and is referred to as type K due to the use of lysine (single amino acid code, K) tRNA as a reverse transcription primer. HERV-K is further classified into 10 families denoted HML-1 to HML-10 based on their similarity with the mouse mammary tumour virus (MMTV), a prototype used for comparison when new HERVs first became to be described (Subramanian *et al.*, 2011). Human endogenous mouse mammary tumour virus like-2 (HML-2) is the best preserved HERV-K element, maintaining the capability of encoding viral proteins such as the env protein (Hohn *et al.*, 2013). The delineation of HERV-K and HML subtypes is shown in **Figure 1.4** and the HERV-K proviral genome structure can be seen in **Figure 1.6** (Hughes, 2015, Grandi and Tramontano, 2018).

Two LTR regions are also present on a portion of other HERV families (Gifford and Tristem, 2003, Hughes, 2015). HERV-K (HML-2) are further classified into two types based on the expression of accessory genes. HML-2 type I proviruses have a 292 bp deletion within *env* and encode accessory protein, Np9. Type II proviruses do not have this deletion and encode accessory protein, Rec (Chan *et al.*, 2019). *Rec* is similar to HIV-1 *Rev* accessory gene, a protein that is involved in RNA splicing. While the biological role of these proteins is still unclear, mRNA transcripts for Rec and Np9 from multiple HERV-K loci have been found in many human tissue types (Schmitt *et al.*, 2015).

Many of the HERVs that exist in the human genome are in the form of solitary LTRs (Garcia-Montojo *et al.*, 2018, Hughes and Coffin, 2004). However, some HERVs, as described above for HERV-K and HERV-W, retain intact open reading frames (ORFs), with the ability to produce functional proteins (Dewannieux *et al.*, 2005, Boller *et al.*, 2008). Approximately 950 solitary LTRs have been described in the human genome (Subramanian *et al.*, 2011) with 17 identified full length HERV-K (Shin *et al.*, 2013, Turner *et al.*, 2001, Wildschutte *et al.*, 2016). Both the solo LTRs and the HERV-K proviral elements capable of producing RNA and proteins have been implicated in diseases (Wildschutte *et al.*, 2016).

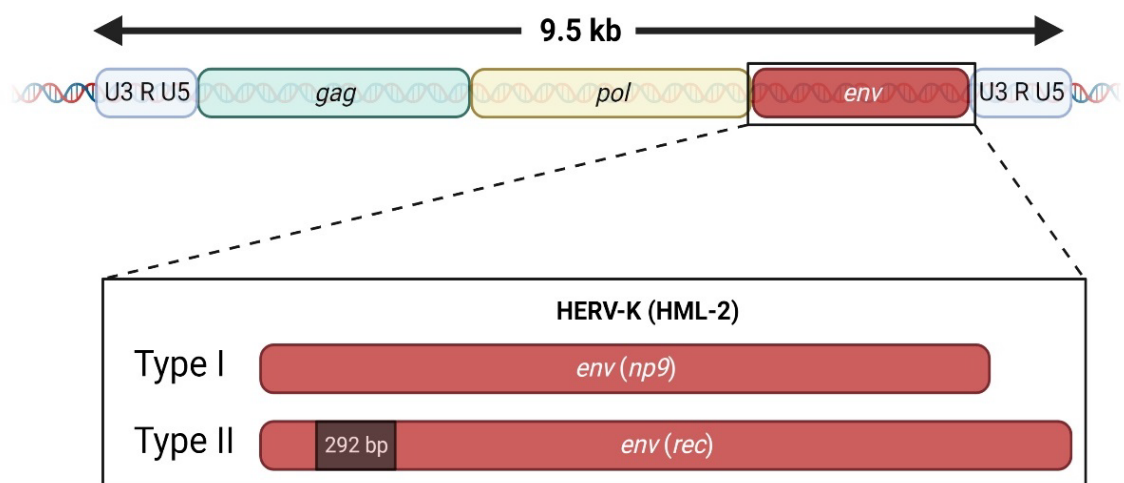


Figure 1.6 Structure of the HERV-K (HML-2) full-length provirus

HERV-K (HML-2) full-length provirus, approximately 9.5 kb, with a capacity to generate infectious virus by virtue of the presence of 2 complete LTR's containing U3, R and U5 regions, that flank the viral structural proteins *gag*, *pol* and *env*. Type I *env* region encodes the accessory protein *np9*, while Type II harbours an additional 292 base pair region in the *env* ORF and encodes the accessory protein *Rec*. Adapted from Li *et al.* (2015). Figure made in BioRender.

1.4.4 Human Endogenous Retrovirus Type-K is Associated with MND

The link between MND and retrovirus activity was first identified in 1975, through discovery of RT activity in brain tissue of two MND patients (Viola *et al.*, 1975). Further studies confirmed this finding with elevated RT levels in serum and CSF of MND patients without exogenous retroviral infection (Andrews *et al.*, 2000, Steele *et al.*, 2005, McCormick *et al.*, 2008). Andrews *et al.* (2000) demonstrated increased RT levels in 59% of the 56 MND patients compared to 5% of the 58 controls. In a separate cohort of 14 MND patients, RT activity in serum was detected in 47% of the MND patients compared to 18% in the controls. However, RT activity was also elevated in blood relatives of the MND patients in this cohort (Steele *et al.*, 2005, Li *et al.*, 2022). Rare cases of an MND-like syndrome were observed in patients infected with exogenous retroviruses such as HIV-1 (Alfahad and Nath, 2013, Moulignier *et al.*, 2001). Additionally, these motor symptoms were observed to be reversed in the HIV positive patients after they were initiated on antiretroviral therapy (ART). This association between HIV and development of MND-like motor symptoms was proposed to occur through activation of a specific endogenous retrovirus, HERV-K with a reduction in the levels of HERV-K DNA within the plasma after ART (Bowen *et al.*, 2016, Garcia-Montojo *et al.*, 2018).

Experimental studies further supported the proposed association between MND and ERVs. Hadlock *et al.* (2004) evaluated the immunoreactivity of MND patient serum to HML-2 gag protein. Their study observed that MND patient serum had greater than 5-fold higher IgG reactivity to recombinant gag (57% vs 11% in MND patients and age-matched controls respectively). This finding suggests that HML-2 gag can induce an antibody response in MND patients and the involvement of ERVs in Immune-mediated MND has been proposed (Alfahad and Nath, 2013).

Recently, an antibody response to specific epitopes of HERV-K (HML-2) env has also been demonstrated with a greater antibody response in MND patients compared to age- and sex-matched controls (Garcia-Montojo *et al.*, 2022). Furthermore, HERV-K pol transcripts, measured through quantitative real-time PCR (RT-qPCR), in brain tissue from the prefrontal cortex, sensory cortex and occipital cortex of 28 MND patients were compared to levels in brain tissue from people who succumbed to other diseases. These HERV-K pol transcripts were found to be significantly higher in MND patients than age-matched controls (Douville *et*

et al., 2011). Post-mortem cortical brain tissue analysis from 11 MND patients using RT-PCR identified increased expression of 3 HERV-K genes, *gag*, *pol* and *env* compared to control brain tissue (Li *et al.*, 2015). However, one study failed to confirm the HERV-K transcript elevation in cortical brain tissue from MND patients compared to controls, measured through RT-qPCR (Garson *et al.*, 2019). Transfection of a construct to express the HERV-K *env* gene in human neuronal cultures derived from iPSCs, has demonstrated the toxicity of *env*, with reduced viable neuronal cell number after *env* transfection (Li *et al.*, 2015). Similarly, Steiner *et al.* (2022) found an increase of HERV-K *env* protein in CSF from 11 out of 15 MND patients measured through Immunocapillary Western Blot, and in only one healthy age-matched control. The authors also demonstrated the neurotoxic properties of HERV-K *env* protein through intracerebral injection of recombinant *env* protein into mice, showing a reduction in neuronal cell number 1-week post-injection compared to control injection. These results provide further support for a role of HERV-K in neurodegeneration in MND.

1.4.4.1 Interaction Between HERV-K, TDP-43 and Inflammation may Cause Neurodegeneration in MND

The association between HERV-K and MND pathology is proposed to occur through an interaction with TDP-43. Importantly, chromatin immunoprecipitation identified 5 binding sites for TDP-43 on the consensus sequence of HERV-K LTR (Li *et al.*, 2015). This suggests that TDP-43 may be involved in HERV-K transcriptional regulation (Ou *et al.*, 1995). HERV-K RT expression is positively correlated with TDP-43 protein levels within cortical brain tissue and human neuronal cells from iPSCs supporting this regulatory link (Douville *et al.*, 2011, Li *et al.*, 2015). An *in vitro* study with cultured human neural progenitor cells transfected with a construct to express mutant human TDP-43, identified an increase in HERV-K RT mRNA levels in the transfected cells compared to untransfected cells (Manghera *et al.*, 2016a).

HERV-K has also been shown to influence TDP-43 expression and aggregation (Li *et al.*, 2015, Chang and Dubnau, 2022). Ibba *et al.* (2018) proposed an association between HERV-K and TDP-43 when disruption of HERV-K *env* throughout the genome resulted in a decrease in TDP-43 mRNA and protein levels in human prostate adenocarcinoma cells. While previous findings

have identified TDP-43-dependent increases in HERV-K expression (Manghera *et al.*, 2016a), the above finding demonstrates the inverse relationship in that HERV-K is capable of regulating TDP-43 mRNA and protein expression levels, suggesting a positive feedback loop of TDP-43 and HERV-K activation (Ibba *et al.*, 2018, Dolei *et al.*, 2019). Chang and Dubnau (2023) established a *Drosophila* model expressing TDP-43 within glial cells to elucidate the mechanisms of ERV-TDP-43 involvement in neuronal damage. In this model, glial TDP-43 protein aggregates increased the expression of *Drosophila* ERVs within the glial cells. This increased ERV expression within glia resulted in increased cellular release of neuronal toxic factors that induced DNA damage and neuronal death in surrounding neurons. These studies provide evidence for a self-perpetuating feedback loop between HERV-K and TDP-43 as a potential mechanism of neurodegeneration in MND.

As outlined in section 1.1.7.7, there is increased activity of transcription factors that drive inflammatory mediator production including IRF-1, IRF-3 and NF- κ B in MND (Taylor *et al.*, 2016, Appel *et al.*, 2021). The TDP-43 promoter has binding sites for IRF-1, IRF-3, and NF- κ B, suggesting the role of activation of these transcription factors in driving increased expression of TDP-43 and potentially TDP-43 proteinopathy. Similarly, HERV-K expression is induced by inflammatory mediators within neurons and non-neuronal cells. HERV-K LTR consensus sequences contain two interferon-stimulated response elements, which will activate HERV-K expression when activated by Type I IFN signalling and activation of the JAK/STAT pathway (Manghera and Douville, 2013). Furthermore, IFN- γ has been experimentally shown to increase transcription of HERV-K *gag* and *pol* determined by RT-qPCR and increased RT activity in an astrocytic cell line (Manghera *et al.*, 2015). Additional evidence for the association between ERVs and inflammation has been demonstrated *in vivo* (Di Curzio *et al.*, 2020, Jönsson *et al.*, 2021, Arru *et al.*, 2021). Genetic deletion of known ERV repressor, Trim28, in mice during development resulted in increased ERV expression in the adult cortex of the mice and increased microglia activation, suggestive of a pro-inflammatory environment in the brain (Jönsson *et al.*, 2021).

In support of the relationship between inflammation and ERVs, NF- κ B is also thought to induce HERV-K expression. Manghera *et al.* (2016) demonstrated increases in HERV-K expression, measured by levels of HERV-K RT activity, when transfected with constructs

expressing NF- κ B in human neural progenitor cells. Neuroinflammatory mediators such as TNF- α and NF- κ B also increase TDP-43 expression which can drive further HERV-K expression and further neuroinflammation. This pathway (**Figure 1.7**) may result in the neurodegeneration observed in MND, with cell-to-cell spread of toxicity (Chang and Dubnau, 2019, Brown and Al-Chalabi, 2015).

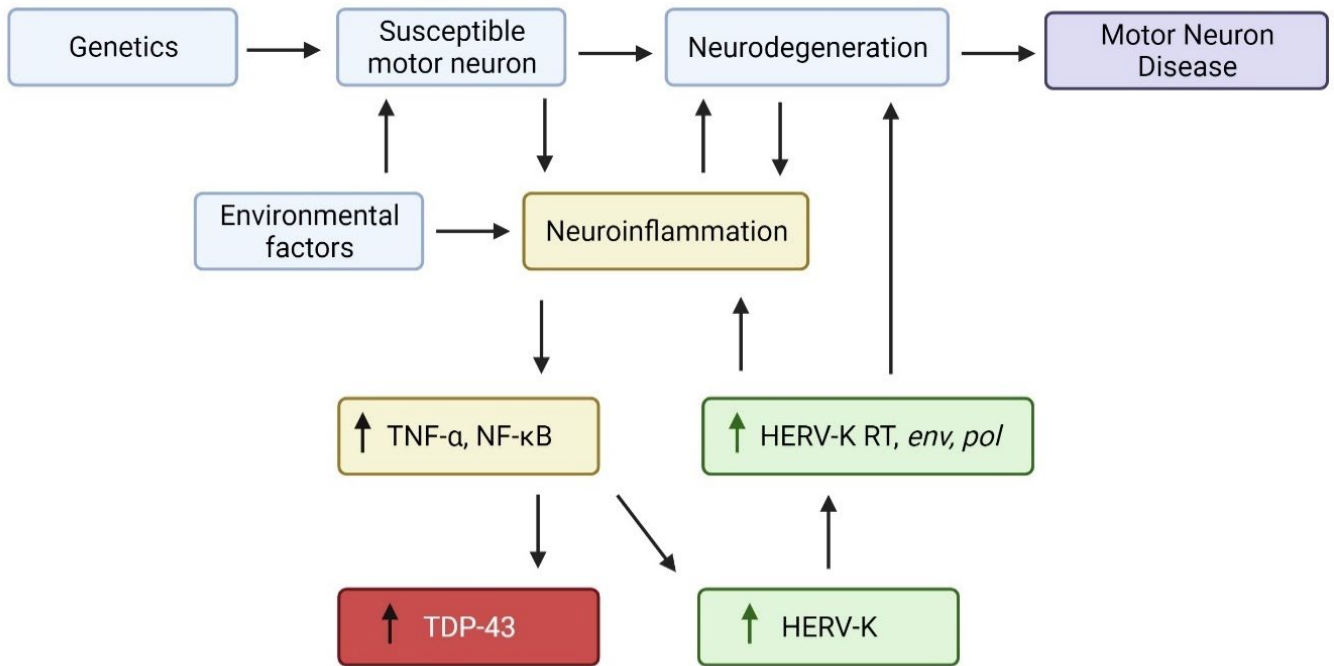


Figure 1.7 Proposed pathway leading to motor neuron disease involving neuroinflammation and HERV-K

MND (ALS) is proposed to be caused by a combination of genetics environmental stimuli and involve neuroinflammation influencing TDP-43 and HERV-K. This feedback loop is proposed to result in impaired motor neurons which results in MND (Brown and Al-Chalabi, 2015). Figure made in BioRender.

1.4.5 Anti-retroviral Therapy

An effective therapy against retroviral infection, most commonly HIV, is anti-retroviral therapy (Cihlar and Fordyce, 2016, Ghosn *et al.*, 2018). Different types of anti-retroviral drugs target different stages of the retroviral replication cycle. Anti-retroviral drugs fall into one of the following categories: Nucleoside Reverse Transcriptase Inhibitors (NRTIs), Non-nucleoside Reverse Transcriptase Inhibitors (NNRTIs), Protease Inhibitors (PIs), Integrase Inhibitors (IIs) and Fusion Inhibitors (FI) (Arts and Hazuda, 2012). NRTIs target the reverse transcription of the viral RNA into DNA by binding to the forming viral DNA strand and causing chain termination. Similarly, NNRTIs also prevent reverse transcription but achieve this through binding to RT directly, impairing its function. PIs inhibit the viral protease function. As described in the retrovirus replication cycle, protease is required for the maturation of the newly formed infectious virion. PIs bind protease, inhibiting its function and prevent virion maturation. IIs prevent the action of integrase, blocking integration of viral DNA into host DNA.

Antiretrovirals (ARVs) were characterised in 1987, as a treatment for HIV with the first ARV being an NRTI, azidothymidine (Furman *et al.*, 1986, St Clair *et al.*, 1987). While this treatment showed significant increases in life expectancy, major side effects questioned its long-term safety and efficacy as a treatment for HIV. Further classes of ARVs were developed, acting on different stages of the replication cycle, as described above, and optimised to reduce side effects. Combination drugs were developed to target multiple mechanisms of the HIV cycle with one tablet (Vella *et al.*, 2012). Hence, treatment adherence was improved through a single tablet, once daily treatment which lowered the cost. Globally, 62% of individuals living with HIV are receiving ARV therapy (ART). While HIV is yet to be eradicated, ART has reduced the number of new HIV infections by 37% between 2000 and 2018 (World Health Organisation, 2018). ART has been proposed as a potential treatment for MND, discussed further below.

1.4.6 Treatment of HERV-K-associated MND Through Antiretroviral Therapy

As described, HERV-K has been implicated in the causation and perpetuation of the signals that drive neurodegeneration in MND. This, and the early clinical anecdotal findings of improved MND-like symptoms in HIV patients on ART, led to the proposal that targeting ERVs could be used as a treatment for MND, through ARTs designed to target HIV (Bowen *et al.*, 2016, Tyagi *et al.*, 2017). Two early clinical trials investigated the effect of two different antiretrovirals in MND patients, a NRTI, Zidovudine, and a PI, Indinavir (Scelsa *et al.*, 2005, Westarp *et al.*, 1993). Neither study identified any slowing of disease progression, although low sample sizes and poor adherence due to the advancing MND symptoms resulted in inconclusive results. An *in vitro* study demonstrated the ability of an NRTI, abacavir, to inhibit HERV-K using a pseudotyped HERV-K with infectious capabilities. Pseudotyped HERV-K-infected HeLa cells were treated with abacavir and HERV-K RT levels were examined through RT assay and determined to be significantly reduced (Tyagi *et al.*, 2017). Interestingly, abacavir was more potent against HERV-K than HIV as determined by significantly lower IC₅₀ and IC₉₀ concentrations of the drug. Triumeq is an example of combination ART that is widely used for treatment of HIV, which is a single tablet, once daily treatment. Triumeq consists of two NRTIs, abacavir and lamivudine and an II, dolutegravir. all of which are capable of penetrating the CNS. (Gubernick *et al.*, 2016, Ene *et al.*, 2011, Letendre *et al.*, 2014). However, while it is capable of CNS penetrance, lamivudine has been shown to have low CNS penetrability compared to abacavir and other NRTIs (Yilmaz *et al.*, 2011, Letendre *et al.*, 2008, Osborne *et al.*, 2020).

Theoretically, the two reverse transcriptase inhibitors within Triumeq, abacavir and lamivudine, could inhibit the formation of HERV-K dsDNA inside cells where HERV-K has been activated. cGAS/STING is a cell sensor that detects dsDNA in the cytoplasm as a danger signal and activation of the cGAS/STING pathway has been suggested to occur in MND (Yu *et al.*, 2020a). Furthermore, cytosolic dsDNA can also trigger the assembly of the AIM2 inflammasome and result in further inflammatory cytokine release including IL-1 β and IL-18 and initiate cell death (Hornung *et al.*, 2009, Rathinam *et al.*, 2010, Adamczak *et al.*, 2014). Thus, NRTI actions to inhibit HERV-K RT activity and reduce production of dsDNA in the cytoplasm that would subsequently activate cGAS/STING and the AIM2 inflammasome can

be envisioned as a mechanism that may underpin the therapeutic success of ART and agents such as Triumeq. It would be expected that such a treatment would reduce production of inflammatory mediators and to slow progression of MND (**Figure 1.8**).

Recently, the de-repression of HERV-K was proposed to be involved in ageing, with increased HERV-K gag, pol and env transcript levels and protein levels in senescent human mesenchymal progenitor cells (hMPCs) compared to phenotypically young cells (Liu *et al.*, 2023). The increased HERV-K levels in these cells, coincided with increased activation of cGAS/STING. Senescent hMPCs treated with abacavir showed reduced HERV-K DNA and reduced levels of inflammatory cytokines IFN- α , IFN- β and IL-1 β measured through q-PCR compared to vehicle treated senescent hMPCs. ARVs have also been shown to have anti-inflammatory properties, decreasing immune activation and inflammatory mechanisms as determined by reductions in TNF- α , IL-6 and IFN- γ in patients with HIV (Hileman and Funderburg, 2017, Hattab *et al.*, 2014).

A phase IIa clinical trial for Triumeq as a treatment for MND has recently been completed (Gold *et al.*, 2019). This clinical trial involved investigating the safety and tolerability of Triumeq in 40 patients with MND across 24 weeks of treatment. During the 24 weeks, the amyotrophic lateral sclerosis functional rating scale – revised (ALSFRS-R) was used as a primary outcome measure of disease progression along with secondary measures of respiratory function, grip strength and the biomarkers, urinary p75^{ECD} and neurofilament-light and phosphorylated neurofilament heavy within CSF. Levels of serum HERV-K were also measured through droplet digital PCR.

The results of the study showed patients on Triumeq treatment had a slower clinical decline as measured by the ALSFRS-R compared to pre-treatment. HERV-K DNA serum levels were significantly decreased over the treatment course (Gold *et al.*, 2019, Garcia-Montojo *et al.*, 2021). This research has progressed to a phase III clinical trial to further assess the efficacy of Triumeq in halting the progression of MND and increasing survival. This will be completed with approximately 400 MND patients from Europe, United Kingdom and Australia. While the Phase IIa clinical trial has shown promise, the mechanism of action of Triumeq for use as an MND therapeutic is still unclear. Interestingly, another antiretroviral, Raltegravir, has been

trialled in relapsing remitting multiple sclerosis, but unfortunately this did not produce any clinical improvement (Gold *et al.*, 2018).

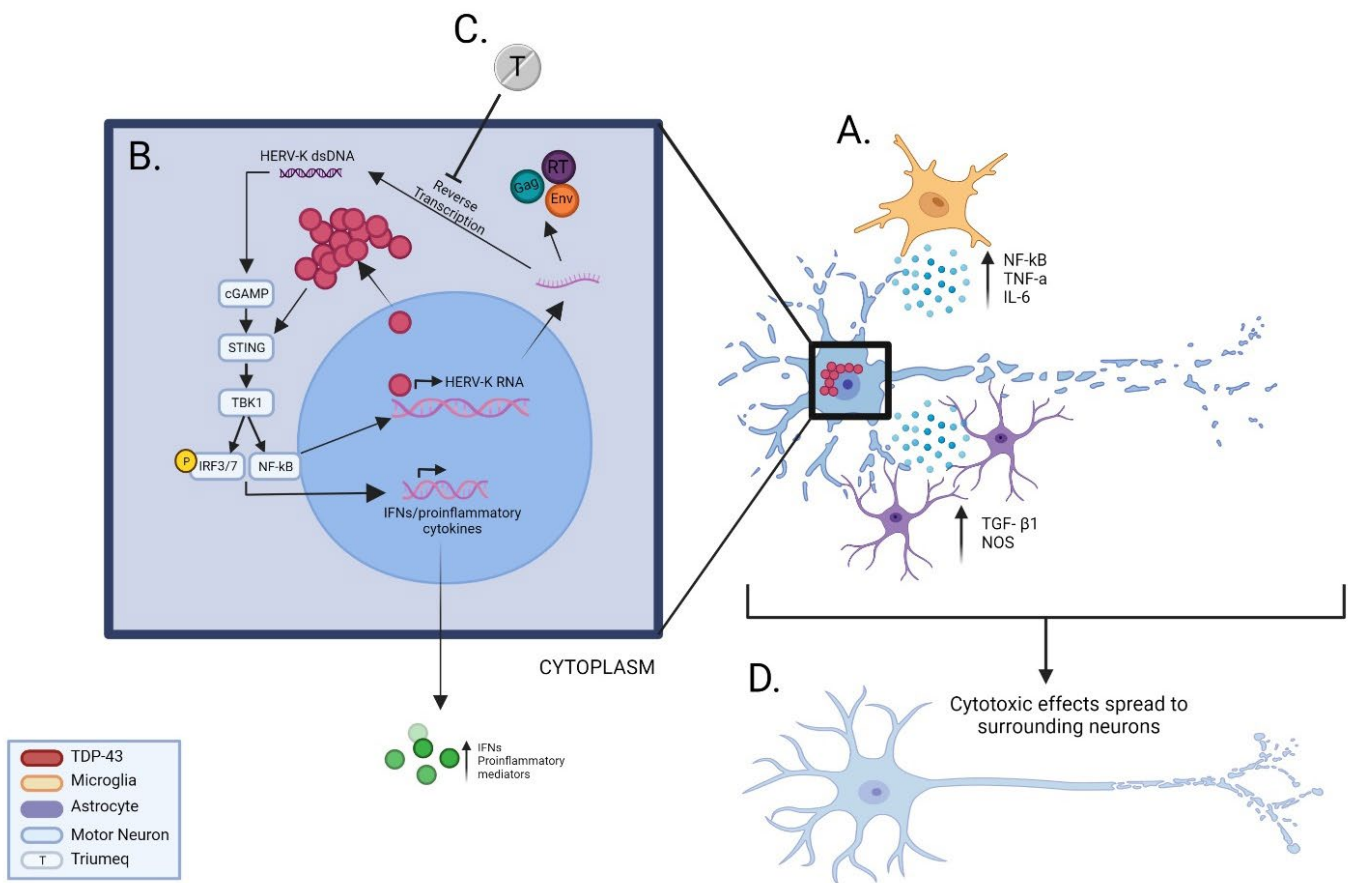


Figure 1.8 Proposed interaction of HERV-K, TDP-43 and inflammatory mediators in the process of neurodegeneration in MND

Depiction of the proposed interactions of HERV-K, TDP-43 and inflammatory mediators in the process of neurodegeneration in MND. **A.** Astrocytes and Microglia release proinflammatory cytokines that is a trigger for TDP-43 cytoplasmic mislocalisation in neurons **B.** Mislocalisation of TDP-43 to the cytoplasm de-represses HERV-K transcription which leads to the production of HERV-K RNA. The HERV-K mRNA is translated into HERV-K proteins including Gag, Envelope (*env*) and the reverse transcriptase enzyme (RT) from the *pol* gene. The RT enzyme acts to reverse transcribe the HERV-K into double stranded DNA (dsDNA). Cytoplasmic dsDNA is a danger signal that is recognised by and activates the cGAS/STING pathway that subsequently activates TBK1 resulting in phosphorylation of IRF3, IRF7 and release of NF- κ B from the cytoplasm. These transcription factors move to the nucleus and subsequently induce transcription of mRNA for multiple inflammatory factors and interferons which can trigger further TDP-43 mislocalisation. Additionally, NF- κ B can further drive HERV-K transcription. **C.** Triumeq contains two RT inhibitors which could act on inhibiting the reverse transcription of HERV-K RNA into dsDNA to prevent the activation of cGAS/STING pathway. **D.** This would be predicted to reduce the release of inflammatory mediators and prevent the spread of toxicity between neurons. IRF3/7 – Interferon regulatory factor 3 and 7, NF- κ B - nuclear factor kappa-light-chain-enhancer of activated B cells, TNF- α – Tumour necrosis factor alpha TGF- β 1 - transforming growth factor β 1, NO – Nitric oxide, P – phosphorylation, TBK1 – Tank Binding Kinase 1, IL-6 – Interleukin 6, T – Triumeq. Figure made in BioRender.

1.4.7 Mouse Endogenous Retroviruses and their association with TDP-43

The mouse genome is made of approximately 10% of endogenous retroviruses. Two mouse retroviruses were identified in the early 1970s, murine leukemia virus (MLV) and mouse mammary tumour virus (MMTV). Endogenous MMTV was proposed after discovery of integrated copies of the cancer-causing MMTV provirus within the mouse genome (Bentvelzen *et al.*, 1970). Endogenous MMTV is present in the genome of all laboratory mice, while the exogenous virus has been eliminated. Many mouse endogenous retroviruses remain mobile within the mouse genome, unlike human ERVs, which are no longer considered mobile within the human genome (Stocking and Kozak, 2008a, Li *et al.*, 2012a). In TDP-43 mouse models of MND, there is an increase in the fraction of bound TDP-43 to transposable element transcripts. This finding suggests that there is an association between mouse ERVs (MERVs) and TDP-43. Previous studies in mice and drosophila have identified the regulation of ERVs from TDP-43 expression suggesting a similar mechanism of TDP-43 binding to ERVs as is seen with HERVs and TDP-43 (Li *et al.*, 2012b, Krug *et al.*, 2017). Furthermore, a recent study has shown the effectiveness of using antiretroviral therapy on inhibiting mouse ERVs and reducing inflammation as shown by a reduction in IL-1 β and IL-6 protein expression in abacavir-treated mice compared to vehicle controls (Liu *et al.*, 2023). Due to the association between TDP-43 and MERVs and the presence of endogenous MMTV in all laboratory mice, MMTV will be used as a measure of endogenous retroviral activity for the current project.

1.5 Concluding Remarks

MND is a relentless neurodegenerative disease with no cure and limited treatment options. While TDP-43 is a hallmark of MND pathology with known involvement in neurodegeneration, there are no treatments that are effective against TDP-43 pathology. The activation of ERVs has been proposed to be involved in neurodegeneration, potentially involving TDP-43. Therefore, targeting ERVs through ART could provide a new therapeutic avenue for reducing TDP-43 pathology and neurodegeneration in MND. However, while currently being used in patients with MND, the mechanisms of ART in MND and how it influences TDP-43 pathology has not been studied in *in vivo* and *in vitro* models. Further understanding of ERVs and their

association with TDP-43 and inflammation through *in vitro* and *in vivo* models after ART could provide insight into increasing the therapeutic benefit of ART for MND.

1.6 Hypothesis and Aims

The overall goal of this PhD project is to determine the role of endogenous retroviruses, inflammation and TDP-43 in MND and how this association is influenced by antiretroviral therapy. If we can determine the efficacy and mechanism of action of Triumeq, and how it relates to TDP-43, inflammation and ERVs, we can determine any potential of increasing the therapeutic benefit of using antiretrovirals for treatment of MND. To achieve the project goals, we proposed the following hypotheses:

Hypothesis 1: In hTDP43 mice, antiretroviral Triumeq treatment decreases endogenous retroviruses, inflammatory signals and TDP-43 pathology in the brain and spinal cord which improves MND-like motor symptoms, increases lifespan and reduces levels of the MND biomarker, urinary p75^{ECD}

Hypothesis 2: Exogenous viral infection or inflammatory stimuli will induce HERV-K expression and increase TDP-43 pathology and the addition of antiretroviral therapy will reduce HERV-K expression and TDP-43 expression

To address these hypotheses, I aim to:

Aim 1:

- a) Determine the effects of antiretroviral therapy on TDP-43 pathology, inflammation, motor symptoms and p75^{ECD} in a TDP-43 mouse model (hTDP43ΔNLS) of MND (**Chapter 3**)
- b) Determine the therapeutic benefit of increasing the dose of Triumeq on disease progression, motor performance and p75^{ECD} in a TDP-43 mouse model (**Chapter 4**)

Aim 2:

- a) Characterise HERV-K expression in multiple human cell lines (**Chapter 5**)
- b) Determine the effect of exogenous viral infection and inflammatory stimuli on TDP-43 and HERV-K expression (**Chapter 5**)

CHAPTER 2. MATERIALS AND METHODS

2 MATERIALS AND METHODS

2.1 Materials

2.1.1 Primers

All oligonucleotide primers were purchased from GeneWorks or Integrated DNA Technologies and a stock concentration of 100 μM was obtained by resuspension in sterile water (Baxter) and stored at $-20\text{ }^{\circ}\text{C}$. Primers were further diluted to 20 μM working solution. Details of human and mouse primer used for the study are provided in **Table 2.1**.

2.1.2 Antibodies

Primary and secondary antibodies used in ELISA and immunofluorescence (IF) throughout this study are presented in **Table 2.2**

2.1.3 Buffers

Details of buffers used in this study are presented in **Table 2.3**

Table 2.1 Primer sequences used for amplification of mRNA

Primer	Species	Accession Number	Sequence Forward (F) and Reverse (R)	Amplicon Size (base pair)
HERV-K (Pan)	Human	Sequence kindly provided by Dr. Avindra Nath	F: ATTTGGTGCCAGGAACTGAG R: GCTGTCTCTTCGGAGCTGTT	179
HERV-K env	Human	Sequence kindly provided by Dr. Avindra Nath	F: CTGAGGCAATTGCAGGAGTT R: GCTGTCTCTTCGGAGCTGTT	164
HERV-K gag	Human	Sequence kindly provided by Dr. Avindra Nath	F: AGCAGGTCAGGTGCCTGTAACATT R: TGGTGCCGTAGGATTAAGTCTCCT	214
HERV-K pol	Human	Sequence kindly provided by Dr. Avindra Nath	F: TCACATGGAAACAGGCAAAA R: AGGTACATGCGTGACATCCA	140
TDP-43	Human	NM_007375.4	F: GTACGGGGATGTGATGGATG R: CTGCGCAATCTGATCATCTG	85
ICAM-1	Human	NM_000201.3	F: TGTTTCCTGCCTCTGAAGC R: CTTCGTTTGTGATCCTCCG	282
Cyclophilin	Human	NM_021130.4	F: GGCAAATGCTGGACCCAACACAAA R: CTAGGCATGGGAGGGAACAAGGAA	355
GAPDH	Mouse	NM_008084.3	F: GACGGCCGCATCTTCTTGTGC R: TGCCACTGCAAATGGCAGCC	120
IFN- β	Mouse	NM_010510.1	F: AGAAAGGACGAACATTCGGAAA R: CCGTCATCTCCATAGGGATCTT	104
MMTV	Mouse	AF243039.1	F: GATGGTATGAAGCAGGATGG R: AAGGGTAAGTAACACAGGCAGATGTA	248
IL-6	Mouse	NM_031168.2	F: GAGGATACCACTCCCAACAGACC R: AAGTGCATCATCGTTGTTCATACA	141
CXCL10	Mouse	NM_021274.2	F: GCCGTCATTTTCTGCCTCAT R: GGCCCGTCATCGATATGG	101
TNF- α	Mouse	NM_013693.3	F: CATCTTCTCAA AATTCGAGTGACAA R: TGGGAGTAGACAAGGTACAACCC	175

Table 2.2 Antibodies used in ELISA and Immunofluorescence

	Antibody	Species	Experiment	Clonality	Supplier
PRIMARY ANTIBODIES	Anti-human p75 antibody (MLR1)	Mouse	ELISA	Monoclonal	Produced from hybridoma cell lines, supplied by A/Prof Rogers (Flinders University, Rogers <i>et al.</i> , 2006)
	Anti-mouse p75	Goat	ELISA	Polyclonal	Sigma-Aldrich Australia (Cat# N5788)
	Anti-NeuN	Mouse	IF	Monoclonal	ProteinTech via United Bioresearch (Cat# 6836-1-Ig)
SECONDARY ANTIBODIES	Anti-hTDP-43	Rabbit	IF	Polyclonal	ProteinTech via United Bioresearch (Cat# 8007-1-RR)
	Biotinylated Anti-goat	Bovine	ELISA	Polyclonal	Jackson ImmunoResearch Laboratories (Cat# 805-065-180)
	649 Anti-mouse	Donkey	IF	Monoclonal	Jackson ImmunoResearch Laboratories (Cat# 715-175-150)
	488 Anti-rabbit	Donkey	IF	Monoclonal	Jackson ImmunoResearch Laboratories (Cat# 75-545-152)

Table 2.3 Buffers used in this project

Buffer	Experimental Use	Components	Supplier
20x Phosphate Buffered Saline (PBS; pH = 7.4)	Buffers	1.46 mM KH ₂ PO ₄ 136.9 mM NaCl 2.68 mM KCl 8.1 mM NaHPO ₄	Chem supply
Sodium Nitrate (pH = 7.4)	Mouse spinal cord and brain fixation	1% (w/v) sodium nitrate 1x PBS	ChemSupply
Zamboni's Fixative (pH = 7.4)	Mouse spinal cord and brain fixation	4% (w/v) PFA 7.5% (v/v) Picric acid 1x PBS pH to 7.4 with HCL	Sigma
30% Sucrose	Mouse spinal cord and brain fixation	30% (w/v) sucrose 0.1% (v/v) sodium azide 1x PBS	ChemSupply
Coating Buffer (pH = 9.6)	ELISA	25mM Na ₂ CO ₃ 25mM NaHCO ₃ 0.01% (w/v) Thimerosal pH to 9.6 with NaOH	ChemSupply
Wash Buffer	ELISA	5% (v/v) 20x PBS 0.05% (v/v) Tween-20	Sigma
Sample Buffer (pH = 7.3)	ELISA	5% (v/v) 20x PBS 0.05% (v/v) Tween-20 0.01% (w/v) Thimerosal 2% (w/v) BSA	Sigma ChemSupply Sigma
Blocking Buffer (pH = 7.3)	ELISA	5% (v/v) 20x PBS 0.05% (v/v) Tween-20 0.01% (w/v) Thimerosal 2% (w/v) BSA	ChemSupply Sigma ChemSupply Merck Millipore
Cell culture media	Cell Culture	DMEM (Gibco; Cat# 11965092) 100 U/mL Penicillin 0.1 mg/ml Streptomycin 1% (v/v) GlutaMAX supplement 10% (v/v) Foetal Calf Serum	Thermo Fisher Scientific

2.2 Methods

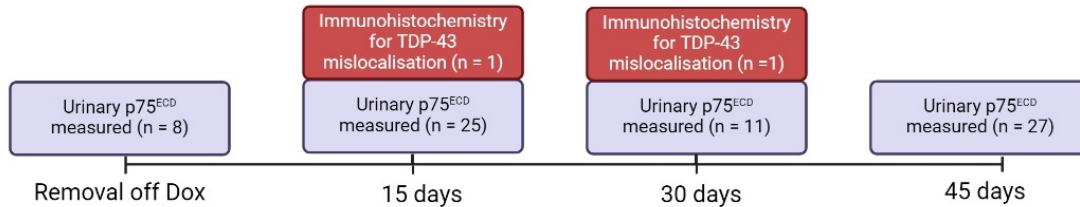
2.2.1 Animal Welfare

All experiments involving mice were reviewed and approved by the Flinders University Animal Welfare Committee (Ethics #2931) and in accordance with the Animal Welfare Act 1985. The TDP-43 transgenic mice (hTDP-43 Δ NLS), as described in section 1.3.2.2 and shown in **Figure 1.3**, were bred at the University of Queensland by Dr. Adam Walker and shipped to Flinders Medical Centre where they were housed in the animal facility. Prior to the start of the experiments, mice were given free access to water and rodent chow with 200 mg/kg Doxycycline (Dox Diet #3888, BioServ). On day one of the experiments, mice were placed on normal rodent chow lacking Dox and continued to be provided with free access to water. Towards disease end-stage, mice were given easier access to food and water through soaked food. Control mice were either non-transgenic C57BL/6 mice, which were age and gender-matched to the transgenic mice, bred at the Flinders Medical Centre Animal House (Ethics #293) or they were litter-matched controls lacking the hTDP-43 Δ NLS transgene, bred alongside the TDP-43 transgenic mice at the University of Queensland. A timeline of each study and the study measurements used can be seen in **Figure 2.1** and **Figure 2.2**.

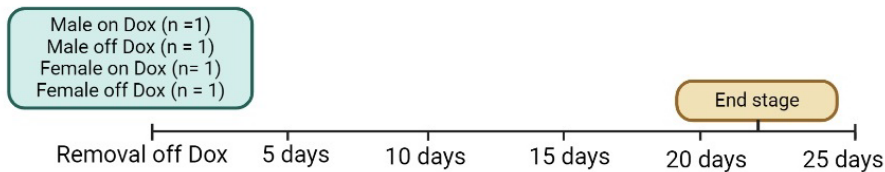
2.2.2 Triumeq Treatment Administration of TDP-43 mice

On day one of the experiments, the mice were placed on Doxycycline-lacking chow and were given the Triumeq treatment. A homogenous mixture of 0.0127 g of crushed Triumeq (ViiV Healthcare; supplied by Professor Julian Gold) and 1.5 g of peanut butter was administered to the mice daily for oral consumption. The mice that were not receiving the treatment were given 1.5 g of peanut butter without Triumeq daily. This procedure continued daily until the mice reached end-stage disease, as defined by a neurological score of 4 (**Table 2.4**) or ethical end point due to weight loss.

A. Validation of TDP-43 mouse model



B. Pilot Study for Dox Removal



C. Pilot Study for Triumeq Treatment

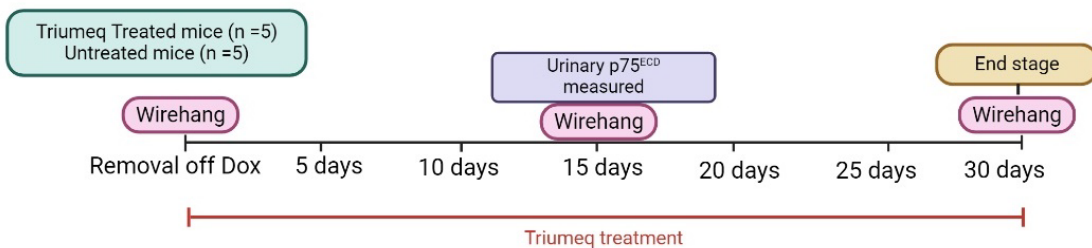
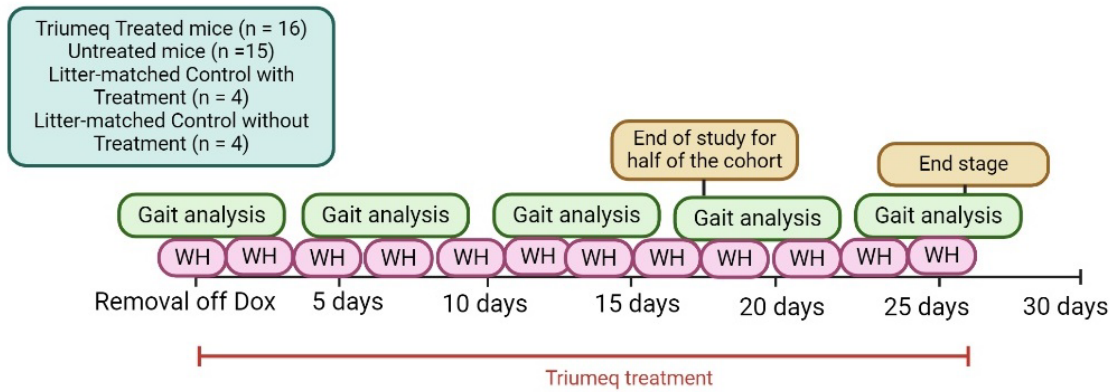


Figure 2.1 Experimental timeline of the validation and pilot studies for Triumeq treatment in hTDP-43 Δ NLS mice

Experimental timeline of treatment and measurements taken for **A.** the validation of the TDP-43 mouse model, **B.** the Pilot study for Dox removal in hTDP-43 Δ NLS mice and **C.** the pilot study for the Triumeq treatment

D. Triumeq Treatment Study



E. Double Dose Triumeq Treatment Study

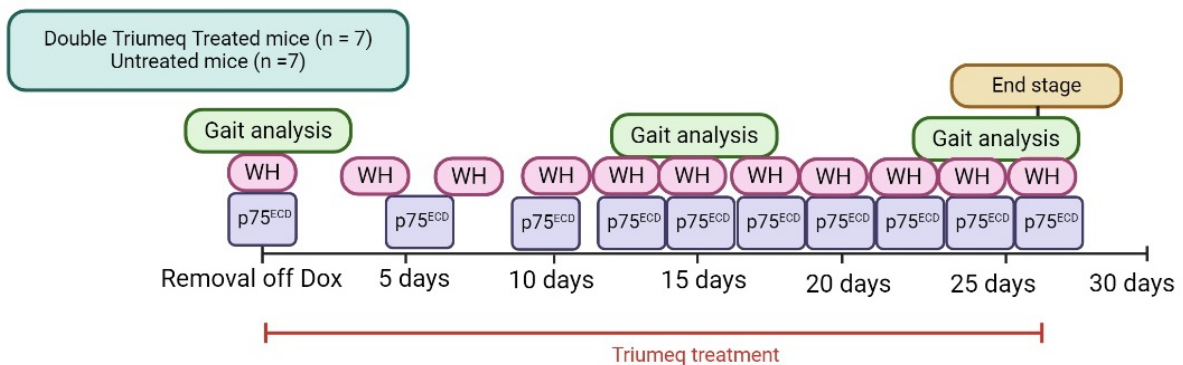


Figure 2.2 Experimental timeline of the Triumeq treatment in hTDP-43 Δ NLS mice

Experimental timeline of treatment and measurements taken for **D.** the Triumeq treatment study in hTDP-43 Δ NLS and **E.** the double dose Triumeq treatment study. WH = Wirehang test

2.2.3 Mouse Behavioural testing

As per ethics, disease end-stage of the mice was determined by a neurological score of 4 (**Table 2.4**) or a weight loss of 15%, whichever occurred first. At a neurological score of 3, mice were given access to soaked food.

2.2.3.1 Weight Measurement

The mice were weighed every day to monitor the overall health of the mice and to determine disease end-stage. At end-stage, the mice weights were recorded twice daily. A 10% weight loss, mice were given access to soaked food.

2.2.3.2 Neurological Scores

Along with their weights, the neurological score of the mice were measured daily. The neurological score system for the mice can be seen in Table 2.4.

Table 2.4 Neurological score explanation for TDP-43 mice (Adapted from Leitner et al., 2009)

Neurological Score	Explanation of score
0	Normal hindlimb extension reflex when mouse is suspended by its tail. Normal gait and normal righting reflex
1	The hindlimb presents abnormal splay as determined by collapse or partial collapse of leg extension towards lateral midline. Showing trembling during tail suspension or clasped hindlimbs during tail suspension. Slightly abnormal gait but normal righting reflex
2	The hindlimb is partially or completely collapsed without much extension. The hindlimb is dragging while walking and the righting reflex is slowed or normal, and toes are curled downwards during a 75cm walk
3	The hindfeet are unable to grasp or there is minimal joint movement. The righting reflex is slowed but the mouse is able to right itself within 30 seconds from both sides
4	Rigid paralysis of both hindlimbs and the mouse is showing no forward motion. The mouse is unable to right itself within 30 seconds from either side

2.2.3.3 Grip Duration using the Wirehang Test

Throughout the study, the motor strength and disease progression of the mice was assessed through grip duration using the wirehang test, as previously described in Crawley (1999) and Miana-Mena *et al.* (2005). The mice were placed on a wire lid and the lid was turned upside down. Latency to fall was measured from the time when the lid was turned upside-down to when the mice fell from the wire. Latency to fall was measured three times per mouse with a rest time of one minute in between trials. A cut-off time was set to 180 seconds.

2.2.3.4 Gait Analysis

Mice were assessed for motor function using the gait analysis test, adapted from Wertman *et al.* (2019). The hindlimbs of the mice were marked with a food-safe blue food colouring. The mice were placed at the start of a 60 cm length of paper where they walked across the page into an enclosed space with access to food. Two trials were undertaken per mouse with a 60 second break in between each trial. Gait was measured through stride width, length and toe spread. Stride length was measured from the middle of one hindlimb print to the middle of the next hindlimb print. Stride width was measured by distance between the hindlimb prints and toe spread measured by the distance between the two outermost toes. An example of the measurements taken with reference to a control mouse with no gait abnormalities can be seen in **Figure A.3** in the appendix.

2.2.3.5 Mice Urine Collection

Urinary samples were collected from untreated and treated TDP-43 mice and litter-matched controls across the study. Mice were placed in a plastic cage and light pressure was applied to the caudal area of the back with a thumb and forefinger to stimulate urine release, adapted from Chew and Chua (2003). Urine was collected immediately and stored in a microcentrifuge tube (Axygen). Samples were centrifuged at 2000 x g for 5 minutes before storage at -80 °C until use.

2.2.4 Spinal Cord and Brain Extraction for Immunohistochemistry

Mice were anaesthetised with isoflurane (Zoetis) and perfused with sodium nitrate and Zamboni's fixative. Spinal cords and brains were extracted and stored in Zamboni's fixative overnight at 4 °C and cryoprotected using 30% sucrose until tissue was no longer yellow. Spinal cords were washed in PBS and placed in Optimal Cutting Temperature (OCT) compound for 5 mins. Spinal cord sections were cut into the lumbar, thoracic and cervical spinal cord regions as described in Sengul and Watson (2012) and placed into embedding cryomolds containing OCT. Whole brain was placed into OCT-filled cryomolds. The cryomolds containing the tissue were placed in isopentane which had been chilled with liquid nitrogen to solidify the OCT. Frozen sections were stored at -20 °C until cut. To cut the brain and spinal cord sections, the cryomolds were frozen onto a specimen stage using OCT and mounted in a Cryostat (Leica) and cut at -20 °C. The tissue was cut into 30 µM sections for spinal cord tissue and 50 µM sections for the brain tissue. Cut tissue sections were stored in 1X PBS with 0.1% sodium azide and stored at 4 °C until used for immunohistochemistry and immunofluorescence.

2.2.5 Brain Extraction for RNA Analysis

Mice were placed in a plastic containment unit and anaesthetised with isoflurane (Zoetis) and transcardially perfused with 30 mL sodium nitrate and 30mL Zamboni's fixative. Brain was extracted and the left hemisphere was stored in 1 mL Trizol (Thermo Fisher Scientific) and flash frozen in liquid nitrogen before storage at -80 °C until RNA extraction.

2.2.6 Enzyme-linked Immunosorbent Assay

An ELISA was used for urinary p75^{ECD} detection, as previously described and validated (Shepherd *et al.*, 2017). 96-well assay plates (Costar Corning, Sigma-Aldrich) were coated with 100 µl of 8 µg/ml capture antibody (mouse anti-human p75 MLR1) in coating buffer and incubated for 18 hrs at 4°C with gentle agitation. Plates were washed for 4x2 mins with wash buffer using a BioRad ImmunoWash 1575 Microplate washer (BioRad). Plates were blocked with 180 µl of Blocking Buffer for 4 hrs at 37°C. Mouse p75 (R&D systems) in sample buffer

was used to create a standard curve (1000 pg/ml – 50 pg/ml) and 100 µl/well was added to the plate in triplicate, for the analysis of human-derived samples. Mouse urine diluted (2.5% v/v and 1.25% v/v) in sample buffer was added to the plates at 100 µl/well, along with the standard curve and incubated for 19 hrs at room temperature with gentle agitation. Plates were washed with wash buffer for 5x2 mins and 100 µl of 1 µg/ml detection antibody in Sample Buffer was added to each well (Goat anti-mouse p75 antibody; Sigma-Aldrich Australia) and incubated for 1 hour at room temperature with gentle agitation. Plates were washed again with wash buffer for 5x2 mins and 100 µl/well secondary antibody (Biotinylated bovine anti-goat; Jackson ImmunoResearch Laboratories) at 1 µg/ml in sample buffer was incubated for 30 mins at RT with gentle agitation. Plates were washed with wash buffer for 5x2 mins and 100 µl of 1 µg/ml Streptavidin Horse Radish Peroxidase (HRP; Jackson ImmunoResearch Laboratories) in sample buffer was added to each well and incubated for 20 mins at room temperature with gentle agitation. Plates were washed for 5x2 mins with wash buffer and 50 µl 3,3',5,5'-Tetramethylbenzidine colour substrate kit (TMB; BioRad Australia) was added to each well after final wash and incubated for 15 mins at room temperature with gentle agitation. 50 µl of 2M sulphuric acid was added to each well to stop the reaction. Colourmetric measurement was performed immediately using the Perkin Elmer Victor X4 Multilabel Plate Reader (Perkin Elmer) at 450 nm at room temperature.

2.2.7 Urinary Creatinine Analysis

Mouse urinary creatinine was measured through a creatinine kit, as per manufacturer's instructions (Enzo Life Sciences). Urine samples were diluted to 1:10 with dH₂O and incubated with creatinine detection reagent for 30 mins. Colourmetric measurement was performed using the Perkin Elmer Victor X4 Multilabel Plate Reader (Perkin Elmer) at 450 nm at room temperature.

2.2.8 Urinary p75^{ECD} calculations

Levels of urinary p75^{ECD} from 2.5% (v/v) and 1.25% (v/v) diluted mouse urine was calculated using the following equation:

$$y = mx + c$$

Where m is the gradient of the slope of the standard curve, x is $p75^{ECD}$ ng in diluted mouse urine and c is the constant which is 0.

$$\therefore \text{Absorbance}_{450nm} = p75^{ECD} \text{ ng} \times m$$

$$\therefore p75^{ECD} \text{ ng/mL} = \frac{\text{Absorbance}_{450nm}}{m} \times \text{dilution factor}$$

Urinary $p75^{ECD}$ values were divided by urinary creatinine values as described in Section 2.2.7 to give a final value of ng of $p75^{ECD}$ /mg of creatinine. Coefficient of variance (CV) was calculated from the following equation from triplicate values in two independent assays:

$$\text{Coefficient of variance (\%)} = \frac{\text{Standard Deviation}}{\text{Mean}} \times 100$$

2.2.9 RNA Analysis

2.2.9.1 RNA Extraction

Total RNA was extracted from mice brain tissue, stored in Trizol, and were homogenised using the TissueLyser (Qiagen) for 3x 30 second bursts at 30 Hz with 15 secs rest in between. In brief, 0.2 mL chloroform (ChemSupply) per 1 mL of Trizol was added and centrifuged for 15 mins at 4 °C at 12,000 x g. The RNA-containing aqueous layer was collected and precipitated with 1 mL 100% (v/v) isopropanol (Univar, Ajax) per 1 mL of Trizol. Samples were incubated at RT for 10 mins and centrifuged for 15 min at 4°C at 12,000 x g. RNA pellet was washed with 1 mL 70% (v/v) ethanol (ChemSupply) per 1 mL Trizol and centrifuged for 5 mins at 7,000 x g. The RNA pellet was air-dried and resuspended in 20 μ L nuclease free water prior to DNase I treatment, as per protocol below to remove genomic DNA.

2.2.9.2 DNase I Treatment

The RNA from section 2.2.9.1 was treated with a DNase solution made up of DNase I enzyme (1 U/ μ L; New England BioLabs) and 1 x DNase I reaction buffer (New England BioLabs) and

incubated for 15 mins at 37°C. The reaction was stopped by addition of 5 mM EDTA and incubated for 10 mins at 75°C. The purified total RNA was quantitated by using a NanoDrop Lite (Thermo Fisher Scientific). RNA integrity was measured using the absorbance ratio at 260 nm and 280 nm and considered acceptable at a 260/280 ratio of approximately 2. RNA was stored at -80°C until use.

2.2.9.3 Reverse Transcription

The extracted RNA was reverse transcribed into cDNA. To do this, 500 ng of RNA was incubated with 30 µM random hexamers (New England BioLabs) and RNase-free water (New England BioLabs) and incubated at 65°C for 5 mins before rapidly cooling to 4°C using a thermocycler (Applied Biosystems). A mix of 10 U Moloney Murine Leukaemia Virus (M-MuLV) reverse transcriptase (New England BioLabs), 5 mM dNTPs (New England BioLabs), 10 U RNase inhibitor (New England BioLabs) and 1X M-MuLV reaction buffer (New England BioLabs) was added to each sample. Using the thermocycler, the samples were incubated for 37°C for 90 mins followed by 5 mins at 95°C and cooled to 4°C. The cDNA was diluted 1:2 with nuclease free water and was stored at -20°C until use.

2.2.9.4 Real-time Quantitative Polymerase Chain Reaction (RT-qPCR)

RT-qPCR was performed on the cDNA produced in section 2.2.9.3 and using the primers described in **Table 2.1**. 2 µL of cDNA samples were mixed with 5 µL iTAQ Universal SYBR green (Bio-Rad), 0.5 µL of 20 µM forward and reverse primer and 2 µL of nuclease free water and cycled using a Rotor-gene Q PCR cycler (Qiagen). Samples were run in duplicate and heated to 95 for 5 mins and then cycled 40 times at 95°C for 15 secs, 59°C for 30 secs and 72°C for 30 secs followed by one cycle of 72°C for 5 mins. Cycle threshold (Ct) values were compared to a standard curve of known value for a positive control. A negative control of H₂O and a no template control was used. Melt curve analysis was used to assess for single symmetrical melt profiles. The melt curve qPCR values were normalised to the housekeeping genes: cyclophilin for human PCR and glyceraldehyde-3-phosphate dehydrogenase (GAPDH) for mouse PCR with values calculated according to the double delta Ct method (Rao *et al.*, 2013). Example melt curve and primer validation shown in **Figure A.3**.

2.2.10 Tissue Imaging

2.2.10.1 *Brain Immunofluorescence*

Cryosections were washed in filtered PBS 4 x 15 mins to remove excess OCT. Sections were blocked in 10% donkey serum (Sigma Aldrich) overnight at 4°C. Sections were incubated with primary antibody solution overnight at 4°C or for 3-4 nights at 4°C. Primary antibodies are described in section 2.1.2 and were diluted in antibody diluent reaction solution (ADRS; Sigma Aldrich) and 1% donkey serum. Control samples were incubated with ADRS and 1% donkey serum without the primary antibody. Sections were washed 4 x 15 mins with filtered 1x PBS and placed in secondary antibody solution for 3 hrs at room temperature. The secondary antibodies used are described in section 2.1.2 and were diluted in antibody diluent reaction solution with 1% donkey serum. Sections were washed 4 x 15 mins with filtered 1x PBS before being mounted onto slides with buffered glycerol in PBS (pH = 7.4) or Fluoromount (Thermo Fisher Scientific) and covered with a coverslip. After drying, sections were viewed on a BX50 fluorescence microscope (Olympus).

2.2.10.2 *Cresyl Violet Staining*

Cut spinal cord sections (collection described in section 2.2.4) were mounted onto SuperFrost Plus Adhesion slides (ThermoFisher Scientific) and dried overnight at 37°C. Slides were rinsed in tap water to remove excess salts prior to defatting the tissue in xylene for 2x 15 mins and 100% ethanol for 2x 5 mins. The sections were rehydrated in 90% ethanol for 2x 3 mins followed by 75% ethanol for 2x 5 mins. After rinsing, the sections were stained using a 0.1% cresyl violet stain (0.1% cresyl violet acetate, 60 mM sodium acetate, 0.25% v/v glacial acetic acid) for 15 mins. Excess stain was removed, and the sections were differentiated in 95% ethanol with glacial acetic acid and microscopically monitored for successful differentiation of nuclei and Nissl bodies. Sections were dehydrated in 100% ethanol for 2x 3 mins and cleared in xylene. Coverslips were mounted using Dibutylphthalate Polystyrene Xylene (DPX) mounting medium (Thermo Fisher Scientific). Sections were imaged on a BX53 Brightfield light Microscope (Olympus).

2.2.10.3 Motor Neuron Counts

A segment of the lumbar region (L3-L5) of the spinal cord was sectioned into 30 µM sections and stained with cresyl violet as outlined in 2.2.10.2. Every third section was stained and the motor neurons within the ventral horn were counted as previously described (Zhou *et al.*, 2010, Huang *et al.*, 2011), with motor neurons over 25 µM included in the count (**Figure A.2**)

2.2.11 Cell Culture

2.2.11.1 Cell Maintenance

HeLa cells (Source code: ATCC® CCL-2™) were maintained using aseptic technique in a class II biosafety cabinet. Cells were passaged every 3-4 days using adherent cell culture media (**Table 2.3**) and incubated in a humidified incubator at 37°C with 5% CO₂. Briefly, cells were washed and trypsinised with 1 ml of 0.25% (v/v) trypsin (Thermo Fisher Scientific) for 2-3 minutes at 37°C. 3 mL complete media was added to inhibit further trypsinisation and cells were harvested. Harvested cells were mixed with 0.4% w/v trypan blue (BDH) and counted using a counting chamber (Hawksley). Following counting, 5 x 10⁵ cells, as determined by the calculation below, were reseeded into a 75 cm² flask in 17mL complete media.

$$\text{Cells/mL} = \frac{\text{Dilution factor} \times \text{cells counted per square}}{\text{chamber volume (mL)}}$$

2.2.11.2 Viral and Inflammatory Stimulation of HeLa Cells

The dengue viral stocks were kindly provided by Professor Jillian Carr and viral infection and inflammatory stimuli of cells was kindly completed by Dr. Joshua Dubowsky. In brief, HeLa cells were seeded onto a 6-well plate (Corning) and incubated at 37°C with 5% CO₂ for 24 hrs. Dengue virus (DENV) and lipopolysaccharide (LPS) was added to a 6-well plate and incubated at 37°C with 5% CO₂ for 24 hrs before cells were harvested for RNA analysis as described in 2.2.9.

2.2.11.3 Cell Lines Provided

Analysis of other cell lines occurred through kind provision of mRNA or cDNA. Details of mRNA or cDNA provided for this project are described in **Table 2.5**.

Table 2.5 Cell lines used for RNA analysis provided for this project

Cell Line	Species	Organ/Tissue	Source
Huh7	Human	Hepatocyte (Liver)	Kindly provided by Professor Jill Carr
ARPE-19	Human	Retinal Pigmented Epithelium	Kindly provided by Professor Jill Carr
U937	Human	Epstein Barr Virus transformed Histiocytic lymphoma	Kindly provided by Professor Jill Carr
HEK293	Human	Human Embryonic Kidney	Kindly provided by Professor Jill Carr
SH-YSY5Y	Human	Neuronal	Kindly provided by Dr. Rita Mejzini
ONS	Human	Olfactory Neuroepithelial	Kindly provided by Professor Jill Carr

2.2.12 Data Analysis

Statistical analyses were performed using Prism 10 (GraphPad). Values are representative of the average \pm standard error of measurement (SEM). For the ELISAs, standard curves were plotted using Microsoft Excel and urinary p75^{ECD} levels analysed using One-way ANOVAs with Sidak's multiple comparisons. Two-way ANOVAs with Sidak's multiple comparisons were used to analyse percentage weight change, latency to fall on the wirehang test and analysis of gait in all mice experiments. mRNA expression was analysed via double delta transformation of RT-qPCR and analysed using a Two-way ANOVA with Sidak's multiple comparisons. mRNA expression from cell lines was analysed with a Two-way ANOVA with Tukey's multiple comparisons or a Student's *t*-test. Statistical significance was considered at $p < 0.05$.

**CHAPTER 3.
EFFECTS OF TRIUMEQ TREATMENT ON AN
MND MOUSE MODEL**

3 EFFECTS OF TRIUMEQ TREATMENT ON AN MND MOUSE MODEL

3.1 Introduction

Antiretroviral therapy has been effectively used to suppress the replication of exogenously acquired retroviruses such as HIV (Ghosn *et al.*, 2018). With a suggested association between ERVs and the causation and progression of MND, antiretroviral therapy has been proposed as a novel therapy for MND (Gold *et al.*, 2019), potentially reducing the progression of MND. A recent clinical trial of using a combination antiretroviral, Triumeq, in MND patients has shown promising results for reducing the level of endogenous retroviral activity measured via HERV-K levels in serum of MND patients (Gold *et al.*, 2019). However, the mechanisms underlying the therapeutic benefit remain unclear, including the involvement of the pathological hallmark of MND, TDP-43.

The current study aimed to determine the effects of antiretroviral therapy, Triumeq, on disease outcomes in a mouse model of MND expressing human TDP-43 with a defective nuclear localisation sequence, hTDP43 Δ NLS, on a Dox-suppressible expression system (Walker *et al.*, 2015). For this study, the TDP-43 mouse model was validated for disease progression and initiation of symptoms after removal from Dox and motor symptoms, weight loss and urinary p75^{ECD} increases were measured. The effects of Triumeq were then assessed through disease progression including weight change and neurological score, motor symptoms including performance on a wirehang test and analysis of gait, TDP-43 pathology including TDP-43 solubility within brain tissue, motor neuron count within the spinal cord and muscle denervation from urinary p75^{ECD} analysis.

This chapter describes the pilot study for validation of the mouse model and tolerability of Triumeq before describing the influences of Triumeq on disease progression measured in a cohort of hTDP43 Δ NLS mice.

3.2 Results

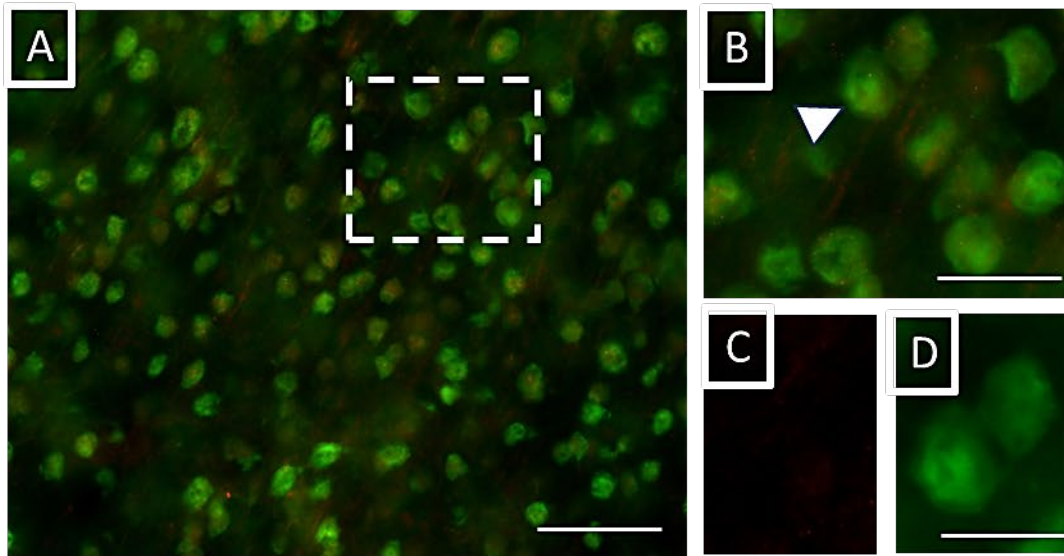
3.2.1 Validation of hTDP-43 Expression and Mislocalisation in hTDP43 Δ NLS mice

To validate the expression and mislocalisation of hTDP-43 in the hTDP43 Δ NLS mice, immunofluorescence of cortical brain sections from non-transgenic control mice on a C57Bl/6 background and the hTDP43 Δ NLS mice on a C57Bl/6 background. Brain sections were stained with hTDP-43 (red) and NeuN (green) as a neuronal marker. **Figure 3.1** shows the lack of hTDP-43 expression in the non-transgenic control mice with a lack of red fluorescence from these sections. In contrast, the cortical brain sections from the hTDP43 Δ NLS mice show hTDP-43 expression as well as mislocalisation of hTDP-43 from the nucleus to the cytoplasm with the hTDP-43 shown surrounding the NeuN-labelled neurons.

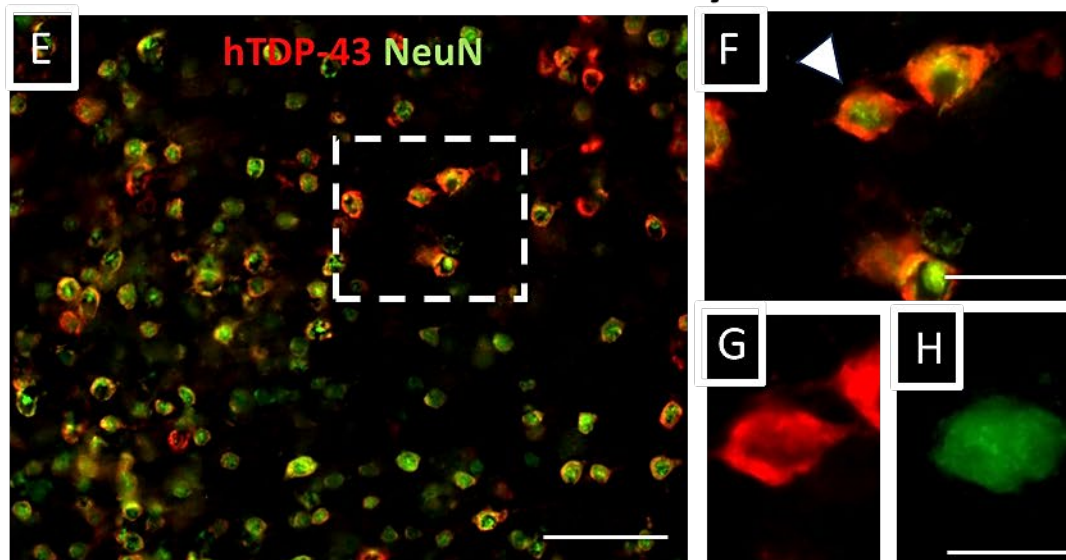
3.2.2 Validation of Urinary p75^{ECD} Levels in hTDP43 Δ NLS mice after Removal from Dox

To confirm that urinary p75^{ECD} was detectable in the hTDP43 Δ NLS mice and to confirm the timeline of disease progression based on p75^{ECD}, urine samples were collected and quantified using a validated ELISA described in section 2.2.6. Urinary p75^{ECD} was detected and quantified in hTDP43 Δ NLS mice on Dox (n = 8) and compared to hTDP43 Δ NLS mice at 2 weeks (n = 25), 4 weeks (n = 11) and 6 weeks (n = 27) off Dox (**Figure 3.2**). There was a significant increase in the level of urinary p75^{ECD} between hTDP43 Δ NLS mice on Dox and 6 weeks off Dox ($p = 0.0329$). There were no significant differences between the hTDP43 Δ NLS mice on Dox and 2 weeks off Dox ($p = 0.983$) or 4 weeks off Dox ($p = 0.0949$). However, there was still a trend towards an increase in the levels of urinary p75^{ECD} from the hTDP43 Δ NLS mice off dox to 2 and 4 weeks off Dox.

Non-transgenic control



hTDP-43 Δ NLS – Day 15



hTDP-43 Δ NLS – Day 30

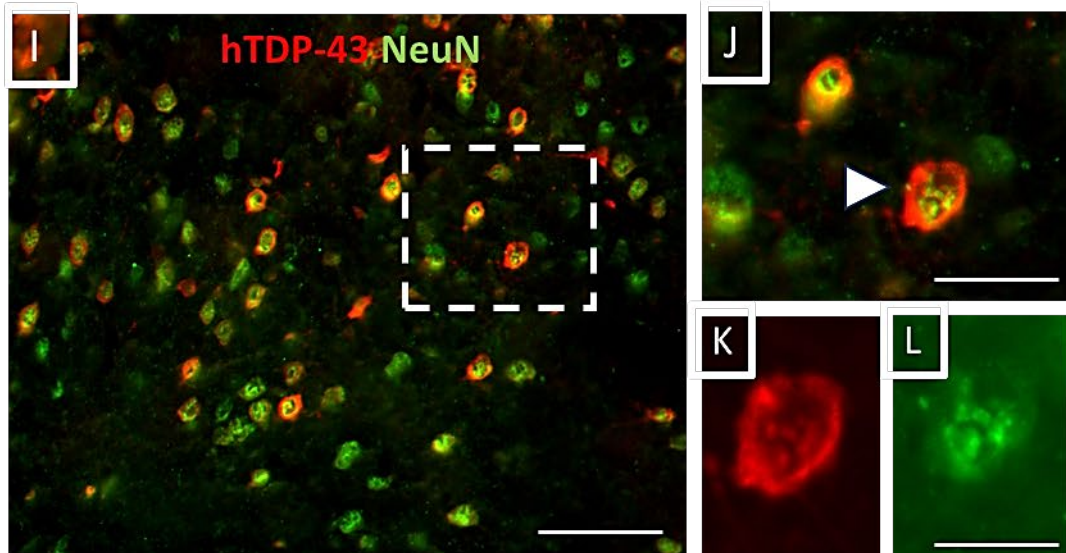


Figure 3.1 hTDP-43 expression and mislocalisation in the cortex of the hTDP-43 Δ NLS mouse model

Representative confocal micrographs (20x) of cortical neurons from hTDP-43 Δ NLS mice off Dox, show hTDP-43 immunofluorescence, which is absent in C57BL/6 control mice **A.** Immunohistochemistry of control mouse cortex labelled with hTDP-43 (red) and NeuN (green) (Scale bar 200 μ M) with inset (**B.**) showing the lack of hTDP-43 within the NeuN labelled neurons (Scale bar 100 μ M). Arrow showing the neuron shown in **C.** and **D.** labelled with hTDP-43 and NeuN, respectively (Scale bar 50 μ M). **E.** Immunohistochemistry of hTDP-43 Δ NLS mouse cortex at 15 days post dox-removal labelled with hTDP-43 (red) and NeuN (green) (Scale bar 200 μ M) with inset (**F.**) showing hTDP-43 in the cytoplasm around the nucleus (Scale bar 100 μ M). Arrow showing the neuron shown in **G.** and **H.** labelled with hTDP-43 and NeuN, respectively (Scale bar 50 μ M). **I.** Immunohistochemistry of hTDP-43 Δ NLS mouse cortex at 30 days post dox-removal labelled with hTDP-43 (red) and NeuN (green) (Scale bar 200 μ M) with inset (**J.**) showing hTDP-43 in the cytoplasm around the nucleus (Scale bar 100 μ M). Arrow showing the neuron shown in **K.** and **L.** labelled with hTDP-43 and NeuN, respectively (Scale bar 50 μ M).

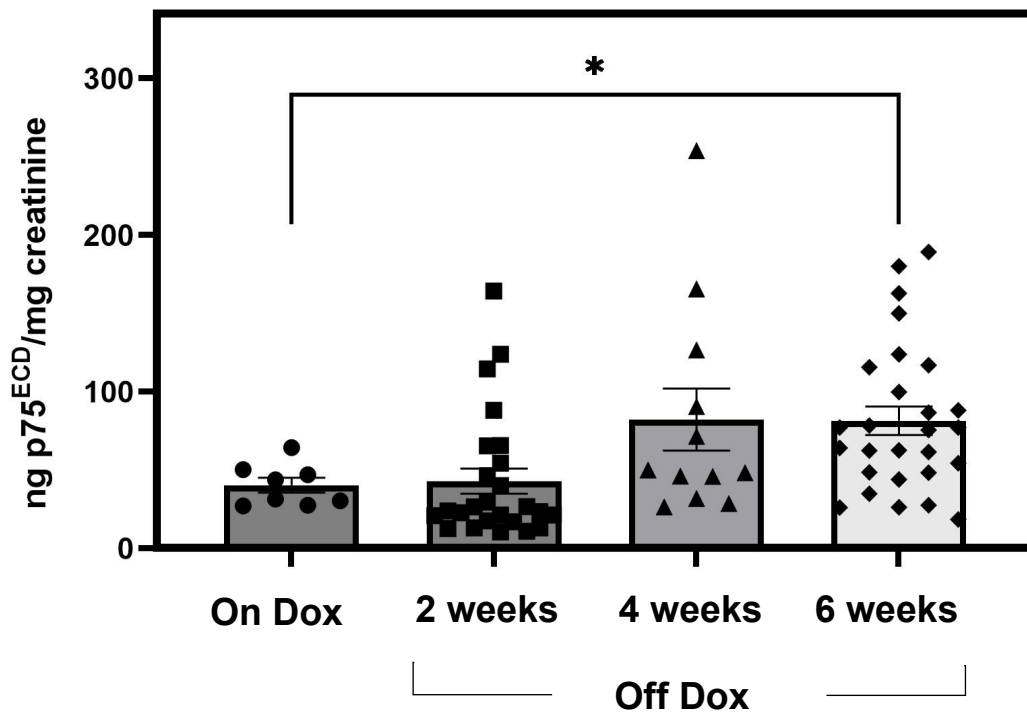


Figure 3.2 Urinary p75^{ECD} levels in hTDP-43ΔNLS mice on Dox and 2, 4 and 6 weeks off Dox

Urinary p75^{ECD} levels were quantified in samples from hTDP-43ΔNLS mice on Dox (n = 8) and compared to p75^{ECD} levels from hTDP-43ΔNLS mice off Dox at the time points 2 weeks (n = 25), 4 weeks (n = 11) and 6 weeks (n = 27). Levels of p75^{ECD} were standardised to urinary creatinine to account for dilution. Results represent the mean ± SEM from 3 biological replicates, 2 technical replicates. One-way ANOVA with Sidak's multiple comparisons test * $p < 0.05$

3.2.3 Pilot Study for the Validation of MND Progression in hTDP43 Δ NLS Mice off Doxycycline

For the pilot study, four hTDP43 Δ NLS mice on a mixed genetic background of B6 and C3H, as described in section 2.2.1 and shown in the timeline in **Figure 2.1B**, were used to assess the progression of disease after removal off Dox and to determine any sex differences in disease progression. Two mice, one female and one male, were removed off Dox and placed onto regular chow to initiate hTDP-43 overexpression and the development of MND-like symptoms. The other two mice remained on the Dox. Mouse weight was used to assess disease progression based on reductions in mass from muscle degeneration and neurological score was used to assess disease progression through the hindlimb function.

Figure 3.3 shows the percentage weight change of the male (**Figure 3.3A**) and female (**Figure 3.3B**) mice on and off Dox. The mice that were removed off Dox showed a significantly higher percentage weight loss compared to the gender and age matched mice that remained on Dox. These mice also developed motor symptoms that mimicked MND-like motor symptoms, including decreased motor function of the hindlimbs according to hindlimb dragging

Male and female differences were observed during the pilot study, including weight loss in the female mouse that was still on Dox, while the male mouse that remained on Dox, did not lose weight. The mice that were removed off the Dox diet reached the ethical endpoint, according to their weight loss, sooner than those that remained on Dox (**Figure 3.3**).

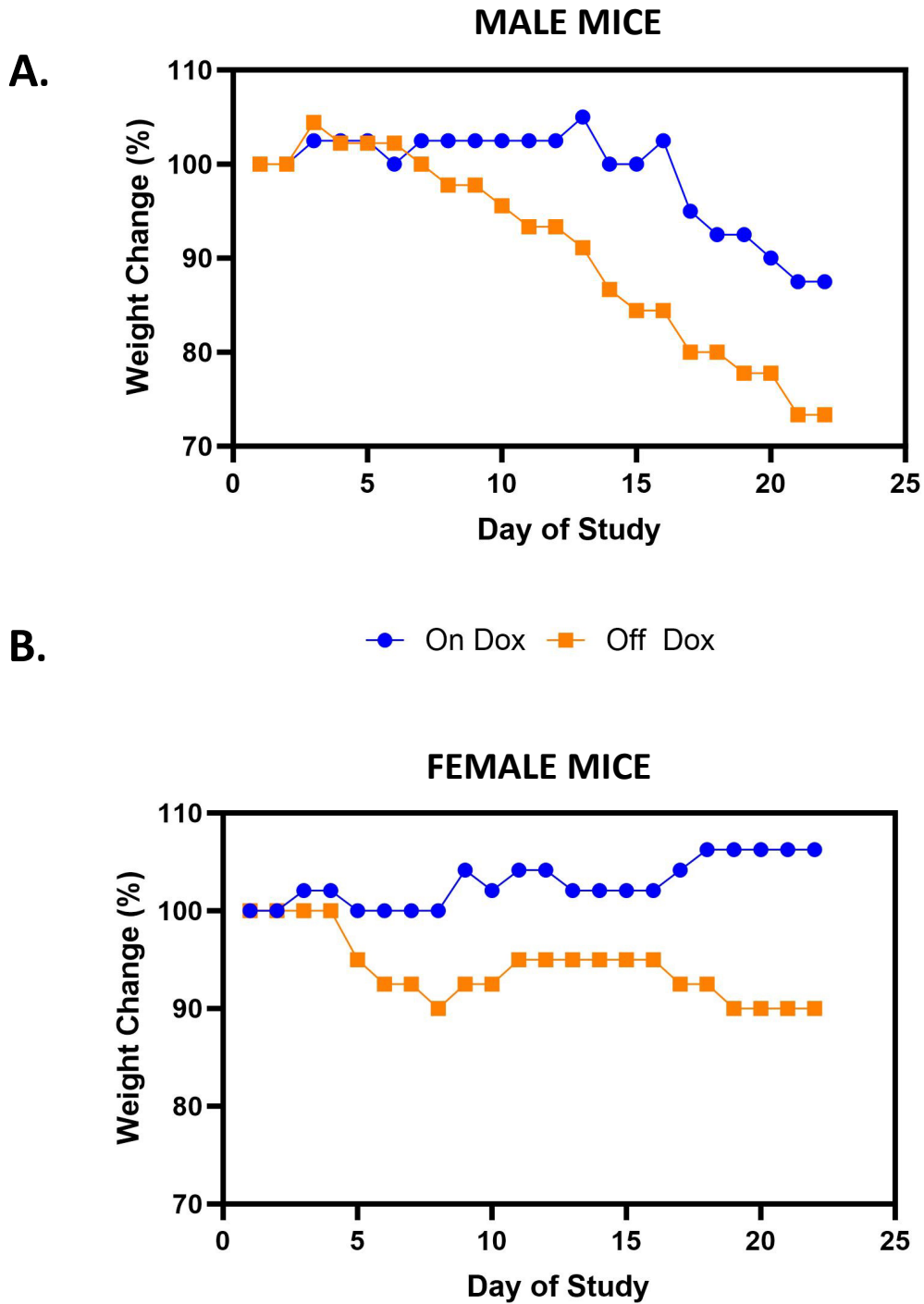


Figure 3.3 Removal of Dox initiates MND-like symptoms in hTDP-43 Δ NLS mice

A pilot study to validate the removal of Dox and initiation of MND-like symptoms in the hTDP-43 Δ NLS mouse model. **A.** male hTDP-43 Δ NLS mice (n= 2) and **B.** female hTDP-43 Δ NLS mice (n = 2) on and off Dox were compared based on percentage weight change as a measure of disease progression.

3.2.4 Pilot Study to Assess the Tolerability and Palatability of Triumeq in hTDP43ΔNLS Mice

3.2.4.1 *Triumeq Does not Influence Disease Progression*

After previous validation that Dox removal induces the onset of MND-like disease, the tolerability and palatability of Triumeq was assessed using mice bred on a C57BL/6 background resulting in a lower starting weight than the mice bred on the mixed B6 and C3H background. Based on the sex difference noted in the previous study, only female mice were used in the following studies. A small cohort of hTDP-43ΔNLS mice (n = 10) were removed off Dox, with half the cohort treated with Triumeq. Disease progression was assessed through weight loss and neurological score, and the wirehang test was used as a measure of motor performance. The study timeline can be seen in **Figure 2.1C**. Dox removal did initiate disease in both the untreated and treated mice as shown by weight loss and motor symptoms shown through an increase in neurological score. However, there was no difference between the treated and untreated mice according to weight loss (**Figure 3.4A**) and neurological score (**Figure 3.4B**), with both groups showing a similar progression of disease and the study reached the ethical endpoint according to weight loss, around the same time of 30 days post-treatment onset and removal off Dox.

3.2.4.2 *Triumeq Influences Motor Performance at 15 Days Post-treatment Onset*

Motor performance was assessed through the latency to fall on the wirehang test, measuring hindlimb strength. Motor performance was measured on day 1, day 15 and day 30 after removal from Dox and post treatment onset. There was a significantly lower latency to fall for the untreated mice compared to the treated mice at day 15 (**Figure 3.5**; $p = 0.0032$). This effect was no longer seen by the time the mice reached the ethical endpoint, at 30 days post treatment onset.

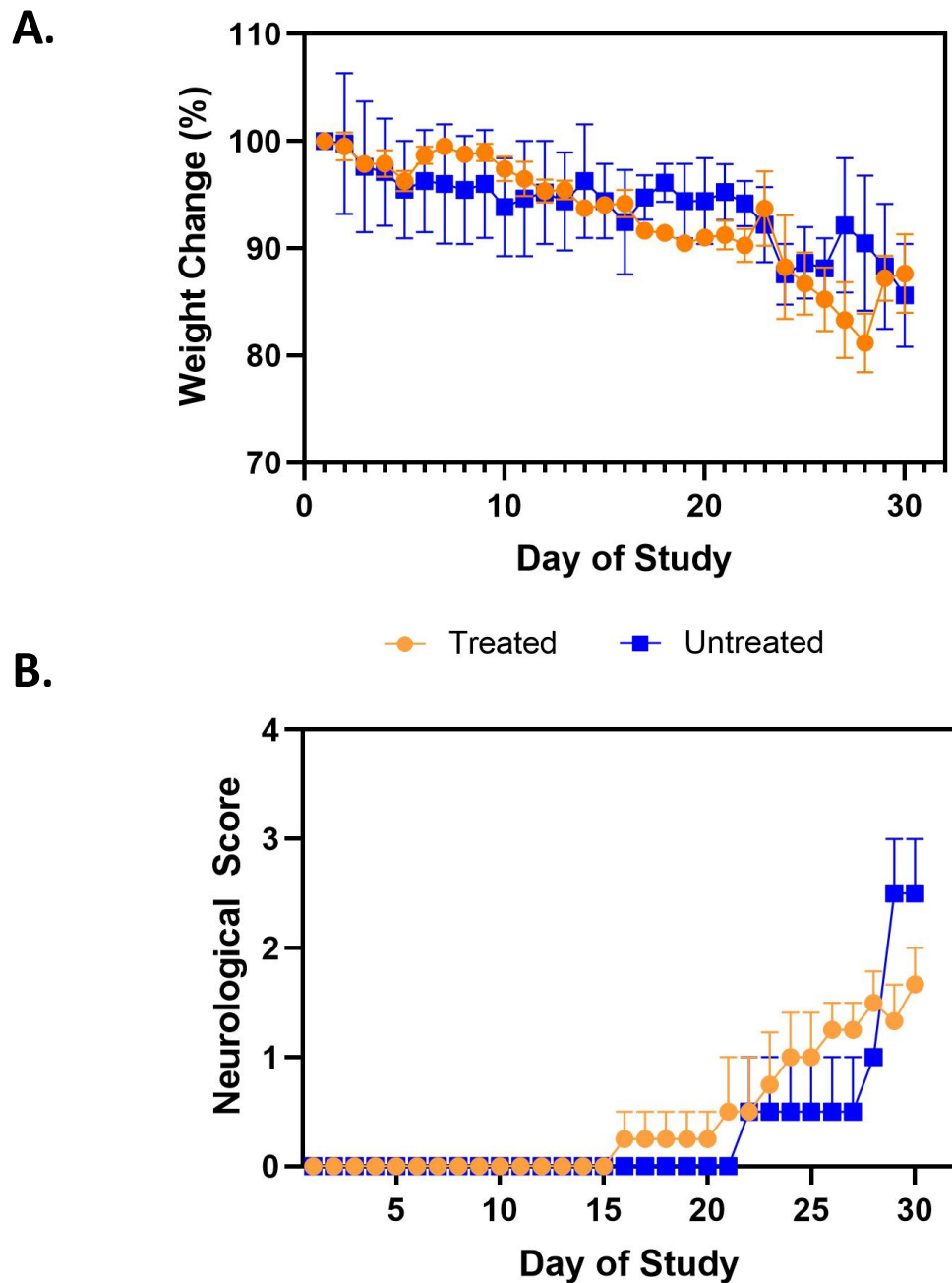


Figure 3.4 Percentage weight change and neurological score after Triumeq treatment in hTDP-43 Δ NLS mice

A cohort of hTDP-43 Δ NLS mice was treated with antiretroviral therapy, Triumeq, (n = 5) and compared to an untreated hTDP-43 Δ NLS cohort (n = 5) and disease progression was measured through **A.** percentage weight change and **B.** neurological score where 0 = normal hindlimb movement and normal gait, 1 = partial hindlimb splay and slightly abnormal gait, 2 = hindlimb dragging while moving forward, 3 = minimal hindlimb movement and slow and abnormal gait and 4 = rigid paralysis in hindlimbs and no forward motion, deemed the ethical end-point. Results represent the mean \pm SEM, Two-way ANOVA with repeated measures and Sidak's multiple comparisons.

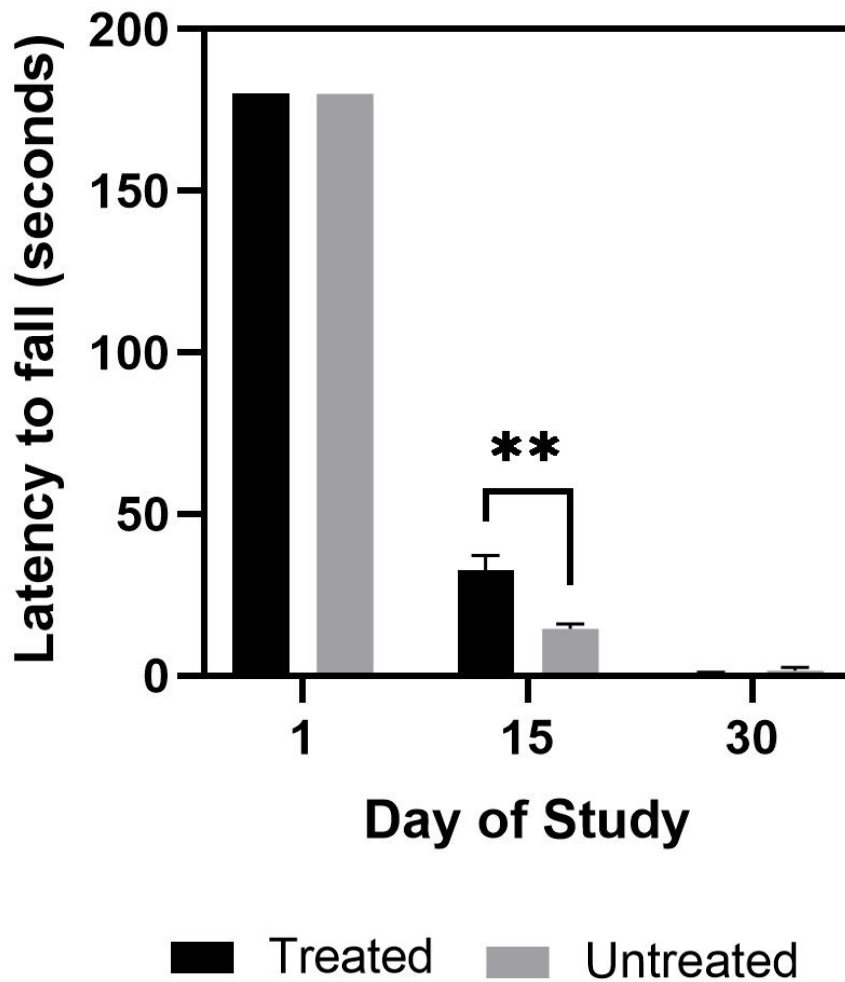


Figure 3.5 Latency to fall on the wirehang test between treated and untreated hTDP-43ΔNLS mice

Mean latency to fall for a cohort of treated hTDP-43ΔNLS mice (n = 5) and untreated hTDP-43ΔNLS mice (n = 5) at day 1, 15 and 30 post-treatment onset. Results represent the mean ± SEM, Two-way ANOVA with Sidak's multiple comparisons. ** = $p < 0.005$

3.2.5 Effects of Triumeq Treatment in hTDP43ΔNLS Mice

3.2.5.1 *Triumeq Treatment Does Not Influence Disease Progression According to Weight Loss and Neurological Score*

After validation of the removal of Dox resulting in MND-like symptoms and promising results for Day 15 being a crucial time point for differential impact of Triumeq, a larger cohort of hTDP43ΔNLS mice were used to assess the effects of Triumeq treatment further. As described in section 2.2.2 and shown in **Figure 2.2D**, mice were administered Triumeq daily and weight and neurological score were used to assess disease progression until mice reached pre-determined ethical endpoints, according to weight loss or neurological score. Treated and untreated hTDP43ΔNLS mice along with treated and untreated litter-matched non-transgenic controls were compared based on percentage weight change (**Figure 3.6A**) and neurological score (**Figure 3.6B**). There was no significant difference according to percentage weight change between the treated and untreated hTDP43ΔNLS mice ($p = 0.833$). There was no significant difference between the treated and untreated litter-matched controls after Dox removal ($p = 0.998$). However, there was a significant difference between the litter-matched controls and the hTDP43ΔNLS mice regardless of treatment group at the end of the study course ($p = <0.0001$) showing an induction of disease from Dox removal but a lack of affect from Triumeq.

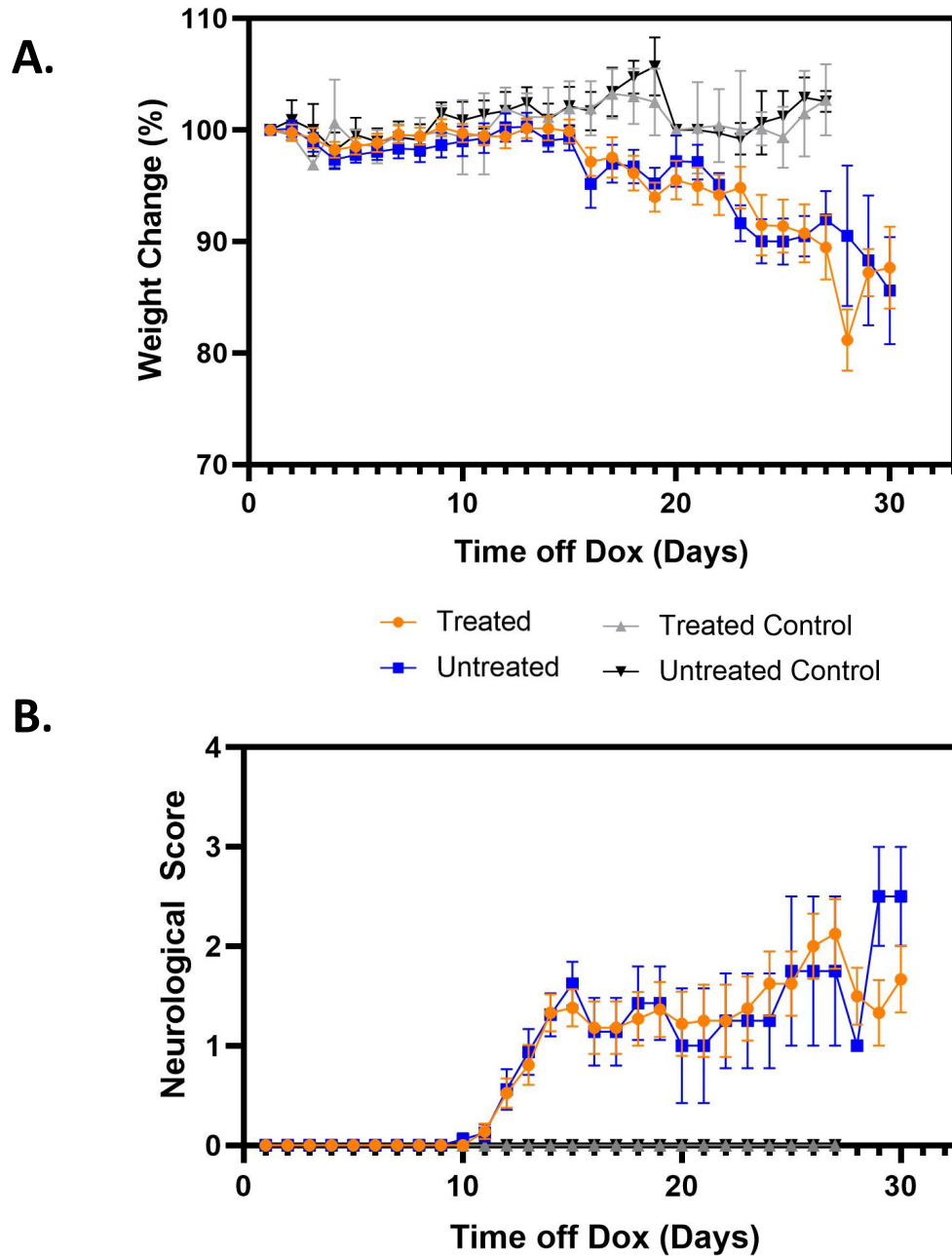


Figure 3.6 Percentage weight change and neurological score in a large cohort of hTDP-43ΔNLS mice

A cohort of hTDP-43ΔNLS mice was treated with antiretroviral therapy, Triumeq, (n = 21) and compared to an untreated hTDP-43ΔNLS cohort (n = 19), treated litter-matched control cohort (n = 4) and an untreated litter-matched control cohort (n = 4) and compared **A.** percentage weight change and **B.** neurological score where 0 = normal hindlimb movement and normal gait, 1 = partial hindlimb splay and slightly abnormal gait, 2 = hindlimb dragging while moving forward, 3 = minimal hindlimb movement and slow and abnormal gait and 4 = rigid paralysis in hindlimbs and no forward motion, deemed the ethical end-point. Results represent the mean ± SEM, Two-way ANOVA with Sidak's multiple comparisons test. 119

3.2.5.2 *Triumeq Treatment Influences Motor Performance*

Motor performance was assessed through the latency to fall on the wirehang test, measured at multiple time points across the experimental study. A cohort of treated hTDP43 Δ NLS mice (n = 21), untreated hTDP43 Δ NLS mice (n = 19), treated litter-matched controls (n = 4) and untreated litter-matched controls (n = 4) were compared based on the latency to fall (**Figure 3.7**). The litter-matched controls, regardless of treatment group, consistently had a latency to fall at the cut-off time of 180 seconds. The treated and untreated hTDP43 Δ NLS mice showed the first drop in latency to fall on day 15 of the study which was followed by a large drop in the latency to fall by day 17. On day 17, there was a significant difference between the treated and untreated hTDP43 Δ NLS mice with the untreated group showing a significantly lower latency to fall compared to the treated group ($p < 0.0001$). While there was a trend for a lower latency to fall for the untreated group for the study course, this was not significantly different to any other time point in the study.

3.2.5.3 *Triumeq Treatment Influences Gait*

Gait analysis was also used as another measure of motor performance, completed on day 1, 8, 15, 22 and 27. Stride length was measured from the distance of one hindlimb pawprint to the following hindlimb pawprint on the same side of the body. Stride width was measured as the distance between left and right hindlimb pawprints. There were no significant differences between treated and untreated hTDP43 Δ NLS mice on day 1, day 8, day 22 or day 27. However, there was a significantly lower stride length in untreated mice on day 15 compared to the treated mice (**Figure 3.8**; $p = 0.0375$). There were no significant differences in stride width between the treated and untreated mice on any day of measurement.

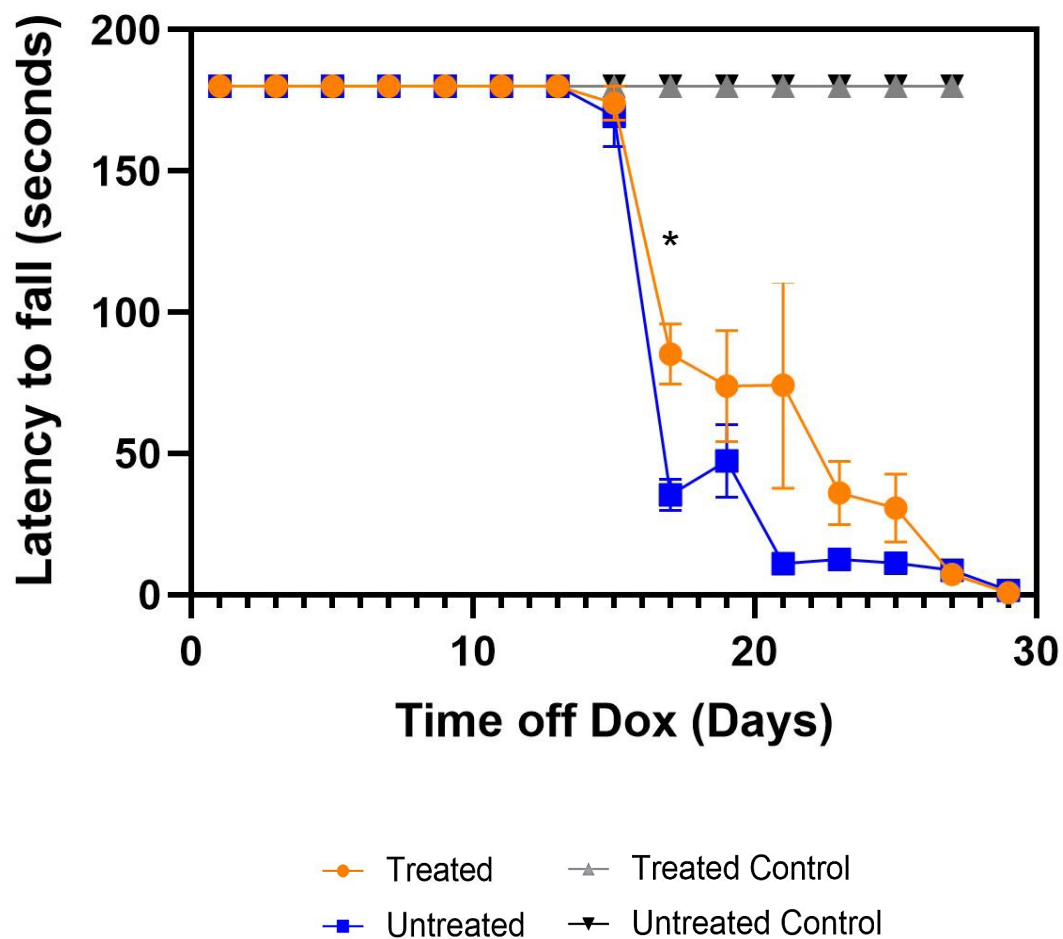


Figure 3.7 Latency to fall on the wirehang test for a large cohort of hTDP-43ΔNLS mice

Mean latency to fall for a cohort of treated hTDP-43ΔNLS mice (n = 21), untreated hTDP-43ΔNLS mice (n = 19), treated litter-matched control cohort (n = 4) and an untreated litter-matched control cohort (n = 4) across the course of the experimental study. Results represent the mean ± SEM, Two-way ANOVA with Sidak's multiple comparisons test. * $p < 0.05$

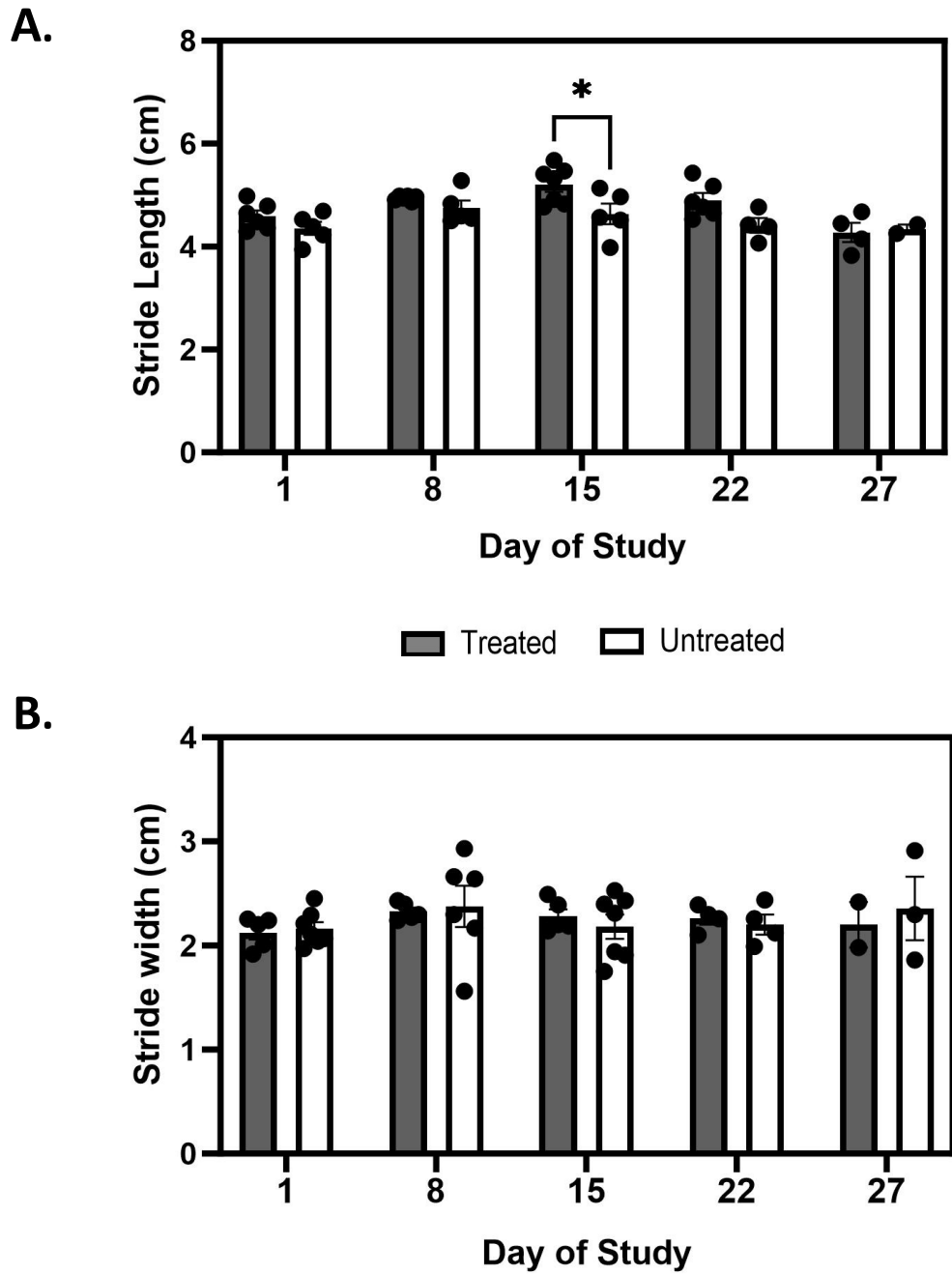


Figure 3.8 Gait analysis including stride length and stride width in treated and untreated hTDP-43ΔNLS mice

Gait analysis of treated hTDP-43ΔNLS mice (n = 7) and untreated hTDP-43ΔNLS mice (n = 5) was measured and assessed by **A.** mean stride length and **B.** mean stride width across the course of the treatment study. Results represent the mean ± SEM, Two-way ANOVA with Tukey's multiple comparisons test. * $p < 0.05$

3.2.5.4 *Triumeq Influences p75^{ECD} Levels*

Using the p75^{ECD} ELISA, urinary p75^{ECD} was detected and quantified in the treated hTDP43ΔNLS mice (n = 6-8) and untreated hTDP43ΔNLS mice (n = 5) at day 1 and day 15. There was no significant difference in the levels of urinary p75^{ECD} levels on day 1 between the treated and untreated mice. On day 15, p75^{ECD} were significantly higher in the untreated hTDP43ΔNLS mice compared to the treated mice (**Figure 3.9**, $p = 0.0489$).

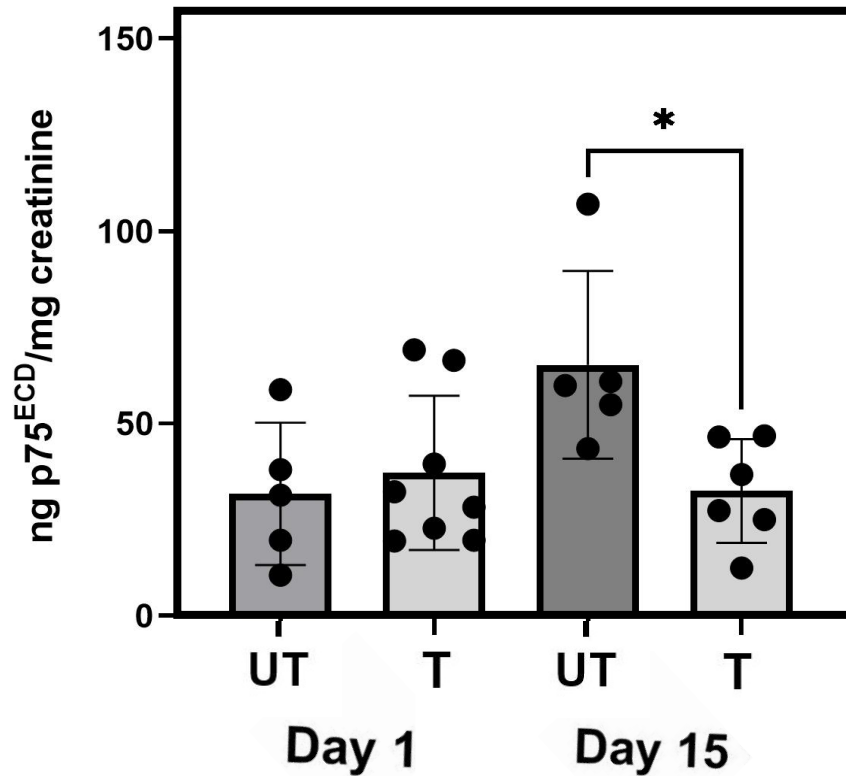


Figure 3.9 Urinary p75^{ECD} levels in treated and untreated hTDP-43ΔNLS mice on day 1 and day 15 post-treatment onset

Urinary p75^{ECD} levels were quantified in samples from treated hTDP-43ΔNLS mice (n = 6-8) and untreated (n = 5) on day 1 and day 15 post-treatment onset. Levels of p75^{ECD} were standardised to urinary creatinine to account for dilution. Results represent the mean ± SEM from 3 biological replicates, 2 technical replicates. One-way ANOVA with Sidak's multiple comparisons test. * $p < 0.05$. UT = Untreated T = Treated

3.2.5.5 *Triumeq Influences Motor Neuron Count in the Spinal Cord*

Using cresyl violet staining, sections of the lumbar spinal cord from treated and untreated hTDP-43 Δ NLS mice and litter-matched controls were analysed for motor neuron count on Day 19 post-treatment onset. **Figure 3.10** shows the histological analysis used to assess motor neuron count within the spinal cord. Based on the histological staining, motor neuron number was counted from 5 sections per mouse from treated mice, untreated mice and litter-matched controls. Shown in **Figure 3.11**, there was a significant difference in the number of motor neurons within the lumbar region between the litter-matched controls and the treated hTDP-43 Δ NLS mice ($p = 0.0001$) and untreated mice ($p = 0.0001$). There was also a significantly lower amount of motor neurons within the untreated hTDP-43 Δ NLS mice compared to the treated mice ($p = 0.00165$).

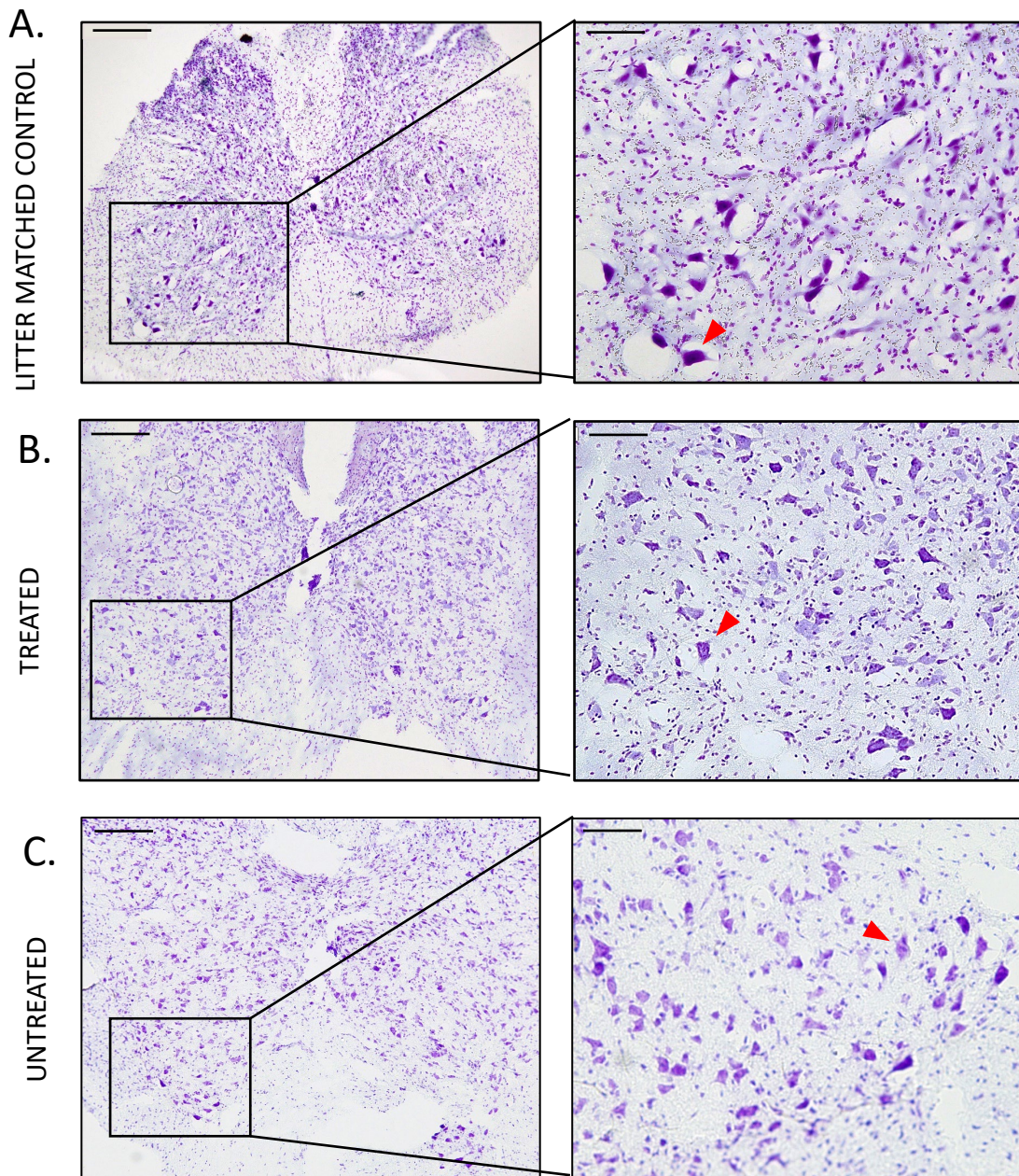


Figure 3.10 Histological presentation of motor neurons within the lumbar spinal cord from treated and untreated hTDP-43 Δ NLS mice

Histological analysis of motor neurons in the lumbar spinal cord from **A.** litter-matched controls **B.** treated and **C.** untreated hTDP-43 Δ NLS mice at day 19 stained with cresyl violet. Red arrows represent a motor neuron included in the count. Scale bar represents 200 μ m for images on the left-hand side and 50 μ m for the images on the right-hand side

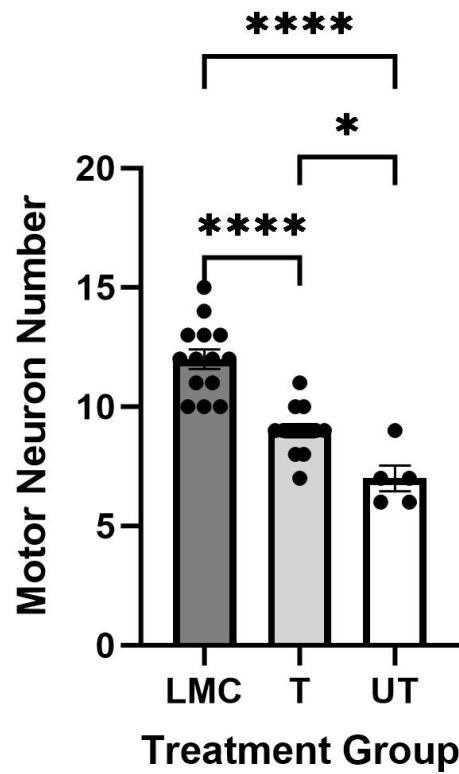


Figure 3.11 Motor neuron count from lumbar spinal cord of treated and untreated hTDP-43ΔNLS mice

Motor neuron count per section from the lumbar region of the spinal cord from litter-matched controls (n = 14), treated (n = 9) and untreated (n = 5) hTDP-43ΔNLS mice at Day 19, counted from the cresyl violet staining depicted in Figure 3.10. Data is representative of mean motor neuron count per section ± SEM. LMC = litter-matched control T = Treated, UT = Untreated. One-way ANOVA with Tukey's multiple comparisons test * = $p < 0.005$, **** = $p < 0.0001$

3.2.5.6 *Triumeq Does Not Influence Expression of TDP-43, MMTV, TNF- α or CXCL10*

Brain tissue from mice that were 19 days post-treatment was analysed for expression of TDP-43, MMTV, CXCL10 and TNF- α . Expression levels were compared between treated hTDP-43 Δ NLS mice, untreated hTDP-43 Δ NLS mice and litter-matched non-transgenic controls. There was significantly higher expression of TDP-43 in the treated hTDP-43 Δ NLS mice compared to the litter-matched non-transgenic controls validating the TDP-43 expression system in the TDP-43 mice (**Figure 3.12A**). However, there was no significant differences between the expression of TDP-43 between the treated and untreated hTDP-43 Δ NLS mice.

The influence of Triumeq on a mouse endogenous retrovirus, MMTV, was analysed and compared between the treated and untreated hTDP-43 Δ NLS mice and the litter-matched controls. There was no significant difference in the expression of MMTV between either treatment group or the litter-matched controls (**Figure 3.12B**).

Due to their involvement in neurodegeneration in MND, the expression of inflammatory markers CXCL10, TNF- α , IL-6 and IFN- β were also analysed. There was low expression of either inflammatory marker in the litter-matched non-transgenic controls. There was induction of inflammatory markers in the hTDP-43 Δ NLS mice with significantly higher expression of TNF- α (**Figure 3.12C**; $p = 0.0073$) and CXCL10 (**Figure 3.12D**; $p = 0.026$) in the treated hTDP-43 Δ NLS mice compared to the litter-matched controls. There were no significant differences in the expression of TNF- α or CXCL10 between the treated and untreated hTDP-43 Δ NLS mice. Other inflammatory markers such as IFN- β and IL-6 were also analysed but there were no significant expression differences between the non-transgenic litter-matched controls and the hTDP-43 Δ NLS mice for either marker, although a trend towards an induction of IFN- β in hTDP-43 Δ NLS mice was found (**Figure 3.12E-F**).

3.2.5.7 TDP-43 Expression Correlates with Inflammatory Marker Expression

Due to the significant induction of TNF- α , CXCL10 and TDP-43 in the transgenic hTDP-43 Δ NLS mice compared to the litter-matched controls, the correlation between TDP-43 and TNF- α and TDP-43 and CXCL10 was analysed. The expression levels were pooled for the treated and untreated mice due to there being no significant differences in the expression levels between the treatment groups. There was no significant correlation between TDP-43 and TNF- α (**Figure 3.13A**; $R^2 = 0.129$, $p = 0.343$). There was a strong and significant correlation between TDP-43 and CXCL10 (**Figure 3.13B**; $R^2 = 0.885$, $p = 0.0002$). There is also a significant moderate correlation between TNF- α and CXCL10 ; $R^2 = 0.609$, $p = 0.0019$).

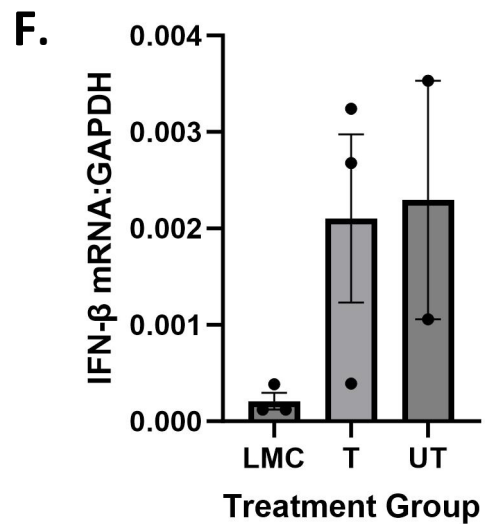
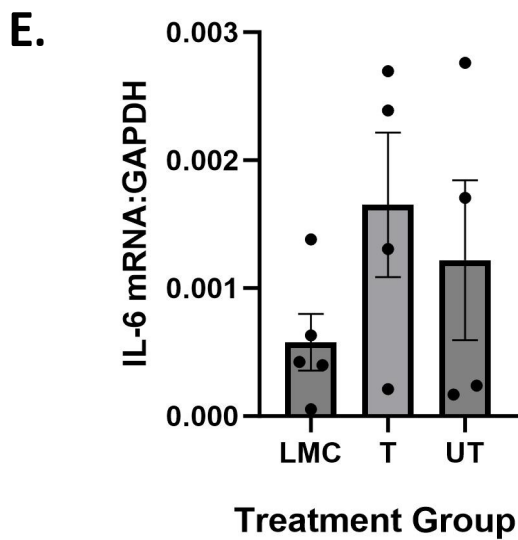
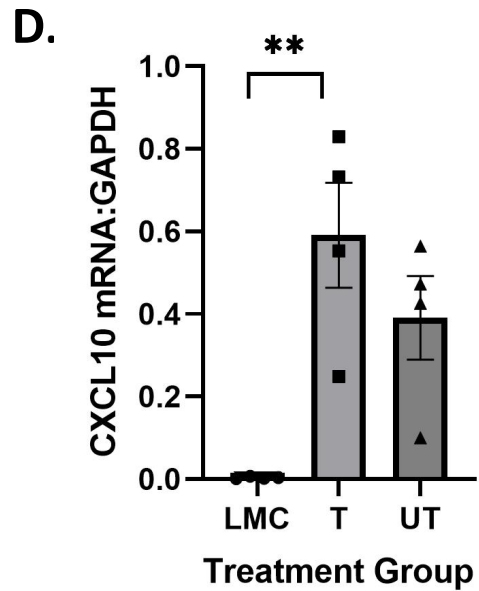
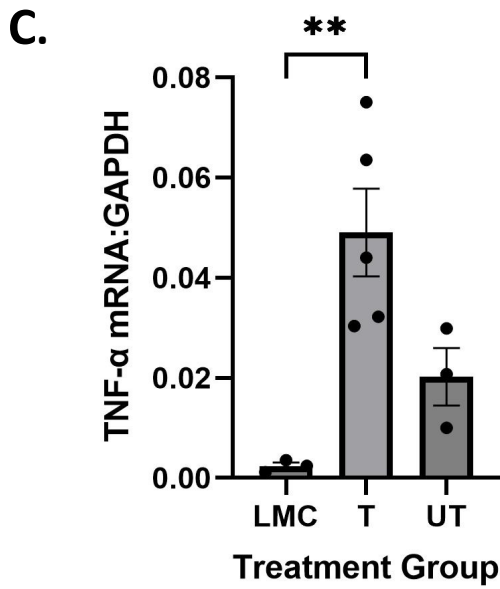
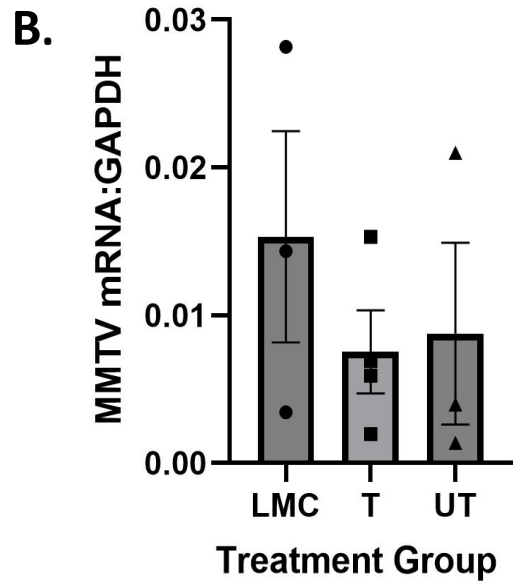
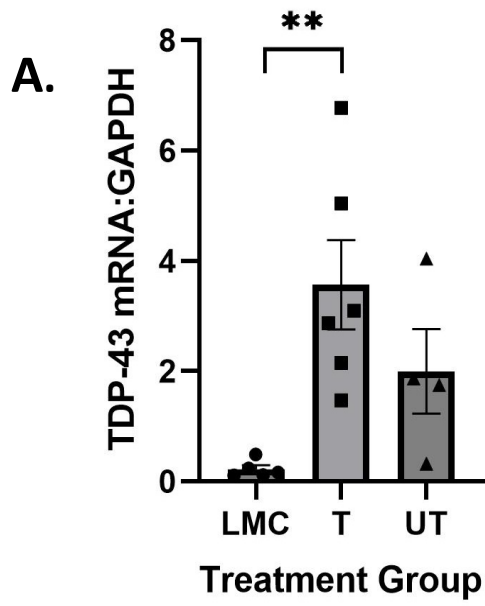


Figure 3.12 mRNA analysis of brain tissue from treated and untreated hTDP-43 Δ NLS mice

mRNA was quantified from brain tissue from treated hTDP-43 Δ NLS mice (n = 4-5) untreated hTDP-43 Δ NLS mice (n = 3-4) and litter-matched controls (n = 4) from day 19 post treatment onset by RT-qPCR using primers for **A.** TDP-43, **B.** MMTV, **C.** TNF- α , **D.** CXCL10, **E.** IL-6, **F.** IFN- β . Expression for all mRNA candidates were normalised to GAPDH. Results represent the mean \pm SEM from duplicate values. LMC = litter-matched controls, T = Treated, UT= untreated, Two-way ANOVA with Sidak's multiple comparisons test. ** $p < 0.005$

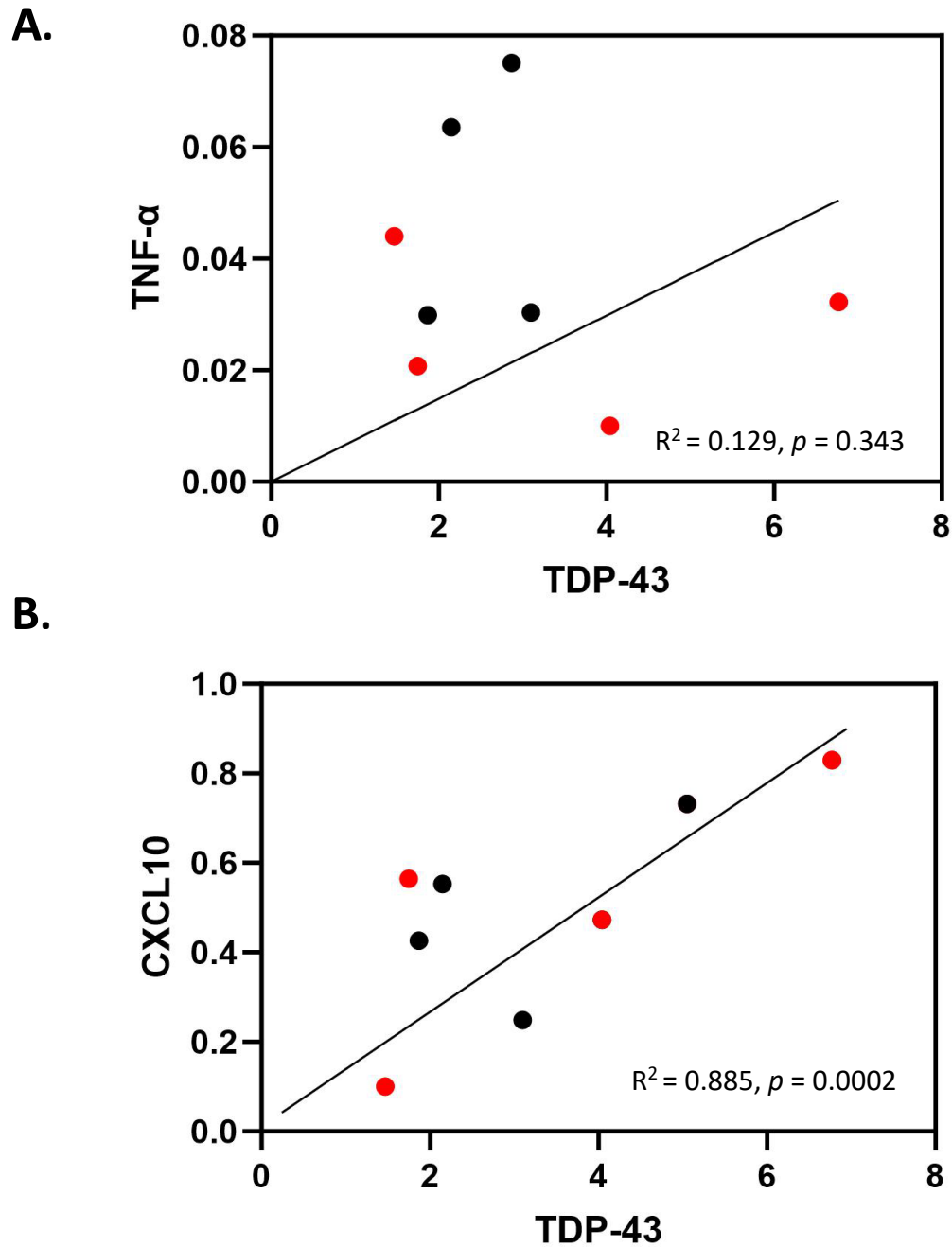


Figure 3.13 Relationship between TDP-43 expression and TNF- α and CXCL10 expression from brain tissue of treated and untreated hTDP-43 Δ NLS mice

The relationship between the expression of **A.** TNF- α and **B.** CXCL10 to mRNA expression of TDP-43 was quantified from brain tissue from pooled treated and untreated hTDP-43 Δ NLS mice (n = 11). Red data points are representative of the treated hTDP-43 Δ NLS mice and black data points are representative of untreated hTDP-43 Δ NLS mice.

3.3 Discussion

3.3.1 Summary

Endogenous retroviruses have been a proposed cause of MND and be involved in the progression of MND neurodegeneration (Li *et al.*, 2022). While nuclear TDP-43 mislocalisation is a hallmark of MND pathology and the involvement of inflammation in neurodegeneration is well established, the association between TDP-43, inflammation and ERVs, specifically HERV-K, is not well known. Due to the association between MND and ERVs, antiretroviral therapy, Triumeq, was investigated as a potential therapy. While promising results were obtained after a Phase II clinical trial of Triumeq (Gold *et al.*, 2019), the mechanisms of benefit of Triumeq for MND and the influence of TDP-43 was not defined. The effect of Triumeq on inflammatory pathways was also unclear. The aim of this study, therefore, was to investigate the effects of Triumeq on a TDP-43 mouse model of MND to further understand where in the pathway of brain to muscle, Triumeq was influencing. Determining the effects of Triumeq in a MND mouse model will aid in the understanding of the mechanisms of action of antiretroviral therapy for MND to potentially increase the therapeutic benefit.

3.3.2 Dox Removal in hTDP-43 Δ NLS Mice Induces Disease

Prior to testing the influence of Triumeq in a large cohort of hTDP-43 Δ NLS mice, a cohort of mice were used to validate the removal of Dox to initiate disease and disease progression in the mice, as shown by previous data with this mouse model (Walker *et al.*, 2015). Firstly, to confirm the expression and mislocalisation of hTDP-43 in this mouse model, immunohistochemistry was used to assess the hTDP-43 expression in cortical brain tissue from hTDP-43 Δ NLS mice and non-transgenic control mice. This confirmed the expression and cytoplasmic mislocalisation of hTDP-43 in the hTDP-43 Δ NLS mice while there was no expression in the control mice (**Figure 3.1**). A large cohort of hTDP-43 Δ NLS mice were then removed off Dox to measure the levels of urinary p75^{ECD} at 2 weeks, 4 weeks and 6 weeks off Dox and were compared to mice that remained on Dox. The removal of Dox in this cohort resulted in increases of the level of urinary p75^{ECD} at 2 weeks, 4 weeks and 6 weeks off Dox (**Figure 3.2**). This suggests that removal of Dox within this mouse model results in neurodegeneration, as seen in human MND, with increased levels able to be detected at 2

weeks off Dox. This increase of p75^{ECD} with disease is consistent with human MND, where p75^{ECD} has been well described as a progression biomarker of MND (Shepherd *et al.*, 2017) and consistent with what is seen in the SOD1^{G93A} mouse model (Matusica *et al.*, 2016). Further validation of disease progression was then completed in a small cohort of hTDP-43ΔNLS mice and sex differences were explored.

Dox removal from the hTDP-43ΔNLS mice resulted in progressive weight loss (**Figure 3.3**). This suggests that with Dox removal, there is initiation of disease that progresses over time, with mice reaching end stage disease at approximately 23 days post-Dox removal. Sex differences were observed in this validation study with the male mouse on Dox losing weight across the study course while the female mouse did not drop below the starting weight. Based on this finding, female mice were used for the remainder of the mice studies. Although the validation cohort was small, this study was consistent from previous findings with this mouse model and was therefore, deemed an appropriate model for a pilot study of Triumeq treatment using female hTDP-43ΔNLS mice.

3.3.3 Pilot Study for Triumeq Use in hTDP-43ΔNLS Mice

Following the validation of Dox removal inducing disease in the hTDP-43ΔNLS mice, a pilot study was conducted to examine the use of Triumeq in this mouse model, measuring disease progression through weight loss, neurological score and motor performance through the latency to fall on the wirehang test. There was no effect of Triumeq on disease progression according to weight loss and neurological score (**Figure 3.4**), although weight loss coincided with an increase in neurological score and continued to have an inverse association for the remainder of the study. This suggests that the observed weight loss may be due to muscle degeneration, causing the decreased hindlimb motor function and the increase in neurological score. This study also found a difference between the treated and untreated mice according to the motor performance was first observed in this cohort, at approximately 15 days post treatment onset and Dox removal (**Figure 3.5**). It is also at this point where p75^{ECD} increases were observed in mice removed off Dox, suggesting this timepoint may be of interest for disease progression.

While this finding suggests that Triumeq is influencing motor performance, it remained unclear where Triumeq is influencing and if this difference in motor performance is consistent with any other measures of disease pathology including alterations in mRNA expression in cortical brain tissue or motor neuron count within the spinal cord. These measures were analysed in a larger cohort, discussed below.

3.3.4 Effects of Triumeq Treatment on Disease Progression and Pathology

A larger cohort of hTDP-43 Δ NLS mice (n = 40) was used to enable the understanding of the action of Triumeq on the pathway from brain to muscle. Since Triumeq treatment resulted in an improvement of motor performance at 15-17 days post-treatment onset, it suggests that Triumeq is influencing the neurodegeneration pathway. A difference in motor performance at day 15 was also noted in another measure of motor function through the gait analysis test. While not seen on any other day of the study, there was a difference between the treated and untreated hTDP-43 Δ NLS mice in the stride length at day 15. This finding is consistent with the wirehang results from the same cohort, where an improved performance was observed for Triumeq treated mice between day 15-19 that is no longer seen at end stage disease. The reduced stride length is also consistent with what has been observed in human disease where gait abnormalities and a reduction in stride length is seen in human MND with a slower walking pace as disease progresses (Sanjak *et al.*, 2010). Furthermore, a comparison of day 1 and day 15 urine from treated and untreated hTDP-43 Δ NLS mice showed a lower level of urinary p75^{ECD} in treated mice at day 15. This is suggestive of less motor neuron degeneration in the treated mice and suggestive of reduced muscle degeneration due to the simultaneous improved performance on the wirehang test.

In this study, there was expression of human TDP-43 in the hTDP-43 Δ NLS mice off Dox but no hTDP-43 expression in non-transgenic controls, validating the TDP-43 expression system in this model. However, there was no effect of Triumeq on the expression of TDP-43 from cortical brain tissue from mice 15-17 days post-treatment onset. This suggests that the increased level of motor function observed in the Triumeq-treated mice, is not due to differences in expression of hTDP-43 within the cortex but could be due to differences other TDP-43

pathology including mislocalisation. Interestingly, there inflammatory markers TNF- α and CXCL10 trended higher in the Triumeq-treated mice but not in the untreated mice. In addition, there was a correlation between TDP-43 and CXCL10 expression, regardless of treatment group, suggesting that TDP-43 expression in the transgenic mice may be associated with the inflammatory pathway involving CXCL10 and not TNF- α , not influenced by Triumeq. The finding of increased expression of CXCL10 and the correlation to TDP-43 is consistent with previous research. Using the hTDP-43 Δ NLS mouse model, Hunter *et al.* (2021) found increased gene expression of CXCL10 occurred early in the disease process and remained at an increased level through late stage disease also. CXCL10 is an inflammatory cytokine involved in T-cell recruitment, including recruitment of CD4⁺ and CD8⁺ T-cells with T-cell infiltrate found within the brain and spinal cord of MND patients (Engelhardt *et al.*, 1993, Garofalo *et al.*, 2022). CD8⁺ T-cells have been shown to have direct cytotoxic contact with motor neurons in MND, potentially involved in the neurodegenerative process (Coque *et al.*, 2019). Although not examined in the current study, previous research with other TDP-43 mouse models has identified cellular infiltration in the brain and spinal cord, supporting the increased CXCL10 expression seen in the present study (Garofalo *et al.*, 2020). The lack of significant difference in the levels of IL-6 and IFN- β between the transgenic TDP-43 mice and the litter-matched controls could be explained by the low sample size for this analysis. Further research with greater numbers should be used to confirm the induction of these, and further, inflammatory mediators within the cortex.

Further RNA analysis from cortical brain tissue also looked at expression levels of a mouse endogenous retrovirus, MMTV. Due to the lack of human ERVs in mice, the MMTV ERV was selected as a measure of ERV expression due to its high expression in all laboratory mice (Subramanian *et al.*, 2011). There were no differences in the levels of MMTV expression between the hTDP-43 Δ NLS mice and non-transgenic litter-matched controls which suggests that MMTV was not induced from TDP-43 mislocalisation in this mouse model. The absence of a significant difference between treatment groups also suggests that Triumeq is not influencing MMTV expression at this stage of disease in this model. The improved motor performance in this model from Triumeq treatment is consistent with recent research which found improved grip strength in mice after abacavir, a component of Triumeq, treatment but no differences in MMTV expression after abacavir treatment (Liu *et al.*, 2023). Future research

could include measures of other HERV analogues to confirm this finding due to the number of active ERVs present within the mouse genome (Stocking and Kozak, 2008b).

The histological analysis of the lumbar section of the spinal cord also identified further significant differences between treated and untreated mice. Here, there was a significantly lower number of motor neurons in the spinal cord of the untreated mice compared to the treated mice on Day 19. This lower motor neuron number coincides with the lower p75^{ECD} levels in treated mice and the significantly higher latency to fall on the wirehang test. This finding suggests that at this stage of disease, Triumeq is influencing the degeneration of the motor neurons stimulating the muscles, but this may not yet be coinciding with muscle atrophy. Further research will analyse the muscle to determine if Triumeq is influencing muscle atrophy at this stage of disease.

Although Triumeq was not shown to have an influence on TDP-43 expression or CXCL10 expression, there is a significant effect on the motor performance, p75^{ECD} levels and motor neuron number within the lumbar spinal cord at the 15-19 day timepoint. This suggests that Triumeq could be having a direct influence on motor neuron degeneration which is not associated with inflammation or reducing expression of TDP-43, although it is still unknown if mislocalisation was improved. An overview of the significant differences found after Triumeq treatment is outlined in **Table 3.1** Antiretroviral therapy has been shown to induce neurocognitive disorder with prolonged use that may involve pyramidal neuron excitability (Stern *et al.*, 2018, Chen *et al.*, 2020, Akay *et al.*, 2014). However, Triumeq, or other antiretrovirals, are not linked to change in motor function. Hence, it is unlikely that Triumeq is causing a toxic effect and instead, is protective at 15-19 days in regard to motor neuron numbers, improved motor function and lower urinary p75^{ECD}. With chronic TDP-43 overexpression and cytoplasmic aggregation, this protective effect is not maintained. The mechanism of action that improves motor neuron numbers does not appear to involve inflammatory cytokines, IL-1 β , IL-6 or CXCL10. This is different to what has been previously published for this mouse model where IL-1 β and IL-6 were up-regulated at 14 days off Dox in the hTDP-43 Δ NLS mice (Luan *et al.*, 2023). Further work would use a greater sample size for the immune response to confirm if these markers changed at 15-19 days in the hTDP-43 Δ NLS

mice treated with Triumeq. TDP-43 mislocalisation analysis would also be included in further analysis.

This study demonstrates a moderate effect of Triumeq treatment on motor performance a promising result for use as a treatment for MND patients. One approved pharmaceutical therapy for MND, Riluzole, described in section 1.2.5.1, has not been shown to have any effect in mice models of MND, including the mouse model used for this study (Hogg *et al.*, 2018, Wright *et al.*, 2021). Therefore, the moderate effect observed here could have a greater benefit on motor performance in MND patients. In an attempt to increase the therapeutic benefit of Triumeq, the following chapter outlines the effects of increasing the dose of Triumeq in the hTDP-43 Δ NLS mouse model.

3.3.5 Conclusions

In summary, this chapter validates the parameters of the testing model and outlines the validity of using Triumeq *in vivo*. This chapter validated the expression and mislocalisation of hTDP-43 in hTDP-43 Δ NLS mice compared to controls and identified an increase in urinary p75^{ECD} from 2 weeks post-dox removal. Importantly, Triumeq is influencing the motor performance in TDP-43 compared to untreated TDP-43 mice suggesting that Triumeq is influencing muscle degeneration at 15-20 days post-treatment onset. Furthermore, Triumeq is influencing the number of motor neurons in the lumbar region of the spinal cord with improved motor neuron retention at this same timepoint. The strong correlation between TDP-43 and CXCL10 also suggests that TDP-43 expression is associated with inflammatory process, however the relationship is not fully defined and was not shown to be influenced by Triumeq treatment. While this chapter did not show any effect on survival with all mice reaching end-stage at a similar time regardless of treatment, the following chapter examines the effect of increasing the dose to determine if this provides any further therapeutic benefit.

Table 3.1 Overview of significant effects from Triumeq treatment on the pathways from brain through to muscle

Part of the pathway analysed	Significantly different between treated and untreated mice on Day 15-20	Figure reference
Disease progression		
Weight change across study	N	Figure 3.5A
Neurological score across study	N	Figure 3.5B
Urinary p75 ^{ECD}	Y	Figure 3.8
Motor performance		
Wirehang	Y	Figure 3.6
Gait analysis	Y	Figure 3.7
Endogenous retrovirus measure		
Endogenous retrovirus expression	N	Figure 3.11B
TDP-43 pathology		
TDP-43 expression	N	Figure 3.11A
TDP-43 solubility and mislocalisation	N/A – still to be completed	N/A
Inflammatory profile		
TNF- α	N	Figure 3.11C
CXCL10	N	Figure 3.11D
IL-6	N	Figure 3.11E
IFN- β	N	Figure 3.11F
Motor Neuron number		
Motor Neuron Count in spinal cord	Y	Figure 3.10
Muscle atrophy		
Muscle fibre analysis	N/A – still to be completed	N/A

CHAPTER 4.
EFFECTS OF AN INCREASED DOSE OF
TRIUMEQ TREATMENT ON THE hTDP-
43 Δ NLS MND MOUSE MODEL

4 EFFECTS OF AN INCREASED DOSE OF TRIUMEQ TREATMENT ON AN MND MOUSE MODEL

4.1 Introduction

After **Chapter 3** outlined a therapeutic benefit of Triumeq through improved motor performance, the therapeutic window of benefit for Triumeq was investigated. Increasing the dose of Triumeq would either increase the benefit that was outlined in chapter 3, or it will provide insight about the most effective dosing. A double dose of 400mg/kg per day or the equivalent human dose of 2 tablets of Triumeq per day was administered to a small cohort of hTDP-43 Δ NLS mice. In the previous chapter, the benefit from Triumeq was found in changes in motor performance according to wirehang and gait analysis and changes in p75^{ECD} levels between day 15-17 of the study. Based on these changes, the current chapter aimed to understand the upper therapeutic limit of Triumeq, focused on determining the effects of the increased dose on mouse motor performance and levels of urinary p75^{ECD}.

4.2 Results

4.2.1 Increased Triumeq Dose Does Not Influence Disease Progression

A small cohort of hTDP43 Δ NLS mice (n = 14) was used to assess the effects of increasing the dose of Triumeq to a two times dose (400 mg/kg per day), equivalent to the human dose of 2 Triumeq tablets per day, as described in section 2.2.2. Weight and neurological score were used to assess disease progression until the mice reached the ethical endpoint according to weight loss at 27 days post Dox removal and treatment onset. There was no significant difference between the treated hTDP43 Δ NLS mice (n = 7) and the untreated hTDP43 Δ NLS mice (n = 7) for percentage weight change (**Figure 4.1A**) or neurological score (**Figure 4.1B**) across the study course.

4.2.2 Increased Triumeq Dose Does Not Affect Weight Loss

The percentage weight change across the study course was compared for double dose treated mice (n = 7), double dose untreated mice (n = 7), single dose treated mice (n = 21) and single dose untreated mice (n = 19). There were no significant differences between any of the treatment groups regardless of dosing, and all treatment and dosing groups followed a similar progression of disease according to weight loss (**Figure 4.2**).

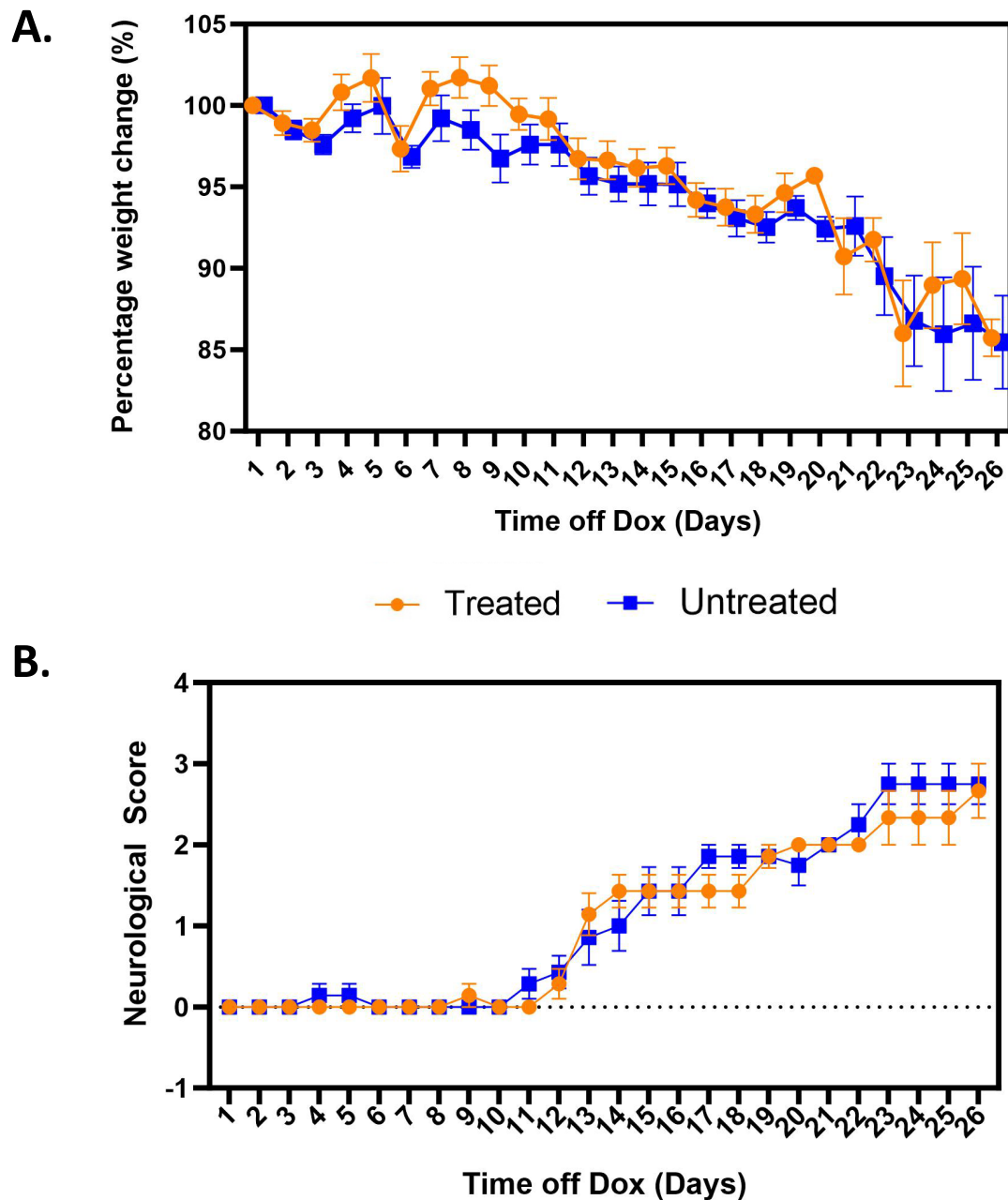


Figure 4.1 Percentage weight change and neurological score in a cohort of hTDP-43ΔNLS mice after increased dose of Triumeq treatment

A cohort of hTDP-43ΔNLS mice were treated with a 2 times dose of antiretroviral therapy, Triumeq, (n = 7) and compared to an untreated hTDP-43ΔNLS cohort (n = 7) and compared **A.** percentage weight change and **B.** neurological score where 0 = normal hindlimb movement and normal gait, 1 = partial hindlimb splay and slightly abnormal gait, 2 = hindlimb dragging while moving forward, 3 = minimal hindlimb movement and slow and abnormal gait and 4 = rigid paralysis in hindlimbs and no forward motion, deemed the ethical end-point. Results represent the mean ± SEM, Two-way ANOVA with Sidak's multiple comparisons.

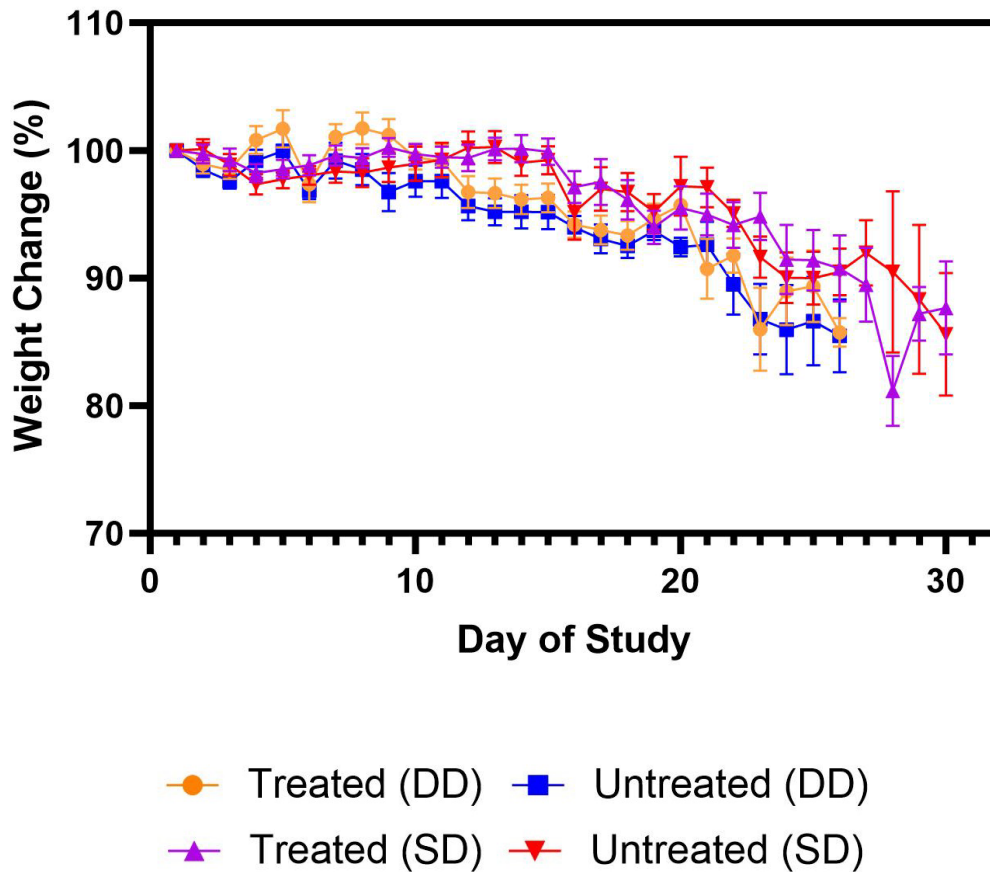


Figure 4.2 Percentage weight change of treated single dose and double dose hTDP-43 Δ NLS mice compared to untreated mice

The double dose (DD) cohort of hTDP-43 Δ NLS mice, treated (n = 7) and untreated (n = 7), were compared to the original single dose (SD) cohort, treated (n = 21) and untreated (n = 19) by percentage weight change over the course of the study. Results represent the mean \pm SEM, Two-way ANOVA with Sidak's multiple comparisons.

4.2.3 Increased Triumeq Dose Does Not Influence Motor Performance According to Wirehang

Motor performance was assessed using the wirehang test to measure hindlimb strength and gait analysis was performed as described in sections 2.2.3.3 and 2.2.3.4. A small cohort of hTDP-43 Δ NLS mice ($n = 7$) were treated with a double dose of Triumeq and compared to an untreated hTDP-43 Δ NLS cohort ($n = 7$) according to latency to fall on the wirehang test. There was no significant difference between the double dose treated group and the untreated group in terms of the latency to fall with similar fall times observed regardless of treatment group across the study course (**Figure 4.3A**)

As shown in **Figure 4.3B**, all mice across treatment and dose groups were compared for latency to fall on the wirehang test. At day 17, there was no significant difference in the wirehang time between the treated single dose mice or the treated ($p = 0.997$) and untreated double dose mice ($p = 0.551$). There was, however, a significantly lower latency to fall for the single dose untreated mice ($p = 0.009$). There were no other significant differences between the treatment groups regardless of dose across the rest of the study course.

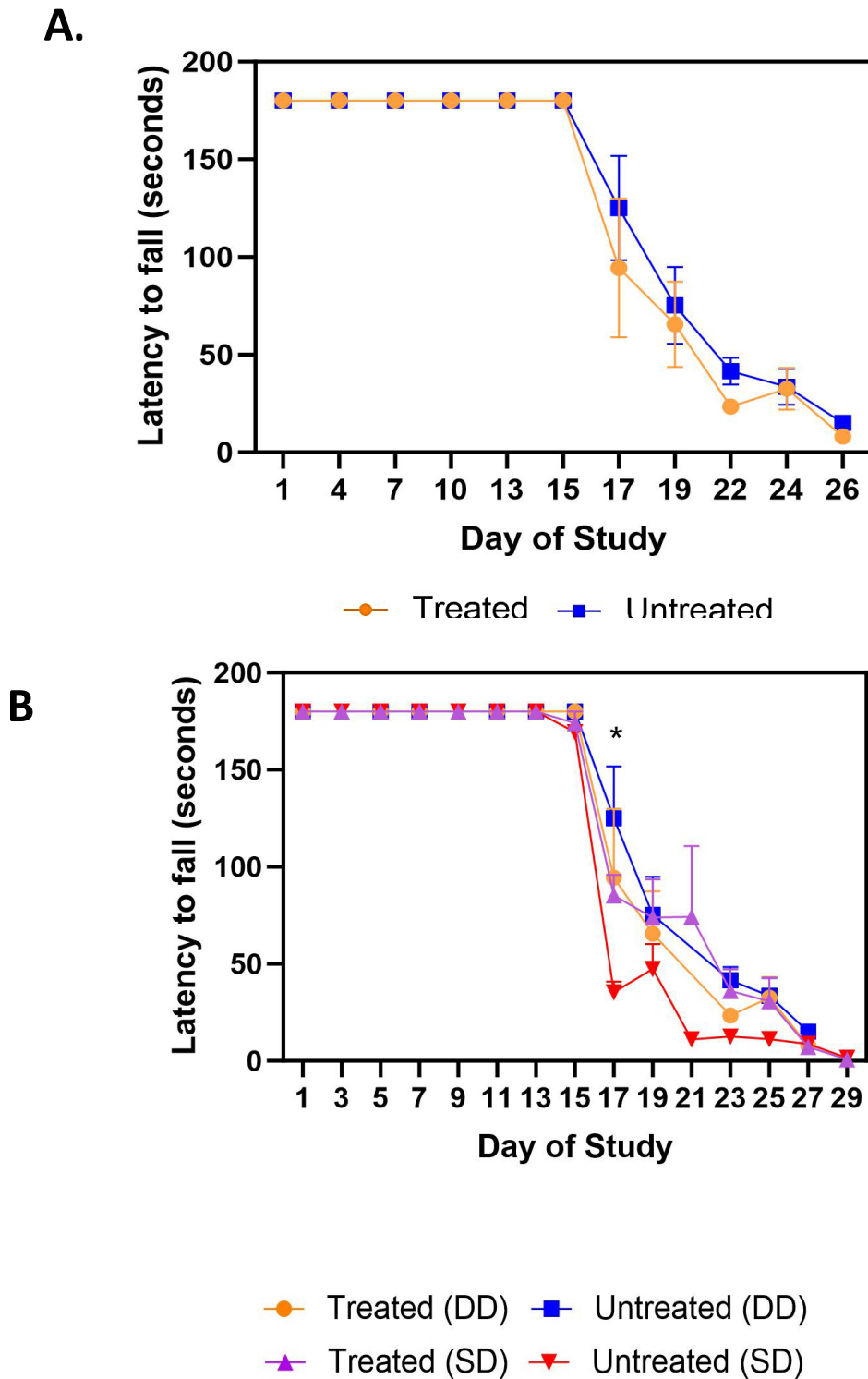


Figure 4.3 Latency to fall from the wirehang test for the double dose study

Mean latency to fall for a cohort of treated hTDP-43ΔNLS mice (n = 7), untreated hTDP-43ΔNLS mice (n = 7), treated with a 2 times dose of Triumeq across the course of the experimental study. Results represent the mean ± SEM, Two-way ANOVA with Sidak's multiple comparisons test. DD = Double Dose SD = Single Dose * $p < 0.05$

4.2.4 Increased Triumeq Dose Does Not Influence Gait

Gait analysis was assessed on the treated ($n = 7$) and untreated ($n = 7$) hTDP-43 Δ NLS mice on day 1, 15 and 30 of the study. There were no significant differences in stride length between the treated and untreated hTDP-43 Δ NLS mice on Day 1 (**Figure 4.4A**; $p = 0.708$). By Day 15, there was a significantly higher stride length in the untreated mice compared to the treated mice ($p = 0.013$). This significant difference was not seen by the end of the study course on Day 30. For the stride width (**Figure 4.4B**), there were no significant differences between treated and untreated mice on any day of the study. However, there was a significant decrease in stride width from Day 1 of the study to Day 15 in the untreated mice. There was also a trend for this significant decrease in stride width for the untreated mice also, it just did not reach statistical significance.

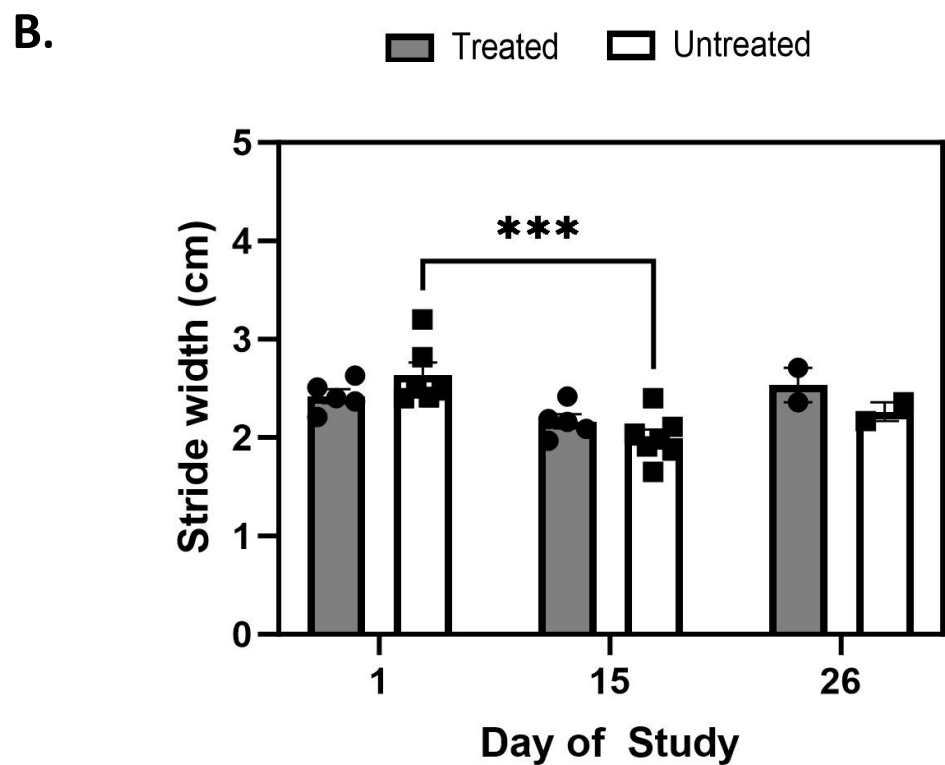
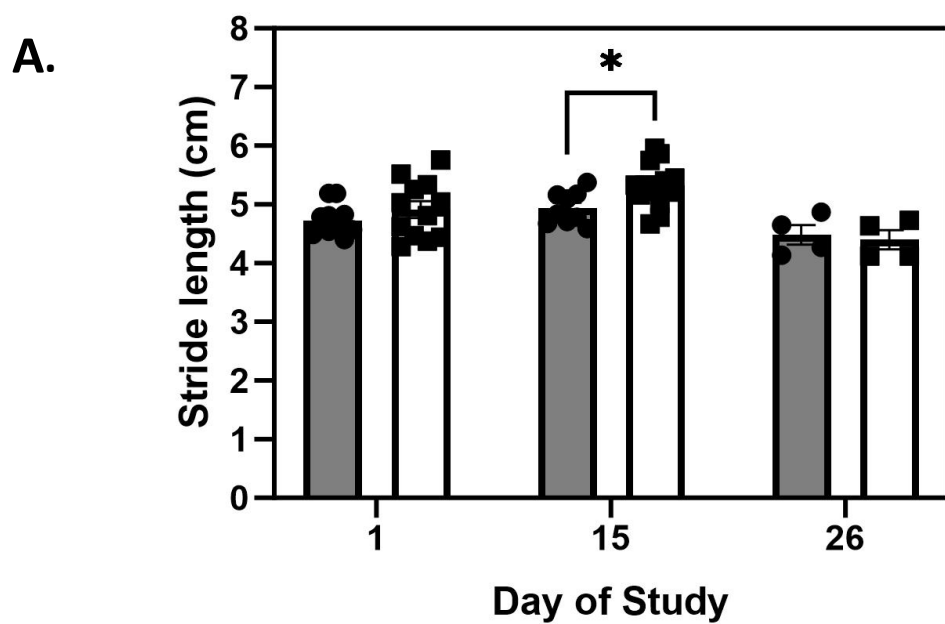


Figure 4.4 Gait analysis including stride length and stride width in double dose treated and untreated hTDP-43ΔNLS mice

Gait analysis of treated hTDP-43ΔNLS mice (n = 7) and untreated hTDP-43ΔNLS mice (n = 5) was measured and assessed by **A.** mean stride length and **B.** mean stride width across the course of the treatment study. Results represent the mean ± SEM, Two-way ANOVA with Tukey's multiple comparisons test. * $p < 0.05$

4.2.5 Increased Triumeq Dose Does Not Influence Urinary p75^{ECD}

Across the study course, urine was collected from the hTDP-43 Δ NLS mice and compared for urinary p75^{ECD} levels between the treatment groups. There were no significant differences in the level of p75^{ECD} between the treated mice with the increased Triumeq dose and the untreated mice at any day of the study. Interestingly, p75^{ECD} within the urine did not increase with disease progression with the highest values of p75^{ECD} seen within the urine on day 6 (**Figure 4.5**).

The urinary p75^{ECD} levels were also compared between the single dose treated (n = 6) and untreated mice (n = 6) and the double dose treated (n = 5) and untreated mice (n = 5) from Day 1 to Day 15 of the study. There were no significant differences between the levels of p75^{ECD} on Day 1 between any of the treatment groups or dose groups. On Day 15, however, there was a significantly higher level of urinary p75^{ECD} in the single dose untreated mice compared to the single dose treated mice ($p = 0.0059$) and both untreated ($p = 0.0040$) and treated ($p = 0.0009$) double dose mice (**Figure 4.6**)

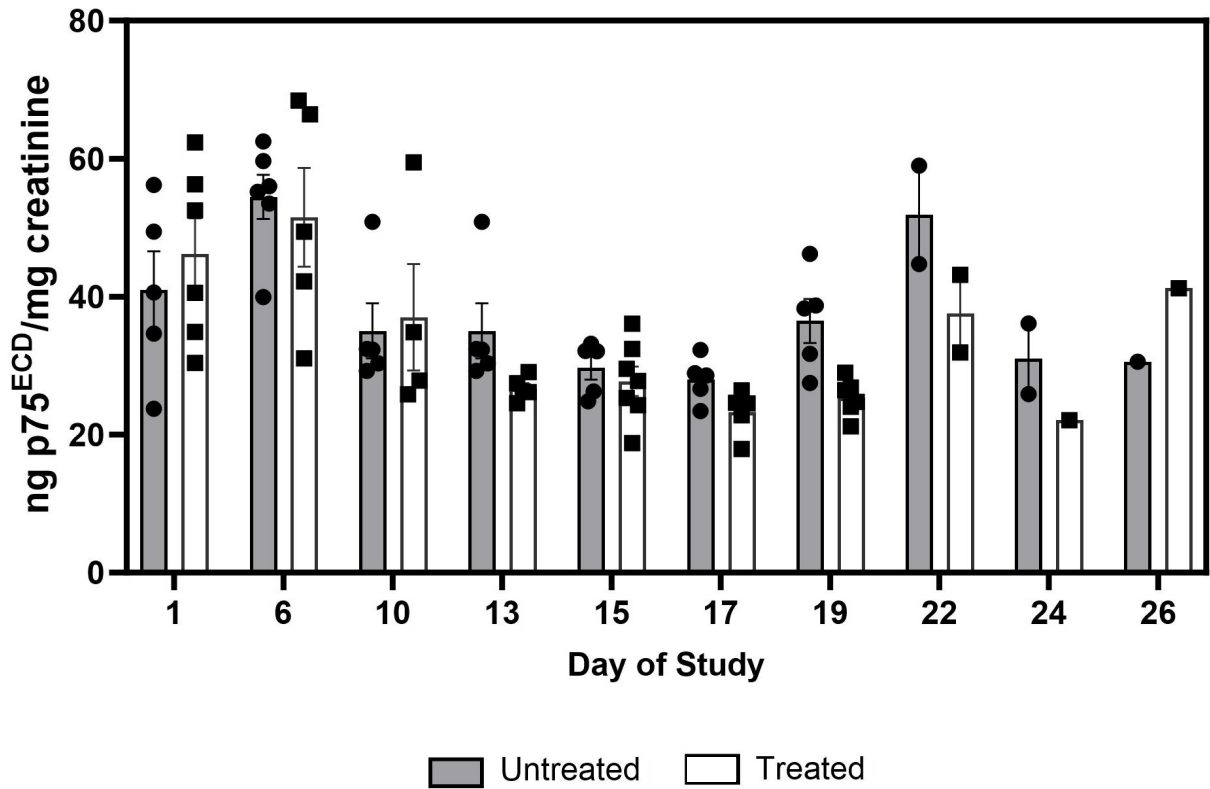


Figure 4.5 Urinary p75^{ECD} levels in double dose treated and untreated hTDP-43ΔNLS mice across study course

Urinary p75^{ECD} levels were quantified in samples from double dose treated hTDP-43ΔNLS mice (n = 2-6) and untreated (n = 2-7) across study course. Levels of p75^{ECD} were standardised to urinary creatinine to account for dilution. Results represent the mean ± SEM from 3 biological replicates, 2 technical replicates. One-way ANOVA with Sidak's multiple comparisons test.

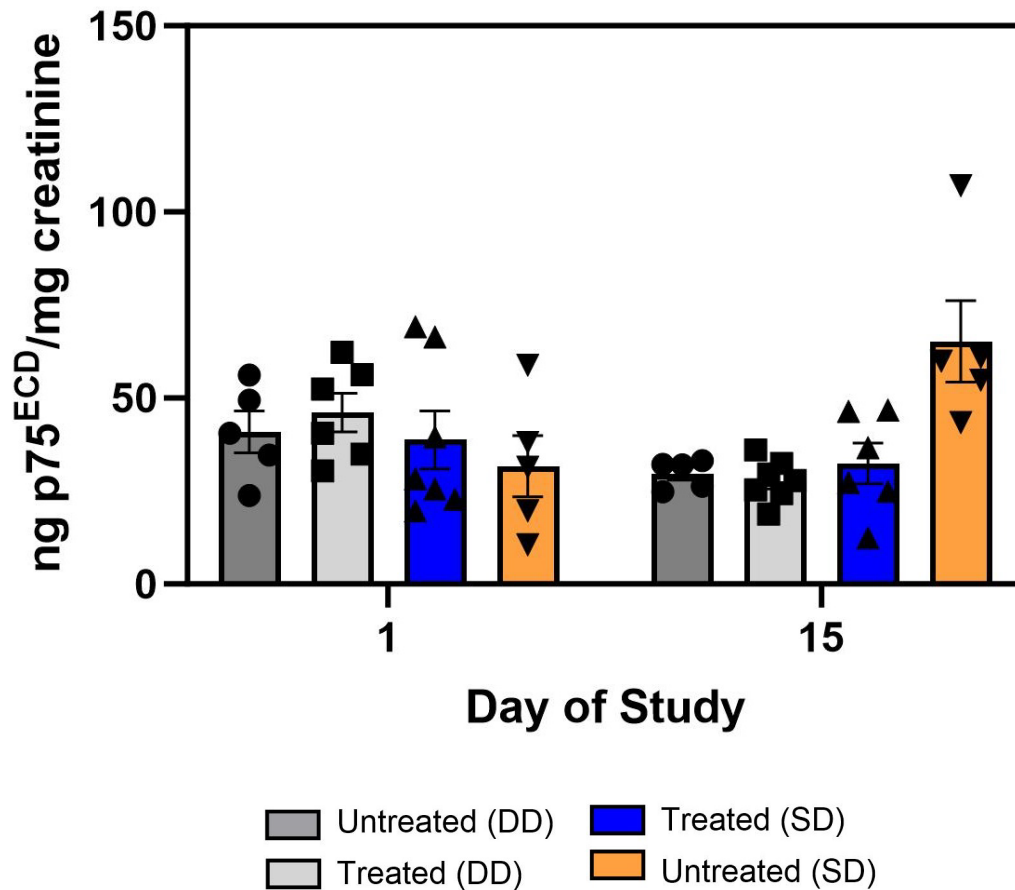


Figure 4.6 Urinary p75^{ECD} levels in double dose treated and untreated hTDP-43ΔNLS compared to single dose treated and untreated mice

Urinary p75^{ECD} levels were quantified in samples from double dose treated hTDP-43ΔNLS mice (n = 5) and untreated (n = 6) as well as single dose treated (n = 6) and untreated (n = 5) mice on Day 1 and Day 15 post-treatment onset. Levels of p75^{ECD} were standardised to urinary creatinine to account for dilution. Results represent the mean ± SEM from 3 biological replicates, 2 technical replicates. One-way ANOVA with Sidak's multiple comparisons test. * $p < 0.05$. SD = Single Dose DD = Double Dose

4.3 Discussion

4.3.1 Summary

Chapter 3 outlined the therapeutic benefit of Triumeq showing increased motor performance, reduced urinary p75^{ECD} levels and a higher number of motor neurons within the lumbar spinal cord of hTDP-43ΔNLS mice. This finding lead to the hypothesis that increasing the dose of Triumeq in TDP-43 mouse model will improve the benefits outlined in Chapter 3, using the regular dose of Triumeq. Hence, the aim of this chapter was to elucidate the therapeutic benefit of Triumeq in a small cohort of hTDP-43ΔNLS mice. The experimental timeline for this study can be seen in **Figure 2.2E**. This chapter describes no further increase of the therapeutic benefit of Triumeq by increasing the dose.

4.3.2 Increasing the Dose of Triumeq in a small cohort of hTDP-43ΔNLS mice

A small cohort of hTDP-43ΔNLS mice (n = 14) were used to investigate the effects of increasing the dose of Triumeq from the equivalent human daily dose of one tablet to two tablets. Firstly, the weight and neurological score of the double dose treated and untreated mice were compared but no significant differences were noted, with all mice reaching the ethical end point of the disease at a similar time regardless of treatment group (**Figure 4.1**). According to weight change, there was a similar disease progression seen for all mice regardless of treatment group and dosing amount with all single dose treated mice and double dose treated mice following a similar weight loss pattern across the study course. It should be noted here that the mice in the double dose cohort reached the ethical end point of the study according to weight loss and neurological score, sooner than the single dose cohort, outlining the disease variability in this mouse model (**Figure 4.2**).

Motor performance was assessed through the latency to fall on the wirehang, and stride width and stride length were measured through gait analysis. There was no significant difference between the mice treated with the double dose of Triumeq and untreated mice for latency to fall on the wirehang test (**Figure 4.3A**). This was a surprising result given that this was the first study where a significant difference in motor performance was not found between the treated and untreated mice and no motor benefits that have been seen in all previous single dose

studies were not seen in this cohort. The double dose cohort was compared to the single dose treated and untreated mice for the wirehang. There was a significantly lower latency to fall for the untreated single dose mice, but no other significant differences were seen between the mice regardless of treatment dose or group at any other point in the study. The untreated double dose mice showed similar motor performance progression to the single dose treated mice in the prior studies. This finding further describes the variability in the mouse model. For the gait analysis, there was a significantly lower stride length for the treated mice compared to the untreated mice, a contradictory finding from the previous single dose studies and not consistent with human MND where a lower stride length occurs with increased motor dysfunction (Sanjak *et al.*, 2010).

Urinary p75^{ECD} was measured at multiple time points across the study. While urinary p75^{ECD} has been previously validated as a progression marker of MND (Shepherd *et al.*, 2017) and also found to increase with disease progression in SOD1^{G93A} mice (Shepherd *et al.*, 2014) and the hTDP-43ΔNLS mice (**Figure 3.2**), the current study did not find the same increase with disease progression. Not only were there no significant differences between treated and untreated mice across the study course, but there was also variability in the levels of p75^{ECD}, with the highest levels seen on Day 6 of the study. This finding is not consistent with the previously described p75^{ECD} progression rates increasing with disease progression. Part of this contradictory finding could be due to the low numbers of the study, particularly towards the end of the study where urine collection in the mice is more difficult to obtain. When compared to the single dose treated and untreated mice, the double dose treated and untreated mice had a similar urinary p75^{ECD} level on Day 15 to the single dose treated mice. On Day 15, the single dose untreated mice had significantly higher levels compared to any other treatment group (**Figure 4.6**).

Overall, these findings suggest that increasing the dose of Triumeq does not improve the therapeutic benefit. However, the variability seen in the progression of disease across mice studies could be influencing the results. Furthermore, ERV activity in the mouse brain was not measured due to a lack of induction or difference in MMTV in the single dose studies. Further analysis should investigate the effect of Triumeq on mouse ERV expression within the mouse brain. While only a small cohort of hTDP-43ΔNLS mice were used for the current study, the

lack of any significant improvement in any measure of disease progression meant there was no ethical basis for continuing to a larger cohort.

Previous research has investigated the therapeutic benefit of increasing the dose of other FDA-approved therapeutics for MND. An early study of Riluzole, a FDA-approved drug for MND described in section 1.2.5, determined that increasing the dose from 100 mg daily treatment to 200 mg daily did not provide any further benefit (Lacomblez *et al.*, 1996). In fact, a greater number of adverse effects occurred at the increased dose although the survival benefit remained the same as the 100 mg dose. Further Phase II clinical trials for other treatments for MND have shown similar results with the higher doses of Toprimate, a glutamate antagonist and Xaliproden, a serotonin antagonist, showing the greatest adverse effects without showing any increase in the benefit and in some cases, accelerating disease progression (Cudkowicz *et al.*, 2003, Meininger *et al.*, 2004).

The toxicity of the components of Triumeq, dolutegravir, abacavir and lamivudine have also been assessed at increasing doses. Dolutegravir has been shown to be non-toxic, even at high doses, including the dose given to the mice in the current study (Shah *et al.*, 2014). Similarly, despite cases of abacavir hypersensitivity regardless of dose, increased doses of abacavir have been shown to be tolerable and non-toxic (Kumar *et al.*, 1999, Jesson *et al.*, 2022). Lamivudine, however, has been shown to have toxic effects at higher doses. Olaniyan *et al.* (2015) showed increased liver toxicity from higher doses of lamivudine in rats, due to increased oxidative stress. Furthermore, lamivudine treatment has been reported to have neurotoxic properties with neurodegeneration seen in the cerebellum of Wistar rats treated with lamivudine compared to control rats, also causing gait abnormalities (Li *et al.*, 2007, Peter *et al.*, 2017). Thus, the effects observed in the current study could be explained by neurotoxic effects from increased lamivudine dose.

4.3.3 Conclusions

In summary, this chapter investigated the effects of increasing the dose of Triumeq on a small cohort of hTDP-43 Δ NLS mice. The effect of the increased dose on weight change, neurological score, motor performance and urinary p75^{ECD} was investigated. Only one significant difference

between treated and untreated mice was observed with a significantly higher stride length for the untreated mice seen at Day 15, an opposing result to the previous single dose studies. However, this finding could be explained by variability of disease progression seen in this mouse model. Furthermore, the p75^{ECD} levels did not follow a consistent progression increase, previously seen. Although only a small cohort was used, the lack of significant effects of Triumeq on any measure did not warrant the use of more mice. Overall, this current study does not provide evidence of an increase in therapeutic benefit from increasing the dose of Triumeq.

**CHAPTER 5.
INVESTIGATING THE RELATIONSHIP
BETWEEN HERV-K, TDP-43 AND
INFLAMMATION IN VITRO**

5 INVESTIGATING THE RELATIONSHIP BETWEEN HERV-K, TDP-43 AND INFLAMMATION *IN VITRO*

5.1 Introduction

The previous chapters have demonstrated the use of antiretrovirals, specifically Triumeq, for MND to target endogenous retroviruses and determine their association with TDP-43 in a TDP-43 mouse model of MND. Due to the lack of expression of human endogenous retroviruses in these mice, specifically HERV-K, which is associated with MND, *in vitro* studies are beneficial for investigation of the association between HERV-K and TDP-43. Although Triumeq is currently being trialled in a Phase III clinical trial, elucidating the effects and mechanisms of Triumeq on the relationship between TDP-43, HERV-K and inflammation could be beneficial to improving its therapeutic benefit.

Therefore, the aim of this chapter is to assess transcription factors that bind HERV-K, quantify the expression of HERV-K targets in human cell lines and investigate the association between HERV-K and TDP-43 with Triumeq treatment *in vitro*. To do this, HERV-K and TDP-43 expression levels were analysed in multiple cell lines including non-neuronal cell lines, a neuronal cell line and a primary cell line from MND patients and controls. Determining the best cell line for HERV-K and TDP-43 expression will help to understand the hypothesis that exogenous viral infection or inflammatory stimuli will induce HERV-K expression and increase TDP-43 pathology and the addition of antiretroviral therapy will reduce HERV-K expression and TDP-43 expression.

5.2 Results

5.2.1 *In silico* Analysis of Transcription Factors Predicted to Regulate HERV-K Gene Expression

Due to COVID-19 lockdowns and interruptions to lab access and mouse breeding to continue the *in vivo* work, the focus of the project shifted to computer-based *in silico* analysis. *In silico* analysis was used to predict the transcription factors that regulate HERV-K gene expression. For this analysis, 1100 base pairs upstream of the transcription start site for full length HERV-K across 20 loci in the human genome were analysed through the promotor analysis online tool PROMO (Alggen). The transcription factors and the number of binding sites across the 20 full length HERV-K loci are displayed in **Table 5.1**, ordered from highest number of binding sites to least number of binding sites. 51 transcription factors were identified and predicted to regulate full length HERV-K expression. Of these transcription factors, 18 were involved in development or differentiation, 8 were oncogenic, 7 were related to immune function and 2 were known repressor of mouse endogenous retrovirus, MMTV. Highlighted in red boxes are the transcription factors that are of importance for MND, discussed further in the Section 5.3.3.

These transcription factors were also analysed for the number of loci they bind to determine which transcription factors were common across the 20 HERV-K loci. **Table 5.2** depicts these transcription factors according to the number of loci they bind with green squares showing one or more binding sites for that locus and red showing no binding sites for that locus, in order from greatest number of loci to least. Transcription factors outlined in bold indicate importance for MND.

Table 5.1 Transcription factors upstream of full length HERV-K and the number of binding sites across 20 HERV-K loci

Abbreviation	Transcription Factor	Total number of binding sites
OCT1	Octamer transcription factor 1	122
FOXD3	Forkhead box D3	99
AP-1	Activator protein 1	54
Pax-4	Paired-homeodomain transcription factor 4	54
HNF-4	Hepatocyte nuclear factor 4	43
CDP CR1	CCAAT Displacement protein – cut repeat 1	39
Evi-1	Ecotropic viral integration site1	39
HNF-3 β	Hepatocyte nuclear factor 3-beta	38
c-Rel	Rel proto-oncogene protein	32
USF	Upstream stimulatory factor	31
GATA-3	GATA binding protein 3	27
GATA-1	GATA binding protein 1	26
FOXJ2	Forkhead Box J2	25
GATA-2	GATA binding protein 2	23
MyoD	Myogenic differentiation 1	21
COMP1	Cooperates with myogenic protein 1	20
NF- κ B	Nuclear factor kappa-light-chain-enhancer of activated B cells	20
NF-Y	Nuclear transcription factor Y	19
Sox-9	SRY-box transcription factor 9	19
Pax-6	Paired-homeodomain transcription factor 6	17
CP2	Transcription factor CP2	16
v-Myb	Avian myeloblastosis viral oncogene homolog	16
IK-1	Ikaros isoform 1	15
RFX1	Regulatory Factor X1	15
Freac-7	Forkhead related transcription factor 7	14
v-Maf	Musculoaponeurotic fibrosarcoma oncogene homolog	14
Hand1	Hand and neural crest derivatives expressed 1	14

Brn-2	Brain-2	12
POU3F2	POU Class 3 homeobox 2	12
AREB6	ATP1a1 regulatory element binding factor 6	11
Elk-1	ETS domain-containing protein	11
HNF-1	Hepatocyte nuclear factor 1	10
Lmo2	LIM domain only 2	10
Sox-5	SRY-box transcription factor 5	10
HFH-3	Hepatocyte nuclear factor-3 (HNF-3)/fork head homolog	8
XFD-2	Xenopus fork head domain related multigene 2	8
TATA	TATA binding protein	7
TGIF	TGFB induced factor homeobox 1	7
Gfi-1	Growth factor independent 1	7
CDP CR3+HD	CCAAT Displacement protein – cut repeat 3	7
N-Myc	MYCN Proto-oncogene protein	6
STAT	Signal transducer and activator of transcription	6
C-Myc	MYC Proto-oncogene protein	5
CHOP-C	C/EBP homologous protein C	5
E47	E2A immunoglobulin enhancer-binding factor	5
MYOG	Myogenin	5
P54	Paraspeckle regulatory protein 54-kDa	4
NF-E2	Nuclear factor erythroid-derived 2	4
Olf-1	Olfactory 1	3
HFH-8	Hepatocyte nuclear factor-3 (HNF-8)/fork head homolog	3
HFH-1	Hepatocyte nuclear factor-3 (HNF-1)/fork head homolog	2
HNF-3	Hepatocyte nuclear factor 3	1
YY1	Yin-yang 1	1
Mef-2	Myocyte-enhancer factor 2	1

Table 5.2 Transcription factors predicted to regulate HERV-K expression showing the number of binding sites on each locus with red representing no binding sites and green representing 1 or more binding sites

	Loci																				TOTAL
	1	2	3	4	5	6	7	8	9	10	11	12	13	14	15	16	17	18	19	20	
OCT_1	1	2	13	12	6	3	3	4	5	1	3	8	13	16	5	4	2	12	8	1	122
FOXD3	3	7	1	2	1	3	4	10	3	2	5	6	3	10	4	1	3	27	4	0	99
HNF-3beta	4	5	1	1	0	2	1	2	3	2	0	2	1	3	1	1	0	4	5	0	38
CDP CR1	0	3	0	4	4	2	2	1	1	4	4	2	1	4	2	0	2	1	2	0	39
Pax-4	5	5	1	0	2	4	0	0	2	4	2	1	0	2	2	4	4	2	5	9	54
HNF-4	4	2	0	1	1	4	0	0	0	3	4	4	2	2	5	5	3	1	1	1	43
GATA-1	0	3	1	5	2	1	1	0	1	0	1	1	1	1	1	2	2	0	3	0	26
FOXJ2	2	1	2	2	1	0	1	4	1	1	1	0	0	3	0	1	0	1	2	2	25
AP-1	4	2	0	0	2	8	5	5	6	0	0	5	0	4	2	6	1	1	1	2	54
Ik-1	0	1	0	0	2	1	1	1	1	0	1	2	0	1	0	2	1	0	0	1	15
Evi-1	2	3	0	3	6	3	1	1	0	2	0	5	1	3	1	1	0	6	1	0	39
USF	2	0	0	0	1	2	3	2	0	2	0	6	0	0	1	1	1	3	6	1	31
c-Rel	0	0	0	2	2	2	3	2	1	0	0	1	0	2	2	5	5	0	1	4	32
GATA-3	0	2	6	4	2	1	1	2	0	0	1	2	1	0	0	0	0	2	3	0	27
Sox-9	3	0	0	0	1	1	2	2	2	0	1	1	0	1	1	2	0	2	0	0	19
Brn-2	1	1	1	1	0	1	0	0	0	0	1	1	0	2	1	0	0	1	1	0	12
COMP1	0	1	0	0	2	0	4	1	0	0	3	2	0	1	2	1	0	2	1	0	20
GATA-2	0	2	3	4	3	0	0	0	1	0	0	3	1	3	0	1	0	1	1	0	23
MyoD	4	1	0	0	0	3	1	2	1	1	0	0	0	0	1	1	2	1	0	3	21
Pax-6	1	0	2	0	0	1	1	1	1	1	0	0	1	1	0	0	2	0	5	0	17
RFX1	1	0	0	1	0	2	0	0	1	2	1	2	0	1	2	0	1	0	0	1	15
Hand1	1	0	0	2	0	0	0	0	1	1	0	0	1	3	1	1	2	0	0	1	14
Elk-1	0	0	0	0	1	1	0	0	2	0	1	0	1	1	1	1	0	1	1	0	11
Freac-7	2	1	0	2	0	0	1	2	2	1	0	1	0	0	0	0	1	1	0	0	14
v-Myb	0	1	0	0	0	1	3	2	2	2	1	1	0	0	0	0	0	0	3	0	16
NF-Y	0	1	1	0	3	4	2	2	3	0	1	0	0	0	2	0	0	0	0	0	19
HNF-1	2	1	1	1	1	1	0	0	1	0	0	0	1	1	0	0	0	0	0	0	10
Lmo2	1	2	1	1	0	1	0	0	0	0	0	0	1	1	0	0	1	0	1	0	10
CP2	2	0	0	0	1	0	0	1	0	0	1	1	1	0	2	2	5	0	0	0	16
v-Maf	0	2	0	1	0	0	0	0	0	1	1	2	0	0	1	1	0	0	1	4	14
AREB6	1	1	0	0	0	2	0	0	1	0	0	0	0	0	0	1	0	2	0	3	11
XFD-2	1	0	0	0	0	0	1	2	2	1	0	0	0	0	0	0	1	0	0	0	8
Sox-5	3	0	0	0	0	1	0	1	2	0	0	0	0	1	1	0	0	1	0	0	10
Gfi-1	1	0	0	0	1	0	1	1	1	0	1	0	0	0	1	0	0	0	0	0	7
TGIF	0	0	0	1	0	0	0	0	2	0	0	1	1	0	1	0	0	0	1	0	7
HFH-3	2	1	0	0	0	0	0	0	1	0	1	2	0	0	1	0	0	0	0	0	8
TATA	0	0	0	1	0	0	0	0	0	0	1	1	0	0	0	1	0	2	0	1	7
STAT	0	0	0	0	1	0	1	1	0	0	0	0	0	0	1	0	1	0	1	0	6
NF-KB	0	0	0	0	0	0	1	1	0	0	0	0	0	0	0	4	3	0	0	11	20
CDP CR3+HD	0	1	0	0	0	0	0	0	1	0	0	0	0	3	1	0	1	0	0	0	7
E47	0	2	0	0	0	1	0	0	0	0	1	0	0	0	0	1	0	0	0	0	5
p54	0	0	0	0	0	0	0	0	1	0	0	0	0	0	1	0	0	0	2	0	4
Myogenin	0	0	0	0	0	0	0	0	2	0	0	0	0	0	1	0	2	0	0	0	5
N-Myc	0	0	0	0	0	0	0	0	0	0	0	2	0	0	0	0	0	2	2	0	6
CHOP-C	1	0	0	0	0	0	0	0	3	0	0	0	0	0	1	0	0	0	0	0	5
C-Myc	0	0	0	0	0	0	0	0	0	0	0	2	0	0	0	0	0	2	1	0	5
HFH-8	0	0	0	0	0	0	0	1	1	0	0	0	0	0	0	0	1	0	0	0	3
HFH-1	0	0	0	0	0	0	0	1	1	0	0	0	0	0	0	0	0	0	0	0	2
HNF-3	0	0	0	1	0	0	0	0	0	0	0	0	0	0	0	0	0	0	0	0	1
Mef-2	0	0	0	0	0	0	0	0	0	0	0	0	0	1	0	0	0	0	0	0	1
E47	0	0	0	0	0	0	0	0	0	1	0	0	0	0	0	0	0	0	0	0	1
YY1	1	0	0	0	0	0	0	0	0	0	0	0	0	0	0	0	0	0	0	0	1

5.2.2 Antisense Oligonucleotide against TARDBP reduces TDP-43 expression

During the current study, a collaboration with the MND laboratory at the Perron Institute for Neurological and Translational Science allowed for the opportunity to visit and undergo the following research. Professor Anthony Akkari and Dr. Rita Mejzini developed phosphorodiamidate morpholino oligomers (PMO), an antisense oligonucleotide chemistry, against TARDBP to knockdown TDP-43. Therefore, using this PMO, the relationship between TDP-43 and HERV-K expression *in vitro* using a neuronal cell line, SH-SY5Y, was assessed. Using Western Blot (**Figure 5.1A**), Dr. Rita Mejzini assessed protein levels in the SH-SY5Y with increasing concentrations of the PMO which was quantitated and expressed as fold change of untreated cells, normalised to total protein. The concentration of the PMO was increased and the fold change of TDP-43 expression to untreated cells was compared. With an increase in concentration of the PMO from 0.79 μM through to 100 μM , there was a decrease in the fold change of TDP-43 compared to untreated suggesting successful knockdown of TDP-43 with increasing PMO concentrations (**Figure 5.1B**).

Following the western blot analysis, TDP-43 mRNA expression as well as two HERV-K targets (visualised in **Figure 1.6**), Pan HERV-K, HERV-K env and inflammatory markers intracellular adhesion molecule 1 (ICAM-1) and TNF- α was analysed at each concentration of the PMO against TDP-43. Due to the low expression of immune markers in the SH-SY5Y neuronal cell culture without a microglia co-culture, ICAM-1 was chosen due to its innate expression and its known induction by TNF- α (Myers *et al.*, 1992, Singh *et al.*, 2023). There was no association between the expression of TDP-43 (**Figure 5.2A**), Pan HERV-K (**Figure 5.2B**), HERV-K env (**Figure 5.2C**), ICAM-1 (**Figure 5.2D**) or TNF- α (**Figure 5.2E**) with the increasing PMO concentration.

5.2.3 TDP-43 Expression is Not Correlated with HERV-K Expression *In Vitro*

To assess the relationship between TDP-43 and HERV-K in the SH-SY5Y neuronal cell line, the expression of TDP-43 at the various concentrations of the PMO was correlated against Pan HERV-K and HERV-K env. There was no correlation between TDP-43 and pan HERV-K (**Figure**

5.3A; $R^2 = 0.3215$, $p = 0.4263$) or between TDP-43 and HERV-K env (**Figure 5.3B**; $R^2 = 0.1506$, $p = 0.3284$).

5.2.4 TDP-43 Expression is Correlated with Immune Markers *In Vitro*

Following on from the previous investigation of the TDP-43 and HERV-K relationship *in vitro*, the relationship between immune markers and TDP-43 was also investigated. **Figure 5.4A** shows the moderate correlation between TDP-43 and TNF- α ($R^2 = 0.563$, $p = 0.0125$). TDP-43 expression was strongly correlated with ICAM-1 expression in the SH-SY5Y cell line (**Figure 5.4B**; $R^2 = 0.787$, $p = 0.006$).

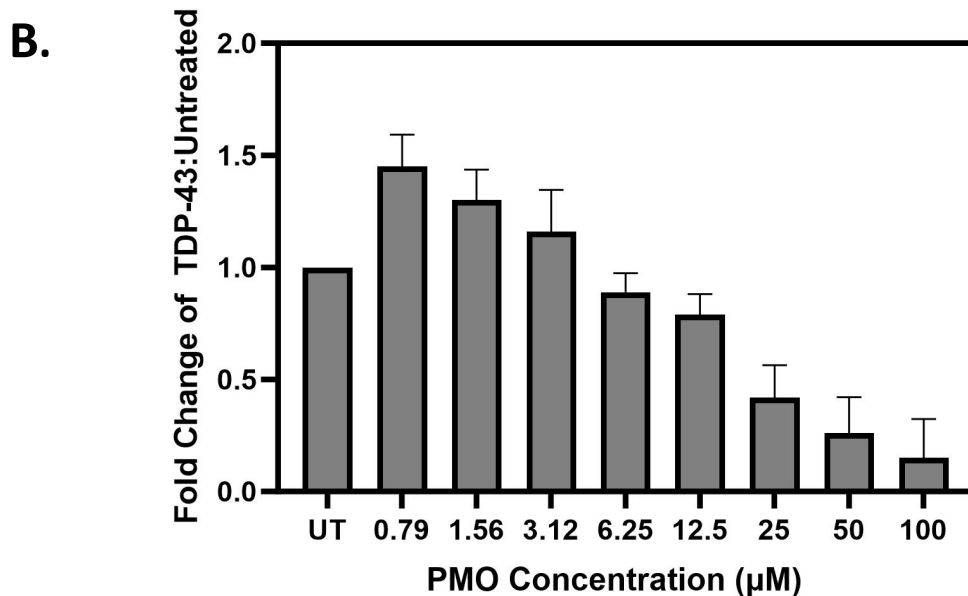
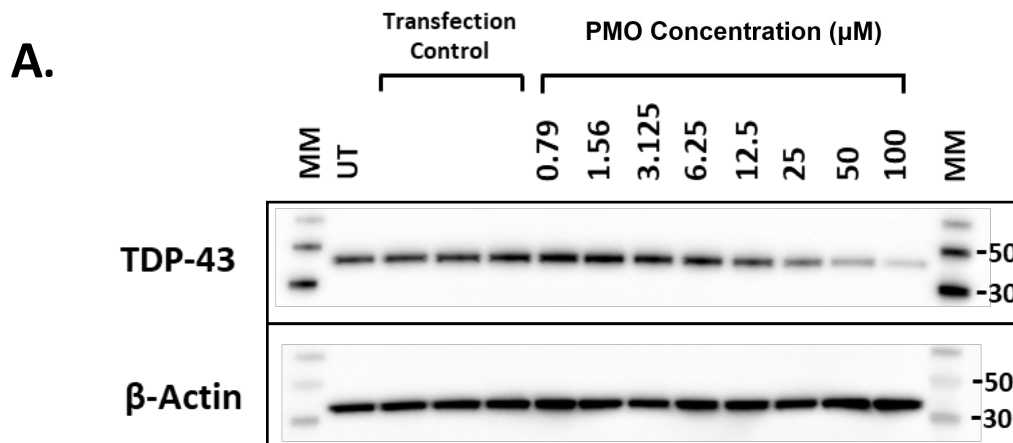


Figure 5.1 Change of TDP-43 expression to untreated SH-SY5Y after treatment with various concentrations of a PMO against TARDBP

SH-SY5Y neuronal cell line was transfected with different concentrations of a type of antisense oligonucleotide, PMO, against *TARDBP* to reduce TDP-43 expression. **A.** Western Blot showing TDP-43 protein present after transfection with increasing levels of PMO targeting TARDBP. B-actin used as housekeeping gene. **B.** Quantification of data shown in A with fold change of TDP-43 protein levels of different concentrations compared to untreated SH-SY5Y cells, normalised to total protein. Data from PMO-knockdown of TDP-43 in SH-SY5Ys was kindly provided by Dr. Rita Mejzini. Results expressed as mean \pm SEM from duplicate values and analysed with One-way ANOVA with Tukey's multiple comparisons UT = untreated, MM = molecular marker

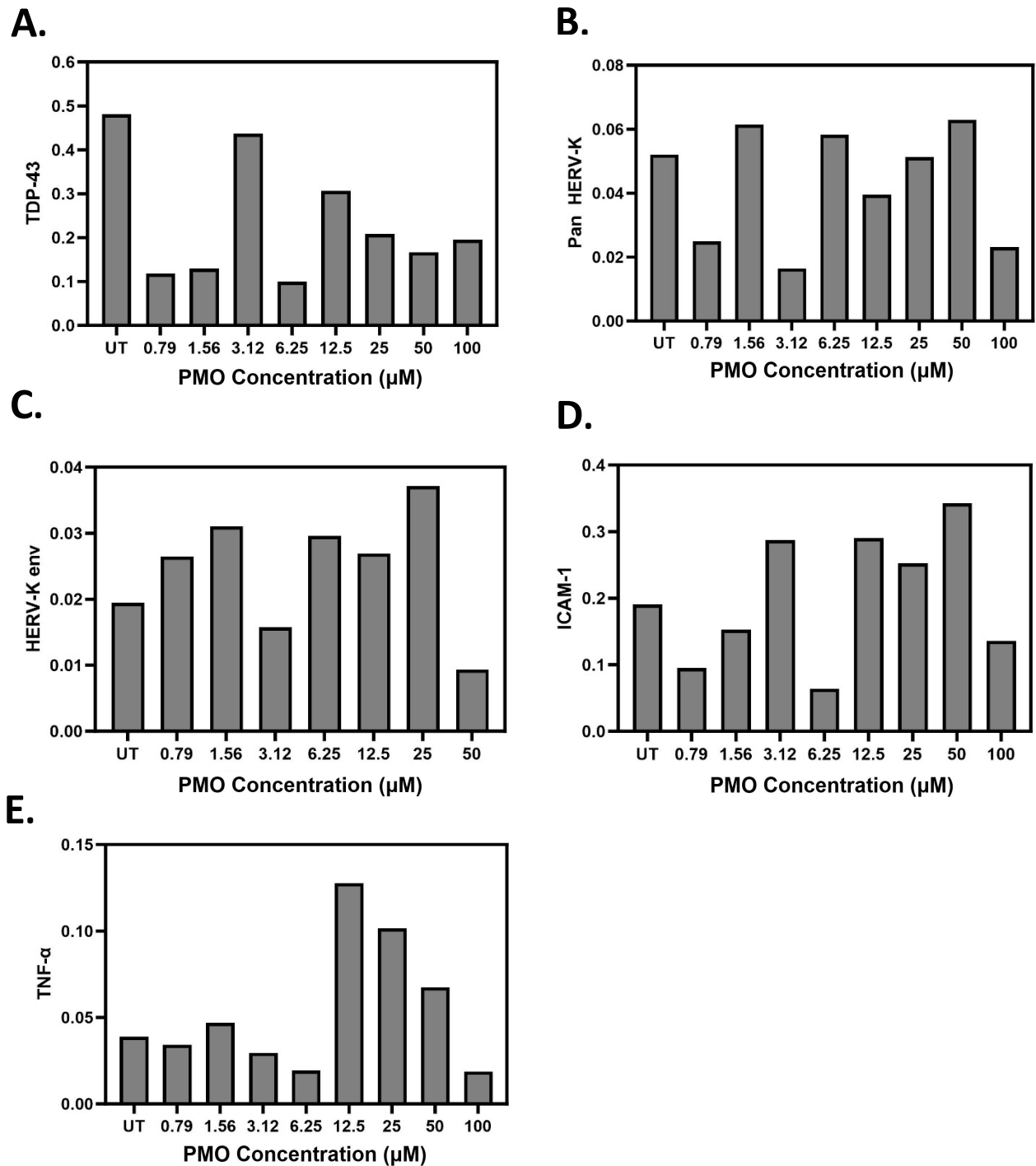


Figure 5.2 Expression of HERV-K and inflammatory markers at different concentrations of a PMO against TARDBP

SH-SY5Y neuronal cell line was transfected with different concentrations of a type of antisense oligonucleotide, PMO, against TARDBP to reduce TDP-43 expression. Expression of **A.** TDP-43, **B.** Pan HERV-K, **C.** HERV-K env, **D.** ICAM-1 and **E.** TNF- α at different concentrations of the PMO.

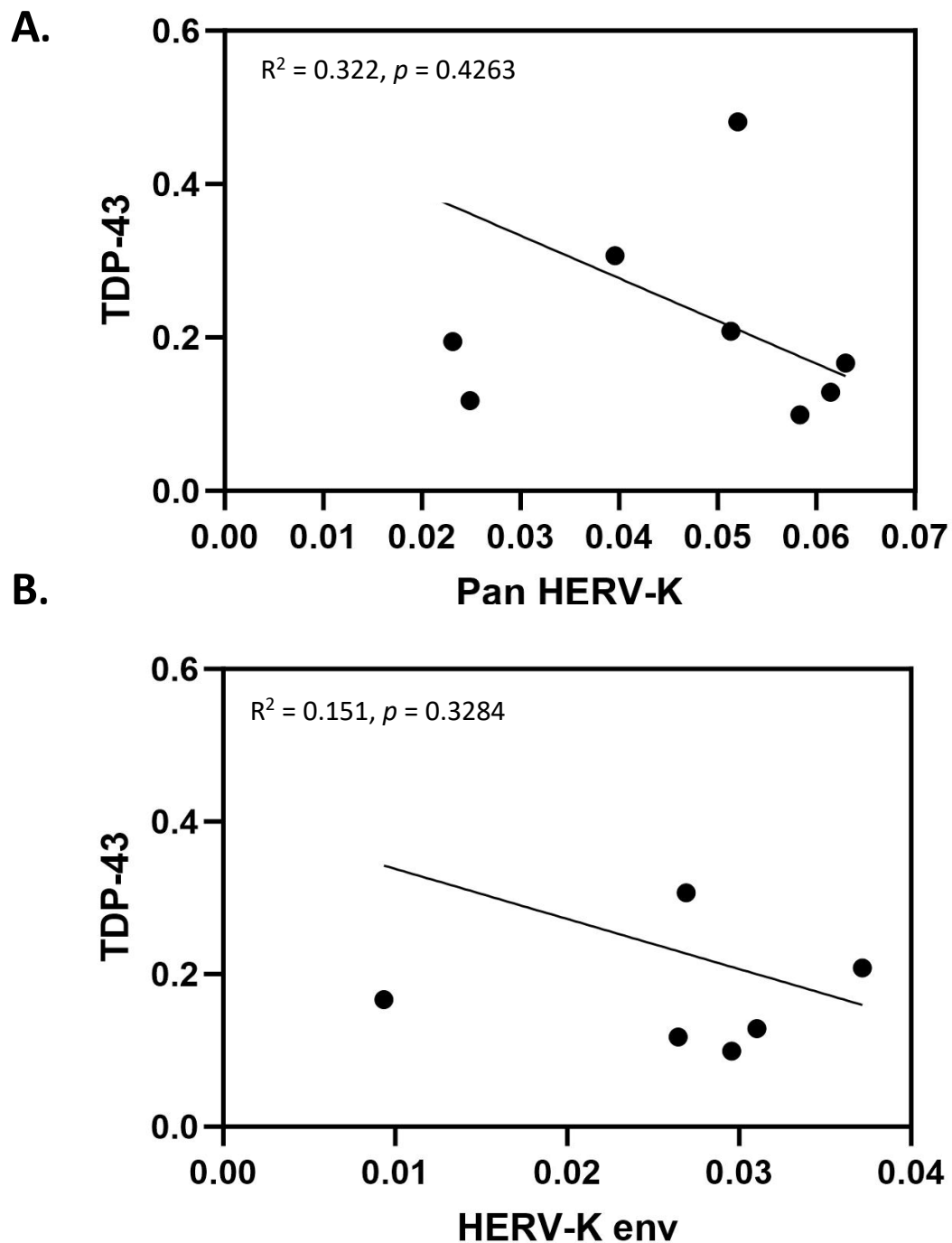


Figure 5.3 Correlation of TDP-43 expression to Pan HERV-K and HERV-K env expression in a TDP-43-knockdown SH-SY5Y cell line

The relationship between the expression of **A.** Pan HERV-K ($n = 9$) and **B.** HERV-K env ($n = 9$) to mRNA expression of TDP-43 was quantified from SH-SY5Y neuronal cell line transfected with different concentrations of a type of antisense oligonucleotide, PMO, against *TARDBP* to reduce TDP-43 expression.

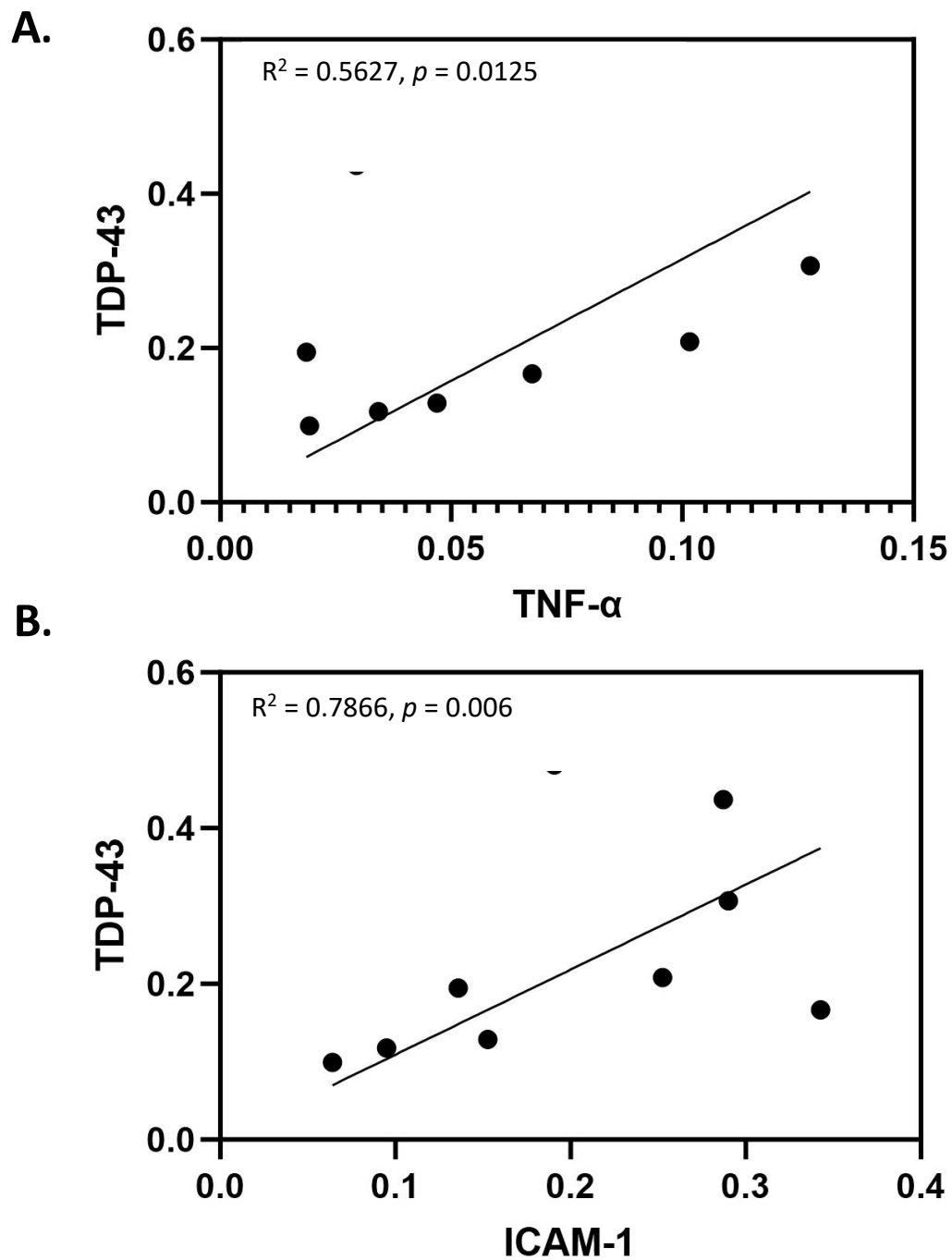


Figure 5.4 Correlation of TDP-43 expression to ICAM-1 and TNF- α expression in a TDP-43-knockdown SH-SY5Y cell line

The relationship between the expression of **A.** TNF- α (n = 9) and **B.** ICAM-1 (n = 9) to mRNA expression of TDP-43 was quantified from SH-SY5Y neuronal cell line transfected with different concentrations of a type of antisense oligonucleotide, PMO, against *TARDBP* to reduce TDP-43 expression.

5.2.5 HERV-K and TDP-43 Expression is Not Increased in a Primary Cell Line of MND

The previous findings outlined the ability to detect and investigate HERV-K expression in a neuronal cell line. After investigating the levels of HERV-K in this cell line and assessing the relationship with TDP-43, the expression of Pan HERV-K, HERV-K pol, HERV-K env and TDP-43 were quantified in a primary cell line. Due to accessibility of the cell line, olfactory neuroepithelial-derived stem (ONS) cells were used to examine HERV-K and TDP-43 expression. ONS cells were obtained from sporadic MND patients (n = 5) and controls (n = 6). There were no significant differences in the expression levels of pan HERV-K (**Figure 5.5A**; $p = 0.964$), HERV-K env (**Figure 5.5B**; $p = 0.234$), HERV-K pol (**Figure 5.5C**; $p = 0.879$) or TDP-43 (**Figure 5.5D**; $p = 0.085$) between MND patients and controls.

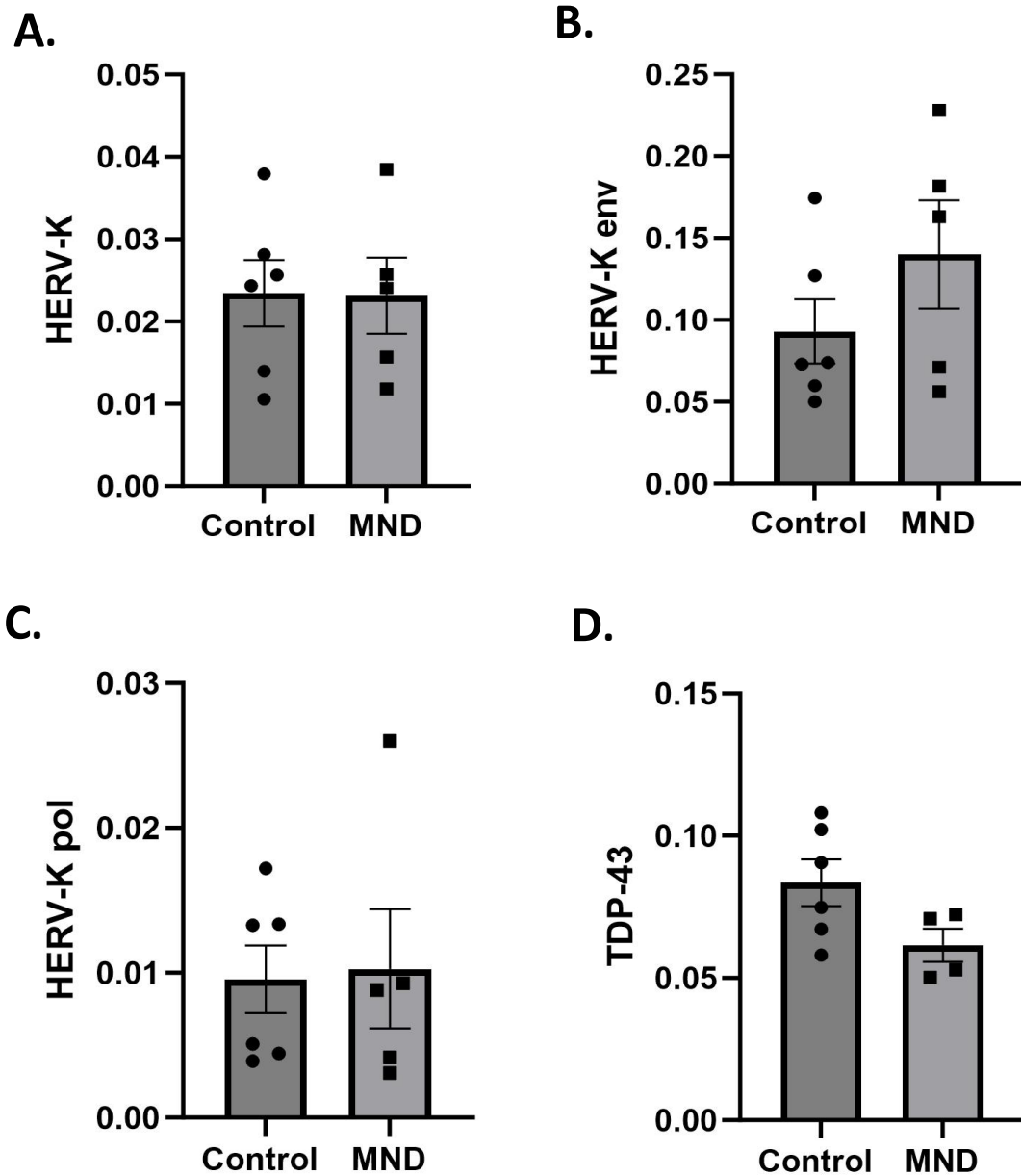


Figure 5.5 TDP-43 and HERV-K expression from olfactory neuroepithelial derived stem cells from MND patients and controls

mRNA extracted from olfactory neuroepithelial derived stem cells from MND patients (n= 4-5) and controls (n = 6) was quantified using RT-qPCR using primers for **A.** pan HERV-K, **B.** HERV-K env, **C.** HERV-K pol and **D.** TDP-43. Ct values were normalised to cyclophilin. Results represent the mean \pm SEM from duplicate values and were analysed with Student's *t*-test.

5.2.6 Expression of HERV-K in Multiple Cell Lines

To determine the optimal cell line to use for assessing the influence of Triumeq *in vitro*, multiple cell lines that were readily available were assessed for their expression of TDP-43 and HERV-K gene targets, HERV-K gag, HERV-K pol, HERV-K env shown in **Figure 1.6**, as well as Pan HERV-K depicting full length HERV-K by binding the consensus LTR sequence. The cell lines analysed were 1. HeLa, a cervical cancer cell line 2. U937, Epstein Barr Virus transformed Histiocytic lymphoma cell line 3. Huh7, a hepatoma cell line 4. HEK293, an embryonic kidney cell line and 5. ARPE-19, a retinal epithelial cell line. There were no significant differences in the expression of pan HERV-K, HERV-K gag, HERV-K env or HERV-K pol between any of the cell lines used (**Figure 5.6**). There was, however, a significant increase in the level of TDP-43 expression in the HeLa cell line compared to ARPE-19 ($p = 0.0013$), Huh7 ($p = 0.0024$), HEK293 ($p = 0.024$) and U937 ($p = 0.0052$). There was also a correlation between expression of HERV-K env and TDP-43 across all cell lines (; $R^2 = 0.702$, $p = 0.0132$).

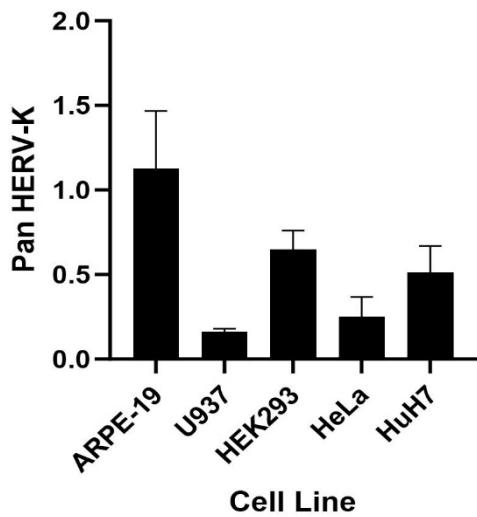
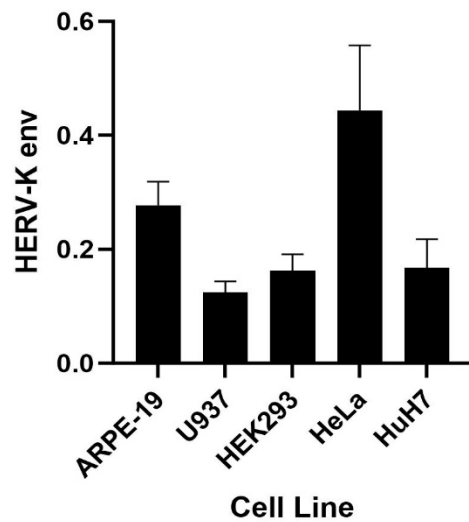
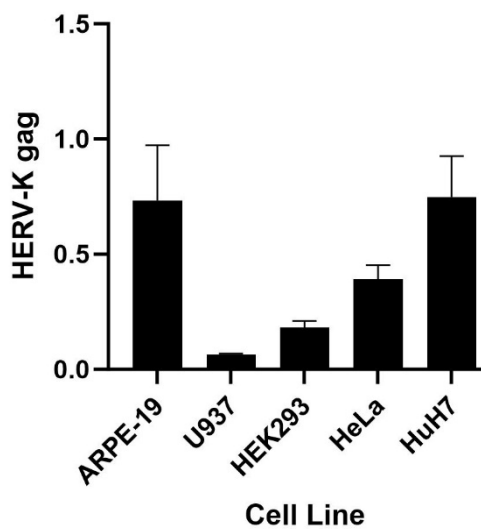
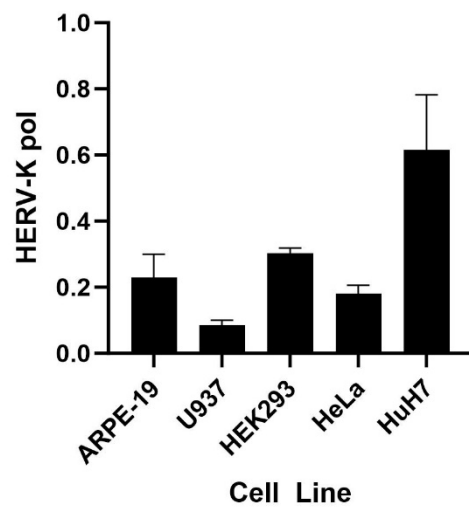
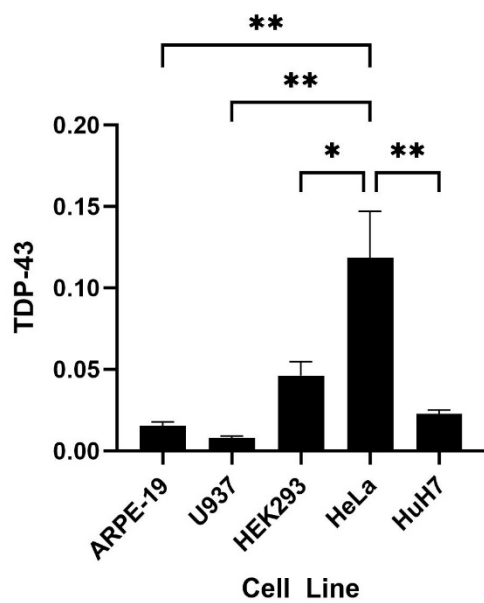
A.**B.****C.****D.****E.**

Figure 5.6 HERV-K expression in multiple cell lines

mRNA from uninfected HeLa, Huh7, U937, HEK293 and ARPE-19 cell lines were used to quantify the expression of **A.** Pan HERV-K, **B.** HERV-K env, **C.** HERV-K gag, **D.** HERV-K pol and **E.** TDP-43. Ct values were normalised to cyclophilin, and results are expressed as the mean \pm SEM from triplicate values. Two-way ANOVA with Tukey's multiple comparisons. * $p < 0.05$, ** $p > 0.01$

5.2.7 Dengue Virus Infection or LPS stimulation does not increase HERV-K or TDP-43 expression in a HeLa cell line

Due to HeLa being an established and validated non-neuronal cell line for MND research, (Figure 5.6), this cell line was used to investigate the ability to stimulate HERV-K expression through exogenous viral infection and an immune response stimulation. To do this, as described in Section 2.2.11.1, HeLa cells were infected with dengue virus (DENV) or stimulated with lipopolysaccharide (LPS) to induce an immune response and compared to uninfected (UI) cells. Pan HERV-K, HERV-K gag, HERV-K env and TDP-43 expression levels were analysed from the DENV infected, LPS stimulated or uninfected (UI) cells. There were no significant differences in the expression of any HERV-K targets or TDP-43 between the DENV-infected, LPS-stimulated or UI cells (**Figure 5.7**).

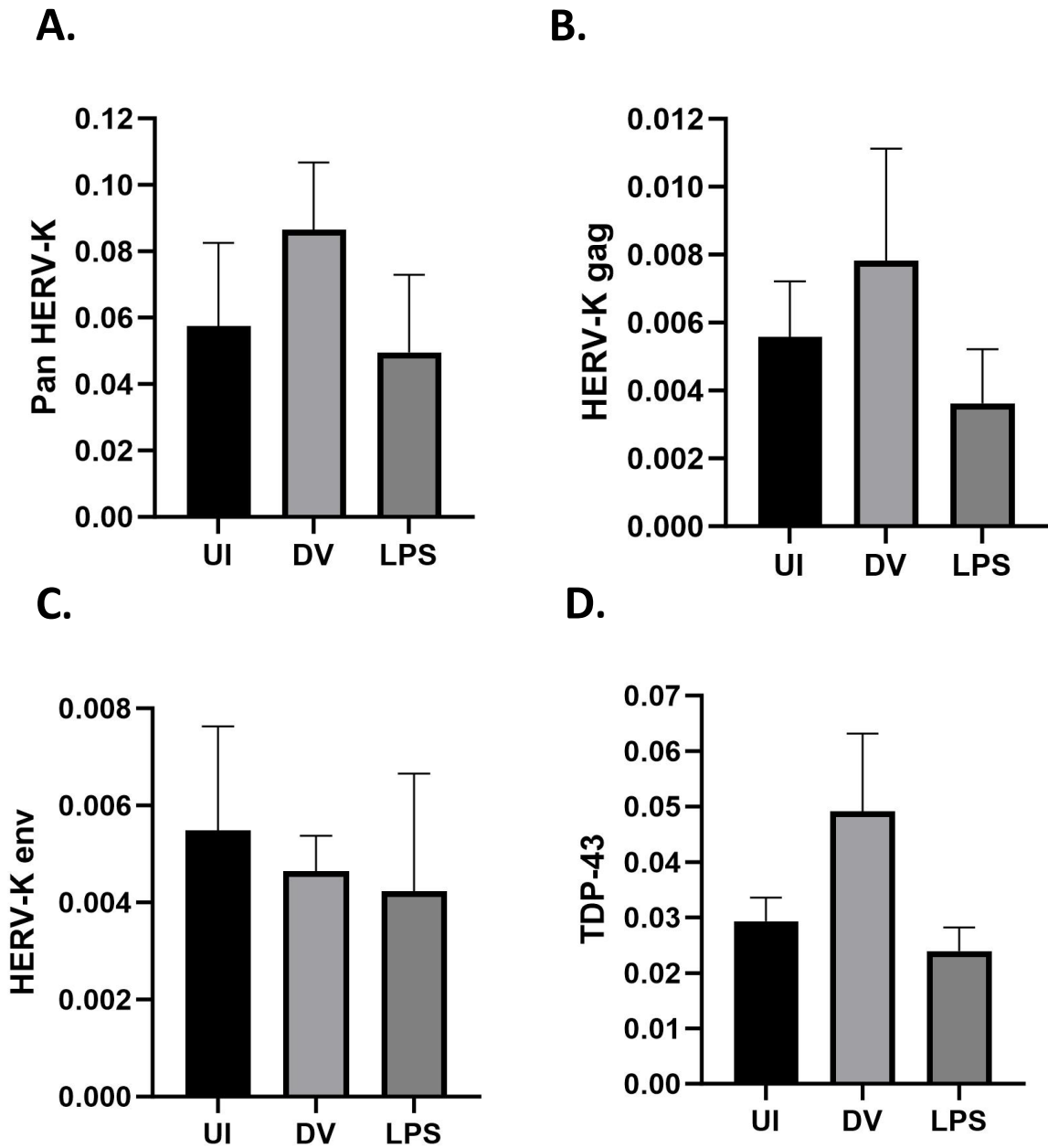


Figure 5.7 Expression of TDP-43 and HERV-K in a HeLa cell line with Dengue Virus Infection and LPS stimulation

HeLa cells were uninfected (UI), dengue virus (DENV) infected, or lipopolysaccharide (LPS) stimulated and incubated for 24 hours. Cells were harvested and analysed for mRNA expression of **A.** Pan HERV-K, **B.** HERV-K gag, **C.** HERV-K env and **D.** TDP-43. Ct values were normalised to cyclophilin, and results are expressed as the mean \pm SEM from triplicate values. Two-way ANOVA with Tukey's multiple comparisons.

5.2.8 Expression of HERV-K pan and HERV-K env is Increased Following Zika Virus Infection *In Vitro*

Following the previous finding where Triumeq did not have a significant effect on the expression of HERV-K or TDP-43 *in vitro* after DENV or LPS stimulation (Figure 5.7), the expression of pan HERV-K and HERV-K env was investigated in another cell line of neuronal origin, ARPE-19. ARPE-19 cell line was chosen due to the trend to increased expression of pan HERV-K compared to the other cell lines analysed, including HeLa cells (Figure 5.6A). The expression of Pan HERV-K, HERV-K env and TDP-43 was compared between ARPE-19 that had been infected with DENV, Zika Virus (ZIKV), LPS stimulated or Poly I:C stimulated. For pan HERV-K (Figure 5.8A), there was a significantly higher expression in the ARPE-19 cells infected with ZIKV compared to uninfected cells ($p = 0.0001$) DENV ($p = 0.0002$), LPS ($p = 0.0001$), or Poly I:C ($p = 0.0001$). Similarly, as shown in Figure 5.8B, there was a significantly higher expression of HERV-K env in the ZIKV-infected ARPE-19 compared to uninfected ($p = 0.0051$), DENV-infected ($p = 0.0049$), LPS stimulated ($p = 0.001$) or transfected with Poly I:C ($p = 0.0012$). For TDP-43 (Figure 5.8C), there was significantly higher expression in DENV-infected ARPE-19 compared to UI ($p = 0.0002$), LPS ($p = 0.0007$), and Poly I:C ($p = 0.0008$). There was not significantly higher expression in the DENV-infected ARPE-19 compared to ZIKV-infected ($p = 0.326$).

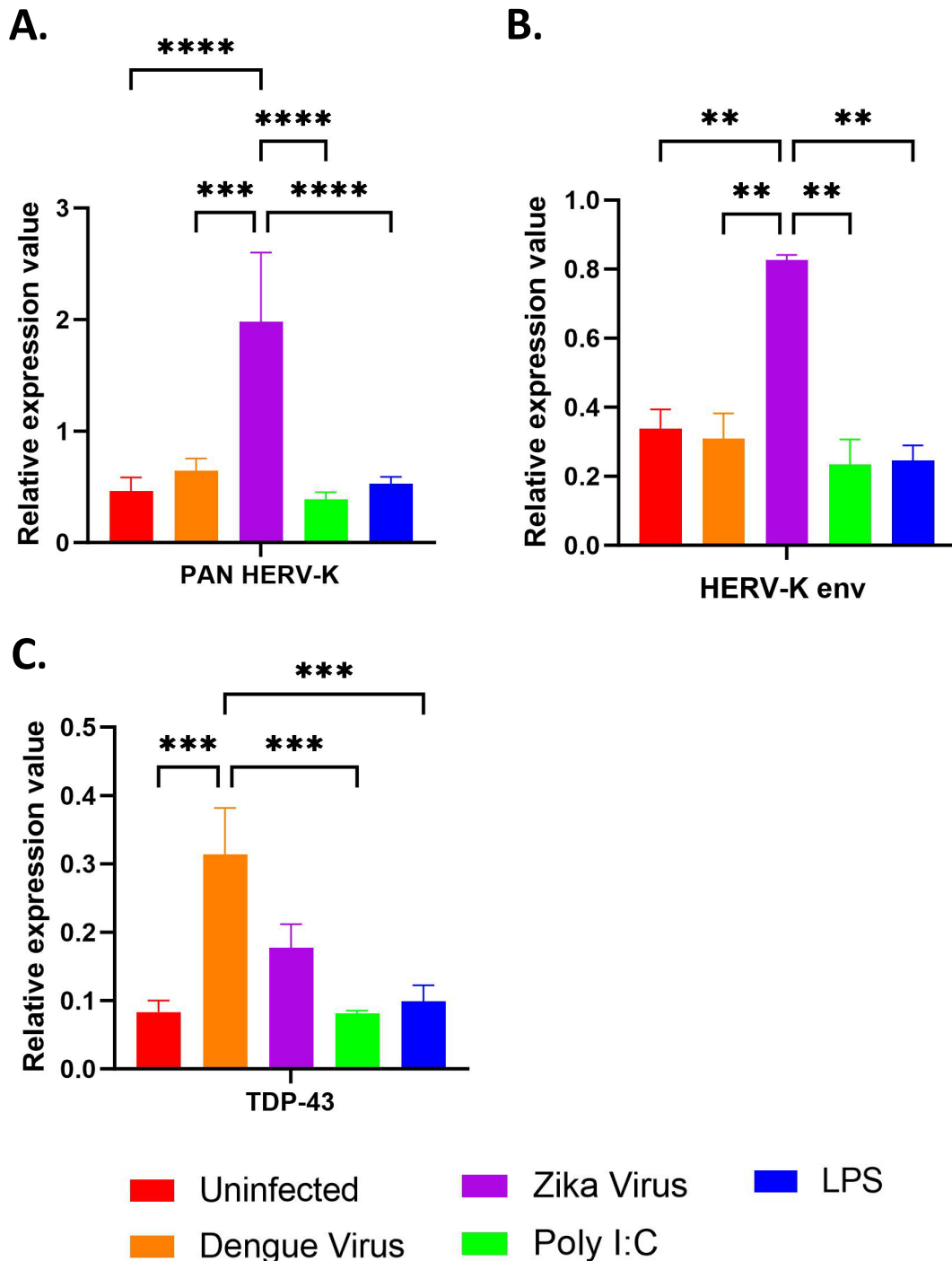


Figure 5.8 Expression of pan HERV-K and HERV-K env in ARPE-19 with Zika virus or dengue virus infection and LPS and Poly-IC stimulation

ARPE-19 were uninfected (UI) (n = 4), zika virus (ZIKV) infected (n = 2), dengue virus (DENV) infected (n = 3), lipopolysaccharide (LPS) stimulated (n = 4) or Poly I:C stimulated (n = 3) and incubated for 24 hours before cells were harvested and analysed for mRNA expression of **A.** Pan HERV-K, **B.** HERV-K env and **C.** TDP-43. Ct values were normalised to cyclophilin, and results are expressed as the mean \pm SEM. One-way ANOVA with Tukey's multiple comparisons. ** $p < 0.001$, *** $p < 0.0001$, **** $p < 0.00001$

5.3 Discussion

5.3.1 Summary

Although Triumeq is currently being trialled for MND in a phase III clinical trial, there are still unknowns regarding the mechanism of action of Triumeq, particularly its effects on the association between HERV-K and TDP-43. The previous chapters outlined the effect of Triumeq *In vivo*, providing valuable insight into the mechanism of action of Triumeq in a mouse model of MND. However, due to the lack of expression of human endogenous retroviruses in all mice, the previous chapters do not provide insight into the effects of Triumeq on HERV-K expression and its association with TDP-43. Hence, the aim of this chapter was to characterise the expression of HERV-K and TDP-43 *in vitro*, including *in silico* analysis of the transcription factors that are predicted to regulate HERV-K expression. This chapter also aimed to further elucidate the relationship between HERV-K and TDP-43 *in vitro*.

5.3.2 In Silico Analysis of Transcription Factors Regulating HERV-K Expression

During COVID-19 lockdowns with limited lab access, computer-based analysis became the focus. The *in silico* analysis of the transcription factors that are predicted to regulate the expression of full length HERV-K provided some interesting results (**Table 5.1** and **5.2**). This work expanded on previous research identifying binding sites for transcription factors on four HERV-K loci (Manghera and Douville, 2013) and looked at a further 20 HERV-K loci. Firstly, one transcription factor that had 46 total binding sites across 16 of the 20 full length HERV-K loci was CCCAAT displacement protein with cut repeats 1 and 3 (CDP CR1-3). This is of particular interest for ERV analysis as these transcription factors are known repressors of mouse endogenous retrovirus MMTV, binding the MMTV LTR (Zhu *et al.*, 2000). Similarly, Octamer transcription factor 1 (OCT1) which had the highest number of total binding sites and common across all 20 HERV-K loci, has been shown to stimulate HERV-W through exogenous viral infection (Lee *et al.*, 2003).

Of the predicted transcription factors in Table 5.1, NF- κ B, with 20 binding sites across the 20 loci, has been experimentally shown to stimulate HERV-K expression in MND with increased levels of HERV-K activity after transfection with NF- κ B-expressing constructs in a human

neural progenitor cell line (Manghera *et al.*, 2016b). Furthermore, NF- κ B and AP-1, with 54 binding sites across 15 of the 20 HERV-K loci identified in the current study, have also been shown to be stimulated from TDP-43 overexpression and mislocalisation (Zhao *et al.*, 2015), providing support for an association between TDP-43 and HERV-K. Transcription factor STAT had 6 binding sites across 5 of the 20 full length HERV-K, consistent with previous research identifying STAT involvement in HERV-K regulation (Russ *et al.*, 2023, Manghera and Douville, 2013). The STAT involvement in HERV-K regulation could be a link between TDP-43, inflammation and HERV-K with a known association between STAT signalling and CXCL10 expression reported in the literature (Burke *et al.*, 2013, Makuch *et al.*, 2022) and the TDP-43 and CXCL10 expression correlation observed in the current study (Figure 3.13).

Some of the transcription factors shown in **Table 5.1** are known to be activated through exogenous viral infection also. For example, human simplex virus 1 (HSV-1) is known to stimulate activation of HERV-W and HERV-K through OCT-1 and AP-1 and could therefore, be a link between exogenous viral infection and endogenous retroviral activation (Kwun *et al.*, 2002, Lee *et al.*, 2003). Furthermore, HIV-1 has been shown to activate HERV-K through NF- κ B and Tat (Vincendeau *et al.*, 2015, Gonzalez-Hernandez *et al.*, 2012) and has been shown to increase TDP-43 expression (Douville and Nath, 2017). The exogenous viral infection activating endogenous retroviral activity through transcription factors involved in immune function also supports the previous finding of ZIKV infection resulting in greater HERV-K expression in ARPE-19 (**Figure 5.9**). The transcription factors identified in the current study that are predicted to regulate HERV-K expression validate and expands on previous research which identified transcription factor sites within HERV-K LTR consensus sequences (Manghera and Douville, 2013). Overall, these results support the previous research and findings from **Chapter 3** that increased HERV-K expression could be due to immune function.

5.3.3 Analysis of HERV-K and TDP-43 Expression in Multiple Cell Lines

The *in silico* analysis outlined the involvement of an association between HERV-K and inflammation with multiple HERV-K loci containing binding sites for transcription factors associated with immune function. To elucidate this finding further, *in vitro* analysis included investigation of HERV-K, TDP-43 and inflammatory marker expression in a neuronal cell line,

SH-SY5Y. To investigate the relationship of TDP-43 and HERV-K *in vitro*, SH-SY5Ys were treated with a type of antisense oligonucleotide, a PMO, to target and knockdown TARDBP at different concentrations, resulting in significantly lower TDP-43 expression with higher PMO concentration as determined by quantitative western blot analysis performed by Dr. Rita Mejzini (**Figure 5.1**). TDP-43 mRNA levels were also quantified through PCR analysis and with TDP-43 expression reduced with increased concentration of the PMO (**Figure A.6A**). The current study then aimed to determine the relationship between TDP-43 and HERV-K expression in this cell type through RT-qPCR (**Figure 5.2**). There was no relationship seen between TDP-43 expression and concentration of the PMO in the current study (**Figure 5.3A**) suggesting the PMO has not successfully altered the TDP-43 RNA levels. However, the inconsistent TDP-43 RNA expression between the current study and the study performed by Dr. Rita Mejzini could be explained through the different methods of detection of TDP-43 expression and the primers used for TDP-43 detection. To detect TDP-43, Dr. Rita Mejzini used PCR, targeting the full-length TDP-43 sequence, shown in **Figure A.6B**. The current study, instead, used RT-qPCR for quantitative analysis of TDP-43 expression using primers described in section 2.1.1, with primer binding location shown as the red line in **Figure A.6B**, binding exon 5, a location not affected by the PMO knockdown. Future research will reassess TDP-43 RNA levels using primers validated for detection of full-length TDP-43 and the exon skipped transcripts to ensure accurate quantification after TDP-43 knockdown. Such methods for assessing PMO knockdown have been achieved for Duchenne Muscular Dystrophy (López-Martínez *et al.*, 2022) Furthermore, the qPCR analysis was completed from a single experiment. Repetition of the analysis from further TDP-43 knockdown experiments would be beneficial prior to drawing conclusions.

Although TDP-43 expression was not correlated with the concentration of the PMO in the current study, correlation analysis between HERV-K and TDP-43 was still completed to assess the relationship between TDP-43 and HERV-K expression in a neuronal cell line. The levels of pan HERV-K and HERV-K env were assessed at the different concentrations of the PMO and the correlation with TDP-43 examined. There was no correlation between pan HERV-K or HERV-K env and TDP-43 expression in the current study, not consistent with previous *in vivo* or *in vitro* studies (Manghera *et al.*, 2016a, Li *et al.*, 2015). To assess the relationship between TDP-43 expression and inflammatory markers in this cell type, TDP-43 expression was also

correlated with inflammatory markers. This finding is consistent with research suggesting neuronal TDP-43 expression induces inflammation, potentially involved in neurodegenerative processes (Bright *et al.*, 2021). Only two inflammatory markers were assessed based on the limited amount innately expressed inflammatory markers in neuronal cells in the absence of a microglial co-culture, where cytokines and inflammatory mediators are predominately produced (Smith *et al.*, 2012, Haenseler *et al.*, 2017). There was a correlation between the two markers assessed, however, with a moderate and strong correlation between TDP-43 and TNF- α and ICAM-1, respectively. Although the involvement of ICAM-1 in neurodegeneration and how the TDP-43/ICAM-1 association may be involved is unclear, it is understood that ICAM-1 expression promotes an inflammatory response (Singh *et al.*, 2023) and is induced by TNF- α (Burke-Gaffney and Hellewell, 1996, Myers *et al.*, 1992). Furthermore, serum levels of ICAM-1 have been shown to be higher in MND patients compared to controls (Brodovitch *et al.*, 2021). Therefore, TDP-43 expression could induce an inflammatory state through TNF- α which is further exacerbating pro-inflammatory processes and may be involved in neurodegeneration. With a lack of correlation between HERV-K and TDP-43 in this model, TDP-43 expression may be inducing the inflammatory state prior to the involvement of HERV-K. Further research is required to elucidate this pathway with future directions discussed in **Chapter 6**.

Analysis of HERV-K and TDP-43 expression in ONS cells did not show any statistical significance in expression between MND patients and controls for HERV-K or TDP-43 (**Figure 5.5**). While surprising, the limited sample size could be contributing to the lack of differences observed. Furthermore, while this cell type was readily available and less invasive to obtain from MND patients and controls, there is a lack of data regarding disease pathology in this model, particularly regarding TDP-43 pathology (Mejzini *et al.*, 2019). The trend towards higher expression of HERV-K env in the MND patient cells compared to control patient cells is promising with HERV-K env being shown to have elevated expression in MND patient CSF and serum and is associated with neurotoxicity in vitro (Steiner *et al.*, 2022). To further this research in primary cells with cells that also produce a disease phenotype including TDP-43 mislocalisation, readily available induced pluripotent stem cells (iPSCs) from MND patients and healthy controls will be used to analyse the expression levels of HERV-K and TDP-43 at the different differentiation stages from iPSCs through to iPSC-motor neurons. Furthermore,

the lack of significant difference in TDP-43 expression between MND patients and controls could be due to the pathology of TDP-43. Alternative splicing of TDP-43 pre-mRNA can produce TDP-43 C-terminal and N-terminal fragments of TDP-43 (Igaz *et al.*, 2009). These fragmented forms of TDP-43 have been shown to contribute to disease pathology, specifically, TDP-43 cytoplasmic accumulation (Chhangani *et al.*, 2021, Che *et al.*, 2015) but may not be detectable by primers designed for full-length TDP-43 in the current study (as indicated in section 2.1.1). Furthermore, recent research showed cryptic exons in TDP-43 generating de novo proteins in iPSCs and CSF of MND patients (Seddighi *et al.*, 2024). Therefore, the TDP-43 expression profile may not be adequately reflecting disease pathology in these patients.

Following on from the research in a primary cell line, the expression levels of HERV-K and TDP-43 were assessed using readily available secondary cell lines to determine which cell lines had highest expression levels of HERV-K or TDP-43. (**Figure 5.6**). While there were no significant differences in the expression of HERV-K between any cell lines, HeLa not only had a trend towards a significant increase in the expression of HERV-K *env*, but there was also significantly higher expression of TDP-43. This finding is consistent with previous research where the use of HeLa cells for TDP-43 pathology research has been validated as a non-neuronal model for MND (Liu *et al.*, 2013, Giannini *et al.*, 2020).

Based on this finding, HeLa were used to stimulate HERV-K expression through exogenous viral infection and inflammatory stimulation. Due to availability and the previous *in silico* finding of NF- κ B and STAT transcription factors predicted to regulate HERV-K expression, DENV infection and inflammatory stimulation through addition of LPS was used to potentially stimulate HERV-K expression. However, there were no effects of the DENV or LPS stimulation on HERV-K or TDP-43 expression. With a lack of effect of DENV infection on HERV-K expression, further analysis was conducted to assess the effects of another viral infection, ZIKV, on HERV-K expression in a cell line of neuronal origin. ARPE-19 were chosen based on the trend towards increased pan HERV-K expression compared to other cell lines. HERV-K *env* expression was significantly increased in ARPE-19 with ZIKV infection compared to DENV infection or inflammatory stimulation with Poly: IC or LPS (**Figure 5.3**). This finding is of

particular interest due to the ability of ZIKV to modulate an immune response within the eye (Simonin *et al.*, 2019, Singh *et al.*, 2017, Cowell *et al.*, 2023).

The increased HERV-K expression within the ZIKV-infected ARPE-19 suggest a link between exogenous infection, immune response and endogenous retrovirus activation. TDP-43 expression analysis from these cells also showed that DENV significantly increased TDP-43 expression but ZIKV did not. This finding suggests that while ZIKV increases HERV-K expression, it does not occur through increased TDP-43 expression. Furthermore, previous research from has shown a significantly higher expression of TNF- α in ZIKV-infected ARPE-19 but not in DENV-infected ARPE-19 (Shown in Appendix **Figure A.5**). This suggests a link between increased inflammatory response from exogenous viral infection and increased HERV expression that is independent of TDP-43. Research to build upon the results summarised in this chapter will include analysis of Triumeq treatment on ZIKV-infected ARPE-19 which was not completed in the current study due to time constraints.

5.3.4 Conclusions

In summary, this chapter reports the expression of HERV-K in multiple cell lines including a neuronal cell line with TDP-43 knockdown and a primary cell line obtained from MND patients. This chapter investigated the expression of TDP-43 and HERV-K in other cell lines including ARPE-19, a cell line of neuronal origin. ARPE-19 was found to have increased expression of HERV-K after infection with ZIKV, an infection that occurs in the CNS. This was independent of TDP-43 expression, but potentially involving TNF- α , as shown by previous research. Future work should explore further cell lines to be used for HERV-K analysis *in vitro* including iPSCs from MND patients and controls and investigate treatment of ARPE-19 with Triumeq after exogenous viral infection. Understanding the transcription factors that are predicted to regulate HERV-K expression could also allow for *in vitro* stimulation of HERV-K expression to evaluate the effects of Triumeq on HERV-K expression.

CHAPTER 6. DISCUSSION

6 DISCUSSION

6.1 Overview

Despite the great effort from many research groups worldwide, MND remains an incurable and for the most part, an untreatable disease. The current treatment landscape of MND provides dismal results for motor improvement or increases to survival time for MND patients (Outlined in **Chapter 1**). This highlights the need for further treatment options for MND patients. Understanding the neurodegenerative mechanisms that underpin the progressive loss of motor function and eventual death in MND patients is vital for developing new treatments or improving the therapeutic benefit of currently available treatments. Endogenous retroviruses and their reactivation have been linked to MND and could, therefore, be a therapeutic avenue for reducing neurodegeneration occurring in MND (Li *et al.*, 2022). Antiretroviral therapy, Triumeq, to target ERVs is currently being investigated as a treatment for MND in a Phase III clinical trial with a Phase II trial showing promising outcomes for reducing HERV-K in serum of MND patients (Gold *et al.*, 2019). However, the mechanism of action of Triumeq remains unclear with the effect on TDP-43, a hallmark of MND pathology, still unknown. The central aims of this study were to determine the effects of Triumeq in a TDP-43 mouse model of MND. Based on the inability to detect human ERVs in mice, the last aim of the study was to further elucidate the mechanism of Triumeq and its effects on HERV-K and TDP-43 *in vitro*.

6.1.1 Triumeq Treatment in a TDP-43 mouse model of MND

A TDP-43 mouse model of MND, hTDP-43 Δ NLS, was chosen for the analysis of Triumeq treatment *in vivo*. The pilot study assessed the tolerability and palatability of Triumeq and the onset of disease after Dox removal prior to assessing Triumeq efficacy in a large cohort. As outlined in **Chapter 3**, there was a consistent and significant difference in the motor performance according to the wirehang test, at the approximate half-way point of the study between the treated and untreated mice. This improvement in motor performance in the treated mice at this point of the study also coincided with a significant reduction in the level of urinary p75^{ECD} and a significantly higher motor neuron count within the lumbar spinal cord

region at the same time point. This finding suggests that during the treatment course, the treated mice had less motor neuron degradation resulting in greater motor performance outcomes and lower levels of p75^{ECD}. These differences were not observed at the end of the study, however, with all mice having similar performances on motor tests at the end of the study course. This reduction in urinary p75^{ECD} post-treatment has been previously shown in the SOD1^{G93A} MND mouse model (Matusica *et al.*, 2016). p75^{ECD} is reflective of motor neuron degeneration, with this result indicating that Triumeq is reducing motor neuron loss at the early stage of treatment, confirmed by the motor neuron counts within the lumbar spinal cord. As shown in **Chapter 3**, there is an increase in urinary p75^{ECD} over disease progression in hTDP-43ΔNLS as they express TDP-43, post Dox removal. In humans, urinary p75^{ECD} has been shown as a potential pharmacodynamic marker in MND and the current study confirms the use of p75^{ECD} as a pharmacodynamic marker in mice also.

These results suggest that while there may be slower progression of motor neuron loss as a result of Triumeq treatment in the mice, there is no effect on survival outcomes. However, this is still a promising result for the use of this drug in human MND patients for two reasons. Firstly, the currently approved therapeutics for MND, Riluzole and Edaravone, that are resulting in moderate improvements to survival time have been shown to be ineffective in changing disease outcomes in mouse models of MND, including in the hTDP-43ΔNLS mouse model used in the current project (Hogg *et al.*, 2018, Wright *et al.*, 2021). Therefore, the small improvement from the treatment observed in the current study in mice could provide a greater improvement in humans. Secondly, while changes to survival outcomes were not observed from the treatment in the current study, the improvement to motor function could provide MND patients with an increase in the quality of life. Further measures of disease pathology should also be included in future analysis to fully elucidate the pathway from brain to muscle including TDP-43 solubility to assess aggregation within the nucleus and cytoplasm and muscle fibre analysis to determine the state of the muscle atrophy, particularly at the timepoint where other significant effects of Triumeq treatment were noted.

This study showed induction of inflammatory markers including TNF-α and CXCL10 in the hTDP-43ΔNLS mouse model by 2 weeks after Dox removal but did not show any significant influence of Triumeq on expression of these markers. However, the correlation between TDP-

43 expression and CXCL10 at this time point suggests an association between TDP-43 and inflammatory mediators in disease progression. Recent analysis using the hTDP-43 Δ NLS model has shown significantly increased expression of TNF- α and other inflammatory response elements such as IL-6 by 2 weeks off Dox suggesting inflammatory processes occurs early on in TDP-43-mediated disease progression (Luan *et al.*, 2023). This finding, alongside the current study where TNF- α , IL-6 and CXCL10 were induced in this model by 2 weeks off Dox, suggest that targeting inflammatory processes could be a potential avenue for treatment, discussed further in section 6.2.

A limitation of the current finding presenting in this thesis is the use of the animal model. While animal models are a valuable asset for understanding disease mechanisms and ideal pre-clinical testing models, they still have major flaws. Specific to the current study and the use of the hTDP-43 Δ NLS model, variability in disease progression was noted between mice and between litters. While some cohorts of mice had a slower disease progression with first symptoms noted at 9 days post-Dox removal and treatment onset, other cohorts had earlier disease onset with symptoms noted at an earlier time of 6 days. This variability means assessments of treatment efficacy is more difficult to assess. This disease heterogeneity has also been established in the SOD1^{G93A} mouse model (Pfohl *et al.*, 2015, Synofzik *et al.*, 2010).

Furthermore, while a TDP-43 mouse model is ideal for understanding disease mechanisms with TDP-43 pathology being a hallmark of MND, measuring HERVs and the association between HERV-K and TDP-43 was not possible. Instead, a measure of MMTV was used under the assumption that HERVs and MMTV may have similar functions and could be involved in disease pathology. If MMTV does not have a similar function, any effects of the treatment that was observed during the current study would not be due to ERV involvement. Instead, the effect of Triumeq on improving motor function and reducing motor neuron count within the lumbar spinal cord could be due to an alternative mechanism. For example, the improvement from Triumeq seen in the current study could be due to the anti-inflammatory properties of antiretrovirals (Hileman and Funderburg, 2017, Hattab *et al.*, 2014). Therefore, the anti-inflammatory effects could be acting on the TDP-43 and inflammation relationship described previously and in the current study. While significant differences in inflammatory mediator expression was not found from Triumeq treatment in the current study, it could be

explained by other inflammatory mediators that were not measured. For example, peripheral inflammatory markers were not measured and could be affected without affecting the levels of expression within the cortex measured in the current study. Furthermore, a recent study using has identified significant expression of inflammatory chemokine (c-c motif) ligand 12 (CCL12) in the hTDP-43 Δ NLS mouse model by 2 weeks off Dox which was not measured in the current study and should be investigated in future research to determine any changes after Triumeq treatment. Furthermore, levels of abacavir or lamivudine were not measured to confirm the presence within brain tissue of the mice and should be investigated prior to drawing conclusions about therapeutic efficacy in this mouse model.

Further research could also include the use of a HERV-K mouse model such as the model described in Li *et al.* (2015). Using this HERV-K mouse model and treating with Triumeq or combination therapies including anti-inflammatories and measuring HERV-K and inflammatory marker levels could further elucidate the mechanism of action of Triumeq *in vivo* and establish the association between HERV-K and inflammatory processes. However, use of this mouse model would not allow for understanding of the HERV-K/TDP-43 relationship. Other reverse transcriptase inhibitors with higher CNS penetrance could also be investigated in future studies to resolve the limitation of the current study which exclusively examined the use of Triumeq as a method to reduce ERV expression.

Based on the results from **Chapter 3**, it was hypothesised that doubling the dose of Triumeq could improve the therapeutic benefit. **Chapter 4** investigated the effects of increasing the dose of Triumeq in a small cohort of TDP-43 mice. There were no significant differences between the treated mice and untreated mice in the increased dose study for any measures of disease pathology. However, only a limited number of mice were used for this study. The guidelines for the use of SOD1^{G93A} mice in MND research suggest the use of at least 12 animals of a single sex for each treatment group (Ludolph *et al.*, 2010, Scott *et al.*, 2008). While this number was used for measurements of disease progression such as neurological score, weight changes and motor performance for the single dose study, the double dose treatment pilot study used only 14 mice divided into two treatment groups. This sample size is under the recommended sample size to be drawing conclusions into the use of increasing the dose. Furthermore, heterogeneity in disease onset was observed in the double dose study with

some mice showing a delayed symptom onset after Dox removal as determined by weight loss, neurological score and motor performance remaining unaffected after 10 days off Dox. This limitation highlights the need for greater mice numbers to reduce the effects of symptom onset heterogeneity. However, with no significant effects observed from the treatment, there was no ethical basis to continue to a larger cohort of mice. Another limitation of the double dose study includes the lack of measure of the circulating levels of Triumeq in the mice. A measure of Triumeq levels was not taken throughout the single or double dose study. To fully elucidate the efficacy of the increased dose of Triumeq, serum levels of the drug should be determined at the single and double to ensure the increased oral dose correlates with increased circulating levels.

Overall, **Chapter 3** and **Chapter 4** partially supported the hypothesis that in hTDP43 mice, antiretroviral Triumeq treatment decreases endogenous retroviruses, inflammatory signals and TDP-43 pathology in the brain and spinal cord which improves MND-like motor symptoms, increases lifespan and reduces levels of the MND biomarker, urinary p75^{ECD}.

6.1.2 *In Vitro* Analysis of HERV-K and TDP-43

Chapter 5 investigated the relation between HERV-K, TDP-43 and inflammatory mediators *in vitro*. *In silico* analysis of the transcription factors predicted to bind and regulate HERV-K transcription found an association between inflammatory mediators, such as NF- κ B, and HERV-K regulation. Transcription factors that are known to be associated with exogenous viral infection including OCT1 were found to be common across all HERV-K loci examined. Further *in vitro* analysis of ARPE-19 infected with exogenous virus, ZIKV and DENV found an increase in HERV-K expression from ZIKV infection. Here, TDP-43 levels were not correlated with HERV-K expression suggesting the increased HERV-K expression was occurring independently of TDP-43. This finding alongside previous research showing increased expression of TNF- α in ZIKV-infected ARPE-19 compared to DENV-infected ARPE-19 (Cowell *et al.*, 2023) suggests that increased HERV-K expression is perhaps occurring through inflammatory mediators such as TNF- α .

Using SH-SY5Ys, a neuroblastoma cell line, with an antisense oligonucleotide targeting TDP-43 to reduce expression showed no correlation between TDP-43 expression and HERV-K expression. However, there was a correlation between TDP-43 and TNF- α and TDP-43 and CXCL10 found in this cell line. This finding suggests that an association between TDP-43 and inflammation could be occurring independently but alongside of a HERV-K and inflammation association. Further assessment of other inflammatory markers that are established to be involved in MND, such as interleukins and interferons, were not able to be detected due to low expression of cytokines and inflammatory mediators in this cell type (Smith *et al.*, 2012, Haenseler *et al.*, 2017) and hence, the relationship between HERV-K, TDP-43 and inflammation was not able to be completely assessed.

Further *in vitro* investigation using the primary cell line, ONS, from MND patients and controls showed no significant differences between the expression levels of TDP-43 or HERV-K between MND patients and controls. However, this could be explained by the limited sample size and lack of TDP-43 pathology in this cell type. Further investigations in a primary cell line will involve iPSCs from MND patients and controls with known TDP-43 pathology in iPSC-derived motor neurons from MND patients. A further limitation to the *in vitro* analysis of HERV-K expression is the reliance on RT-qPCR as the method for detecting HERV-K in the cell lines. For future analysis, an antibody against HERV-K env will be used for immunofluorescence and ELISA analysis. This will allow for a thorough investigation of expressed HERV-K within different cell types and will allow for analysis of the localisation of HERV-K env and TDP-43 within neurons.

Overall, Chapter 5 supported the hypothesis that exogenous viral infection or inflammatory stimuli will induce HERV-K expression and increase TDP-43 pathology and the addition of antiretroviral therapy will reduce HERV-K expression and TDP-43 expression. Due to time constraints, *in vitro* analysis of Triumeq and its effects on HERV-K and TDP-43 expression were unable to be investigated but should be included in future research.

6.2 The future of Triumeq treatment for MND

Overall, the current study found that Triumeq did not influence survival of hTDP-43 Δ NLS mice with treated mice and untreated mice reaching ethical end-state at a similar timeframe. However, as outlined previously, Chapter 3 found significant benefits from Triumeq treatment including improvement in motor performance. **Chapter 3** and **Chapter 5** was the inflammatory involvement and association between TDP-43 and HERV-K. These results suggest that targeting the inflammatory response could be beneficial for increasing the therapeutic benefit of Triumeq. During the course of this study, new research identified the involvement of cGAS/STING in neurodegeneration in MND, described in Section 1.1.7.7.1. With HERV-K potentially exacerbating this pathway, future research could focus on further elucidating the involvement of HERV-K in this pathway and determine the effect of Triumeq on proinflammatory markers which are produced as a result of cGAS/STING activation.

Outlined in **Figure 6.1**, a potential way of increasing the therapeutic benefit of Triumeq could be targeting another aspect of the pathway to reduce the inflammatory effects that have been associated with increased neurodegeneration. For example, a combination therapy of Triumeq and a STING inhibitor, already showing promise in reducing neurodegeneration *in vivo* and *in vitro* (Yu *et al.*, 2020), could reduce the production of pro-inflammatory cytokines that are exacerbating neurodegeneration. This combination therapy would be a way of targeting the association between TDP-43 and inflammation, and HERV-K and inflammation. With Triumeq being shown to be safe and effective for use in MND in a Phase II clinical trial (Gold *et al.*, 2018) and being shown in the current study to have an effect on measures of disease outcomes including motor performance, it has promise for use as a treatment for MND.

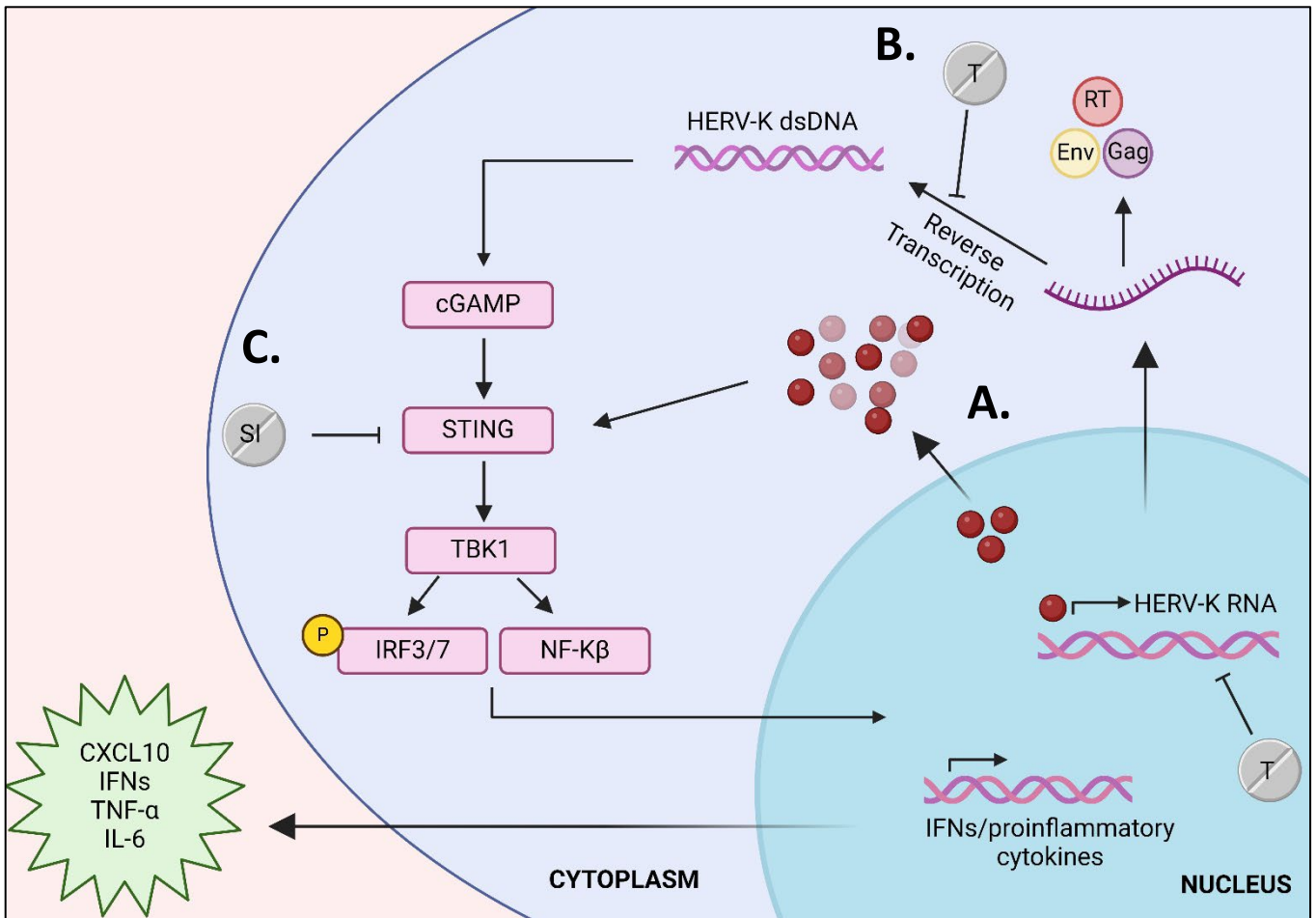


Figure 6.1 Proposed therapeutic targets and interaction of HERV-K, TDP-43 and inflammatory mediators in MND

A. Mislocalisation of TDP-43 to the cytoplasm de-represses HERV-K transcription which leads to the production of HERV-K RNA. The HERV-K mRNA is translated into HERV-K proteins including Gag, Envelope (env) and the reverse transcriptase enzyme (RT) from the pol gene. The RT enzyme acts to reverse transcribe the HERV-K into double stranded DNA (dsDNA). Cytoplasmic dsDNA is a danger signal that is recognised by and activates the cGAS/STING pathway that subsequently activates TBK1 resulting in phosphorylation of IRF3, IRF7 and release of NF- κ B from the cytoplasm. These transcription factors move to the nucleus and subsequently induce transcription of mRNA for multiple inflammatory factors and interferons. Additionally, NF- κ B can further drive HERV-K transcription. **B.** Triumeq contains two RT inhibitors which could act on inhibiting the reverse transcription of HERV-K RNA into dsDNA to prevent the activation of cGAS/STING pathway. It also contains an integrase inhibitor which could act on blocking HERV-K DNA integration **C.** STING inhibitors are proposed as a therapeutic avenue to prevent further activation of this pathway. This would be predicted to reduce the release of inflammatory mediators and prevent the spread of toxicity between neurons. IRF3/7 – Interferon regulatory factor 3 and 7, NF- κ B – nuclear factor kappa-light-chain-enhancer of activated B cells, TNF- α – Tumour necrosis factor alpha TGF- β 1 – transforming growth factor β 1, NO – Nitric oxide, P – phosphorylation, TBK1 – Tank Binding Kinase 1, IL-6 – Interleukin 6, T – Triumeq. Figure made in BioRender.

6.3 Future directions

While this study has answered some of the research questions regarding Triumeq treatment for use in MND, there are questions that remain unanswered that should be investigated further. This study provided insight into association between TDP-43, HERV-K and inflammation *in vivo* and *in vitro* but these associations should be further investigated, addressing the limitations of the present study. For example, using an established neuronal cell line, such as iPSC, with a microglia and astrocytic co-culture would allow for a thorough investigation of the inflammation, TDP-43 and HERV-K relationship *in vitro* to elucidate immune targets, such as members of the cGAS/STING pathway, that could be a therapeutic target. Using iPSCs with a co-culture of microglia and astrocytes, the effects of Triumeq treatment could be assessed *in vitro* through RNAseq analysis, including measures of HERV-K envelope expression, TDP-43 pathology including expression and mislocalisation and expression of inflammatory mediators such as TNF- α . This model should be used for assessment of combination therapies for MND including Triumeq with anti-inflammatories, including those trialled for MND previously where clinical benefit was not found (Mizwicki *et al.*, 2012, Kiaei *et al.*, 2006) or STING inhibitors as outlined in **Figure 6.1**. This cell model would be a closer representation of MND disease pathology to elucidate the association between HERV-K, TDP-43 and inflammation further. Further *in vitro* research should also include analysis of the association between HERV-K, TDP-43 and inflammation from exogenous viral infection in ARPE-19 including treatment with Triumeq after ZIKV infection and measures of TDP-43 pathology including mislocalisation in this cell type also.

While Triumeq is an established treatment for HIV and has promising benefits as a treatment for MND, further treatments targeting different aspects of HERV-K should be explored also. For example, a RT inhibitor specifically targeting HERV-K RT could increase the therapeutic benefit compared to Triumeq, which specifically targets HIV RT. This has already been investigated targeting retrotransposon activity with an RT inhibitor designed specifically against LINE-1 retrotransposon RT found to be more effective in reducing in retrotransposition in HeLa cells than the commercially available HIV RT inhibitors, including abacavir (Banuelos-Sanchez *et al.*, 2019).

Another aspect of HERV-K pathology that could be therapeutically targeted is the HERV-K envelope protein. The expression of the HERV-K envelope protein has been found to have neurotoxic effects, *in vivo*, with a reduction in neuronal cell number after injection of recombinant env protein (Steiner *et al.*, 2022). Therefore, an antisense oligonucleotide targeting HERV-K envelope protein has been proposed as a treatment option (Li *et al.*, 2022). *In vitro* investigations of this potential therapy using the iPSC and microglia cell models described above, should include analysis of TDP-43 pathology and immune response after knockdown of HERV-K env to elucidate the relationship further and determine if this treatment option is comparable to Triumeq in this model. A combination therapy of Triumeq and an antisense oligonucleotide against HERV-K env protein, targeting multiple HERV-K pathological mechanisms could be a novel therapeutic approach to reducing HERV-K-associated disease progression.

6.4 Conclusions

This project has investigated the role of association between ERVs, TDP-43 and inflammation *in vitro* and *in vivo*. The research presented in this study promote the use of Triumeq as a treatment for MND. While not prolonging survival in the hTDP-43 Δ NLS mouse model, this project identified significant effects from Triumeq in the treated mice including significantly improved motor performance and motor neuron count within the spinal cord. Outcomes of the study also further implicated inflammation in progression of disease with associations between HERV-K and inflammation and TDP-43 and inflammation seen, potentially occurring independently of the association between HERV-K and TDP-43. Altogether, this study provides promise for the continued use of Triumeq for MND and has identified the potential of combination therapy involving Triumeq that targets further inflammatory pathways to increase the therapeutic benefit. MND remains an incurable and relentless disease with limited treatment options. Investigating neurodegenerative mechanisms and determining the effectiveness of novel therapies is vital for progression towards MND being a treatable and curable disease.

APPENDIX

7 APPENDIX

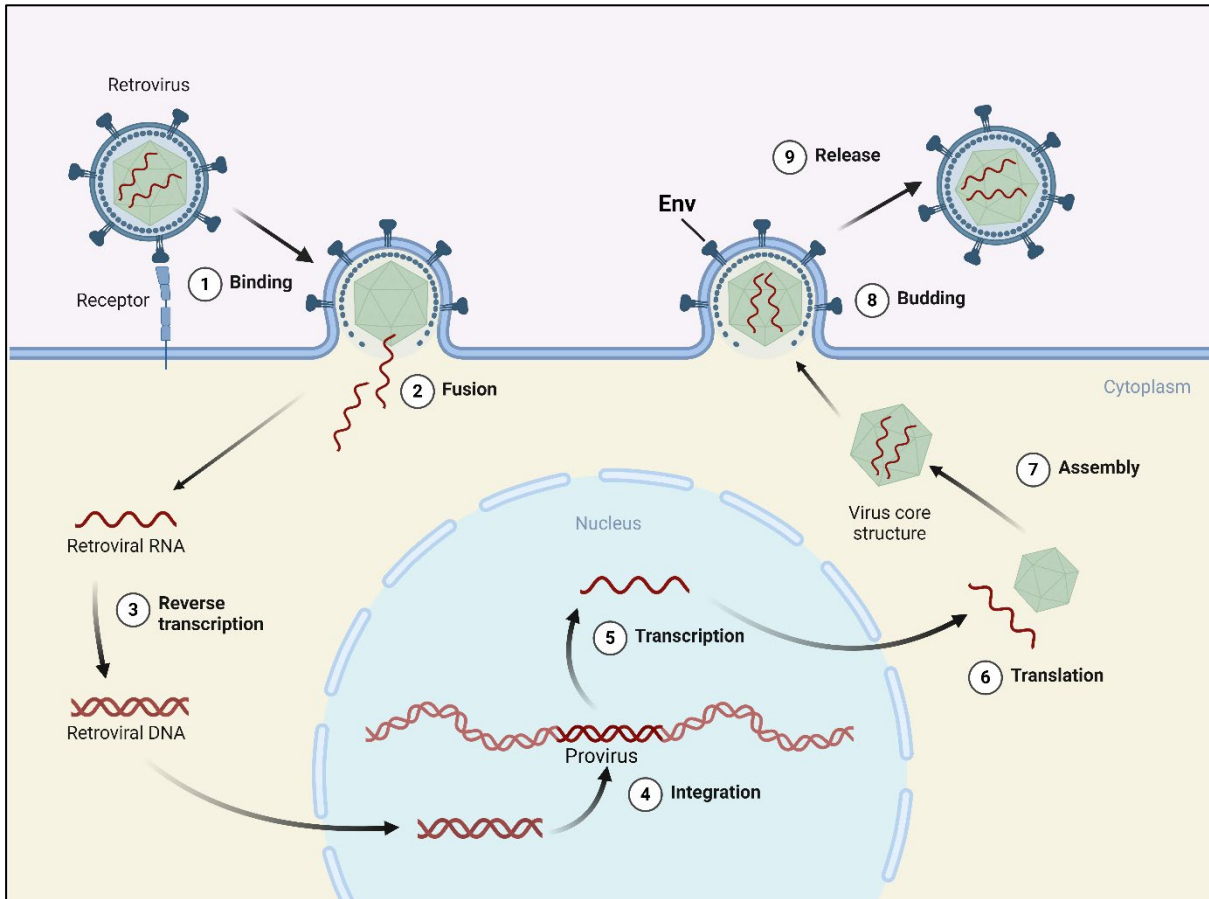


Figure A.1 Formation of a provirus from exogenous retroviral infection to release from a host cell

The retrovirus particle consists of an RNA genome packaged with replication machinery, including integrase and RT inside the capsid core and surrounded by the envelope containing viral glycoproteins and lipid derived from cell membranes. When an exogenous retrovirus infects a cell (1 and 2), the genomic RNA is reverse transcribed into double stranded DNA (3) in the cytoplasm, that then moves to the nucleus and integrates into the chromosome of the host cell forming a provirus (4). This proviral DNA gets transcribed (5) and translated (6) forming proviral RNA and proteins to form a retroviral particle that gets released from the host cell (7-9). Figure adapted from template provided by BioRender.

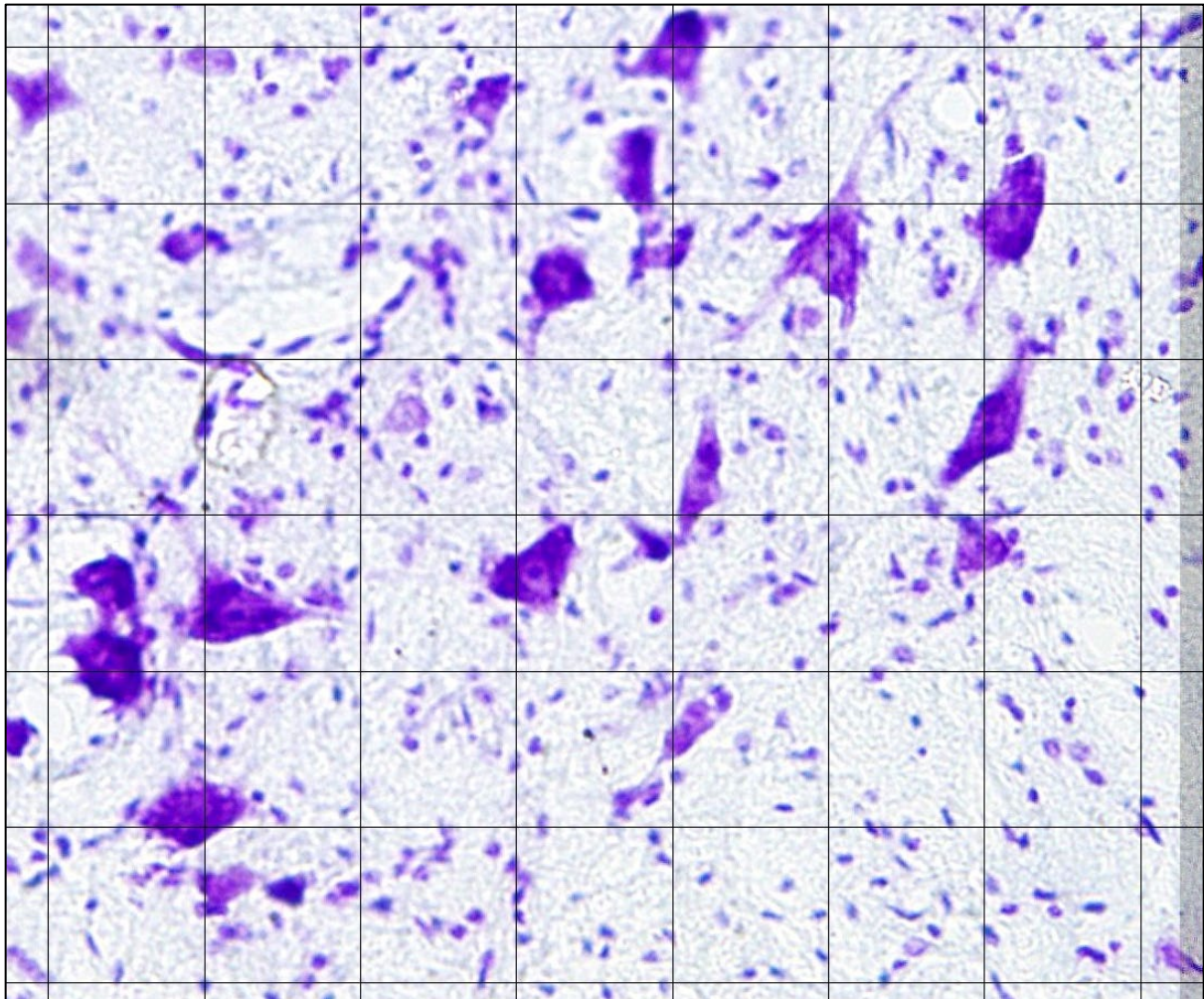


Figure A.2 Motor neurons within the lumbar spinal cord of a hTDP-43ΔNLS mouse

An example of the motor neuron numbers within the spinal cord where motor neurons that are nucleated and above 25 μm in size were included in the count. The grid lines represent 25 μm which was used as a method for counting the motor neurons in each section.

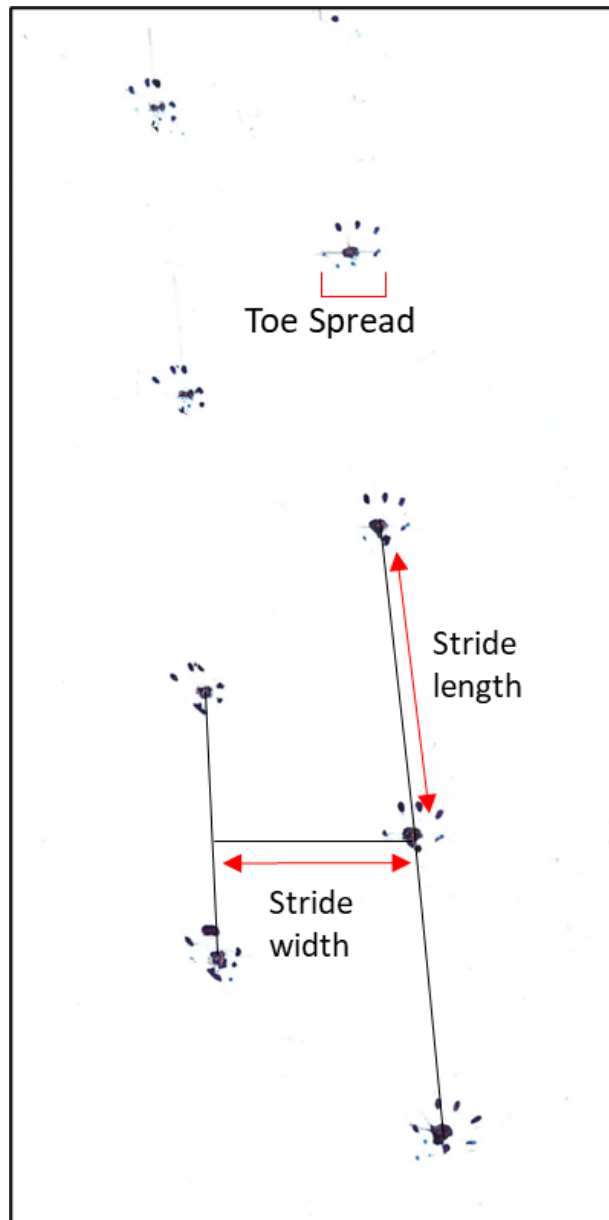
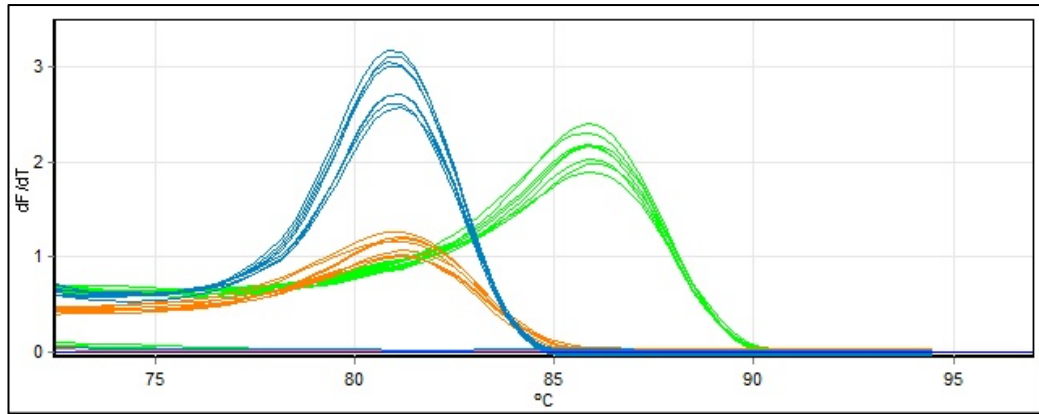


Figure A.3 Example gait analysis from a healthy litter-matched control mouse

The hindlimbs of the mice were gently painted with blue food colouring and they were placed on a blank sheet of paper to walk across. As shown by the red arrows, stride length was measured from the middle of one hindlimb paw print to the next hindlimb paw print on the same side. Stride width was measured from the middle of one hindlimb paw print to the adjacent stride length line. Toe spread was measured from the two outermost toes. Mice completed two trials with a minute rest in between.

A.**B.**

Predicted (bp)	214	140	164
	gag	H ₂ O	pol env

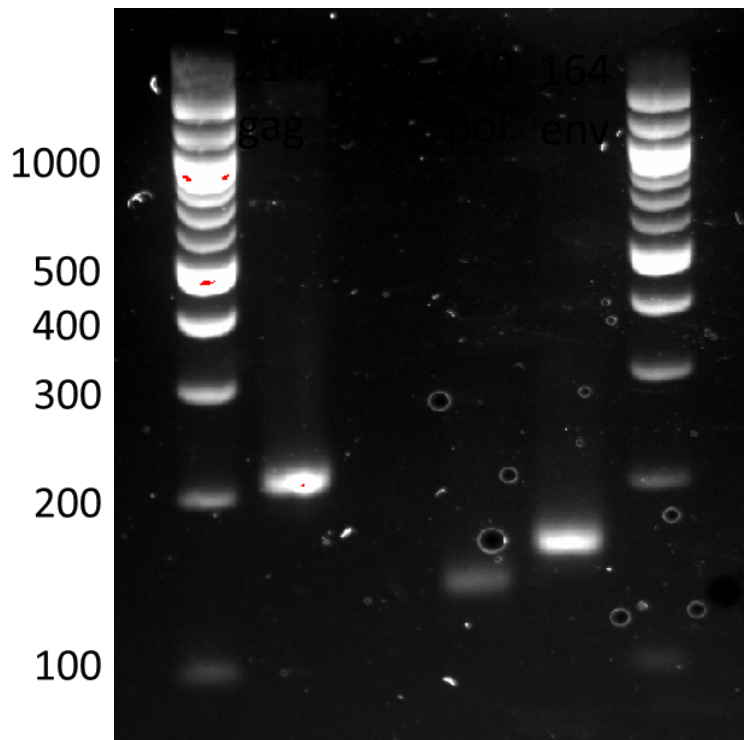


Figure A.4 HERV-K pol, HERV-K gag and HERV-K env primer validation in ARPE-19

ARPE-19 were lysed in Trizol and RNA extracted for RT-PCR. **A.** Melt curve for cDNA at 1/10, 1/100, 1/1000 and 1/10000, analysed by qPCR for HERV-K pol (orange), HERV-K gag (green) and HERV-K env (blue) along with a no template control (not visible). **B.** Amplicon size was estimated through agarose gel electrophoresis. Lane 1: NEB 1500 bp ladder, Lane 2: HERV-K gag amplicon, Lane 3: H₂O, Lane 4: HERV-K pol amplicon, Lane 5: HERV-K env amplicon, Lane 6: NEB ladder. Bp = Base pairs

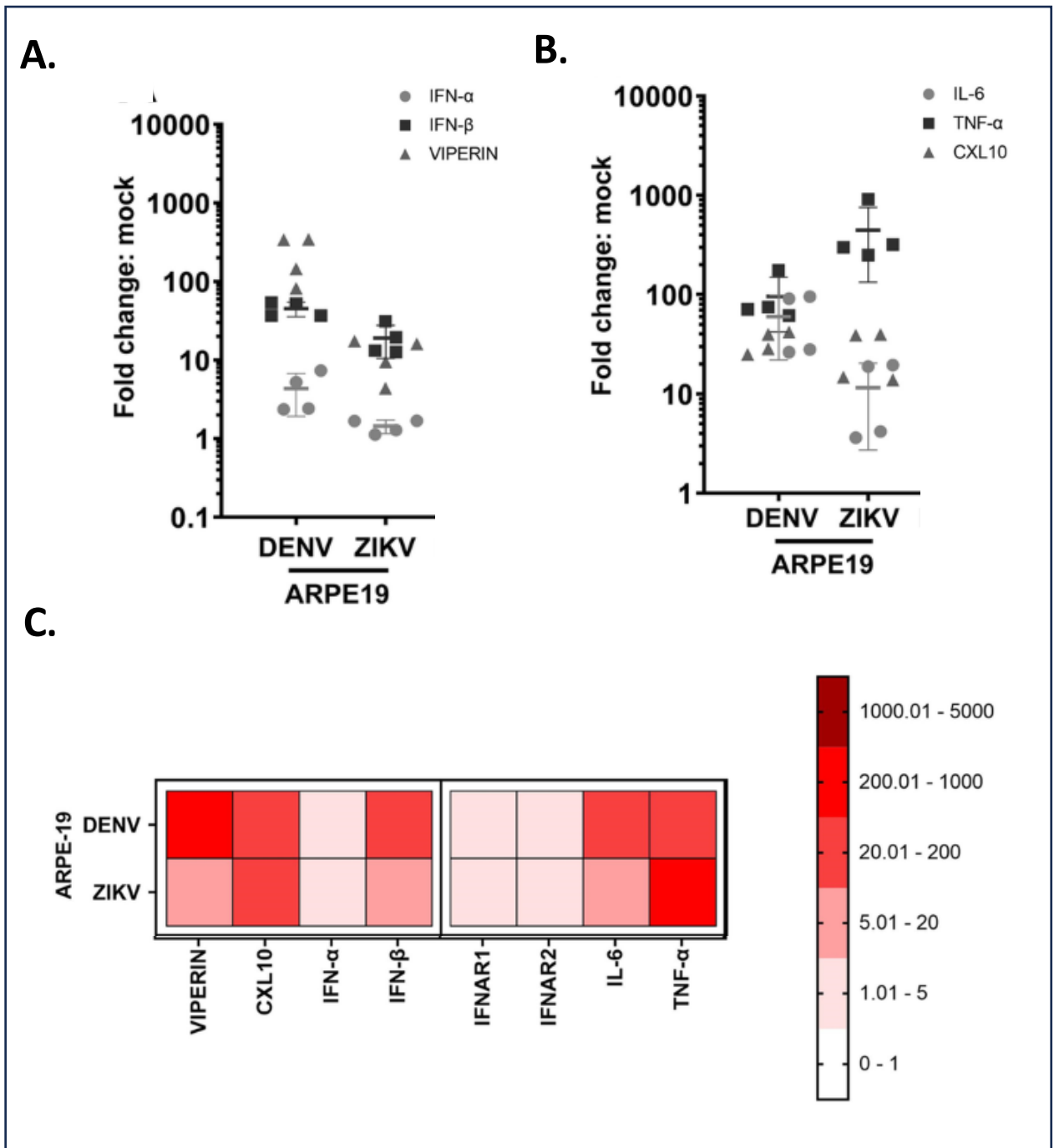
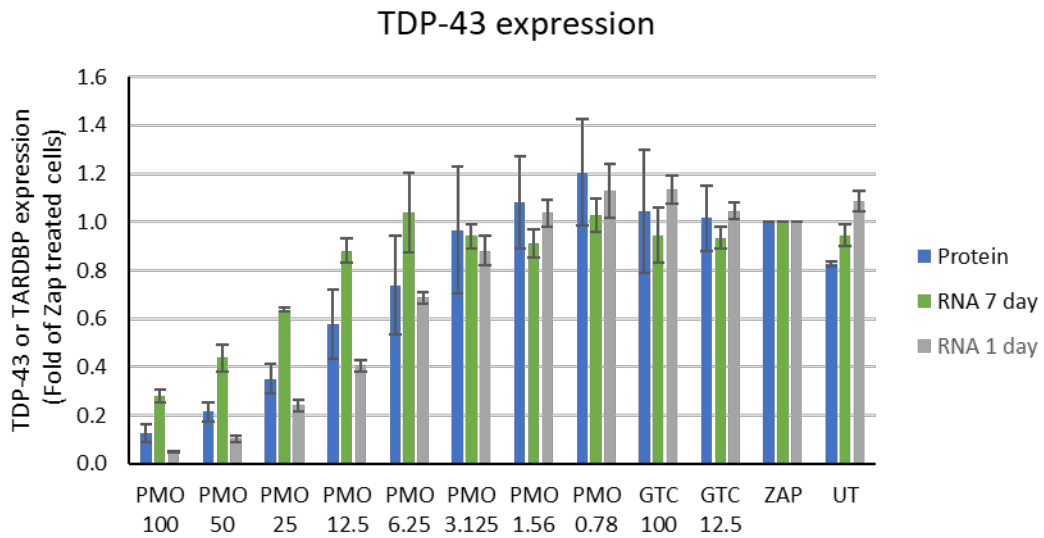


Figure A.5 Inflammatory expression in DENV and ZIKV-infected ARPE-19

Figure adapted from Cowell *et al.* (2023). Inflammatory profile from ARPE-19 infected with ZIKV or DENV. **A.** Relative expression of IFN- α , IFN- β and Viperin in DENV or ZIKV-infected ARPE-19 compared to mock infected ARPE-19. **B.** Relative expression of IL-6, TNF- α and CXCL10 in DENV or ZIKV-infected ARPE-19 compared to mock infected ARPE-19. **C.** Heat map representation of data presented in **A** and **B**.

A.



B.

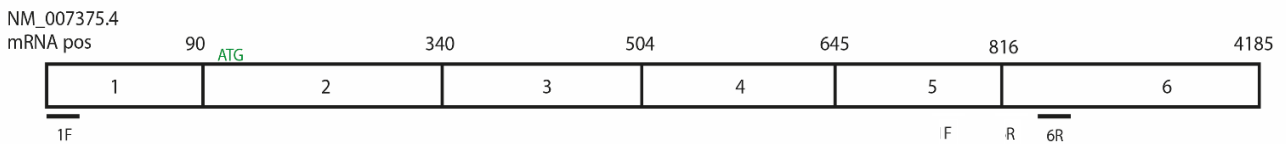


Figure A.6 TDP-43 expression with different concentrations of PMO and primer binding locations shown on TDP-43 sequence

A. TDP-43 protein and RNA expression data provided by Dr. Rita Mejzini showing an increase in TDP-43 protein and RNA expression with decreasing PMO concentration. **B.** TDP-43 sequence with numbers representing the exons showing primer binding location for primers used in the current study (shown as red line) and primers used by Dr. Rita Mejzini (shown as black line) for measuring TDP-43 expression after PMO knockdown.

REFERENCES

- Abe, K., Aoki, M., Tsuji, S., Itoyama, Y., Sobue, G., Togo, M., Hamada, C., Tanaka, M., Akimoto, M. & Nakamura, K. 2017. Safety and efficacy of edaravone in well defined patients with amyotrophic lateral sclerosis: a randomised, double-blind, placebo-controlled trial. *The Lancet Neurology*, 16, 505-512.
- Abel, E. L. 2007. Football increases the risk for Lou Gehrig's disease, amyotrophic lateral sclerosis. *Perceptual and motor skills*, 104, 1251-1254.
- Acharya, K. K., Govind, C. K., Shore, A. N., Stoler, M. H. & Reddi, P. P. 2006. cis-Requirement for the maintenance of round spermatid-specific transcription. *Developmental biology*, 295, 781-790.
- Adamczak, S. E., De Rivero Vaccari, J. P., Dale, G., Brand, F. J., Nonner, D., Bullock, M., Dahl, G. P., Dietrich, W. D. & Keane, R. W. 2014. Pyroptotic Neuronal Cell Death Mediated by the AIM2 Inflammasome. *Journal of Cerebral Blood Flow & Metabolism*, 34, 621-629.
- Afroz, T., Perez-Berlanga, M. & Polymenidou, M. 2019. Structural Transition, Function and Dysfunction of TDP-43 in Neurodegenerative Diseases. *CHIMIA International Journal for Chemistry*, 73, 380-390.
- Agosta, F., Al-Chalabi, A., Filippi, M., Hardiman, O., Kaji, R., Meininger, V., Nakano, I., Shaw, P., Shefner, J. & Van Den Berg, L. H. 2015. The El Escorial criteria: strengths and weaknesses. *Amyotrophic Lateral Sclerosis and Frontotemporal Degeneration*, 16, 1-7.
- Ahmad, I., Fernando, A., Gurgel, R., Jason Clark, J., Xu, L. & Hansen, M. R. 2015. Merlin status regulates p75NTR expression and apoptotic signaling in Schwann cells following nerve injury. *Neurobiology of Disease*, 82, 114-122.
- Ahmad, L., Zhang, S.-Y., Casanova, J.-L. & Sancho-Shimizu, V. 2016. Human TBK1: A Gatekeeper of Neuroinflammation. *Trends in Molecular Medicine*, 22, 511-527.
- Akay, C., Cooper, M., Odeleye, A., Jensen, B. K., White, M. G., Vassoler, F., Gannon, P. J., Mankowski, J., Dorsey, J. L. & Buch, A. M. 2014. Antiretroviral drugs induce oxidative stress and neuronal damage in the central nervous system. *Journal of neurovirology*, 20, 39-53.
- Al-Chalabi, A., Fang, F., Hanby, M. F., Leigh, P. N., Shaw, C. E., Ye, W. & Rijdsdijk, F. 2010. An estimate of amyotrophic lateral sclerosis heritability using twin data. *Journal of Neurology, Neurosurgery & Psychiatry*, 81, 1324-1326.
- Al-Chalabi, A., Hardiman, O., Kiernan, M. C., Chiò, A., Rix-Brooks, B. & Van Den Berg, L. H. 2016. Amyotrophic lateral sclerosis: moving towards a new classification system. *The Lancet Neurology*, 15, 1182-1194.
- Alami, N. H., Smith, R. B., Carrasco, M. A., Williams, L. A., Winborn, C. S., Han, S. S., Kiskinis, E., Winborn, B., Freibaum, B. D. & Kanagaraj, A. 2014. Axonal transport of TDP-43 mRNA granules is impaired by ALS-causing mutations. *Neuron*, 81, 536-543.
- Alfahad, T. & Nath, A. 2013. Retroviruses and amyotrophic lateral sclerosis. *Antiviral research*, 99, 180-187.
- Allodi, I., Comley, L., Nichterwitz, S., Nizzardo, M., Simone, C., Benitez, J. A., Cao, M., Corti, S. & Hedlund, E. 2016. Differential neuronal vulnerability identifies IGF-2 as a protective factor in ALS. *Scientific Reports*, 6, 25960.

- Altman, T., Ionescu, A., Ibraheem, A., Priesmann, D., Gradus-Pery, T., Farberov, L., Alexandra, G., Shelestovich, N., Dafinca, R. & Shomron, N. 2021. Axonal TDP-43 condensates drive neuromuscular junction disruption through inhibition of local synthesis of nuclear encoded mitochondrial proteins. *Nature Communications*, 12, 1-17.
- Anderson, E. N., Gochenaur, L., Singh, A., Grant, R., Patel, K., Watkins, S., Wu, J. Y. & Pandey, U. B. 2018. Traumatic injury induces stress granule formation and enhances motor dysfunctions in ALS/FTD models. *Human Molecular Genetics*, 27, 1366-1381.
- Andrew, A. S., Caller, T. A., Tandan, R., Duell, E. J., Henegan, P. L., Field, N. C., Bradley, W. G. & Stommel, E. W. 2017. Environmental and Occupational Exposures and Amyotrophic Lateral Sclerosis in New England. *Neurodegenerative Diseases*, 17, 110-116.
- Andrews, W., Tuke, P., Al-Chalabi, A., Gaudin, P., Ijaz, S., Parton, M. & Garson, J. 2000. Detection of reverse transcriptase activity in the serum of patients with motor neurone disease. *Journal of medical virology*, 61, 527-532.
- Appel, S. H., Beers, D. R. & Zhao, W. 2021. Amyotrophic lateral sclerosis is a systemic disease: peripheral contributions to inflammation-mediated neurodegeneration. *Current opinion in neurology*, 34, 765-772.
- Araki, E., Tsuboi, Y., Daechsel, J., Milnerwood, A., Vilarino-Guell, C., Fujii, N., Mishima, T., Oka, T., Hara, H., Fukae, J. & Farrer, M. J. 2014. A Novel DCTN1 mutation with late-onset parkinsonism and frontotemporal atrophy. *Movement Disorders*, 29, 1201-1204.
- Armon, C. 2018. From Snow to Hill to ALS: An epidemiological odyssey in search of ALS causation. *Journal of the Neurological Sciences*, 391, 134-140.
- Arru, G., Galleri, G., Deiana, G. A., Zarbo, I. R., Sechi, E., Bo, M., Cadoni, M. P. L., Corda, D. G., Frau, C. & Simula, E. R. 2021. HERV-K modulates the immune response in ALS patients. *Microorganisms*, 9, 1784.
- Arts, E. J. & Hazuda, D. J. 2012. HIV-1 antiretroviral drug therapy. *Cold Spring Harbor perspectives in medicine*, 2, a007161.
- Ash, P. E., Dhawan, U., Boudeau, S., Lei, S., Carlomagno, Y., Knobel, M., Al Mohanna, L. F., Boomhower, S. R., Newland, M. C. & Sherr, D. H. 2018. Heavy metal neurotoxicants induce ALS-linked TDP-43 pathology. *Toxicological Sciences*, 167, 105-115.
- Ayala, Y. M., De Conti, L., Avendaño-Vázquez, S. E., Dhir, A., Romano, M., D'ambrogio, A., Tollervey, J., Ule, J., Baralle, M., Buratti, E. & Baralle, F. E. 2011. TDP-43 regulates its mRNA levels through a negative feedback loop. *The EMBO journal*, 30, 277-288.
- Balchin, D., Hayer-Hartl, M. & Hartl, F. U. 2016. In vivo aspects of protein folding and quality control. *Science*, 353.
- Banuelos-Sanchez, G., Sanchez, L., Benitez-Guijarro, M., Sanchez-Carnerero, V., Salvador-Palomeque, C., Tristan-Ramos, P., Benkaddour-Boumzaouad, M., Morell, S., Garcia-Puche, J. L. & Heras, S. R. 2019. Synthesis and characterization of specific reverse transcriptase inhibitors for mammalian LINE-1 retrotransposons. *Cell Chemical Biology*, 26, 1095-1109. e14.
- Barmada, S. J., Skibinski, G., Korb, E., Rao, E. J., Wu, J. Y. & Finkbeiner, S. 2010. Cytoplasmic Mislocalization of TDP-43 Is Toxic to Neurons and Enhanced by a Mutation Associated with Familial Amyotrophic Lateral Sclerosis. *The Journal of Neuroscience*, 30, 639.

- Baugh, R. F. 2017. Murky Water: Cyanobacteria, BMAA and ALS. *Journal of Neurological Research and Therapy*, 2, 34.
- Beers, D. R. & Appel, S. H. 2019. Immune dysregulation in amyotrophic lateral sclerosis: mechanisms and emerging therapies. *The Lancet Neurology*, 18, 211-220.
- Belli, S. & Vanacore, N. 2005. Proportionate mortality of Italian soccer players: is amyotrophic lateral sclerosis an occupational disease? *European journal of epidemiology*, 20, 237-242.
- Benatar, M., Boylan, K., Jeromin, A., Rutkove, S. B., Berry, J., Atassi, N. & Bruijn, L. 2016. ALS biomarkers for therapy development: state of the field and future directions. *Muscle & nerve*, 53, 169-182.
- Benjaminsen, E., Alstadhaug, K. B., Gulsvik, M., Baloch, F. K. & Odeh, F. 2018. Amyotrophic lateral sclerosis in Nordland county, Norway, 2000–2015: prevalence, incidence, and clinical features. *Amyotrophic Lateral Sclerosis and Frontotemporal Degeneration*, 19, 522-527.
- Bensimon, G., Lacomblez, L., Meininger, V. F. & Group, A. R. S. 1994. A controlled trial of riluzole in amyotrophic lateral sclerosis. *New England Journal of Medicine*, 330, 585-591.
- Bentvelzen, P., Daams, J., Hageman, P. & Calafat, J. 1970. Genetic transmission of viruses that incite mammary tumor in mice. National Acad Sciences.
- Berlowitz, D. J., Howard, M. E., Fiore, J. F., Vander Hoorn, S., Donoghue, F. J., Westlake, J., Smith, A., Beer, F., Mathers, S. & Talman, P. 2016. Identifying who will benefit from non-invasive ventilation in amyotrophic lateral sclerosis/motor neurone disease in a clinical cohort. *Journal of Neurology, Neurosurgery & Psychiatry*, 87, 280.
- Bhat, A. H., Dar, K. B., Anees, S., Zargar, M. A., Masood, A., Sofi, M. A. & Ganie, S. A. 2015. Oxidative stress, mitochondrial dysfunction and neurodegenerative diseases; a mechanistic insight. *Biomedicine & Pharmacotherapy*, 74, 101-110.
- Bilsland, L. G., Sahai, E., Kelly, G., Golding, M., Greensmith, L. & Schiavo, G. 2010. Deficits in axonal transport precede ALS symptoms in vivo. *Proceedings of the National Academy of Sciences*, 107, 20523.
- Birsa, N., Bentham, M. P. & Fratta, P. 2019. Cytoplasmic functions of TDP-43 and FUS and their role in ALS. *Seminars in Cell & Developmental Biology*.
- Bjork, R. T., Mortimore, N. P., Loganathan, S. & Zarnescu, D. C. 2022. Dysregulation of Translation in TDP-43 Proteinopathies: Deficits in the RNA Supply Chain and Local Protein Production. *Frontiers in Neuroscience*, 16, 840357.
- Blasco, H., Garcon, G., Patin, F., Veyrat-Durebex, C., Boyer, J., Devos, D., Vourc'h, P., Andres, C. R. & Corcia, P. 2017. Panel of oxidative stress and inflammatory biomarkers in ALS: a pilot study. *Canadian Journal of Neurological Sciences*, 44, 90-95.
- Blizzard, C. A., Southam, K. A., Dawkins, E., Lewis, K. E., King, A. E., Clark, J. A. & Dickson, T. C. 2015. Identifying the primary site of pathogenesis in amyotrophic lateral sclerosis—vulnerability of lower motor neurons to proximal excitotoxicity. *Disease models & mechanisms*, 8, 215-224.
- Boller, K., Schönfeld, K., Lischer, S., Fischer, N., Hoffmann, A., Kurth, R. & Tönjes, R. R. 2008. Human endogenous retrovirus HERV-K113 is capable of producing intact viral particles. *Journal of General Virology*, 89, 567-572.
- Bonvicini, F., Marcello, N., Mandrioli, J., Pietrini, V. & Vinceti, M. 2010. Exposure to pesticides and risk of amyotrophic lateral sclerosis: a population-based case-control study. *Annali dell'Istituto superiore di sanita*, 46, 284-287.

- Bose, J. K., Wang, I.-F., Hung, L., Tarn, W.-Y. & Shen, C.-K. J. 2008. TDP-43 Overexpression Enhances Exon 7 Inclusion during the Survival of Motor Neuron Pre-mRNA Splicing*. *Journal of Biological Chemistry*, 283, 28852-28859.
- Bothwell, M. 2016. Recent advances in understanding neurotrophin signaling. *F1000Research*, 5, F1000 Faculty Rev-1885.
- Bourbouli, M., Rentzos, M., Bougea, A., Zouvelou, V., Constantinides, V. C., Zaganas, I., Evdokimidis, I., Kapaki, E. & Paraskevas, G. P. 2017. Cerebrospinal fluid TAR DNA-binding protein 43 combined with tau proteins as a candidate biomarker for amyotrophic lateral sclerosis and frontotemporal dementia spectrum disorders. *Dementia and geriatric cognitive disorders*, 44, 144-152.
- Bourque, G., Burns, K. H., Gehring, M., Gorbunova, V., Seluanov, A., Hammell, M., Imbeault, M., Izsvák, Z., Levin, H. L., Macfarlan, T. S., Mager, D. L. & Feschotte, C. 2018. Ten things you should know about transposable elements. *Genome Biology*, 19, 199.
- Bowen, L. N., Tyagi, R., Li, W., Alfahad, T., Smith, B., Wright, M., Singer, E. J. & Nath, A. 2016. HIV-associated motor neuron disease: HERV-K activation and response to antiretroviral therapy. *Neurology*, 87, 1756-1762.
- Bozdagi, O., Sakurai, T., Dorr, N., Pilorge, M., Takahashi, N. & Buxbaum, J. D. 2012. Haploinsufficiency of Cyfip1 produces fragile X-like phenotypes in mice. *PLoS One*, 7, e42422.
- Bozzo, F., Mirra, A. & Carri, M. T. 2017. Oxidative stress and mitochondrial damage in the pathogenesis of ALS: New perspectives. *Neuroscience Letters*, 636, 3-8.
- Brady, S. T. & Morfini, G. A. 2017. Regulation of motor proteins, axonal transport deficits and adult-onset neurodegenerative diseases. *Neurobiology of Disease*, 105, 273-282.
- Brand, L. E., Pablo, J., Compton, A., Hammerschlag, N. & Mash, D. C. 2010. Cyanobacterial blooms and the occurrence of the neurotoxin, beta-N-methylamino-L-alanine (BMAA), in South Florida aquatic food webs. *Harmful algae*, 9, 620-635.
- Brettschneider, J., Del Tredici, K., Toledo, J. B., Robinson, J. L., Irwin, D. J., Grossman, M., Suh, E., Van Deerlin, V. M., Wood, E. M. & Baek, Y. 2013. Stages of pTDP-43 pathology in amyotrophic lateral sclerosis. *Annals of neurology*, 74, 20-38.
- Brigadski, T. & Leßmann, V. 2020. The physiology of regulated BDNF release. *Cell and Tissue Research*, 382, 15-45.
- Bright, F., Chan, G., Van Hummel, A., Ittner, L. M. & Ke, Y. D. 2021. TDP-43 and inflammation: Implications for amyotrophic lateral sclerosis and frontotemporal dementia. *International Journal of Molecular Sciences*, 22, 7781.
- Brodovitch, A., Boucraut, J., Delmont, E., Parlanti, A., Grapperon, A.-M., Attarian, S. & Verschuere, A. 2021. Combination of serum and CSF neurofilament-light and neuroinflammatory biomarkers to evaluate ALS. *Scientific Reports*, 11, 703.
- Brown, A.-L., Wilkins, O. G., Keuss, M. J., Hill, S. E., Zanovello, M., Lee, W. C., Bampton, A., Lee, F. C. Y., Masino, L., Qi, Y. A., Bryce-Smith, S., Gatt, A., Hallegger, M., Fagegaltier, D., Phatnani, H., Phatnani, H., Kwan, J., Sareen, D., Broach, J. R., Simmons, Z., Arcila-Londono, X., Lee, E. B., Van Deerlin, V. M., Shneider, N. A., Fraenkel, E., Ostrow, L. W., Baas, F., Zaitlen, N., Berry, J. D., Malaspina, A., Fratta, P., Cox, G. A., Thompson, L. M., Finkbeiner, S., Dardiotis, E., Miller, T. M., Chandran, S., Pal, S., Hornstein, E., Macgowan, D. J., Heiman-Patterson, T., Hammell, M. G., Patsopoulos, N. A., Butovsky, O., Dubnau, J., Nath, A., Bowser, R., Harms, M., Aronica, E., Poss, M., Phillips-Cremins, J., Crary, J., Atassi, N., Lange, D. J., Adams, D. J., Stefanis, L., Gotkine, M., Baloh, R. H., Babu, S., Raj, T., Paganoni, S., Shalem, O., Smith, C., Zhang,

- B., Harris, B., Broce, I., Drory, V., Ravits, J., Mcmillan, C., Menon, V., Wu, L., Altschuler, S., Lerner, Y., Sattler, R., Van Keuren-Jensen, K., Rozenblatt-Rosen, O., Lindblad-Toh, K., Nicholson, K., Gregersen, P., Lee, J.-H., Koks, S., Muljo, S., Newcombe, J., Gustavsson, E. K., Seddighi, S., Reyes, J. F., Coon, S. L., Ramos, D., Schiavo, G., Fisher, E. M. C., Raj, T., Secrier, M., Lashley, T., Ule, J., Buratti, E., Humphrey, J., Ward, M. E., Fratta, P. & Consortium, N. A. 2022. TDP-43 loss and ALS-risk SNPs drive mis-splicing and depletion of UNC13A. *Nature*, 603, 131-137.
- Brown, R. H. & Al-Chalabi, A. 2015. Endogenous retroviruses in ALS: A reawakening? *Science translational medicine*, 7, 307fs40-307fs40.
- Brown, R. H. & Al-Chalabi, A. 2017. Amyotrophic lateral sclerosis. *New England Journal of Medicine*, 377, 162-172.
- Brujin, L. I., Houseweart, M. K., Kato, S., Anderson, K. L., Anderson, S. D., Ohama, E., Reaume, A. G., Scott, R. W. & Cleveland, D. W. 1998. Aggregation and motor neuron toxicity of an ALS-linked SOD1 mutant independent from wild-type SOD1. *Science*, 281, 1851-1854.
- Bryan, L., Kaye, W., Antao, V., Mehta, P., Muravov, O. & Horton, D. K. 2016. Preliminary Results of National Amyotrophic Lateral Sclerosis (ALS) Registry Risk Factor Survey Data. *PLOS ONE*, 11, e0153683.
- Bunina, T. 1962. On intracellular inclusions in familial amyotrophic lateral sclerosis. *Zh Nevropatol Psikhiatr Im SS Korsakova*, 62, 1293-1299.
- Buratti, E. & Baralle, F. E. 2001. Characterization and Functional Implications of the RNA Binding Properties of Nuclear Factor TDP-43, a Novel Splicing Regulator of CFTR Exon 9. *Journal of Biological Chemistry*, 276, 36337-36343.
- Buratti, E., Brindisi, A., Giombi, M., Tisminetzky, S., Ayala, Y. M. & Baralle, F. E. 2005. TDP-43 binds heterogeneous nuclear ribonucleoprotein a/b through its c-terminal tail an important region for the inhibition of cystic fibrosis transmembrane conductance regulator exon 9 splicing. *Journal of Biological Chemistry*, 280, 37572-37584.
- Buratti, E., Dörk, T., Zuccato, E., Pagani, F., Romano, M. & Baralle, F. E. 2001. Nuclear factor TDP-43 and SR proteins promote in vitro and in vivo CFTR exon 9 skipping. *The EMBO Journal*, 20, 1774-1784.
- Burberry, A., Suzuki, N., Wang, J.-Y., Moccia, R., Mordes, D. A., Stewart, M. H., Suzuki-Uematsu, S., Ghosh, S., Singh, A. & Merkle, F. T. 2016. Loss-of-function mutations in the C9ORF72 mouse ortholog cause fatal autoimmune disease. *Science translational medicine*, 8, 347ra93-347ra93.
- Burke-Gaffney, A. & Hellewell, P. G. 1996. Tumour necrosis factor-alpha-induced ICAM-1 expression in human vascular endothelial and lung epithelial cells: modulation by tyrosine kinase inhibitors. *Br J Pharmacol*, 119, 1149-58.
- Burke, S. J., Goff, M. R., Lu, D., Proud, D., Karlstad, M. D. & Collier, J. J. 2013. Synergistic Expression of the CXCL10 Gene in Response to IL-1 β and IFN- γ Involves NF- κ B, Phosphorylation of STAT1 at Tyr701, and Acetylation of Histones H3 and H4. *The Journal of Immunology*, 191, 323-336.
- Byrne, S., Walsh, C., Lynch, C., Bede, P., Elamin, M., Kenna, K., Mclaughlin, R. & Hardiman, O. 2010. Rate of familial amyotrophic lateral sclerosis: a systematic review and meta-analysis. *Journal of Neurology, Neurosurgery & Psychiatry*.
- Cady, J., Allred, P., Bali, T., Pestronk, A., Goate, A., Miller, T. M., Mitra, R. D., Ravits, J., Harms, M. B. & Baloh, R. H. 2015. Amyotrophic lateral sclerosis onset is influenced

- by the burden of rare variants in known amyotrophic lateral sclerosis genes. *Annals of Neurology*, 77, 100-113.
- Cairns, N. J., Neumann, M., Bigio, E. H., Holm, I. E., Troost, D., Hatanpaa, K. J., Foong, C., White III, C. L., Schneider, J. A. & Kretzschmar, H. A. 2007. TDP-43 in familial and sporadic frontotemporal lobar degeneration with ubiquitin inclusions. *The American journal of pathology*, 171, 227-240.
- Calvo, A., Moglia, C., Lunetta, C., Marinou, K., Ticozzi, N., Ferrante, G. D., Scialo, C., Sorarù, G., Trojsi, F. & Conte, A. 2017. Factors predicting survival in ALS: a multicenter Italian study. *Journal of neurology*, 264, 54-63.
- Camu, W., Tremblier, B., Plassot, C., Alphandery, S., Salsac, C., Pageot, N., Juntas-Morales, R., Scamps, F., Daures, J.-P. & Raoul, C. 2014. Vitamin D confers protection to motoneurons and is a prognostic factor of amyotrophic lateral sclerosis. *Neurobiology of aging*, 35, 1198-1205.
- Carra, S., Crippa, V., Rusmini, P., Boncoraglio, A., Minoia, M., Giorgetti, E., Kampinga, H. H. & Poletti, A. 2012. Alteration of protein folding and degradation in motor neuron diseases: Implications and protective functions of small heat shock proteins. *Progress in Neurobiology*, 97, 83-100.
- Carri, M. T., D'ambrosi, N. & Cozzolino, M. 2017. Pathways to mitochondrial dysfunction in ALS pathogenesis. *Biochemical and Biophysical Research Communications*, 483, 1187-1193.
- Cascella, R., Capitini, C., Fani, G., Dobson, C. M., Cecchi, C. & Chiti, F. 2016. Quantification of the relative contributions of loss-of-function and gain-of-function mechanisms in TAR DNA-binding protein 43 (TDP-43) proteinopathies. *Journal of Biological Chemistry*, 291, 19437-19448.
- Chan, S. M., Sapir, T., Park, S.-S., Rual, J.-F., Contreras-Galindo, R., Reiner, O. & Markovitz, D. M. 2019. The HERV-K accessory protein Np9 controls viability and migration of teratocarcinoma cells. *PLOS ONE*, 14, e0212970.
- Chang, X.-L., Tan, M.-S., Tan, L. & Yu, J.-T. 2016. The role of TDP-43 in Alzheimer's disease. *Molecular neurobiology*, 53, 3349-3359.
- Chang, Y.-H. & Dubnau, J. 2019. The Gypsy Endogenous Retrovirus Drives Non-Cell-Autonomous Propagation in a Drosophila TDP-43 Model of Neurodegeneration. *Current Biology*, 29, 3135-3152.e4.
- Chang, Y.-H. & Dubnau, J. 2022. Endogenous Retroviruses and TDP-43 Proteinopathy Form a Sustaining Feedback to Drive the Intercellular Spread of Neurodegeneration. *bioRxiv*, 2022.07. 20.500816.
- Chang, Y.-H. & Dubnau, J. 2023. Endogenous retroviruses and TDP-43 proteinopathy form a sustaining feedback driving intercellular spread of Drosophila neurodegeneration. *Nature Communications*, 14, 966.
- Charcot, J.-M. 1869. Deux cas d'atrophie musculaire progressive avec lesions de la substance grise et des faisceaux anterolateraux de la moelle epiniere. *Arch Physiol Norm Pathol*, 2, 354,629,744.
- Che, M.-X., Jiang, L.-L., Li, H.-Y., Jiang, Y.-J. & Hu, H.-Y. 2015. TDP-35 sequesters TDP-43 into cytoplasmic inclusions through binding with RNA. *FEBS letters*, 589, 1920-1928.
- Chen, L., Al-Harhi, L. & Hu, X. T. 2020. Triumeq Increases Excitability of Pyramidal Neurons in the Medial Prefrontal Cortex by Facilitating Voltage-Gated Ca(2+) Channel Function. *Front Pharmacol*, 11, 617149.

- Chen, Y. 2012. Organophosphate-induced brain damage: Mechanisms, neuropsychiatric and neurological consequences, and potential therapeutic strategies. *NeuroToxicology*, 33, 391-400.
- Cherry, J. D., Olschowka, J. A. & O'banion, M. K. 2014. Neuroinflammation and M2 microglia: the good, the bad, and the inflamed. *Journal of Neuroinflammation*, 11, 98.
- Chew, J. L. & Chua, K. Y. 2003. Collection of mouse urine for bioassays. *Lab animal*, 32, 48-50.
- Chhangani, D., Martín-Peña, A. & Rincon-Limas, D. 2021. Molecular, functional and pathological aspects of TDP-43 fragmentation. *iScience*, 24, 102459.
- Chiò, A., Calvo, A., Dossena, M., Ghiglione, P., Mutani, R. & Mora, G. 2009. ALS in Italian professional soccer players: the risk is still present and could be soccer-specific. *Amyotrophic lateral sclerosis*, 10, 205-209.
- Chiò, A., Calvo, A., Moglia, C., Mazzini, L. & Mora, G. 2011. Phenotypic heterogeneity of amyotrophic lateral sclerosis: a population based study. *Journal of Neurology, Neurosurgery & Psychiatry*, 82, 740-746.
- Chiò, A., Logroscino, G., Traynor, B., Collins, J., Simeone, J., Goldstein, L. & White, L. 2013. Global epidemiology of amyotrophic lateral sclerosis: a systematic review of the published literature. *Neuroepidemiology*, 41, 118-130.
- Chiò, A. & Traynor, B. J. 2015. Motor neuron disease in 2014: Biomarkers for ALS--in search of the Promised Land. *Nature reviews. Neurology*, 11, 72.
- Chipika, R. H., Finegan, E., Shing, S. L. H., Hardiman, O. & Bede, P. 2019. Tracking a fast-moving disease: longitudinal markers, monitoring, and clinical trial endpoints in ALS. *Frontiers in neurology*, 10.
- Christensen, T. 2010. HERVs in neuropathogenesis. *Journal of Neuroimmune Pharmacology*, 5, 326-335.
- Chung, T., Park, J. S., Kim, S., Montes, N., Walston, J. & Höke, A. 2017. Evidence for dying-back axonal degeneration in age-associated skeletal muscle decline. *Muscle & Nerve*, 55, 894-901.
- Chuong, E. B. 2018. The placenta goes viral: Retroviruses control gene expression in pregnancy. *PLoS biology*, 16, e3000028-e3000028.
- Cicero, C. E., Mostile, G., Vasta, R., Rapisarda, V., Santo Signorelli, S., Ferrante, M., Zappia, M. & Nicoletti, A. 2017. Metals and neurodegenerative diseases. A systematic review. *Environmental research*, 159, 82-94.
- Cihlar, T. & Fordyce, M. 2016. Current status and prospects of HIV treatment. *Current Opinion in Virology*, 18, 50-56.
- Cirulli, E. T., Lasseigne, B. N., Petrovski, S., Sapp, P. C., Dion, P. A., Leblond, C. S., Couthouis, J., Lu, Y.-F., Wang, Q. & Krueger, B. J. 2015. Exome sequencing in amyotrophic lateral sclerosis identifies risk genes and pathways. *Science*, 347, 1436-1441.
- Ciura, S., Lattante, S., Le Ber, I., Latouche, M., Tostivint, H., Brice, A. & Kabashi, E. 2013. Loss of function of C9orf72 causes motor deficits in a zebrafish model of amyotrophic lateral sclerosis. *Annals of neurology*, 74, 180-187.
- Clarke, B. E. & Patani, R. 2020. The microglial component of amyotrophic lateral sclerosis. *Brain*, 143, 3526-3539.
- Coffin, J. M. 2018. Replication of retrovirus genomes. *RNA Genetics: Volume II: Retroviruses, Viroids, and RNA Recombination*.

- Cohen, T. J., Lee, V. M. & Trojanowski, J. Q. 2011. TDP-43 functions and pathogenic mechanisms implicated in TDP-43 proteinopathies. *Trends in molecular medicine*, 17, 659-667.
- Colombrita, C., Zennaro, E., Fallini, C., Weber, M., Sommacal, A., Buratti, E., Silani, V. & Ratti, A. 2009. TDP-43 is recruited to stress granules in conditions of oxidative insult. *Journal of neurochemistry*, 111, 1051-1061.
- Copray, J., Jaarsma, D., Kst, B., Bruggeman, R., Mantingh, I., Brouwer, N. & Boddeke, H. 2003. Expression of the low affinity neurotrophin receptor p75 in spinal motoneurons in a transgenic mouse model for amyotrophic lateral sclerosis. *Neuroscience*, 116, 685-694.
- Coque, E., Salsac, C., Espinosa-Carrasco, G., Varga, B., Degauque, N., Cadoux, M., Crabé, R., Virenque, A., Soulard, C. & Fierle, J. K. 2019. Cytotoxic CD8+ T lymphocytes expressing ALS-causing SOD1 mutant selectively trigger death of spinal motoneurons. *Proceedings of the National Academy of Sciences*, 116, 2312-2317.
- Cowell, E., Kris, L. P., Bracho-Granado, G., Jaber, H., Smith, J. R. & Carr, J. M. 2023. Zika virus infection of retinal cells and the developing mouse eye induces host responses that contrasts to the brain and dengue virus infection. *Journal of NeuroVirology*, 29, 187-202.
- Cox, P. A., Kostrzewa, R. M. & Guillemin, G. J. 2018. BMAA and neurodegenerative illness. *Neurotoxicity research*, 33, 178-183.
- Crawley, J. N. 1999. Behavioral phenotyping of transgenic and knockout mice: experimental design and evaluation of general health, sensory functions, motor abilities, and specific behavioral tests. *Brain research*, 835, 18-26.
- Creemers, H., Grupstra, H., Nollet, F., Van Den Berg, L. H. & Beelen, A. 2015. Prognostic factors for the course of functional status of patients with ALS: a systematic review. *Journal of neurology*, 262, 1407-1423.
- Cudkovicz, M. E., Shefner, J., Schoenfeld, D., Brown Jr, R., Johnson, H., Qureshi, M., Jacobs, M., Rothstein, J., Appel, S. H. & Pascuzzi, R. 2003. A randomized, placebo-controlled trial of topiramate in amyotrophic lateral sclerosis. *Neurology*, 61, 456-464.
- Dai, J., Lin, W., Zheng, M., Liu, Q., He, B., Luo, C., Lu, X., Pei, Z., Su, H. & Yao, X. 2017. Alterations in AQP4 expression and polarization in the course of motor neuron degeneration in SOD1G93A mice. *Molecular medicine reports*, 16, 1739-1746.
- Danial, N. N., Hartman, A. L., Stafstrom, C. E. & Thio, L. L. 2013. How Does the Ketogenic Diet Work? Four Potential Mechanisms. *Journal of Child Neurology*, 28, 1027-1033.
- De Giorgio, F., Maduro, C., Fisher, E. M. & Acevedo-Arozena, A. 2019. Transgenic and physiological mouse models give insights into different aspects of amyotrophic lateral sclerosis. *Disease models & mechanisms*, 12.
- De Jong, S. W., Huisman, M. H. B., Sutedia, N. A., Van Der Kooi, A. J., De Visser, M., Schelhaas, H. J., Fischer, K., Veldink, J. H. & Van Den Berg, L. H. 2012. Smoking, Alcohol Consumption, and the Risk of Amyotrophic Lateral Sclerosis: A Population-based Study. *American Journal of Epidemiology*, 176, 233-239.
- De Vos, K. J. & Hafezparast, M. 2017. Neurobiology of axonal transport defects in motor neuron diseases: opportunities for translational research? *Neurobiology of disease*, 105, 283-299.
- Decout, A., Katz, J. D., Venkatraman, S. & Ablasser, A. 2021. The cGAS–STING pathway as a therapeutic target in inflammatory diseases. *Nature Reviews Immunology*, 21, 548-569.

- Dejesus-Hernandez, M., Mackenzie, Ian r., Boeve, Bradley f., Boxer, Adam l., Baker, M., Rutherford, Nicola j., Nicholson, Alexandra m., Finch, Nicole a., Flynn, H., Adamson, J., Kouri, N., Wojtas, A., Sengdy, P., Hsiung, G.-Yuek r., Karydas, A., Seeley, William w., Josephs, Keith a., Coppola, G., Geschwind, Daniel h., Wszolek, Zbigniew k., Feldman, H., Knopman, David s., Petersen, Ronald c., Miller, Bruce l., Dickson, Dennis w., Boylan, Kevin b., Graff-Radford, Neill r. & Rademakers, R. 2011. Expanded GGGGCC Hexanucleotide Repeat in Noncoding Region of C9ORF72 Causes Chromosome 9p-Linked FTD and ALS. *Neuron*, 72, 245-256.
- Del Aguila, M., Longstreth, W., Mcguire, V., Koepsell, T. & Van Belle, G. 2003. Prognosis in amyotrophic lateral sclerosis A population-based study. *Neurology*, 60, 813-819.
- Deng, H.-X., Hentati, A., Tainer, J. A., Iqbal, Z., Cayabyab, A., Hung, W.-Y., Getzoff, E. D., Hu, P., Herzfeldt, B. & Roos, R. P. 1993. Amyotrophic lateral sclerosis and structural defects in Cu, Zn superoxide dismutase. *Science*, 261, 1047-1051.
- Deng, H., Gao, K. & Jankovic, J. 2014. The role of FUS gene variants in neurodegenerative diseases. *Nature Reviews Neurology*, 10, 337-348.
- Dewannieux, M., Blaise, S. & Heidmann, T. 2005. Identification of a functional envelope protein from the HERV-K family of human endogenous retroviruses. *Journal of virology*, 79, 15573-15577.
- Di Curzio, D., Gurm, M., Turnbull, M., Nadeau, M.-J., Meek, B., Rempel, J. D., Fineblit, S., Jonasson, M., Hebert, S. & Ferguson-Parry, J. 2020. Pro-inflammatory signaling upregulates a neurotoxic conotoxin-like protein encrypted within human endogenous retrovirus-K. *Cells*, 9, 1584.
- Dickerson, A., Hansen, J., Kiumourzoglou, M.-A., Specht, A., Gredal, O. & Weisskopf, M. 2019. O6E. 5 Occupation and risk of amyotrophic laterals sclerosis (ALS) in denmark. BMJ Publishing Group Ltd.
- Diehl, W. E., Patel, N., Halm, K. & Johnson, W. E. 2016. Tracking interspecies transmission and long-term evolution of an ancient retrovirus using the genomes of modern mammals. *Elife*, 5, e12704.
- Dion, P. A., Daoud, H. & Rouleau, G. A. 2009. Genetics of motor neuron disorders: new insights into pathogenic mechanisms. *Nature Reviews Genetics*, 10, 769.
- Distefano, P. S. & Johnson, E. M. 1988. Identification of a truncated form of the nerve growth factor receptor. *Proceedings of the National Academy of Sciences*, 85, 270-274.
- Doble, A. 1996a. The pharmacology and mechanism of action of riluzole. *Neurology*, 47, 233S-241S.
- Doble, A. 1996b. The pharmacology and mechanism of action of riluzole. *Neurology*, 47, 233S.
- Dolei, A. 2018. The aliens inside us: HERV-W endogenous retroviruses and multiple sclerosis. *Multiple Sclerosis Journal*, 24, 42-47.
- Dolei, A., Ibba, G., Piu, C. & Serra, C. 2019. Expression of HERV Genes as Possible Biomarker and Target in Neurodegenerative Diseases. *International journal of molecular sciences*, 20, 3706.
- Dong, Y. & Chen, Y. 2018. The role of ubiquitinated TDP-43 in amyotrophic lateral sclerosis. *Neuroimmunol Neuroinflammation*, 5.
- Dorst, J., Chen, L., Rosenbohm, A., Dreyhaupt, J., Hübers, A., Schuster, J., Weishaupt, J. H., Kassubek, J., Gess, B. & Meyer, T. 2019. Prognostic factors in ALS: a comparison between Germany and China. *Journal of Neurology*, 1-10.

- Douville, R., Liu, J., Rothstein, J. & Nath, A. 2011. Identification of active loci of a human endogenous retrovirus in neurons of patients with amyotrophic lateral sclerosis. *Annals of neurology*, 69, 141-151.
- Douville, R. N. & Nath, A. 2014. Chapter 22 - Human endogenous retroviruses and the nervous system. *In: TSELIS, A. C. & BOOSS, J. (eds.) Handbook of Clinical Neurology*. Elsevier.
- Douville, R. N. & Nath, A. 2017. Human endogenous retrovirus-K and TDP-43 expression bridges ALS and HIV neuropathology. *Frontiers in microbiology*, 8, 1986.
- Dunlop, R. A., Cox, P. A., Banack, S. A. & Rodgers, K. J. 2013. The non-protein amino acid BMAA is misincorporated into human proteins in place of L-serine causing protein misfolding and aggregation. *PloS one*, 8, e75376.
- Egawa, N., Kitaoka, S., Tsukita, K., Naitoh, M., Takahashi, K., Yamamoto, T., Adachi, F., Kondo, T., Okita, K. & Asaka, I. 2012. Drug screening for ALS using patient-specific induced pluripotent stem cells. *Science translational medicine*, 4, 145ra104-145ra104.
- Eisen, A., Kim, S. & Pant, B. 1992. Amyotrophic lateral sclerosis (ALS): a phylogenetic disease of the corticomotoneuron? *Muscle & nerve*, 15, 219-224.
- Endo, F., Komine, O., Fujimori-Tonou, N., Katsuno, M., Jin, S., Watanabe, S., Sobue, G., Dezawa, M., Wyss-Coray, T. & Yamanaka, K. 2015. Astrocyte-Derived TGF- β 1 Accelerates Disease Progression in ALS Mice by Interfering with the Neuroprotective Functions of Microglia and T Cells. *Cell Reports*, 11, 592-604.
- Endo, F., Komine, O. & Yamanaka, K. 2016. Neuroinflammation in motor neuron disease. *Clinical and Experimental Neuroimmunology*, 7, 126-138.
- Ene, L., Duiculescu, D. & Ruta, S. 2011. How much do antiretroviral drugs penetrate into the central nervous system? *Journal of medicine and life*, 4, 432.
- Engelhardt, J. I., Tajti, J. & Appel, S. H. 1993. Lymphocytic infiltrates in the spinal cord in amyotrophic lateral sclerosis. *Archives of neurology*, 50, 30-36.
- Fairless, R., Williams, S. K. & Diem, R. 2019. Calcium-Binding Proteins as Determinants of Central Nervous System Neuronal Vulnerability to Disease. *International journal of molecular sciences*, 20, 2146.
- Fakhri-Bafghi, M. S., Ghasemi-Niri, S. F., Mostafalou, S., Navaei-Nigjeh, M., Baeri, M., Mohammadirad, A. & Abdollahi, M. 2016. Protective effect of selenium-based medicines on toxicity of three common organophosphorus compounds in human erythrocytes in vitro. *Cell Journal (Yakhteh)*, 17, 740.
- Fang, F., Kwee, L. C., Allen, K. D., Umbach, D. M., Ye, W., Watson, M., Keller, J., Oddone, E. Z., Sandler, D. P. & Schmidt, S. 2010. Association between blood lead and the risk of amyotrophic lateral sclerosis. *American journal of epidemiology*, 171, 1126-1133.
- Farrarwell, N. E., Lambert-Smith, I., Mitchell, K., Mckenna, J., Mcalary, L., Ciryam, P., Vine, K. L., Saunders, D. N. & Yerbury, J. J. 2018. SOD1^{&A4V}; aggregation alters ubiquitin homeostasis in a cell model of ALS. *Journal of Cell Science*.
- Feneberg, E., Gray, E., Ansoerge, O., Talbot, K. & Turner, M. R. 2018. Towards a TDP-43-based biomarker for ALS and FTL. *Molecular neurobiology*, 55, 7789-7801.
- Ferraiuolo, L., Kirby, J., Grierson, A. J., Sendtner, M. & Shaw, P. J. 2011. Molecular pathways of motor neuron injury in amyotrophic lateral sclerosis. *Nature Reviews Neurology*, 7, 616.

- Fitzgerald, K. C., O'reilly, É. J., Falcone, G. J., Mccullough, M. L., Park, Y., Kolonel, L. N. & Ascherio, A. 2014. Dietary ω -3 Polyunsaturated Fatty Acid Intake and Risk for Amyotrophic Lateral Sclerosis. *JAMA Neurology*, 71, 1102-1110.
- Foran, E. & Trotti, D. 2009. Glutamate Transporters and the Excitotoxic Path to Motor Neuron Degeneration in Amyotrophic Lateral Sclerosis. *Antioxidants & Redox Signaling*, 11, 1587-1602.
- Foster, L. A. & Salajegheh, M. K. 2018. Motor Neuron Disease: Pathophysiology, Diagnosis, and Management. *The American journal of medicine*.
- Frakes, A. E., Ferraiuolo, L., Haidet-Phillips, A. M., Schmelzer, L., Braun, L., Miranda, C. J., Ladner, K. J., Bevan, A. K., Foust, K. D. & Godbout, J. P. 2014. Microglia induce motor neuron death via the classical NF- κ B pathway in amyotrophic lateral sclerosis. *Neuron*, 81, 1009-1023.
- Freischmidt, A., Müller, K., Ludolph, A. C., Weishaupt, J. H. & Andersen, P. M. 2017. Association of Mutations in TBK1 With Sporadic and Familial Amyotrophic Lateral Sclerosis and Frontotemporal Dementia. *JAMA Neurology*, 74, 110-113.
- Freischmidt, A., Wieland, T., Richter, B., Ruf, W., Schaeffer, V., Müller, K., Marroquin, N., Nordin, F., Hübers, A. & Weydt, P. 2015. Haploinsufficiency of TBK1 causes familial ALS and fronto-temporal dementia. *Nature neuroscience*, 18, 631-636.
- Fryer, A. L., Abdullah, A., Taylor, J. M. & Crack, P. J. 2021. The complexity of the cGAS-STING pathway in CNS pathologies. *Frontiers in neuroscience*, 15, 621501.
- Furman, P. A., Fyfe, J. A., St Clair, M. H., Weinhold, K., Rideout, J. L., Freeman, G. A., Lehrman, S. N., Bolognesi, D. P., Broder, S. & Mitsuya, H. 1986. Phosphorylation of 3'-azido-3'-deoxythymidine and selective interaction of the 5'-triphosphate with human immunodeficiency virus reverse transcriptase. *Proceedings of the National Academy of Sciences*, 83, 8333-8337.
- Gaiani, A., Martinelli, I., Bello, L., Querin, G., Puthenparampil, M., Ruggero, S., Toffanin, E., Cagnin, A., Briani, C. & Pegoraro, E. 2017. Diagnostic and prognostic biomarkers in amyotrophic lateral sclerosis: neurofilament light chain levels in definite subtypes of disease. *JAMA neurology*, 74, 525-532.
- Gao, J., Wang, L., Huntley, M. L., Perry, G. & Wang, X. 2018. Pathomechanisms of TDP-43 in neurodegeneration. *Journal of Neurochemistry*, 146, 7-20.
- Gao, J., Wang, L., Yan, T., Perry, G. & Wang, X. 2019. TDP-43 proteinopathy and mitochondrial abnormalities in neurodegeneration. *Molecular and Cellular Neuroscience*, 100, 103396.
- Garbuzova-Davis, S., Ehrhart, J., Sanberg, P. R. & Borlongan, C. V. 2018. Potential Role of Humoral IL-6 Cytokine in Mediating Pro-Inflammatory Endothelial Cell Response in Amyotrophic Lateral Sclerosis. *International journal of molecular sciences*, 19, 423.
- Garcia-Montojo, M., Doucet-O'hare, T., Henderson, L. & Nath, A. 2018. Human endogenous retrovirus-K (HML-2): a comprehensive review. *Critical Reviews in Microbiology*, 44, 715-738.
- Garcia-Montojo, M., Fathi, S., Norato, G., Smith, B., Rowe, D., Kiernan, M., Vucic, S., Mathers, S., Van Eijk, R. & Santamaria, U. 2021. Inhibition of HERV-K (HML-2) in amyotrophic lateral sclerosis patients on antiretroviral therapy. *Journal of the neurological sciences*, 423, 117358.
- Garcia-Montojo, M., Simula, E. R., Fathi, S., McMahan, C., Ghosal, A., Berry, J. D., Cudkovicz, M., Elkhouloun, A., Johnson, K., Norato, G., Jensen, P., James, T., Sechi, L. A. & Nath, A.

2022. Antibody Response to HML-2 May Be Protective in Amyotrophic Lateral Sclerosis. *Annals of Neurology*, 92, 782-792.
- Gardner, R. C. & Yaffe, K. 2015. Epidemiology of mild traumatic brain injury and neurodegenerative disease. *Molecular and Cellular Neuroscience*, 66, 75-80.
- Garofalo, S., Coccozza, G., Bernardini, G., Savage, J., Raspa, M., Aronica, E., Tremblay, M.-E., Ransohoff, R. M., Santoni, A. & Limatola, C. 2022. Blocking immune cell infiltration of the central nervous system to tame Neuroinflammation in Amyotrophic lateral sclerosis. *Brain, Behavior, and Immunity*, 105, 1-14.
- Garofalo, S., Coccozza, G., Porzia, A., Inghilleri, M., Raspa, M., Scavizzi, F., Aronica, E., Bernardini, G., Peng, L., Ransohoff, R. M., Santoni, A. & Limatola, C. 2020. Natural killer cells modulate motor neuron-immune cell cross talk in models of Amyotrophic Lateral Sclerosis. *Nature Communications*, 11, 1773.
- Garson, J. A., Usher, L., Al-Chalabi, A., Huggett, J., Day, E. F. & McCormick, A. L. 2019. Quantitative analysis of human endogenous retrovirus-K transcripts in postmortem premotor cortex fails to confirm elevated expression of HERV-K RNA in amyotrophic lateral sclerosis. *Acta neuropathologica communications*, 7, 1-9.
- Geloso, M. C., Corvino, V., Marchese, E., Serrano, A., Michetti, F. & D'ambrosi, N. 2017. The Dual Role of Microglia in ALS: Mechanisms and Therapeutic Approaches. *Frontiers in Aging Neuroscience*, 9.
- Gendron, T. F., Rademakers, R. & Petrucelli, L. 2013. TARDBP mutation analysis in TDP-43 proteinopathies and deciphering the toxicity of mutant TDP-43. *Journal of Alzheimer's Disease*, 33, S35-S45.
- Georges, M., Attali, V., Golmard, J. L., Morélot-Panzini, C., Crevier-Buchman, L., Collet, J.-M., Tintignac, A., Morawiec, E., Trosini-Desert, V., Salachas, F., Similowski, T. & Gonzalez-Bermejo, J. 2016. Reduced survival in patients with ALS with upper airway obstructive events on non-invasive ventilation. *Journal of Neurology, Neurosurgery & Psychiatry*, 87, 1045.
- Ghiasi, P., Hosseinkhani, S., Noori, A., Nafissi, S. & Khajeh, K. 2012. Mitochondrial complex I deficiency and ATP/ADP ratio in lymphocytes of amyotrophic lateral sclerosis patients. *Neurological Research*, 34, 297-303.
- Ghosn, J., Taiwo, B., Seedat, S., Autran, B. & Katlama, C. 2018. HIV. *The Lancet*, 392, 685-697.
- Giannini, M., Bayona-Feliu, A., Sproviero, D., Barroso, S. I., Cereda, C. & Aguilera, A. 2020. TDP-43 mutations link Amyotrophic Lateral Sclerosis with R-loop homeostasis and R loop-mediated DNA damage. *PLOS Genetics*, 16, e1009260.
- Gifford, R. & Tristem, M. 2003. *The Evolution, Distribution and Diversity of Endogenous Retroviruses*.
- Gifford, R. J., Blomberg, J., Coffin, J. M., Fan, H., Heidmann, T., Mayer, J., Stoye, J., Tristem, M. & Johnson, W. E. 2018. Nomenclature for endogenous retrovirus (ERV) loci. *Retrovirology*, 15, 59.
- Gijssels, I., Van Langenhove, T., Van Der Zee, J., Slegers, K., Philtjens, S., Kleinberger, G., Janssens, J., Bettens, K., Van Cauwenberghe, C. & Pereson, S. 2012. A C9orf72 promoter repeat expansion in a Flanders-Belgian cohort with disorders of the frontotemporal lobar degeneration-amyotrophic lateral sclerosis spectrum: a gene identification study. *The Lancet Neurology*, 11, 54-65.
- Gille, B., De Schaepdryver, M., Dedeene, L., Goossens, J., Claeys, K. G., Van Den Bosch, L., Tournoy, J., Van Damme, P. & Poesen, K. 2019. Inflammatory markers in

- cerebrospinal fluid: independent prognostic biomarkers in amyotrophic lateral sclerosis? *Journal of Neurology, Neurosurgery & Psychiatry*, 90, 1338-1346.
- Gitler, A. D. & Tsuiji, H. 2016. There has been an awakening: emerging mechanisms of C9orf72 mutations in FTD/ALS. *Brain research*, 1647, 19-29.
- Gold, J., Marta, M., Meier, U. C., Christensen, T., Miller, D., Altmann, D., Holden, D., Bianchi, L., Adiutori, R. & Macmanus, D. 2018. A phase II baseline versus treatment study to determine the efficacy of raltegravir (Isentress) in preventing progression of relapsing remitting multiple sclerosis as determined by gadolinium-enhanced MRI: The INSPIRE study. *Multiple sclerosis and related disorders*, 24, 123-128.
- Gold, J., Rowe, D. B., Kiernan, M. C., Vucic, S., Mathers, S., Van Eijk, R. P., Nath, A., Garcia Montojo, M., Norato, G. & Santamaria, U. A. 2019. Safety and Tolerability of Triumeq in Amyotrophic Lateral Sclerosis: The Lighthouse Trial.
- Golpich, M., Amini, E., Mohamed, Z., Azman Ali, R., Mohamed Ibrahim, N. & Ahmadiani, A. 2017. Mitochondrial dysfunction and biogenesis in neurodegenerative diseases: pathogenesis and treatment. *CNS neuroscience & therapeutics*, 23, 5-22.
- Gonzalez-Hernandez, M. J., Swanson, M. D., Contreras-Galindo, R., Cookinham, S., King, S. R., Noel Jr, R. J., Kaplan, M. H. & Markovitz, D. M. 2012. Expression of human endogenous retrovirus type K (HML-2) is activated by the Tat protein of HIV-1. *Journal of virology*, 86, 7790-7805.
- Goutman, S. A., Boss, J., Patterson, A., Mukherjee, B., Batterman, S. & Feldman, E. L. 2019. High plasma concentrations of organic pollutants negatively impact survival in amyotrophic lateral sclerosis. *Journal of Neurology, Neurosurgery & Psychiatry*, jnnp-2018-319785.
- Govaarts, R., Beeldman, E., Kampelmacher, M. J., Van Tol, M.-J., Van Den Berg, L. H., Van Der Kooij, A. J., Wijkstra, P. J., Zijnen-Suyker, M., Cobben, N. a. M., Schmand, B. A., De Haan, R. J., De Visser, M. & Raaphorst, J. 2016. The frontotemporal syndrome of ALS is associated with poor survival. *Journal of Neurology*, 263, 2476-2483.
- Grandi, N. & Tramontano, E. 2017. Type W Human Endogenous Retrovirus (HERV-W) Integrations and Their Mobilization by L1 Machinery: Contribution to the Human Transcriptome and Impact on the Host Physiopathology. *Viruses*, 9.
- Grandi, N. & Tramontano, E. 2018. HERV Envelope Proteins: Physiological Role and Pathogenic Potential in Cancer and Autoimmunity. *Frontiers in Microbiology*, 9.
- Gregory, J. M., Livesey, M. R., Mcdade, K., Selvaraj, B. T., Barton, S. K., Chandran, S. & Smith, C. 2020. Dysregulation of AMPA receptor subunit expression in sporadic ALS post-mortem brain. *The Journal of Pathology*, 250, 67-78.
- Gubernick, S. I., Félix, N., Lee, D., Xu, J. J. & Hamad, B. 2016. The HIV therapy market. Nature Publishing Group.
- Gunnarsson, L. G., Bodin, L., Söderfeldt, B. & Axelson, O. 1992. A case-control study of motor neurone disease: its relation to heritability, and occupational exposures, particularly to solvents. *British journal of industrial medicine*, 49, 791-798.
- Guo, W., Chen, Y., Zhou, X., Kar, A., Ray, P., Chen, X., Rao, E. J., Yang, M., Ye, H. & Zhu, L. 2011. An ALS-associated mutation affecting TDP-43 enhances protein aggregation, fibril formation and neurotoxicity. *Nature Structural and Molecular Biology*, 18, 822.
- Gurney, M. E., Pu, H., Chiu, A. Y., Dal Canto, M. C., Polchow, C. Y., Alexander, D. D., Caliendo, J., Hentati, A., Kwon, Y. W. & Deng, H.-X. 1994. Motor neuron degeneration in mice that express a human Cu, Zn superoxide dismutase mutation. *Science*, 264, 1772-1775.

- Guttenplan, K. A., Weigel, M. K., Prakash, P., Wijewardhane, P. R., Hasel, P., Rufen-Blanchette, U., Münch, A. E., Blum, J. A., Fine, J., Neal, M. C., Bruce, K. D., Gitler, A. D., Chopra, G., Liddelow, S. A. & Barres, B. A. 2021. Neurotoxic reactive astrocytes induce cell death via saturated lipids. *Nature*, 599, 102-107.
- Haag, S. M., Gulen, M. F., Reymond, L., Gibelin, A., Abrami, L., Decout, A., Heymann, M., Van Der Goot, F. G., Turcatti, G. & Behrendt, R. 2018. Targeting STING with covalent small-molecule inhibitors. *Nature*, 559, 269-273.
- Hadlock, K., Miller, R., Jin, X., Yu, S., Reis, J., Mass, J., Gelinas, D. & Mcgrath, M. Elevated rates of antibody reactivity to HML-2/HERV-K but not other endogenous retroviruses in ALS. *Neurology*, 2004. LIPPINCOTT WILLIAMS & WILKINS 530 WALNUT ST, PHILADELPHIA, PA 19106-3621 USA, A37-A38.
- Haenseler, W., Sansom, S. N., Buchrieser, J., Newey, S. E., Moore, C. S., Nicholls, F. J., Chintawar, S., Schnell, C., Antel, J. P. & Allen, N. D. 2017. A highly efficient human pluripotent stem cell microglia model displays a neuronal-co-culture-specific expression profile and inflammatory response. *Stem cell reports*, 8, 1727-1742.
- Hardiman, O., Al-Chalabi, A., Chio, A., Corr, E. M., Logroscino, G., Robberecht, W., Shaw, P. J., Simmons, Z. & Van Den Berg, L. H. 2017a. Amyotrophic lateral sclerosis. *Nature Reviews Disease Primers*, 3, 17071.
- Hardiman, O., Al-Chalabi, A., Chio, A., Corr, E. M., Logroscino, G., Robberecht, W., Shaw, P. J., Simmons, Z. & Van Den Berg, L. H. 2017b. Amyotrophic lateral sclerosis. *Nature Reviews Disease Primers*, 3, 1-19.
- Hardiman, O., Van Den Berg, L. H. & Kiernan, M. C. 2011. Clinical diagnosis and management of amyotrophic lateral sclerosis. *Nature reviews neurology*, 7, 639.
- Hartl, F. U., Bracher, A. & Hayer-Hartl, M. 2011. Molecular chaperones in protein folding and proteostasis. *Nature*, 475, 324.
- Hashimoto, Y., Kurita, M., Aiso, S., Nishimoto, I. & Matsuoka, M. 2009. Humanin inhibits neuronal cell death by interacting with a cytokine receptor complex or complexes involving CNTF receptor alpha/WSX-1/gp130. *Mol Biol Cell*, 20, 2864-73.
- Hattab, S., Guihot, A., Guiguet, M., Fourati, S., Carcelain, G., Caby, F., Marcelin, A.-G., Autran, B., Costagliola, D. & Katlama, C. 2014. Comparative impact of antiretroviral drugs on markers of inflammation and immune activation during the first two years of effective therapy for HIV-1 infection: an observational study. *BMC infectious diseases*, 14, 1-9.
- Hatzipetros, T., Bogdanik, L. P., Tassinari, V. R., Kidd, J. D., Moreno, A. J., Davis, C., Osborne, M., Austin, A., Vieira, F. G. & Lutz, C. 2014. C57BL/6J congenic Prp-TDP43A315T mice develop progressive neurodegeneration in the myenteric plexus of the colon without exhibiting key features of ALS. *Brain research*, 1584, 59-72.
- Hayashi, Y., Homma, K. & Ichijo, H. 2016. SOD1 in neurotoxicity and its controversial roles in SOD1 mutation-negative ALS. *Advances in Biological Regulation*, 60, 95-104.
- He, F. & Todd, P. K. 2011. Epigenetics in Nucleotide Repeat Expansion Disorders. *Semin Neurol*, 31, 470-483.
- Hetz, C., Chevet, E. & Oakes, S. A. 2015. Proteostasis control by the unfolded protein response. *Nature cell biology*, 17, 829.
- Heyburn, L. & Moussa, C. E. H. 2017. TDP-43 in the spectrum of MND-FTLD pathologies. *Molecular and Cellular Neuroscience*, 83, 46-54.
- Highley, J. R., Kirby, J., Jansweijer, J. A., Webb, P. S., Hewamadduma, C. A., Heath, P. R., Higginbottom, A., Raman, R., Ferraiuolo, L., Cooper-Knock, J., Mcdermott, C. J.,

- Wharton, S. B., Shaw, P. J. & Ince, P. G. 2014. Loss of nuclear TDP-43 in amyotrophic lateral sclerosis (ALS) causes altered expression of splicing machinery and widespread dysregulation of RNA splicing in motor neurones. *Neuropathology and Applied Neurobiology*, 40, 670-685.
- Hileman, C. O. & Funderburg, N. T. 2017. Inflammation, Immune Activation, and Antiretroviral Therapy in HIV. *Current HIV/AIDS Reports*, 14, 93-100.
- Hilton, J. B., White, A. R. & Crouch, P. J. 2015. Metal-deficient SOD1 in amyotrophic lateral sclerosis. *Journal of Molecular Medicine*, 93, 481-487.
- Hipp, M. S., Park, S.-H. & Hartl, F. U. 2014. Proteostasis impairment in protein-misfolding and -aggregation diseases. *Trends in Cell Biology*, 24, 506-514.
- Hofer, M. J. & Campbell, I. L. 2013. Type I interferon in neurological disease—The devil from within. *Cytokine & Growth Factor Reviews*, 24, 257-267.
- Hogg, M. C., Halang, L., Woods, I., Coughlan, K. S. & Prehn, J. H. 2018. Riluzole does not improve lifespan or motor function in three ALS mouse models. *Amyotrophic Lateral Sclerosis and Frontotemporal Degeneration*, 19, 438-445.
- Hohn, O., Hanke, K. & Bannert, N. 2013. HERV-K(HML-2), the Best Preserved Family of HERVs: Endogenization, Expression, and Implications in Health and Disease. *Frontiers in oncology*, 3, 246-246.
- Holtcamp, W. 2012. The emerging science of BMAA: do cyanobacteria contribute to neurodegenerative disease? : National Institute of Environmental Health Sciences.
- Hor, J.-H., Santosa, M. M., Lim, V. J. W., Ho, B. X., Taylor, A., Khong, Z. J., Ravits, J., Fan, Y., Liou, Y.-C., Soh, B.-S. & Ng, S.-Y. 2021. ALS motor neurons exhibit hallmark metabolic defects that are rescued by SIRT3 activation. *Cell Death & Differentiation*, 28, 1379-1397.
- Horning, K. J., Caito, S. W., Tipps, K. G., Bowman, A. B. & Aschner, M. 2015. Manganese Is Essential for Neuronal Health. *Annual Review of Nutrition*, 35, 71-108.
- Hornung, V., Ablasser, A., Charrel-Dennis, M., Bauernfeind, F., Horvath, G., Caffrey, D. R., Latz, E. & Fitzgerald, K. A. 2009. AIM2 recognizes cytosolic dsDNA and forms a caspase-1-activating inflammasome with ASC. *Nature*, 458, 514-518.
- Huang, C., Zhou, H., Tong, J., Chen, H., Liu, Y.-J., Wang, D., Wei, X. & Xia, X.-G. 2011. FUS Transgenic Rats Develop the Phenotypes of Amyotrophic Lateral Sclerosis and Frontotemporal Lobar Degeneration. *PLOS Genetics*, 7, e1002011.
- Huang, F., Zhu, Y., Hsiao-Nakamoto, J., Tang, X., Dugas, J. C., Moscovitch-Lopatin, M., Glass, J. D., Brown Jr, R. H., Ladha, S. S. & Lacomis, D. 2020. Longitudinal biomarkers in amyotrophic lateral sclerosis. *Annals of clinical and translational neurology*, 7, 1103-1116.
- Hughes, J. F. & Coffin, J. M. 2004. Human endogenous retrovirus K solo-LTR formation and insertional polymorphisms: implications for human and viral evolution. *Proceedings of the National Academy of Sciences*, 101, 1668-1672.
- Hughes, S. H. 2015. Reverse transcription of retroviruses and LTR retrotransposons. *Mobile DNA III*. American Society of Microbiology.
- Hunter, M., Spiller, K. J., Dominique, M. A., Xu, H., Hunter, F. W., Fang, T. C., Canter, R. G., Roberts, C. J., Ransohoff, R. M., Trojanowski, J. Q. & Lee, V. M. Y. 2021. Microglial transcriptome analysis in the rNLS8 mouse model of TDP-43 proteinopathy reveals discrete expression profiles associated with neurodegenerative progression and recovery. *Acta Neuropathologica Communications*, 9, 140.

- Ibba, G., Piu, C., Uleri, E., Serra, C. & Dolei, A. 2018. Disruption by SaCas9 endonuclease of HERV-Kenv, a retroviral gene with oncogenic and neuropathogenic potential, inhibits molecules involved in cancer and amyotrophic lateral sclerosis. *Viruses*, 10, 412.
- Igaz, L. M., Kwong, L. K., Chen-Plotkin, A., Winton, M. J., Unger, T. L., Xu, Y., Neumann, M., Trojanowski, J. Q. & Lee, V. M. Y. 2009. Expression of TDP-43 C-terminal Fragments in Vitro Recapitulates Pathological Features of TDP-43 Proteinopathies*. *Journal of Biological Chemistry*, 284, 8516-8524.
- Ighodaro, O. M. & Akinloye, O. A. 2017. First line defence antioxidants-superoxide dismutase (SOD), catalase (CAT) and glutathione peroxidase (GPX): Their fundamental role in the entire antioxidant defence grid. *Alexandria Journal of Medicine*.
- Ikeda, K. & Iwasaki, Y. 2015. Edaravone, a free radical scavenger, delayed symptomatic and pathological progression of motor neuron disease in the wobbler mouse. *PLoS one*, 10, e0140316.
- Ikenaka, K., Kawai, K., Katsuno, M., Huang, Z., Jiang, Y.-M., Iguchi, Y., Kobayashi, K., Kimata, T., Waza, M. & Tanaka, F. 2013. dnc-1/dynactin 1 knockdown disrupts transport of autophagosomes and induces motor neuron degeneration. *PLoS One*, 8, e54511.
- Ingre, C., Roos, P. M., Piehl, F., Kamel, F. & Fang, F. 2015. Risk factors for amyotrophic lateral sclerosis. *Clinical epidemiology*, 7, 181-193.
- Isache, C., Sands, M., Guzman, N. & Figueroa, D. 2016. HTLV-1 and HIV-1 co-infection: A case report and review of the literature. *IDCases*, 4, 53-55.
- Ishigaki, S. & Sobue, G. 2018. Importance of functional loss of FUS in FTLD/ALS. *Frontiers in molecular biosciences*, 5.
- Jara, J. H., Genç, B., Stanford, M. J., Pytel, P., Roos, R. P., Weintraub, S., Mesulam, M. M., Bigio, E. H., Miller, R. J. & Özdinler, P. H. 2017. Evidence for an early innate immune response in the motor cortex of ALS. *Journal of neuroinflammation*, 14, 1-20.
- Jayaraj, R., Megha, P. & Sreedev, P. 2016. Organochlorine pesticides, their toxic effects on living organisms and their fate in the environment. *Interdisciplinary toxicology*, 9, 90-100.
- Je, H. S., Yang, F., Ji, Y., Potluri, S., Fu, X.-Q., Luo, Z.-G., Nagappan, G., Chan, J. P., Hempstead, B. & Son, Y.-J. 2013. ProBDNF and mature BDNF as punishment and reward signals for synapse elimination at mouse neuromuscular junctions. *Journal of Neuroscience*, 33, 9957-9962.
- Jennum, P., Ibsen, R., Pedersen, S. W. & Kjellberg, J. 2013. Mortality, health, social and economic consequences of amyotrophic lateral sclerosis: a controlled national study. *Journal of Neurology*, 260, 785-793.
- Jesson, J., Saint-Lary, L., Revegue, M. H. D. T., O'rourke, J., Townsend, C. L., Renaud, F., Penazzato, M. & Leroy, V. 2022. Safety and efficacy of abacavir for treating infants, children, and adolescents living with HIV: a systematic review and meta-analysis. *The Lancet Child & Adolescent Health*.
- Ježek, J., Cooper, K. F. & Strich, R. 2018. Reactive Oxygen Species and Mitochondrial Dynamics: The Yin and Yang of Mitochondrial Dysfunction and Cancer Progression. *Antioxidants (Basel, Switzerland)*, 7, 13.
- Jin, M., Günther, R., Akgün, K., Hermann, A. & Ziemssen, T. 2020. Peripheral proinflammatory Th1/Th17 immune cell shift is linked to disease severity in amyotrophic lateral sclerosis. *Scientific reports*, 10, 1-13.

- Jönsson, M. E., Garza, R., Sharma, Y., Petri, R., Södersten, E., Johansson, J. G., Johansson, P. A., Atacho, D. A., Piracs, K. & Madsen, S. 2021. Activation of endogenous retroviruses during brain development causes an inflammatory response. *The EMBO journal*, 40, e106423.
- Jonsson, P. A., Graffmo, K. S., Brännström, T., Nilsson, P., Andersen, P. M. & Marklund, S. L. 2006. Motor neuron disease in mice expressing the wild type-like D90A mutant superoxide dismutase-1. *Journal of Neuropathology & Experimental Neurology*, 65, 1126-1136.
- Joyce, P. I., Fratta, P., Fisher, E. M. & Acevedo-Arozena, A. 2011. SOD1 and TDP-43 animal models of amyotrophic lateral sclerosis: recent advances in understanding disease toward the development of clinical treatments. *Mammalian Genome*, 22, 420-448.
- Kamel, F., Umbach, D. M., Bedlack, R. S., Richards, M., Watson, M., Alavanja, M. C., Blair, A., Hoppin, J. A., Schmidt, S. & Sandler, D. P. 2012. Pesticide exposure and amyotrophic lateral sclerosis. *Neurotoxicology*, 33, 457-462.
- Kaufmann, P., Levy, G., Thompson, J., Delbene, M., Battista, V., Gordon, P., Rowland, L., Levin, B. & Mitsumoto, H. 2005. The ALSFRS_r predicts survival time in an ALS clinic population. *Neurology*, 64, 38-43.
- Kiaei, M., Petri, S., Kipiani, K., Gardian, G., Choi, D.-K., Chen, J., Calingasan, N. Y., Schafer, P., Muller, G. W. & Stewart, C. 2006. Thalidomide and lenalidomide extend survival in a transgenic mouse model of amyotrophic lateral sclerosis. *Journal of Neuroscience*, 26, 2467-2473.
- Kiernan, M. C. 2018. Motor neuron disease in 2017: Progress towards therapy in motor neuron disease. *Nature Reviews Neurology*, 14, 65.
- King, A. E., Woodhouse, A., Kirkcaldie, M. T. K. & Vickers, J. C. 2016. Excitotoxicity in ALS: Overstimulation, or overreaction? *Experimental Neurology*, 275, 162-171.
- Klim, J. R., Williams, L. A., Limone, F., Guerra San Juan, I., Davis-Dusenbery, B. N., Mordes, D. A., Burberry, A., Steinbaugh, M. J., Gamage, K. K., Kirchner, R., Moccia, R., Cassel, S. H., Chen, K., Wainger, B. J., Woolf, C. J. & Eggan, K. 2019. ALS-implicated protein TDP-43 sustains levels of STMN2, a mediator of motor neuron growth and repair. *Nature Neuroscience*, 22, 167-179.
- Kremer, D., Gruchot, J., Weyers, V., Oldemeier, L., Goettle, P., Healy, L., Ho, J., Jang, R. D. & Küry, P. Microglial-dependent neurodegeneration in multiple sclerosis is fueled by HERV-W envelope protein. *MULTIPLE SCLEROSIS JOURNAL*, 2018. SAGE PUBLICATIONS LTD 1 OLIVERS YARD, 55 CITY ROAD, LONDON EC1Y 1SP, ENGLAND, 1000-1000.
- Krug, L., Chatterjee, N., Borges-Monroy, R., Hearn, S., Liao, W.-W., Morrill, K., Prazak, L., Rozhkov, N., Theodorou, D. & Hammell, M. 2017. Retrotransposon activation contributes to neurodegeneration in a Drosophila TDP-43 model of ALS. *PLoS genetics*, 13, e1006635.
- Kumar, P. N., Sweet, D. E., Mcdowell, J. A., Symonds, W., Lou, Y., Hetherington, S. & Lafon, S. 1999. Safety and pharmacokinetics of abacavir (1592U89) following oral administration of escalating single doses in human immunodeficiency virus type 1-infected adults. *Antimicrob Agents Chemother*, 43, 603-8.
- Kurland, L., Radhakrishnan, K., Williams, D. & Waring, S. 1994. Amyotrophic lateral sclerosis-parkinsonism dementia complex on Guam: epidemiological and etiological perspectives. *Motor Neuron Disease. A. Willams, Ed*, 109-130.

- Küry, P., Nath, A., Créange, A., Dolei, A., Marche, P., Gold, J., Giovannoni, G., Hartung, H.-P. & Perron, H. 2018. Human endogenous retroviruses in neurological diseases. *Trends in molecular medicine*, 24, 379-394.
- Kwak, S., Hideyama, T., Yamashita, T. & Aizawa, H. 2010. AMPA receptor-mediated neuronal death in sporadic ALS. *Neuropathology*, 30, 182-188.
- Kwiatkowski, T. J., Bosco, D., Leclerc, A., Tamrazian, E., Vanderburg, C., Russ, C., Davis, A., Gilchrist, J., Kasarskis, E. & Munsat, T. 2009. Mutations in the FUS/TLS gene on chromosome 16 cause familial amyotrophic lateral sclerosis. *Science*, 323, 1205-1208.
- Kwun, H. J., Han, H. J., Lee, W. J., Kim, H. S. & Jang, K. L. 2002. Transactivation of the human endogenous retrovirus K long terminal repeat by herpes simplex virus type 1 immediate early protein 0. *Virus research*, 86, 93-100.
- Lacomblez, L., Bensimon, G., Meininger, V., Leigh, P. & Guillet, P. 1996. Dose-ranging study of riluzole in amyotrophic lateral sclerosis. *The Lancet*, 347, 1425-1431.
- Lacorte, E., Ferrigno, L., Leoncini, E., Corbo, M., Boccia, S. & Vanacore, N. 2016. Physical activity, and physical activity related to sports, leisure and occupational activity as risk factors for ALS: A systematic review. *Neuroscience & biobehavioral reviews*, 66, 61-79.
- Lalmansingh, A. S., Urekar, C. J. & Reddi, P. P. 2011. TDP-43 is a transcriptional repressor: the testis-specific mouse acrv1 gene is a TDP-43 target in vivo. *Journal of Biological Chemistry*, 286, 10970-10982.
- Lance, E., Arnich, N., Maignien, T. & Biré, R. 2018. Occurrence of β -N-methylamino-l-alanine (BMAA) and Isomers in Aquatic Environments and Aquatic Food Sources for Humans. *Toxins*, 10, 83.
- Lander, E. S., Linton, L. M., Birren, B., Nusbaum, C., Zody, M. C., Baldwin, J., Devon, K., Dewar, K., Doyle, M. & Fitzhugh, W. 2001. Initial sequencing and analysis of the human genome.
- Le masson, G., Przedborski, S. & Abbott, L. F. 2014. A Computational Model of Motor Neuron Degeneration. *Neuron*, 83, 975-988.
- Leboyer, M., Tamouza, R., Charron, D., Faucard, R. & Perron, H. 2013. Human endogenous retrovirus type W (HERV-W) in schizophrenia: a new avenue of research at the gene-environment interface. *The World Journal of Biological Psychiatry*, 14, 80-90.
- Lee, C. T.-C., Chiu, Y.-W., Wang, K.-C., Hwang, C.-S., Lin, K.-H., Lee, I.-T. & Tsai, C.-P. 2013. Riluzole and prognostic factors in amyotrophic lateral sclerosis long-term and short-term survival: a population-based study of 1149 cases in Taiwan. *Journal of epidemiology*, JE20120119.
- Lee, E. B., Lee, V. M. Y. & Trojanowski, J. Q. 2011. Gains or losses: molecular mechanisms of TDP43-mediated neurodegeneration. *Nature Reviews Neuroscience*, 13, 38.
- Lee, J. D., Levin, S. C., Willis, E. F., Li, R., Woodruff, T. M. & Noakes, P. G. 2018. Complement components are upregulated and correlate with disease progression in the TDP-43Q331K mouse model of amyotrophic lateral sclerosis. *Journal of Neuroinflammation*, 15, 171.
- Lee, S. & Kim, H.-J. 2015. Prion-like mechanism in amyotrophic lateral sclerosis: are protein aggregates the key? *Experimental neurobiology*, 24, 1-7.
- Lee, W. J., Kwun, H. J., Kim, H. S. & Jang, K. L. 2003. Activation of the human endogenous retrovirus W long terminal repeat by herpes simplex virus type 1 immediate early protein 1. *Molecules and cells*, 15, 75-80.

- Leigh, P., Whitwell, H., Garofalo, O., Buller, J., Swash, M., Martin, J., Gallo, J.-M., Weller, R. & Anderton, B. 1991. Ubiquitin-immunoreactive intraneuronal inclusions in amyotrophic lateral sclerosis: morphology, distribution, and specificity. *Brain*, 114, 775-788.
- Leitner, M., Menzies, S. & Lutz, C. 2009. Working with ALS mice: Guidelines for preclinical testing & colony management. *The Jackson Laboratory*.
- Lenz, J. 2016. HERV-K HML-2 diversity among humans. *Proceedings of the National Academy of Sciences*, 113, 4240.
- Letendre, S., Marquie-Beck, J., Capparelli, E., Best, B., Clifford, D., Collier, A. C., Gelman, B. B., McArthur, J. C., Mccutchan, J. A. & Morgello, S. 2008. Validation of the CNS penetration-effectiveness rank for quantifying antiretroviral penetration into the central nervous system. *Archives of neurology*, 65, 65-70.
- Letendre, S. L., Mills, A. M., Tashima, K. T., Thomas, D. A., Min, S. S., Chen, S., Song, I. H. & Piscitelli, S. C. 2014. ING116070: A study of the pharmacokinetics and antiviral activity of Dolutegravir in cerebrospinal fluid in HIV-1-infected, antiretroviral therapy-naïve subjects. *Clinical Infectious Diseases*, 59, 1032-1037.
- Levine, T. D., Miller, R. G., Bradley, W. G., Moore, D. H., Saperstein, D. S., Flynn, L. E., Katz, J. S., Forshew, D. A., Metcalf, J. S. & Banack, S. A. 2017. Phase I clinical trial of safety of L-serine for ALS patients. *Amyotrophic Lateral Sclerosis and Frontotemporal Degeneration*, 18, 107-111.
- Li, B., Yu, S., Li, G., Chen, X., Huang, M., Liao, X., Li, H., Hu, F. & Wu, J. 2019. Transfer of a cyanobacterial neurotoxin, β -methylamino-l-alanine from soil to crop and its bioaccumulation in Chinese cabbage. *Chemosphere*, 219, 997-1001.
- Li, J., Akagi, K., Hu, Y., Trivett, A. L., Hlynialuk, C. J., Swing, D. A., Volfovsky, N., Morgan, T. C., Golubeva, Y. & Stephens, R. M. 2012a. Mouse endogenous retroviruses can trigger premature transcriptional termination at a distance. *Genome research*, 22, 870-884.
- Li, J., Xiong, G., Huang, Z., Li, G., Xiao, B., Zhu, D., Tan, X. & Liu, Y. 2007. Parkinsonism with long term use of Lamivudine. *Neurology Asia*, 12, 111-113.
- Li, W., Jin, Y., Prazak, L., Hammell, M. & Dubnau, J. 2012b. Transposable Elements in TDP-43-Mediated Neurodegenerative Disorders. *PLOS ONE*, 7, e44099.
- Li, W., Lee, M.-H., Henderson, L., Tyagi, R., Bachani, M., Steiner, J., Campanac, E., Hoffman, D. A., Von Geldern, G. & Johnson, K. 2015. Human endogenous retrovirus-K contributes to motor neuron disease. *Science translational medicine*, 7, 307ra153-307ra153.
- Li, W., Pandya, D., Pasternack, N., Garcia-Montojo, M., Henderson, L., Kozak, C. A. & Nath, A. 2022. Retroviral Elements in Pathophysiology and as Therapeutic Targets for Amyotrophic Lateral Sclerosis. *Neurotherapeutics*, 19, 1085-1101.
- Libonati, L., Onesti, E., Gori, M. C., Ceccanti, M., Cambieri, C., Fabbri, A., Frasca, V. & Inghilleri, M. 2017. Vitamin D in amyotrophic lateral sclerosis. *Functional neurology*, 32, 35-40.
- Liewluck, T. & Saperstein, D. S. 2015. Progressive muscular atrophy. *Neurologic clinics*, 33, 761-773.
- Liu, E. Y., Russ, J., Cali, C. P., Phan, J. M., Amlie-Wolf, A. & Lee, E. B. 2019. Loss of Nuclear TDP-43 Is Associated with Decondensation of LINE Retrotransposons. *Cell Reports*, 27, 1409-1421.e6.
- Liu, J. & Wang, F. 2017. Role of Neuroinflammation in Amyotrophic Lateral Sclerosis: Cellular Mechanisms and Therapeutic Implications. *Frontiers in immunology*, 8, 1005-1005.

- Liu, R., Yang, G., Nonaka, T., Arai, T., Jia, W. & Cynader, M. S. 2013. Reducing TDP-43 aggregation does not prevent its cytotoxicity. *Acta Neuropathologica Communications*, 1, 1-11.
- Liu, X., Liu, Z., Wu, Z., Ren, J., Fan, Y., Sun, L., Cao, G., Niu, Y., Zhang, B. & Ji, Q. 2023. Resurrection of endogenous retroviruses during aging reinforces senescence. *Cell*.
- Livesley, B. & Sissons, C. 1968. Chronic lead intoxication mimicking motor neurone disease. *British medical journal*, 4, 387.
- Loane, D. J., Kumar, A., Stoica, B. A., Cabatbat, R. & Faden, A. I. 2014. Progressive Neurodegeneration After Experimental Brain Trauma: Association With Chronic Microglial Activation. *Journal of Neuropathology & Experimental Neurology*, 73, 14-29.
- Logroscino, G., Piccininni, M., Marin, B., Nichols, E., Abd-Allah, F., Abdelalim, A., Alahdab, F., Asgedom, S. W., Awasthi, A. & Chaiah, Y. 2018. Global, regional, and national burden of motor neuron diseases 1990–2016: a systematic analysis for the Global Burden of Disease Study 2016. *The Lancet Neurology*, 17, 1083-1097.
- López-Martínez, A., Soblechero-Martín, P. & Arechavala-Gomez, V. 2022. Evaluation of Exon Skipping and Dystrophin Restoration in In Vitro Models of Duchenne Muscular Dystrophy. In: ARECHAVALA-GOMEZA, V. & GARANTO, A. (eds.) *Antisense RNA Design, Delivery, and Analysis*. New York, NY: Springer US.
- Luan, W., Wright, A. L., Brown-Wright, H., Le, S., San Gil, R., Madrid San Martin, L., Ling, K., Jafar-Nejad, P., Rigo, F. & Walker, A. K. 2023. Early activation of cellular stress and death pathways caused by cytoplasmic TDP-43 in the rNLS8 mouse model of ALS and FTD. *Molecular Psychiatry*, 28, 2445-2461.
- Ludolph, A. C., Bendotti, C., Blaugrund, E., Chio, A., Greensmith, L., Loeffler, J.-P., Mead, R., Niessen, H. G., Petri, S. & Pradat, P.-F. 2010. Guidelines for preclinical animal research in ALS/MND: A consensus meeting. *Amyotrophic Lateral Sclerosis*, 11, 38-45.
- Ma, X. R., Prudencio, M., Koike, Y., Vatsavayai, S. C., Kim, G., Harbinski, F., Briner, A., Rodriguez, C. M., Guo, C., Akiyama, T., Schmidt, H. B., Cummings, B. B., Wyatt, D. W., Kurylo, K., Miller, G., Mekhoubad, S., Sallee, N., Mekonnen, G., Ganser, L., Rubien, J. D., Jansen-West, K., Cook, C. N., Pickles, S., Oskarsson, B., Graff-Radford, N. R., Boeve, B. F., Knopman, D. S., Petersen, R. C., Dickson, D. W., Shorter, J., Myong, S., Green, E. M., Seeley, W. W., Petrucelli, L. & Gitler, A. D. 2022. TDP-43 represses cryptic exon inclusion in the FTD–ALS gene UNC13A. *Nature*, 603, 124-130.
- Mackenzie, I. R., Bigio, E. H., Ince, P. G., Geser, F., Neumann, M., Cairns, N. J., Kwong, L. K., Forman, M. S., Ravits, J. & Stewart, H. 2007. Pathological TDP-43 distinguishes sporadic amyotrophic lateral sclerosis from amyotrophic lateral sclerosis with SOD1 mutations. *Annals of Neurology: Official Journal of the American Neurological Association and the Child Neurology Society*, 61, 427-434.
- Mackenzie, I. R., Frick, P., Grässer, F. A., Gendron, T. F., Petrucelli, L., Cashman, N. R., Edbauer, D., Kremmer, E., Prudlo, J. & Troost, D. 2015. Quantitative analysis and clinico-pathological correlations of different dipeptide repeat protein pathologies in C9ORF72 mutation carriers. *Acta neuropathologica*, 130, 845-861.
- Magiorkinis, G., Blanco-Melo, D. & Belshaw, R. 2015. The decline of human endogenous retroviruses: extinction and survival. *Retrovirology*, 12, 1-12.

- Majumder, V., Gregory, J. M., Barria, M. A., Green, A. & Pal, S. 2018. TDP-43 as a potential biomarker for amyotrophic lateral sclerosis: a systematic review and meta-analysis. *BMC Neurology*, 18, 90.
- Makuch, E., Jasyk, I., Kula, A., Lipiński, T. & Siednienko, J. 2022. IFN β -Induced CXCL10 Chemokine Expression Is Regulated by Pellino3 Ligase in Monocytes and Macrophages. *International Journal of Molecular Sciences*, 23, 14915.
- Malaspina, A., Puentes, F. & Amor, S. 2015. Disease origin and progression in amyotrophic lateral sclerosis: an immunology perspective. *International immunology*, 27, 117-129.
- Malek, A. M., Barchowsky, A., Bowser, R., Youk, A. & Talbott, E. O. 2012. Pesticide exposure as a risk factor for amyotrophic lateral sclerosis: a meta-analysis of epidemiological studies: pesticide exposure as a risk factor for ALS. *Environmental research*, 117, 112-119.
- Mameli, G., Erre, G. L., Caggiu, E., Mura, S., Cossu, D., Bo, M., Cadoni, M., Piras, A., Mundula, N. & Colombo, E. 2017. Identification of a HERV-K env surface peptide highly recognized in Rheumatoid Arthritis (RA) patients: a cross-sectional case-control study. *Clinical & Experimental Immunology*, 189, 127-131.
- Mandrioli, J., Malerba, S. A., Beghi, E., Fini, N., Fasano, A., Zucchi, E., De Pasqua, S., Guidi, C., Terlizzi, E. & Sette, E. 2018. Riluzole and other prognostic factors in ALS: a population-based registry study in Italy. *Journal of neurology*, 265, 817-827.
- Manghera, M. & Douville, R. N. 2013. Endogenous retrovirus-K promoter: a landing strip for inflammatory transcription factors? *Retrovirology*, 10, 1-11.
- Manghera, M., Ferguson-Parry, J. & Douville, R. N. 2016a. TDP-43 regulates endogenous retrovirus-K viral protein accumulation. *Neurobiology of disease*, 94, 226-236.
- Manghera, M., Ferguson-Parry, J., Lin, R. & Douville, R. N. 2016b. NF- κ B and IRF1 induce endogenous retrovirus K expression via interferon-stimulated response elements in its 5' long terminal repeat. *Journal of virology*, 90, 9338-9349.
- Manghera, M., Ferguson, J. & Douville, R. 2015. ERVK Polyprotein Processing and Reverse Transcriptase Expression in Human Cell Line Models of Neurological Disease. *Viruses*, 7, 320-332.
- Marin, B., Fontana, A., Arcuti, S., Copetti, M., Boumédiène, F., Couratier, P., Beghi, E., Preux, P. M. & Logroscino, G. 2018. Age-specific ALS incidence: a dose-response meta-analysis. *European journal of epidemiology*, 33, 621-634.
- Martin, K., Jackson, C. F., Levy, R. G. & Cooper, P. N. 2016. Ketogenic diet and other dietary treatments for epilepsy. *Cochrane Database of Systematic Reviews*.
- Mathis, S., Goizet, C., Soulages, A., Vallat, J.-M. & Masson, G. L. 2019. Genetics of amyotrophic lateral sclerosis: A review. *Journal of the Neurological Sciences*, 399, 217-226.
- Matusica, D., Alfonsi, F., Turner, B. J., Butler, T. J., Shephard, S. R., Rogers, M.-L., Skeldal, S., Underwood, C. K., Mangelsdorf, M. & Coulson, E. J. 2016. Inhibition of motor neuron death in vitro and in vivo by a p75 neurotrophin receptor intracellular domain fragment. *Journal of Cell Science*, 129, 517-530.
- Mcaleese, K. E., Walker, L., Erskine, D., Thomas, A. J., Mckeith, I. G. & Attems, J. 2017. TDP-43 pathology in Alzheimer's disease, dementia with Lewy bodies and ageing. *Brain pathology*, 27, 472-479.
- Mccauley, M. E., O'rourke, J. G., Yáñez, A., Markman, J. L., Ho, R., Wang, X., Chen, S., Lall, D., Jin, M., Muhammad, A. K. M. G., Bell, S., Landeros, J., Valencia, V., Harms, M., Arditi,

- M., Jefferies, C. & Baloh, R. H. 2020. C9orf72 in myeloid cells suppresses STING-induced inflammation. *Nature*, 585, 96-101.
- Mccombe, P. A. & Henderson, R. D. 2010. Effects of gender in amyotrophic lateral sclerosis. *Gender Medicine*, 7, 557-570.
- Mccormick, A., Brown, R., Cudkowicz, M., Al-Chalabi, A. & Garson, J. 2008. Quantification of reverse transcriptase in ALS and elimination of a novel retroviral candidate. *Neurology*, 70, 278-283.
- Meeker, R. B. & Williams, K. S. 2015. The p75 neurotrophin receptor: at the crossroad of neural repair and death. *Neural regeneration research*, 10, 721.
- Mehta, P., Kaye, W., Raymond, J., Wu, R., Larson, T., Punjani, R., Heller, D., Cohen, J., Peters, T. & Muravov, O. 2018. Prevalence of amyotrophic lateral sclerosis—United States, 2014. *Morbidity and Mortality Weekly Report*, 67, 216.
- Mehta, P. R., Jones, A. R., Opie-Martin, S., Shatunov, A., Iacoangeli, A., Al Khleifat, A., Smith, B. N., Topp, S., Morrison, K. E., Shaw, P. J., Shaw, C. E., Morgan, S., Pittman, A. & Al-Chalabi, A. 2019. Younger age of onset in familial amyotrophic lateral sclerosis is a result of pathogenic gene variants, rather than ascertainment bias. *Journal of Neurology, Neurosurgery & Psychiatry*, 90, 268.
- Meininger, V., Bensimon, G., Bradley, W. G., Brooks, B. R., Douillet, P., Eisen, A. A., Lacomblez, L., Nigel Leigh, P. & Robberecht, W. 2004. Efficacy and safety of xaliproden in amyotrophic lateral sclerosis: results of two phase III trials. *Amyotrophic lateral sclerosis and other motor neuron disorders*, 5, 107-117.
- Mejzini, R., Flynn, L. L., Pitout, I. L., Fletcher, S., Wilton, S. D. & Akkari, P. A. 2019. ALS genetics, mechanisms, and therapeutics: where are we now? *Frontiers in neuroscience*, 13, 1310.
- Mi, S., Lee, X., Li, X.-P., Veldman, G. M., Finnerty, H., Racie, L., Lavallie, E., Tang, X.-Y., Edouard, P., Howes, S., Keith, J. C. & McCoy, J. M. 2000. Syncytin is a captive retroviral envelope protein involved in human placental morphogenesis. *Nature*, 403, 785-789.
- Miana-Mena, F. J., Muñoz, M. J., Yagüe, G., Mendez, M., Moreno, M., Ciriza, J., Zaragoza, P. & Osta, R. 2005. Optimal methods to characterize the G93A mouse model of ALS. *Amyotrophic Lateral Sclerosis*, 6, 55-62.
- Millecamps, S. & Julien, J.-P. 2013. Axonal transport deficits and neurodegenerative diseases. *Nature Reviews Neuroscience*, 14, 161-176.
- Miller, R. G., Block, G., Katz, J. S., Barohn, R. J., Gopalakrishnan, V., Cudkowicz, M., Zhang, J. R., Mcgrath, M. S., Ludington, E., Appel, S. H. & Azhir, A. 2015. Randomized phase 2 trial of NP001—a novel immune regulator: Safety and early efficacy in ALS. *Neuroimmunol Neuroinflamm*, 2, e100.
- Miller, R. G., Bouchard, J. P., Duquette, P., Eisen, A., Gelinas, D., Harati, Y., Munsat, T. L., Powe, L., Rothstein, J., Salzman, P. & Sufit, R. L. 1996. Clinical trials of riluzole in patients with ALS. *Neurology*, 47, 86S.
- Miller, T. M., Cudkowicz, M. E., Genge, A., Shaw, P. J., Sobue, G., Bucelli, R. C., Chiò, A., Van Damme, P., Ludolph, A. C. & Glass, J. D. 2022. Trial of antisense oligonucleotide tofersen for SOD1 ALS. *New England Journal of Medicine*, 387, 1099-1110.
- Mishra, P.-S., Dhull, D. K., Nalini, A., Vijayalakshmi, K., Sathyaprabha, T. N., Alladi, P. A. & Raju, T. R. 2016. Astroglia acquires a toxic neuroinflammatory role in response to the cerebrospinal fluid from amyotrophic lateral sclerosis patients. *Journal of Neuroinflammation*, 13, 212.

- Mitra, J., Guerrero, E. N., Hegde, P. M., Liachko, N. F., Wang, H., Vasquez, V., Gao, J., Pandey, A., Taylor, J. P. & Kraemer, B. C. 2019. Motor neuron disease-associated loss of nuclear TDP-43 is linked to DNA double-strand break repair defects. *Proceedings of the National Academy of Sciences*, 116, 4696-4705.
- Mizuno, Y., Amari, M., Takatama, M., Aizawa, H., Mihara, B. & Okamoto, K. 2006. Transferrin localizes in Bunina bodies in amyotrophic lateral sclerosis. *Acta neuropathologica*, 112, 597-603.
- Mizwicki, M. T., Fiala, M., Magpantay, L., Aziz, N., Sayre, J., Liu, G., Siani, A., Chan, D., Martinez-Maza, O. & Chattopadhyay, M. 2012. Tocilizumab attenuates inflammation in ALS patients through inhibition of IL6 receptor signaling. *American journal of neurodegenerative disease*, 1, 305.
- Mora, G. & Chiò, A. 2015. Disorders of Upper and Lower Motor Neurons. In: SGHIRLANZONI, A., LAURIA, G. & CHIAPPARINI, L. (eds.) *Prognosis of Neurological Diseases*. Milano: Springer Milan.
- Morahan, J. M. & Pamphlett, R. 2006. Amyotrophic lateral sclerosis and exposure to environmental toxins: an Australian case-control study. *Neuroepidemiology*, 27, 130.
- Morfini, G. A., Burns, M., Binder, L. I., Kanaan, N. M., Lapointe, N., Bosco, D. A., Brown, R. H., Brown, H., Tiwari, A. & Hayward, L. 2009. Axonal transport defects in neurodegenerative diseases. *Journal of Neuroscience*, 29, 12776-12786.
- Mori, K., Weng, S.-M., Arzberger, T., May, S., Rentzsch, K., Kremmer, E., Schmid, B., Kretzschmar, H. A., Cruts, M. & Van Broeckhoven, C. 2013. The C9orf72 GGGGCC repeat is translated into aggregating dipeptide-repeat proteins in FTLD/ALS. *Science*, 339, 1335-1338.
- Mori, M. A., Delattre, A. M., Carabelli, B., Pudell, C., Bortolanza, M., Staziaki, P. V., Visentainer, J. V., Montanher, P. F., Del Bel, E. A. & Ferraz, A. C. 2018. Neuroprotective effect of omega-3 polyunsaturated fatty acids in the 6-OHDA model of Parkinson's disease is mediated by a reduction of inducible nitric oxide synthase. *Nutritional Neuroscience*, 21, 341-351.
- Mostafalou, S. & Abdollahi, M. 2017. Pesticides: an update of human exposure and toxicity. *Archives of Toxicology*, 91, 549-599.
- Moullignier, A., Moulonguet, A., Pialoux, G. & Rozenbaum, W. 2001. Reversible ALS-like disorder in HIV infection. *Neurology*, 57, 995-1001.
- Moura, M. C., Novaes, M. R. C. G., Eduardo, E. J., Zago, Y. S., Freitas, R. D. N. B. & Casulari, L. A. 2015. Prognostic factors in amyotrophic lateral sclerosis: a population-based study. *PloS one*, 10, e0141500.
- Myers, C. L., Wertheimer, S. J., Schembri-King, J., Parks, T. & Wallace, R. W. 1992. Induction of ICAM-1 by TNF-alpha, IL-1 beta, and LPS in human endothelial cells after downregulation of PKC. *American Journal of Physiology-Cell Physiology*, 263, C767-C772.
- Nagai, M., Re, D. B., Nagata, T., Chalazonitis, A., Jessell, T. M., Wichterle, H. & Przedborski, S. 2007. Astrocytes expressing ALS-linked mutated SOD1 release factors selectively toxic to motor neurons. *Nature Neuroscience*, 10, 615-622.
- Narayanan, R. K., Mangelsdorf, M., Panwar, A., Butler, T. J., Noakes, P. G. & Wallace, R. H. 2013. Identification of RNA bound to the TDP-43 ribonucleoprotein complex in the adult mouse brain. *Amyotrophic Lateral Sclerosis and Frontotemporal Degeneration*, 14, 252-260.

- Nazmi, A., Field, R. H., Griffin, E. W., Haugh, O., Hennessy, E., Cox, D., Reis, R., Tortorelli, L., Murray, C. L. & Lopez-Rodriguez, A. B. 2019. Chronic neurodegeneration induces type I interferon synthesis via STING, shaping microglial phenotype and accelerating disease progression. *Glia*, 67, 1254-1276.
- Neumann, M., Sampathu, D. M., Kwong, L. K., Truax, A. C., Micsenyi, M. C., Chou, T. T., Bruce, J., Schuck, T., Grossman, M. & Clark, C. M. 2006. Ubiquitinated TDP-43 in frontotemporal lobar degeneration and amyotrophic lateral sclerosis. *Science*, 314, 130-133.
- Nexø, B. A., Villesen, P., Nissen, K. K., Lindegaard, H. M., Rossing, P., Petersen, T., Tarnow, L., Hansen, B., Lorenzen, T. & Hørslev-Petersen, K. 2016. Are human endogenous retroviruses triggers of autoimmune diseases? Unveiling associations of three diseases and viral loci. *Immunologic research*, 64, 55-63.
- Nguyen, H. P., Van Broeckhoven, C. & Van Der Zee, J. 2018. ALS Genes in the Genomic Era and their Implications for FTD. *Trends in Genetics*.
- Nijssen, J., Comley, L. H. & Hedlund, E. 2017. Motor neuron vulnerability and resistance in amyotrophic lateral sclerosis. *Acta neuropathologica*, 133, 863-885.
- Nishat, S., Jessica, F., Owen, H., Seddon, J., Simmons, G., Speight, N., Jasmeet, K., Woolford, L., Emes, R. D. & Farhid, H. 2020. Koala retrovirus viral load and disease burden in distinct northern and southern koala populations. *Scientific Reports (Nature Publisher Group)*, 10.
- Noto, Y.-I., Shibuya, K., Sato, Y., Kanai, K., Misawa, S., Sawai, S., Mori, M., Uchiyama, T., Iose, S., Nasu, S., Sekiguchi, Y., Fujimaki, Y., Kasai, T., Tokuda, T., Nakagawa, M. & Kuwabara, S. 2011. Elevated CSF TDP-43 levels in amyotrophic lateral sclerosis: Specificity, sensitivity, and a possible prognostic value. *Amyotrophic Lateral Sclerosis*, 12, 140-143.
- Oakes, J. A., Davies, M. C. & Collins, M. O. 2017. TBK1: a new player in ALS linking autophagy and neuroinflammation. *Molecular brain*, 10, 5.
- Oggiano, R., Solinas, G., Forte, G., Bocca, B., Farace, C., Pisano, A., Sotgiu, M. A., Clemente, S., Malaguarnera, M., Fois, A. G., Pirina, P., Montella, A. & Madeddu, R. 2018. Trace elements in ALS patients and their relationships with clinical severity. *Chemosphere*, 197, 457-466.
- Okamoto, K. 2019. Risk Factors in Amyotrophic Lateral Sclerosis. *Epidemiological Studies of Specified Rare and Intractable Disease*. Springer.
- Okamoto, K., Hirai, S., Amari, M., Watanabe, M. & Sakurai, A. 1993. Bunina bodies in amyotrophic lateral sclerosis immunostained with rabbit anti-cystatin C serum. *Neuroscience letters*, 162, 125-128.
- Olaniyan, L. W., Maduagwu, E. N., Akintunde, O. W., Oluwayelu, O. O. & Brai, B. I. 2015. Lamivudine-Induced Liver Injury. *Open Access Maced J Med Sci*, 3, 545-50.
- Ono, S., Hu, J., Shimizu, N., Imai, T. & Nakagawa, H. 2001. Increased interleukin-6 of skin and serum in amyotrophic lateral sclerosis. *Journal of the Neurological Sciences*, 187, 27-34.
- Osborne, O., Peyravian, N., Nair, M., Daunert, S. & Toborek, M. 2020. The paradox of HIV blood–brain barrier penetrance and antiretroviral drug delivery deficiencies. *Trends in neurosciences*, 43, 695-708.
- Ottum, P. A., Arellano, G., Reyes, L. I., Iruretagoyena, M. & Naves, R. 2015. Opposing roles of interferon-gamma on cells of the central nervous system in autoimmune neuroinflammation. *Frontiers in immunology*, 6, 539.

- Ou, S. H., Wu, F., Harrich, D., García-Martínez, L. F. & Gaynor, R. B. 1995. Cloning and characterization of a novel cellular protein, TDP-43, that binds to human immunodeficiency virus type 1 TAR DNA sequence motifs. *Journal of Virology*, 69, 3584.
- Ouyang, W., Wang, S., Yan, D., Wu, J., Zhang, Y., Li, W., Hu, J. & Liu, Z. 2023. The cGAS-STING pathway-dependent sensing of mitochondrial DNA mediates ocular surface inflammation. *Signal Transduction and Targeted Therapy*, 8, 371.
- Paganoni, S., Deng, J., Jaffa, M., Cudkowicz, M. E. & Wills, A. M. 2011. Body mass index, not dyslipidemia, is an independent predictor of survival in amyotrophic lateral sclerosis. *Muscle & nerve*, 44, 20-24.
- Paganoni, S., Macklin, E. A., Hendrix, S., Berry, J. D., Elliott, M. A., Maiser, S., Karam, C., Caress, J. B., Owegi, M. A. & Quick, A. 2020. Trial of sodium phenylbutyrate–taurursodiol for amyotrophic lateral sclerosis. *New England Journal of Medicine*, 383, 919-930.
- Paganoni, S., Macklin, E. A., Karam, C., Yu, H., Gonterman, F., Fetterman, K. A., Cudkowicz, M., Berry, J. & Wills, A. M. 2017. Vitamin D levels are associated with gross motor function in amyotrophic lateral sclerosis. *Muscle & nerve*, 56, 726-731.
- Paganoni, S., Macklin, E. A., Lee, A., Murphy, A., Chang, J., Zipf, A., Cudkowicz, M. & Atassi, N. 2014. Diagnostic timelines and delays in diagnosing amyotrophic lateral sclerosis (ALS). *Amyotrophic Lateral Sclerosis and Frontotemporal Degeneration*, 15, 453-456.
- Paganoni, S., Watkins, C., Cawson, M., Hendrix, S., Dickson, S. P., Knowlton, N., Timmons, J., Manuel, M. & Cudkowicz, M. 2022. Survival analyses from the CENTAUR trial in amyotrophic lateral sclerosis: Evaluating the impact of treatment crossover on outcomes. *Muscle & Nerve*, 66, 136-141.
- Paul, B. D., Snyder, S. H. & Bohr, V. A. 2021. Signaling by cGAS–STING in Neurodegeneration, Neuroinflammation, and Aging. *Trends in Neurosciences*, 44, 83-96.
- Penndorf, D., Tadić, V., Witte, O. W., Grosskreutz, J. & Kretz, A. 2017. DNA strand breaks and TDP-43 mislocation are absent in the murine hSOD1G93A model of amyotrophic lateral sclerosis in vivo and in vitro. *PLOS ONE*, 12, e0183684.
- Pérez-Pérez, S., Domínguez-Mozo, M. I., García-Martínez, M. Á., Ballester-González, R., Nieto-Gañán, I., Arroyo, R. & Alvarez-Lafuente, R. 2022. Epstein-Barr virus load correlates with multiple sclerosis-associated retrovirus envelope expression. *Biomedicines*, 10, 387.
- Perron, H., Germi, R., Bernard, C., Garcia-Montojo, M., Deluen, C., Farinelli, L., Faucard, R., Veas, F., Stefas, I. & Fabriek, B. O. 2012. Human endogenous retrovirus type W envelope expression in blood and brain cells provides new insights into multiple sclerosis disease. *Multiple sclerosis journal*, 18, 1721-1736.
- Pesiridis, G. S., Lee, V. M.-Y. & Trojanowski, J. Q. 2009. Mutations in TDP-43 link glycine-rich domain functions to amyotrophic lateral sclerosis. *Human molecular genetics*, 18, R156-R162.
- Peter, A., Udoh, K. & Ekanem, A. 2017. Histomorphological effect of Lamivudine on the Cerebellum of Wistar rats. *Histology, Cytology and Embryology*, 1.
- Peters, S., Broberg, K., Gallo, V., Levi, M., Kippler, M., Vineis, P., Veldink, J., Van Den Berg, L., Middleton, L. & Travis, R. C. 2021. Blood metal levels and amyotrophic lateral sclerosis risk: a prospective cohort. *Annals of neurology*, 89, 125-133.

- Peters, T. L., Beard, J. D., Umbach, D. M., Allen, K., Keller, J., Mariosa, D., Sandler, D. P., Schmidt, S., Fang, F. & Ye, W. 2016. Blood levels of trace metals and amyotrophic lateral sclerosis. *Neurotoxicology*, 54, 119-126.
- Pfohl, S. R., Halicek, M. T. & Mitchell, C. S. 2015. Characterization of the contribution of genetic background and gender to disease progression in the SOD1 G93A mouse model of amyotrophic lateral sclerosis: a meta-analysis. *Journal of neuromuscular diseases*, 2, 137-150.
- Pickles, S., Semmler, S., Broom, H. R., Destroismaisons, L., Legroux, L., Arbour, N., Meiering, E., Cashman, N. R. & Vande Velde, C. 2016. ALS-linked misfolded SOD1 species have divergent impacts on mitochondria. *Acta Neuropathologica Communications*, 4, 43.
- Pinarbasi, E. S., Cağatay, T., Fung, H. Y. J., Li, Y. C., Chook, Y. M. & Thomas, P. J. 2018. Active nuclear import and passive nuclear export are the primary determinants of TDP-43 localization. *Scientific reports*, 8, 7083.
- Polymenidou, M. & Cleveland, D. W. 2011. The seeds of neurodegeneration: prion-like spreading in ALS. *Cell*, 147, 498-508.
- Polymenidou, M., Lagier-Tourenne, C., Hutt, K. R., Huelga, S. C., Moran, J., Liang, T. Y., Ling, S.-C., Sun, E., Wancewicz, E., Mazur, C., Kordasiewicz, H., Sedaghat, Y., Donohue, J. P., Shiue, L., Bennett, C. F., Yeo, G. W. & Cleveland, D. W. 2011. Long pre-mRNA depletion and RNA missplicing contribute to neuronal vulnerability from loss of TDP-43. *Nature Neuroscience*, 14, 459.
- Puentes, F., Malaspina, A., Van Noort, J. M. & Amor, S. 2016. Non-neuronal Cells in ALS: Role of Glial, Immune cells and Blood-CNS Barriers. *Brain Pathology*, 26, 248-257.
- Pupillo, E., Bianchi, E., Poloni, M. & Beghi, E. 2017. Is firstly diagnosed ALS really ALS? Results of a population-based study with long-term follow-up. *Amyotrophic Lateral Sclerosis and Frontotemporal Degeneration*, 18, 221-226.
- Pupillo, E., Messina, P., Logroscino, G., Beghi, E. & The, S. G. 2014. Long-term survival in amyotrophic lateral sclerosis: A population-based study. *Annals of Neurology*, 75, 287-297.
- Qiao, S., Wang, F., Chen, H. & Jiang, S.-W. 2017. Inducible knockout of Syncytin-A gene leads to an extensive placental vasculature deficiency, implications for preeclampsia. *Clinica Chimica Acta*, 474, 137-146.
- Raaphorst, J., Beeldman, E., De Visser, M., De Haan, R. J. & Schmand, B. 2012. A systematic review of behavioural changes in motor neuron disease. *Amyotrophic Lateral Sclerosis*, 13, 493-501.
- Ragagnin, A. M., Shadfar, S., Vidal, M., Jamali, S. & Atkin, J. D. 2019. Motor neuron susceptibility in ALS/FTD. *Frontiers in neuroscience*, 13, 532.
- Rao, X., Huang, X., Zhou, Z. & Lin, X. 2013. An improvement of the $2^{-\Delta\Delta CT}$ method for quantitative real-time polymerase chain reaction data analysis. *Biostatistics, bioinformatics and biomathematics*, 3, 71.
- Rasmussen, H. B., Geny, C., Deforges, L., Perron, H., Tourtelotte, W., Heltberg, A. & Clausen, J. 1995. Expression of endogenous retroviruses in blood mononuclear cells and brain tissue from multiple sclerosis patients. *Multiple Sclerosis Journal*, 1, 82-87.
- Rathinam, V. A., Jiang, Z., Waggoner, S. N., Sharma, S., Cole, L. E., Waggoner, L., Vanaja, S. K., Monks, B. G., Ganesan, S. & Latz, E. 2010. The AIM2 inflammasome is essential for host defense against cytosolic bacteria and DNA viruses. *Nature immunology*, 11, 395-402.

- Ratti, A. & Buratti, E. 2016. Physiological functions and pathobiology of TDP-43 and FUS/TLS proteins. *Journal of neurochemistry*, 138, 95-111.
- Ratti, E., Atassi, N., Macklin, E., Murphy, A., Groberio, A. C., Dickerson, B. & Berry, J. 2016. Evaluation of the Association Between Pattern of Symptoms Onset and Survival within the ALS-FTD Continuum (P1. 138). AAN Enterprises.
- Reaume, A. G., Elliott, J. L., Hoffman, E. K., Kowall, N. W., Ferrante, R. J., Siwek, D. R., Wilcox, H. M., Flood, D. G., Beal, M. F. & Brown Jr, R. H. 1996. Motor neurons in Cu/Zn superoxide dismutase-deficient mice develop normally but exhibit enhanced cell death after axonal injury. *Nature genetics*, 13, 43.
- Reddi, P. P. Transcription and splicing factor TDP-43: role in regulation of gene expression in testis. *Seminars in reproductive medicine*, 2017. Thieme Medical Publishers, 167-172.
- Rehman, K., Fatima, F., Waheed, I. & Akash, M. S. H. 2018. Prevalence of exposure of heavy metals and their impact on health consequences. *Journal of cellular biochemistry*, 119, 157-184.
- Renton, A. E., Chiò, A. & Traynor, B. J. 2014. State of play in amyotrophic lateral sclerosis genetics. *Nature neuroscience*, 17, 17.
- Renton, A. E., Majounie, E., Waite, A., Simón-Sánchez, J., Rollinson, S., Gibbs, J. R., Schymick, J. C., Laaksovirta, H., Van Swieten, J. C. & Myllykangas, L. 2011. A hexanucleotide repeat expansion in C9ORF72 is the cause of chromosome 9p21-linked ALS-FTD. *Neuron*, 72, 257-268.
- Ringholz, G. M., Appel, S. H., Bradshaw, M., Cooke, N. A., Mosnik, D. M. & Schulz, P. E. 2005. Prevalence and patterns of cognitive impairment in sporadic ALS. *Neurology*, 65, 586-590.
- Roberts, A. L., Johnson, N. J., Cudkovic, M. E., Eum, K.-D. & Weisskopf, M. G. 2016. Job-related formaldehyde exposure and ALS mortality in the USA. *J Neurol Neurosurg Psychiatry*, 87, 786-788.
- Roos, P. M. 2013. *Studies on metals in motor neuron disease*, Institutet för miljömedicin/Institute of Environmental Medicine.
- Roos, P. M. 2017. Metals and Motor Neuron Disease. *Biometals in Neurodegenerative Diseases*. Elsevier.
- Roos, P. M., Lierhagen, S., Flaten, T. P., Syversen, T., Vesterberg, O. & Nordberg, M. 2012. Manganese in cerebrospinal fluid and blood plasma of patients with amyotrophic lateral sclerosis. *Experimental Biology and Medicine*, 237, 803-810.
- Rosen, D. R., Siddique, T., Patterson, D., Figlewicz, D. A., Sapp, P., Hentati, A., Donaldson, D., Goto, J., O'regan, J. P., Deng, H.-X., Rahmani, Z., Krizus, A., Mckenna-Yasek, D., Cayabyab, A., Gaston, S. M., Berger, R., Tanzi, R. E., Halperin, J. J., Herzfeldt, B., Van Den Bergh, R., Hung, W.-Y., Bird, T., Deng, G., Mulder, D. W., Smyth, C., Laing, N. G., Soriano, E., Pericak-Vance, M. A., Haines, J., Rouleau, G. A., Gusella, J. S., Horvitz, H. R. & Brown Jr, R. H. 1993. Mutations in Cu/Zn superoxide dismutase gene are associated with familial amyotrophic lateral sclerosis. *Nature*, 362, 59.
- Rostami, E., Krueger, F., Plantman, S., Davidsson, J., Agoston, D., Grafman, J. & Risling, M. 2014. Alteration in BDNF and its receptors, full-length and truncated TrkB and p75NTR following penetrating traumatic brain injury. *Brain Research*, 1542, 195-205.
- Rothstein, J. D., Tsai, G., Kuncl, R. W., Clawson, L., Cornblath, D. R., Drachman, D. B., Pestronk, A., Stauch, B. L. & Coyle, J. T. 1990. Abnormal excitatory amino acid metabolism in amyotrophic lateral sclerosis. *Annals of Neurology*, 28, 18-25.

- Rudnick, N. D., Griffey, C. J., Guarnieri, P., Gerbino, V., Wang, X., Piersaint, J. A., Tapia, J. C., Rich, M. M. & Maniatis, T. 2017. Distinct roles for motor neuron autophagy early and late in the SOD1G93A mouse model of ALS. *Proceedings of the National Academy of Sciences*, 114, E8294-E8303.
- Rueggsegger, C. & Saxena, S. 2016. Proteostasis impairment in ALS. *Brain Research*, 1648, 571-579.
- Ruprecht, K. & Mayer, J. 2019. On the origin of a pathogenic HERV-W envelope protein present in multiple sclerosis lesions. *Proceedings of the National Academy of Sciences*, 201911703.
- Russ, E., Mikhalkevich, N. & Iordanskiy, S. 2023. Expression of human endogenous retrovirus group K (HERV-K) HML-2 correlates with immune activation of macrophages and type I interferon response. *Microbiology Spectrum*, 11, e04438-22.
- Rutter-Locher, Z., Turner, M. R., Leigh, P. N. & Al-Chalabi, A. 2016. Analysis of terms used for the diagnosis and classification of amyotrophic lateral sclerosis and motor neuron disease. *Amyotrophic Lateral Sclerosis and Frontotemporal Degeneration*, 17, 600-604.
- Ryan, M., Heverin, M., Mclaughlin, R. L. & Hardiman, O. 2019. Lifetime Risk and Heritability of Amyotrophic Lateral Sclerosis. *JAMA neurology*, 76, 1367-1374.
- Rycaj, K., Plummer, J. B., Yin, B., Li, M., Garza, J., Radvanyi, L., Ramondetta, L. M., Lin, K., Johanning, G. L. & Tang, D. G. 2015. Cytotoxicity of human endogenous retrovirus K-specific T cells toward autologous ovarian cancer cells. *Clinical Cancer Research*, 21, 471-483.
- Saberi, S., Stauffer, J. E., Schulte, D. J. & Ravits, J. 2015. Neuropathology of Amyotrophic Lateral Sclerosis and Its Variants. *Neurologic clinics*, 33, 855-876.
- Sacson, R. A., Bunton-Stasyshyn, R. K. A., Fisher, E. M. C. & Fratta, P. 2013. Is SOD1 loss of function involved in amyotrophic lateral sclerosis? *Brain*, 136, 2342-2358.
- Sances, S., Bruijn, L. I., Chandran, S., Eggan, K., Ho, R., Klim, J. R., Livesey, M. R., Lowry, E., Macklis, J. D. & Rushton, D. 2016. Modeling ALS with motor neurons derived from human induced pluripotent stem cells. *Nature neuroscience*, 19, 542.
- Sanjak, M., Bravver, E., Bockenek, W. L., Norton, H. J. & Brooks, B. R. 2010. Supported treadmill ambulation for amyotrophic lateral sclerosis: a pilot study. *Archives of physical medicine and rehabilitation*, 91, 1920-1929.
- Sarkar, S., Malovic, E., Jin, H., Kanthasamy, A. & Kanthasamy, A. G. 2019. The role of manganese in neuroinflammation. *Role of Inflammation in Environmental Neurotoxicity*, 3, 121.
- Sasaki, S. & Iwata, M. 2007. Mitochondrial Alterations in the Spinal Cord of Patients With Sporadic Amyotrophic Lateral Sclerosis. *Journal of Neuropathology & Experimental Neurology*, 66, 10-16.
- Saxena, S. K. 2016. *Advances in Molecular Retrovirology*, BoD—Books on Demand.
- Scelsa, S., Macgowan, D., Mitsumoto, H., Imperato, T., Levalley, A., Liu, M., Delbene, M. & Kim, M. 2005. A pilot, double-blind, placebo-controlled trial of indinavir in patients with ALS. *Neurology*, 64, 1298-1300.
- Schellhas, V., Glatz, C., Beecken, I., Okegwo, A., Heidbreder, A., Young, P. & Boentert, M. 2018. Upper airway obstruction induced by non-invasive ventilation using an oronasal interface. *Sleep and Breathing*, 22, 781-788.

- Schmitt, K., Heyne, K., Roemer, K., Meese, E. & Mayer, J. 2015. HERV-K(HML-2) rec and np9 transcripts not restricted to disease but present in many normal human tissues. *Mobile DNA*, 6, 4.
- Scott, S., Kranz, J. E., Cole, J., Lincecum, J. M., Thompson, K., Kelly, N., Bostrom, A., Theodoss, J., Al-Nakhala, B. M. & Vieira, F. G. 2008. Design, power, and interpretation of studies in the standard murine model of ALS. *Amyotrophic Lateral Sclerosis*, 9, 4-15.
- Scotter, E. L., Chen, H.-J. & Shaw, C. E. 2015. TDP-43 proteinopathy and ALS: insights into disease mechanisms and therapeutic targets. *Neurotherapeutics*, 12, 352-363.
- Scotter, E. L., Vance, C., Nishimura, A. L., Lee, Y.-B., Chen, H.-J., Urwin, H., Sardone, V., Mitchell, J. C., Rogelj, B., Rubinsztein, D. C. & Shaw, C. E. 2014. Differential roles of the ubiquitin proteasome system and autophagy in the clearance of soluble and aggregated TDP-43 species. *Journal of Cell Science*, 127, 1263.
- Seals, R. M., Kioumourtoglou, M.-A., Gredal, O., Hansen, J. & Weisskopf, M. G. 2017. Occupational formaldehyde and amyotrophic lateral sclerosis. *European journal of epidemiology*, 32, 893-899.
- Seddighi, S., Qi, Y. A., Brown, A.-L., Wilkins, O. G., Bereda, C., Belair, C., Zhang, Y.-J., Prudencio, M., Keuss, M. J. & Khandeshi, A. 2024. Mis-spliced transcripts generate de novo proteins in TDP-43-related ALS/FTD. *Science Translational Medicine*, eadg7162.
- Sengul, G. & Watson, C. 2012. Chapter 13 - Spinal Cord. In: WATSON, C., PAXINOS, G. & PUELLES, L. (eds.) *The Mouse Nervous System*. San Diego: Academic Press.
- Shah, B. M., Schafer, J. J. & Desimone Jr, J. A. 2014. Dolutegravir: a new integrase strand transfer inhibitor for the treatment of HIV. *Pharmacotherapy: The Journal of Human Pharmacology and Drug Therapy*, 34, 506-520.
- Shah, S. I., Paine, J. G., Perez, C. & Ullah, G. 2019. Mitochondrial fragmentation and network architecture in degenerative diseases. *PLOS ONE*, 14, e0223014.
- Sharma, A., Bemis, M. & Desilets, A. R. 2014. Role of Medium Chain Triglycerides (Axona®) in the Treatment of Mild to Moderate Alzheimer's Disease. *American Journal of Alzheimer's Disease & Other Dementias®*, 29, 409-414.
- Shaw, C., Quinn, A. & Daniel, E. 2014. Amyotrophic lateral sclerosis/motor neuron disease. *Palliative Care in Amyotrophic Lateral Sclerosis: From Diagnosis to Bereavement*, 1.
- Shcherbakova, L., Tel'pukhov, V., Trenin, S., Bashilov, I. & Lapkina, T. 1986. Permeability of the blood-brain barrier to intra-arterial formaldehyde. *Biulleten'eksperimental'noi biologii i meditsiny*, 102, 573-575.
- Sheean, R. K., Mckay, F. C., Cretney, E., Bye, C. R., Perera, N. D., Tomas, D., Weston, R. A., Scheller, K. J., Djouma, E. & Menon, P. 2018. Association of regulatory T-cell expansion with progression of amyotrophic lateral sclerosis: a study of humans and a transgenic mouse model. *JAMA neurology*, 75, 681-689.
- Shellikeri, S., Karthikeyan, V., Martino, R., Black, S. E., Zinman, L., Keith, J. & Yunusova, Y. 2017. The neuropathological signature of bulbar-onset ALS: A systematic review. *Neuroscience & Biobehavioral Reviews*, 75, 378-392.
- Shepherd, S. R., Chataway, T., Schultz, D. W., Rush, R. A. & Rogers, M.-L. 2014. The extracellular domain of neurotrophin receptor p75 as a candidate biomarker for amyotrophic lateral sclerosis. *PLoS One*, 9, e87398.
- Shepherd, S. R., Karnaros, V., Benyamin, B., Schultz, D. W., Dubowsky, M., Wu, J., Chataway, T., Malaspina, A., Benatar, M. & Rogers, M. L. 2022. Urinary neopterin: A

- novel biomarker of disease progression in amyotrophic lateral sclerosis. *European journal of neurology*, 29, 990-999.
- Shepherd, S. R., Wu, J., Cardoso, M., Wiklendt, L., Dinning, P. G., Chataway, T., Schultz, D., Benatar, M. & Rogers, M.-L. 2017. Urinary p75^{ECD} A prognostic, disease progression, and pharmacodynamic biomarker in ALS. *Neurology*, 88, 1137-1143.
- Shi, P., Gal, J., Kwinter, D. M., Liu, X. & Zhu, H. 2010. Mitochondrial dysfunction in amyotrophic lateral sclerosis. *Biochimica et Biophysica Acta (BBA) - Molecular Basis of Disease*, 1802, 45-51.
- Shi, Y., Lin, S., Staats, K. A., Li, Y., Chang, W.-H., Hung, S.-T., Hendricks, E., Linares, G. R., Wang, Y. & Son, E. Y. 2018. Haploinsufficiency leads to neurodegeneration in C9ORF72 ALS/FTD human induced motor neurons. *Nature medicine*, 24, 313.
- Shin, W., Lee, J., Son, S.-Y., Ahn, K., Kim, H.-S. & Han, K. 2013. Human-Specific HERV-K Insertion Causes Genomic Variations in the Human Genome. *PLOS ONE*, 8, e60605.
- Shore, G. C., Papa, F. R. & Oakes, S. A. 2011. Signaling cell death from the endoplasmic reticulum stress response. *Current opinion in cell biology*, 23, 143-149.
- Shu, C., Li, X. & Li, P. 2014. The mechanism of double-stranded DNA sensing through the cGAS-STING pathway. *Cytokine & Growth Factor Reviews*, 25, 641-648.
- Simonin, Y., Erkilic, N., Damodar, K., Clé, M., Desmetz, C., Bolloré, K., Taleb, M., Torriano, S., Barthelemy, J. & Dubois, G. 2019. Zika virus induces strong inflammatory responses and impairs homeostasis and function of the human retinal pigment epithelium. *EBioMedicine*, 39, 315-331.
- Singh, K. K., Park, K. J., Hong, E. J., Kramer, B. M., Greenberg, M. E., Kaplan, D. R. & Miller, F. D. 2008. Developmental axon pruning mediated by BDNF-p75^{NTR}-dependent axon degeneration. *Nature Neuroscience*, 11, 649.
- Singh, P. K., Guest, J.-M., Kanwar, M., Boss, J., Gao, N., Juzych, M. S., Abrams, G. W., Yu, F.-S. & Kumar, A. 2017. Zika virus infects cells lining the blood-retinal barrier and causes chorioretinal atrophy in mouse eyes. *JCI insight*, 2.
- Singh, V., Kaur, R., Kumari, P., Pasricha, C. & Singh, R. 2023. ICAM-1 and VCAM-1: Gatekeepers in various inflammatory and cardiovascular disorders. *Clinica Chimica Acta*, 548, 117487.
- Slokar, G. & Hasler, G. 2016. Human endogenous retroviruses as pathogenic factors in the development of schizophrenia. *Frontiers in psychiatry*, 6, 183.
- Smith, E. F., Shaw, P. J. & De Vos, K. J. 2019. The role of mitochondria in amyotrophic lateral sclerosis. *Neuroscience Letters*, 710, 132933.
- Smith, J. A., Das, A., Ray, S. K. & Banik, N. L. 2012. Role of pro-inflammatory cytokines released from microglia in neurodegenerative diseases. *Brain Research Bulletin*, 87, 10-20.
- Smith, K. S., Rush, R. A. & Rogers, M. L. 2015. Characterization and changes in neurotrophin receptor p75-expressing motor neurons in SOD1^{G93AG1H} mice. *Journal of Comparative Neurology*, 523, 1664-1682.
- Soldan, S. S. & Lieberman, P. M. 2023. Epstein-Barr virus and multiple sclerosis. *Nature Reviews Microbiology*, 21, 51-64.
- Spalloni, A., Nutini, M. & Longone, P. 2019. Glutamate in Amyotrophic Lateral Sclerosis: An Ageless Contestant. *Pathology, Prevention and Therapeutics of Neurodegenerative Disease*. Springer.
- Spence, H., Waldron, F. M., Saleeb, R. S., Brown, A.-L., Rifai, O. M., Gilodi, M., Read, F., Roberts, K., Milne, G., Wilkinson, D., O'shaughnessy, J., Pastore, A., Fratta, P.,

- Shneider, N., Tartaglia, G. G., Zacco, E., Horrocks, M. H. & Gregory, J. M. 2024. RNA aptamer reveals nuclear TDP-43 pathology is an early aggregation event that coincides with STMN-2 cryptic splicing and precedes clinical manifestation in ALS. *Acta Neuropathologica*, 147, 50.
- Spencer, P. S. 2018. Formaldehyde, DNA damage, ALS and related neurodegenerative diseases. *Journal of the neurological sciences*, 391, 141-142.
- Sreedharan, J., Blair, I. P., Tripathi, V. B., Hu, X., Vance, C., Rogelj, B., Ackerley, S., Durnall, J. C., Williams, K. L. & Buratti, E. 2008. TDP-43 mutations in familial and sporadic amyotrophic lateral sclerosis. *Science*, 319, 1668-1672.
- St Clair, M. H., Richards, C., Spector, T., Weinhold, K., Miller, W., Langlois, A. J. & Furman, P. 1987. 3'-Azido-3'-deoxythymidine triphosphate as an inhibitor and substrate of purified human immunodeficiency virus reverse transcriptase. *Antimicrobial agents and chemotherapy*, 31, 1972-1977.
- Staats, K. A. & Vandenbosch, L. 2014. Excitotoxicity and Amyotrophic Lateral Sclerosis. *Handbook of Neurotoxicity*. Springer.
- Statland, J. M., Barohn, R. J., Dimachkie, M. M., Floeter, M. K. & Mitsumoto, H. 2015. Primary lateral sclerosis. *Neurologic clinics*, 33, 749-760.
- Steele, A., Al-Chalabi, A., Ferrante, K., Cudkovicz, M., Brown, R. & Garson, J. 2005. Detection of serum reverse transcriptase activity in patients with ALS and unaffected blood relatives. *Neurology*, 64, 454-458.
- Steiner, J. P., Bachani, M., Malik, N., Demarino, C., Li, W., Sampson, K., Lee, M. H., Kowalak, J., Bhaskar, M. & Doucet-O'hare, T. 2022. Human Endogenous Retrovirus K Envelope in Spinal Fluid of Amyotrophic Lateral Sclerosis Is Toxic. *Annals of Neurology*, 92, 545-561.
- Stern, A. L., Lee, R. N., Panvelker, N., Li, J., Harowitz, J., Jordan-Sciutto, K. L. & Akay-Espinoza, C. 2018. Differential effects of antiretroviral drugs on neurons in vitro: roles for oxidative stress and integrated stress response. *Journal of Neuroimmune Pharmacology*, 13, 64-76.
- Stevic, Z., Kostic-Dedic, S., Peric, S., Dedic, V., Basta, I., Rakocevic-Stojanovic, V. & Lavrnic, D. 2016. Prognostic factors and survival of ALS patients from Belgrade, Serbia. *Amyotrophic Lateral Sclerosis and Frontotemporal Degeneration*, 17, 508-514.
- Stocking, C. & Kozak, C. 2008a. Endogenous retroviruses. *Cellular and molecular life sciences*, 65, 3383-3398.
- Stocking, C. & Kozak, C. A. 2008b. Murine endogenous retroviruses. *Cell Mol Life Sci*, 65, 3383-98.
- Stommel, E. W., Cohen, J. A., Fadul, C. E., Cogbill, C. H., Graber, D. J., Kingman, L., Mackenzie, T., Channon Smith, J. Y. & Harris, B. T. 2009. Efficacy of thalidomide for the treatment of amyotrophic lateral sclerosis: A phase II open label clinical trial. *Amyotrophic Lateral Sclerosis*, 10, 393-404.
- Su, F.-C., Goutman, S. A., Chernyak, S., Mukherjee, B., Callaghan, B. C., Batterman, S. & Feldman, E. L. 2016. Association of environmental toxins with amyotrophic lateral sclerosis. *JAMA neurology*, 73, 803-811.
- Subramanian, R. P., Wildschutte, J. H., Russo, C. & Coffin, J. M. 2011. Identification, characterization, and comparative genomic distribution of the HERV-K (HML-2) group of human endogenous retroviruses. *Retrovirology*, 8, 90.

- Sun, Q., Huo, Y., Bai, J., Wang, H., Wang, H., Yang, F., Cui, F., Song, H. & Huang, X. 2021. Inflammatory cytokine levels in patients with sporadic amyotrophic lateral sclerosis. *Neurodegenerative Diseases*, 21, 87-92.
- Sun, S., Xu, Y., Qiu, M., Jiang, S., Cao, Q., Luo, J., Zhang, T., Chen, N., Zheng, W., Meurens, F., Liu, Z. & Zhu, J. 2023. Manganese Mediates Its Antiviral Functions in a cGAS-STING Pathway Independent Manner. *Viruses*, 15.
- Sun, Z., Diaz, Z., Fang, X., Hart, M. P., Chesi, A., Shorter, J. & Gitler, A. D. 2011. Molecular determinants and genetic modifiers of aggregation and toxicity for the ALS disease protein FUS/TLS. *PLoS biology*, 9, e1000614-e1000614.
- Suntsova, M., Garazha, A., Ivanova, A., Kaminsky, D., Zhavoronkov, A. & Buzdin, A. 2015. Molecular functions of human endogenous retroviruses in health and disease. *Cellular and Molecular Life Sciences*, 72, 3653-3675.
- Swarup, V., Phaneuf, D., Dupré, N., Petri, S., Strong, M., Kriz, J. & Julien, J.-P. 2011. Deregulation of TDP-43 in amyotrophic lateral sclerosis triggers nuclear factor κ B-mediated pathogenic pathways. *Journal of Experimental Medicine*, 208, 2429-2447.
- Synofzik, M., Fernández-Santiago, R., Maetzler, W., Schöls, L. & Andersen, P. M. 2010. The human G93A SOD1 phenotype closely resembles sporadic amyotrophic lateral sclerosis. *Journal of Neurology, Neurosurgery & Psychiatry*, 81, 764-767.
- Tafari, F., Ronchi, D., Magri, F., Comi, G. P. & Corti, S. 2015. SOD1 misplacing and mitochondrial dysfunction in amyotrophic lateral sclerosis pathogenesis. *Frontiers in Cellular Neuroscience*, 9, 336.
- Tan, W., Pasinelli, P. & Trotti, D. 2014. Role of mitochondria in mutant SOD1 linked amyotrophic lateral sclerosis. *Biochimica et Biophysica Acta (BBA)-Molecular Basis of Disease*, 1842, 1295-1301.
- Tarry-Adkins, J. L. & Ozanne, S. E. 2017. Nutrition in early life and age-associated diseases. *Ageing Research Reviews*, 39, 96-105.
- Tateishi, T., Yamasaki, R., Tanaka, M., Matsushita, T., Kikuchi, H., Isobe, N., Ohyagi, Y. & Kira, J.-I. 2010. CSF chemokine alterations related to the clinical course of amyotrophic lateral sclerosis. *Journal of Neuroimmunology*, 222, 76-81.
- Taylor, J. M., Moore, Z., Minter, M. R. & Crack, P. J. 2018. Type-I interferon pathway in neuroinflammation and neurodegeneration: focus on Alzheimer's disease. *Journal of Neural Transmission*, 125, 797-807.
- Taylor, J. P., Brown Jr, R. H. & Cleveland, D. W. 2016. Decoding ALS: from genes to mechanism. *Nature*, 539, 197.
- Thakore, N. J., Lapin, B. R., Mitsumoto, H. & Pooled Resource Open-Access, A. L. S. C. T. C. 2022. Early initiation of riluzole may improve absolute survival in amyotrophic lateral sclerosis. *Muscle & Nerve*, 66, 702-708.
- Ticozzi, N. & Silani, V. 2018. Genotypic and Phenotypic Heterogeneity in Amyotrophic Lateral Sclerosis. *Neurodegenerative Diseases*. Springer.
- Tollefsbol, T. O. 2018. Chapter 1 - Epigenetics of Human Disease. *In: TOLLEFSBOL, T. O. (ed.) Epigenetics in Human Disease (Second Edition)*. Academic Press.
- Tollervey, J. R., Curk, T., Rogelj, B., Briese, M., Cereda, M., Kayikci, M., König, J., Hortobágyi, T., Nishimura, A. L., Župunski, V., Patani, R., Chandran, S., Rot, G., Zupan, B., Shaw, C. E. & Ule, J. 2011. Characterizing the RNA targets and position-dependent splicing regulation by TDP-43. *Nature Neuroscience*, 14, 452-458.

- Tong, J., Huang, C., Bi, F., Wu, Q., Huang, B., Liu, X., Li, F., Zhou, H. & Xia, X.-G. 2013. Expression of ALS-linked TDP-43 mutant in astrocytes causes non-cell-autonomous motor neuron death in rats. *The EMBO journal*, 32, 1917-1926.
- Tortarolo, M., Lo Coco, D., Veglianesi, P., Vallarola, A., Giordana, M. T., Marcon, G., Beghi, E., Poloni, M., Strong, M. J. & Iyer, A. M. 2017. Amyotrophic lateral sclerosis, a multisystem pathology: insights into the role of TNF α . *Mediators of inflammation*, 2017.
- Tran, H., Almeida, S., Moore, J., Gendron, T. F., Chalasani, U., Lu, Y., Du, X., Nickerson, J. A., Petrucelli, L. & Weng, Z. 2015. Differential toxicity of nuclear RNA foci versus dipeptide repeat proteins in a Drosophila model of C9ORF72 FTD/ALS. *Neuron*, 87, 1207-1214.
- Tripathi, P., Rodriguez-Muela, N., Klim, J. R., De Boer, A. S., Agrawal, S., Sandoe, J., Lopes, C. S., Ogliari, K. S., Williams, L. A. & Shear, M. 2017. Reactive astrocytes promote ALS-like degeneration and intracellular protein aggregation in human motor neurons by disrupting autophagy through TGF- β 1. *Stem cell reports*, 9, 667-680.
- Trotti, D., Rolfs, A., Danbolt, N. C., Brown, R. H. & Hediger, M. A. 1999. SOD1 mutants linked to amyotrophic lateral sclerosis selectively inactivate a glial glutamate transporter. *Nature Neuroscience*, 2, 427-433.
- Turner, B. J. & Talbot, K. 2008. Transgenics, toxicity and therapeutics in rodent models of mutant SOD1-mediated familial ALS. *Progress in Neurobiology*, 85, 94-134.
- Turner, G., Barbulescu, M., Su, M., Jensen-Seaman, M. I., Kidd, K. K. & Lenz, J. 2001. Insertional polymorphisms of full-length endogenous retroviruses in humans. *Current Biology*, 11, 1531-1535.
- Turner, M. R., Barohn, R. J., Corcia, P., Fink, J. K., Harms, M. B., Kiernan, M. C., Ravits, J., Silani, V., Simmons, Z. & Statland, J. 2020. Primary lateral sclerosis: consensus diagnostic criteria. *Journal of Neurology, Neurosurgery & Psychiatry*, 91, 373-377.
- Turner, M. R., Bowser, R., Bruijn, L., Dupuis, L., Ludolph, A., Mcgrath, M., Manfredi, G., Maragakis, N., Miller, R. G. & Pullman, S. L. 2013a. Mechanisms, models and biomarkers in amyotrophic lateral sclerosis. *Amyotrophic Lateral Sclerosis and Frontotemporal Degeneration*, 14, 19-32.
- Turner, M. R., Hardiman, O., Benatar, M., Brooks, B. R., Chio, A., De Carvalho, M., Ince, P. G., Lin, C., Miller, R. G. & Mitsumoto, H. 2013b. Controversies and priorities in amyotrophic lateral sclerosis. *The Lancet Neurology*, 12, 310-322.
- Tyagi, R., Li, W., Parades, D., Bianchet, M. A. & Nath, A. 2017. Inhibition of human endogenous retrovirus-K by antiretroviral drugs. *Retrovirology*, 14, 21.
- Uittenbogaard, M. & Chiaramello, A. 2014. Mitochondrial biogenesis: a therapeutic target for neurodevelopmental disorders and neurodegenerative diseases. *Current pharmaceutical design*, 20, 5574-5593.
- Van Damme, P. & Robberecht, W. 2021. STING-Induced Inflammation—A Novel Therapeutic Target in ALS? *New England Journal of Medicine*, 384, 765-767.
- Van Den Bos, M. A., Geevasinga, N., Higashihara, M., Menon, P. & Vucic, S. 2019. Pathophysiology and diagnosis of ALS: Insights from advances in neurophysiological techniques. *International Journal of Molecular Sciences*, 20, 2818.
- Van Es, M. A., Hardiman, O., Chio, A., Al-Chalabi, A., Pasterkamp, R. J., Veldink, J. H. & Van Den Berg, L. H. 2017. Amyotrophic lateral sclerosis. *The Lancet*, 390, 2084-2098.

- Vance, C., Rogelj, B., Hortobágyi, T., De Vos, K. J., Nishimura, A. L., Sreedharan, J., Hu, X., Smith, B., Ruddy, D. & Wright, P. 2009. Mutations in FUS, an RNA processing protein, cause familial amyotrophic lateral sclerosis type 6. *Science*, 323, 1208-1211.
- Vandoorne, E., Vrijssen, B., Belge, C., Testelmans, D. & Buyse, B. 2016. Noninvasive ventilation in amyotrophic lateral sclerosis: effects on sleep quality and quality of life. *Acta Clinica Belgica*, 71, 389-394.
- Vandoorne, T., De Bock, K. & Van Den Bosch, L. 2018. Energy metabolism in ALS: an underappreciated opportunity? *Acta Neuropathologica*, 135, 489-509.
- Vaz, S. H., Pinto, S., Sebastião, A. M. & Brites, D. 2021. Astrocytes in Amyotrophic Lateral Sclerosis. *Exon Publications*, 35-53.
- Veech, R. L. 2014. Ketone ester effects on metabolism and transcription. *Journal of lipid research*, 55, 2004-2006.
- Vella, S., Schwartländer, B., Sow, S. P., Eholie, S. P. & Murphy, R. L. 2012. The history of antiretroviral therapy and of its implementation in resource-limited areas of the world. *AIDS*, 26, 1231-1241.
- Veyrat-Durebex, C., Reynier, P., Procaccio, V., Hergesheimer, R., Corcia, P., Andres, C. R. & Blasco, H. 2018. How can a ketogenic diet improve motor function? *Frontiers in molecular neuroscience*, 11, 15.
- Vincendeau, M., Göttesdorfer, I., Schreml, J. M., Wetie, A. G. N., Mayer, J., Greenwood, A. D., Helfer, M., Kramer, S., Seifarth, W. & Hadian, K. 2015. Modulation of human endogenous retrovirus (HERV) transcription during persistent and de novo HIV-1 infection. *Retrovirology*, 12, 1-17.
- Vinceti, G., Olney, N., Mandelli, M. L., Spina, S., Hubbard, H. I., Santos-Santos, M. A., Watson, C., Miller, Z. A., Lomen-Hoerth, C., Nichelli, P., Miller, B. L., Grinberg, L. T., Seeley, W. W. & Gorno-Tempini, M. L. 2019. Primary progressive aphasia and the FTD-MND spectrum disorders: clinical, pathological, and neuroimaging correlates. *Amyotrophic Lateral Sclerosis and Frontotemporal Degeneration*, 1-13.
- Vinceti, M., Filippini, T., Mandrioli, J., Violi, F., Bargellini, A., Weuve, J., Fini, N., Grill, P. & Michalke, B. 2017a. Lead, cadmium and mercury in cerebrospinal fluid and risk of amyotrophic lateral sclerosis: A case-control study. *Journal of Trace Elements in Medicine and Biology*, 43, 121-125.
- Vinceti, M., Filippini, T., Violi, F., Rothman, K. J., Costanzini, S., Malagoli, C., Wise, L. A., Odone, A., Signorelli, C., Iacuzio, L., Arcolin, E., Mandrioli, J., Fini, N., Patti, F., Lo Fermo, S., Pietrini, V., Teggi, S., Ghermandi, G., Scillieri, R., Ledda, C., Mauceri, C., Sciacca, S., Fiore, M. & Ferrante, M. 2017b. Pesticide exposure assessed through agricultural crop proximity and risk of amyotrophic lateral sclerosis. *Environmental Health*, 16, 91.
- Viola, M. V., Frazier, M., White, L., Brody, J. & Spiegelman, S. 1975. RNA-instructed DNA polymerase activity in a cytoplasmic particulate fraction in brains from Guamanian patients. *Journal of Experimental Medicine*, 142, 483-494.
- Viswanad, V., Anand, P. & Shammika, P. 2017. Advancement of Riluzole in Neurodegenerative Disease. *International Journal of Pharmaceutical and Clinical Research*, 9, 214-7.
- Volosin, M., Trotter, C., Cragolini, A., Kenchappa, R. S., Light, M., Hempstead, B. L., Carter, B. D. & Friedman, W. J. 2008. Induction of proneurotrophins and activation of p75NTR-mediated apoptosis via neurotrophin receptor-interacting factor in hippocampal neurons after seizures. *Journal of Neuroscience*, 28, 9870-9879.

- Vu, L. T. & Bowser, R. 2017. Fluid-based biomarkers for amyotrophic lateral sclerosis. *Neurotherapeutics*, 14, 119-134.
- Vucic, S. & Rutkove, S. B. 2018. Neurophysiological biomarkers in amyotrophic lateral sclerosis. *Current opinion in neurology*, 31, 640-647.
- Walker, A. K., Spiller, K. J., Ge, G., Zheng, A., Xu, Y., Zhou, M., Tripathy, K., Kwong, L. K., Trojanowski, J. Q. & Lee, V. M. Y. 2015. Functional recovery in new mouse models of ALS/FTLD after clearance of pathological cytoplasmic TDP-43. *Acta Neuropathologica*, 130, 643-660.
- Wang-Johanning, F., Frost, A. R., Jian, B., Epp, L., Lu, D. W. & Johanning, G. L. 2003. Quantitation of HERV-K env gene expression and splicing in human breast cancer. *Oncogene*, 22, 1528-1535.
- Wang, C., Guan, Y., Lv, M., Zhang, R., Guo, Z., Wei, X., Du, X., Yang, J., Li, T., Wan, Y., Su, X., Huang, X. & Jiang, Z. 2018. Manganese Increases the Sensitivity of the cGAS-STING Pathway for Double-Stranded DNA and Is Required for the Host Defense against DNA Viruses. *Immunity*, 48, 675-687.e7.
- Wang, H., O'reilly, É. J., Weisskopf, M. G., Logroscino, G., Mccullough, M. L., Thun, M. J., Schatzkin, A., Kolonel, L. N. & Ascherio, A. 2011. Smoking and Risk of Amyotrophic Lateral Sclerosis: A Pooled Analysis of 5 Prospective Cohorts Smoking and ALS. *JAMA Neurology*, 68, 207-213.
- Wang, M.-D., Gomes, J., Cashman, N. R., Little, J. & Krewski, D. 2014. A meta-analysis of observational studies of the association between chronic occupational exposure to lead and amyotrophic lateral sclerosis. *Journal of occupational and environmental medicine*, 56, 1235.
- Wang, W., Li, L., Lin, W.-L., Dickson, D. W., Petrucelli, L., Zhang, T. & Wang, X. 2013. The ALS disease-associated mutant TDP-43 impairs mitochondrial dynamics and function in motor neurons. *Human Molecular Genetics*, 22, 4706-4719.
- Wang, W., Wang, L., Lu, J., Siedlak, S. L., Fujioka, H., Liang, J., Jiang, S., Ma, X., Jiang, Z., Da Rocha, E. L., Sheng, M., Choi, H., Lerou, P. H., Li, H. & Wang, X. 2016. The inhibition of TDP-43 mitochondrial localization blocks its neuronal toxicity. *Nature Medicine*, 22, 869-878.
- Watanabe, K., Tanaka, M., Yuki, S., Hirai, M. & Yamamoto, Y. 2018. How is edaravone effective against acute ischemic stroke and amyotrophic lateral sclerosis? *Journal of clinical biochemistry and nutrition*, 62, 20-38.
- Wegorzewska, I. & Baloh, R. H. 2011. TDP-43-based animal models of neurodegeneration: new insights into ALS pathology and pathophysiology. *Neuro-degenerative diseases*, 8, 262-274.
- Wegorzewska, I., Bell, S., Cairns, N. J., Miller, T. M. & Baloh, R. H. 2009. TDP-43 mutant transgenic mice develop features of ALS and frontotemporal lobar degeneration. *Proceedings of the National Academy of Sciences*, 106, 18809.
- Wertman, V., Gromova, A., La Spada, A. R. & Cortes, C. J. 2019. Low-cost gait analysis for behavioral phenotyping of mouse models of neuromuscular disease. *JoVE (Journal of Visualized Experiments)*, e59878.
- Westarp, M. E., Bartmann, P., Rössler, J., Geiger, E., Westphal, K. P., Schreiber, H., Fuchs, D., Westarp, M. P. & Kornhuber, H. H. 1993. Antiretroviral therapy in sporadic adult amyotrophic lateral sclerosis. *Neuroreport*, 4, 819-822.
- Wijesekera, L. C. & Nigel Leigh, P. 2009. Amyotrophic lateral sclerosis. *Orphanet journal of rare diseases*, 4, 1-22.

- Wildschutte, J. H., Williams, Z. H., Montesion, M., Subramanian, R. P., Kidd, J. M. & Coffin, J. M. 2016. Discovery of unfixed endogenous retrovirus insertions in diverse human populations. *Proceedings of the National Academy of Sciences*, 113, E2326-E2334.
- Williams, T. L. 2013. Motor neurone disease: diagnostic pitfalls. *Clinical medicine (London, England)*, 13, 97-100.
- Williamson, T. L. & Cleveland, D. W. 1999. Slowing of axonal transport is a very early event in the toxicity of ALS-linked SOD1 mutants to motor neurons. *Nature neuroscience*, 2, 50.
- Wong, P. C., Pardo, C. A., Borchelt, D. R., Lee, M. K., Copeland, N. G., Jenkins, N. A., Sisodia, S. S., Cleveland, D. W. & Price, D. L. 1995. An adverse property of a familial ALS-linked SOD1 mutation causes motor neuron disease characterized by vacuolar degeneration of mitochondria. *Neuron*, 14, 1105-1116.
- Wright, A. L., Della Gatta, P. A., Le, S., Berning, B. A., Mehta, P., Jacobs, K. R., Gul, H., San Gil, R., Hedl, T. J. & Riddell, W. R. 2021. Riluzole does not ameliorate disease caused by cytoplasmic TDP-43 in a mouse model of amyotrophic lateral sclerosis. *European Journal of Neuroscience*, 54, 6237-6255.
- Wu, L. S., Cheng, W. C., Hou, S. C., Yan, Y. T., Jiang, S. T. & Shen, C. K. J. 2010. TDP-43, a neuro-pathosignature factor, is essential for early mouse embryogenesis. *genesis*, 48, 56-62.
- Wu, X., Wan, T., Gao, X., Fu, M., Duan, Y., Shen, X. & Guo, W. 2022. Microglia pyroptosis: a candidate target for neurological diseases treatment. *Frontiers in Neuroscience*, 16, 922331.
- Xu, Y.-F., Gendron, T. F., Zhang, Y.-J., Lin, W.-L., Alton, S., Sheng, H., Casey, M. C., Tong, J., Knight, J., Yu, X., Rademakers, R., Boylan, K., Hutton, M., McGowan, E., Dickson, D. W., Lewis, J. & Petrucelli, L. 2010. Wild-Type Human TDP-43 Expression Causes TDP-43 Phosphorylation, Mitochondrial Aggregation, Motor Deficits, and Early Mortality in Transgenic Mice. *The Journal of Neuroscience*, 30, 10851.
- Yilmaz, A., Price, R. W. & Gisslén, M. 2011. Antiretroviral drug treatment of CNS HIV-1 infection. *Journal of Antimicrobial Chemotherapy*, 67, 299-311.
- Yoshino, H. & Kimura, A. 2006. Investigation of the therapeutic effects of edaravone, a free radical scavenger, on amyotrophic lateral sclerosis (Phase II study). *Amyotrophic Lateral Sclerosis*, 7, 247-251.
- Yu, C.-H., Davidson, S., Harapas, C. R., Hilton, J. B., Mlodzianoski, M. J., Laohamonthonkul, P., Louis, C., Low, R. R. J., Moecking, J., De Nardo, D., Balka, K. R., Calleja, D. J., Moghaddas, F., Ni, E., Mclean, C. A., Samson, A. L., Tyebji, S., Tonkin, C. J., Bye, C. R., Turner, B. J., Pepin, G., Gantier, M. P., Rogers, K. L., McArthur, K., Crouch, P. J. & Masters, S. L. 2020a. TDP-43 Triggers Mitochondrial DNA Release via mPTP to Activate cGAS/STING in ALS. *Cell*.
- Yu, C. H., Davidson, S., Harapas, C. R., Hilton, J. B., Mlodzianoski, M. J., Laohamonthonkul, P., Louis, C., Low, R. R. J., Moecking, J., De Nardo, D., Balka, K. R., Calleja, D. J., Moghaddas, F., Ni, E., Mclean, C. A., Samson, A. L., Tyebji, S., Tonkin, C. J., Bye, C. R., Turner, B. J., Pepin, G., Gantier, M. P., Rogers, K. L., McArthur, K., Crouch, P. J. & Masters, S. L. 2020b. TDP-43 Triggers Mitochondrial DNA Release via mPTP to Activate cGAS/STING in ALS. *Cell*, 183, 636-649.e18.
- Yu, H. & Cleveland, D. W. 2018. Tuning apoptosis and neuroinflammation: TBK1 restrains RIPK1. *Cell*, 174, 1339-1341.

- Zepeda-Arce, R., Rojas-García, A. E., Benitez-Trinidad, A., Herrera-Moreno, J. F., Medina-Díaz, I. M., Barrón-Vivanco, B. S., Villegas, G. P., Hernández-Ochoa, I., Solís Heredia, M. D. J. & Bernal-Hernández, Y. Y. 2017. Oxidative stress and genetic damage among workers exposed primarily to organophosphate and pyrethroid pesticides. *Environmental toxicology*, 32, 1754-1764.
- Zhan, Y. & Fang, F. 2019. Smoking and amyotrophic lateral sclerosis: A mendelian randomization study. *Annals of Neurology*, 85, 482-484.
- Zhang, Q., Pan, J., Cong, Y. & Mao, J. 2022. Transcriptional regulation of endogenous retroviruses and their misregulation in human diseases. *International Journal of Molecular Sciences*, 23, 10112.
- Zhao, W., Beers, D. R., Bell, S., Wang, J., Wen, S., Baloh, R. H. & Appel, S. H. 2015. TDP-43 activates microglia through NF- κ B and NLRP3 inflammasome. *Experimental Neurology*, 273, 24-35.
- Zhou, H., Huang, C., Chen, H., Wang, D., Landel, C. P., Xia, P. Y., Bowser, R., Liu, Y.-J. & Xia, X. G. 2010. Transgenic Rat Model of Neurodegeneration Caused by Mutation in the TDP Gene. *PLOS Genetics*, 6, e1000887.
- Zhu, Q., Gregg, K., Lozano, M., Liu, J. & Dudley, J. P. 2000. CDP is a repressor of mouse mammary tumor virus expression in the mammary gland. *Journal of Virology*, 74, 6348-6357.
- Zimmer, K. 2019. *Human Endogenous Retroviruses and Disease* [Online]. [Accessed 11/02/2020 2020].
- Zoccolella, S., Beghi, E., Palagano, G., Fraddosio, A., Guerra, V., Samarelli, V., Lepore, V., Simone, I. L., Lamberti, P., Serlenga, L. & Logroscino, G. 2008. Predictors of long survival in amyotrophic lateral sclerosis: A population-based study. *Journal of the Neurological Sciences*, 268, 28-32.
- Zufiria, M., Gil-Bea, F. J., Fernandez-Torron, R., Poza, J. J., Munoz-Blanco, J. L., Rojas-Garcia, R., Riancho, J. & De Munain, A. L. 2016. ALS: a bucket of genes, environment, metabolism and unknown ingredients. *Progress in neurobiology*, 142, 104-129.